

Open Research Online

The Open University's repository of research publications
and other research outputs

Improving Outcome After Cardiac Arrest: New Pharmacological And Electrophysiological Approaches During Cardiopulmonary Resuscitation

Thesis

How to cite:

Ruggeri, Laura (2023). Improving Outcome After Cardiac Arrest: New Pharmacological And Electrophysiological Approaches During Cardiopulmonary Resuscitation. PhD thesis The Open University.

For guidance on citations see [FAQs](#).

© 2022 Laura Ruggeri



<https://creativecommons.org/licenses/by-nc-nd/4.0/>

Version: Version of Record

Link(s) to article on publisher's website:

<http://dx.doi.org/doi:10.21954/ou.ro.0001556e>

Copyright and Moral Rights for the articles on this site are retained by the individual authors and/or other copyright owners. For more information on Open Research Online's data [policy](#) on reuse of materials please consult the policies page.

oro.open.ac.uk

**Improving outcome after cardiac arrest:
new pharmacological and electrophysiological approaches
during cardiopulmonary resuscitation**

Thesis submitted by the student

Laura Ruggeri, MD

for the degree of

Doctor of Philosophy

Discipline of Life, Health & Chemical Sciences

Open University Research School, London, UK

Istituto di Ricerche Farmacologiche “Mario Negri” – IRCCS, Milan, Italy

Director of Studies

Dr. Giuseppe Ristagno

Supervisors

Dr. Derek J. Hausenloy

Dr. Roberto Latini

November 30th, 2022

CONTENTS

CONTENTS	i
1 Abstract	1
2 Abbreviations	4
3 Introduction	6
3.1 Etiology	8
3.1.1 Coronary heart disease	8
3.2 Post cardiac arrest syndrome	10
3.2.1 Post-cardiac arrest brain injury	12
3.2.2 Post-cardiac arrest myocardial dysfunction	18
3.2.3 Post-cardiac arrest systemic inflammatory response	21
3.3 CPR and defibrillation	29
3.3.1 Monitoring effectiveness of CC and predicting DF success	32
3.4 Role of epinephrine	35
3.4.1 Potential role of β 1-adrenergic blockade during CPR	35
3.5 Ventricular Fibrillation Waveform Analysis to Predict Outcome	36
3.5.1 Analyses of ECG features during VF and CPR	36
3.5.2 Overview of principal waveform analyses	40
3.5.3 Evolution of Amplitude spectrum area (AMSA)	44
3.5.4 Applicability of AMSA to a clinical scenario	47
3.5.5 CPR quality and duration of untreated VF	52
3.5.6 CA with underlying myocardial ischemia	54
3.5.7 AMSA and patient's characteristics and medications	55
3.5.8 Artefacts	56
3.5.9 Guideline statement on "Ventricular Fibrillation Waveform Analysis	58
3.5.10 Development of an AMSA guided resuscitation strategy with a two-thresholds approach	59
3.6 The swine model of CA	60
4 Aim of the studies	61
4.1 Study 1: Effects of esmolol during CPR to reduce the total number of defibrillations needed to terminate VF in a porcine model of CA with an underlying AMI	61

4.2	Study 2: AMSA to guide defibrillation during CPR in OHCA patients: a pilot, randomized controlled trial (AMSA TRIAL)	61
4.3	Study 3: Preclinical feasibility of real time AMSA measurement during CPR using a modified clinical defibrillator	61
4.4	Study 4: Identifying an AMI during CPR in a preclinical porcine model of VF	62
5	Study 1. Effects of esmolol during CPR to reduce the total number of defibrillations needed to terminate VF in a porcine model of CA with an underlying AMI	63
5.1	Methods	63
5.1.1	Study design	63
5.1.2	Ethical considerations	63
5.1.3	Animal preparation	63
5.1.4	Experimental procedure	64
5.1.5	Measurements	65
5.1.6	Statistical analyses	66
5.2	Results	67
5.3	Discussion	72
5.3.1	Main findings	72
5.3.2	VF termination	72
5.3.3	Neuroprotection	72
5.3.4	Cardioprotection	73
5.3.5	Limitations	73
6	Study 2. AMSA to guide defibrillation during CPR in OHCA patients: a pilot, randomized controlled trial (AMSA TRIAL)	75
6.1	Methods	75
6.1.1	Study design	75
6.1.2	Patient population	76
6.1.3	Randomization	76
6.1.4	Real-time AMSA analysis	76
6.1.5	Trial interventions	80
6.1.6	Selected AMSA threshold for defibrillation delivery decision	80
6.1.7	EMS training	81
6.1.8	Outcomes	81
6.1.9	Statistical analyses...	83

6.2	Results	84
6.2.1	Study Population	84
6.2.2	Overall defibrillation and clinical outcomes	85
6.2.3	AMSA and defibrillation outcomes	85
6.2.4	AMSA and resuscitation interventions and STEMI	88
6.3	Discussion	91
6.3.1	Main findings	91
6.3.2	Prediction of successful defibrillation	91
6.3.3	AMSA during untreated VF and high -quality CPR	92
6.3.4	Feasibility of AMSA reading during CPR	93
6.3.5	Implications	93
6.3.6	Limitations	93
7	Study 3. Preclinical feasibility of real time AMSA measurement during CPR using a modified clinical defibrillator	95
7.1	Methods	95
7.1.1	Study design	95
7.1.2	Ethical considerations	95
7.1.3	Animal preparation	95
7.1.4	Experimental procedure	97
7.1.5	Measurements	97
7.1.6	Statistical analysis	98
7.2	Results	99
7.3	Discussion	101
7.3.1	Main findings	101
7.3.2	Feasibility of AMSA reading during mechanical CPR	101
7.3.3	Implications	101
7.3.4	Limitations	101
8	Study 4. Identifying an AMI during CPR in a preclinical porcine model of VF	102
8.1	Methods	102
8.1.1	Study Design	102
8.1.2	Ethical considerations	103
8.1.3	Animal preparation	103
8.1.4	Experimental design	104

8.1.5	Measurements _____	105
8.1.6	Endpoints of the study..._____	105
8.1.7	Statistical analysis..._____	106
8.2	Results _____	107
8.4	Discussion _____	112
8.4.1	Main findings _____	112
8.4.2	AMSA and underlying AML..._____	112
8.4.3	Implications _____	114
8.4.4	Limitations _____	114
9	Conclusions _____	116
10	References _____	117
11	Disclosure and Acknowledgements _____	146
11.1	Funding for the thesis work _____	146
11.2	Conflict of Interest _____	146
11.3	Publications derived from the thesis work _____	146
10.3.1	Full articles _____	146
10.3.2	Abstracts _____	146
11.4	Collaborating personnel for the thesis work _____	147

1 ABSTRACT

PRESENTATION OF THE STUDY DESIGN AND THESIS READING

Cardiac arrest (CA) represents a leading cause of death in the western world. CA is a dramatic clinical event that can occur suddenly and often without premonitory signs. This condition is characterized by sudden loss of consciousness caused by the lack of cerebral blood flow, which occurs when the heart ceases to pump. Chest compressions (CCs) and early defibrillation (DF) are the cornerstones of cardiopulmonary resuscitation (CPR) in CA, while the only definitive treatment for ventricular fibrillation (VF) remains prompt DF. The present thesis includes both experimental and clinical studies directed to evaluate new pharmacological and electrophysiological approaches that have a potential benefit in the outcome of patients affected from CA.

In order to achieve such aims, we performed two separate studies concurrently. The first study was directed to investigate experimentally the role of β 1-blockade during CPR, while the second series of study evaluated prospectively the feasibility of a real time VF waveform analysis, in particular Amplitude Spectrum Area (AMSA), to guide interventions during resuscitation and to potentially diagnose underlying cardiac ischemia.

Both the studies therefore concurred to the same goal of identify new tools to improve the outcome of CA and are presented together in this thesis as a single study with an introduction, methods, results, and discussion section. Nevertheless, in order to help the readers going throughout the work, each section is divided into sub-sections presenting separately the studies.

STUDY 1. EFFECTS OF ESMOLOL DURING CPR TO REDUCE THE TOTAL NUMBER OF DEFIBRILLATIONS NEEDED TO TERMINATE VF IN A PORCINE MODEL OF CA WITH AN UNDERLYING AMI

Primary vasopressor efficacy of epinephrine during CPR is due to its α -adrenergic effects. However, epinephrine plays β 1-adrenergic actions, which increasing myocardial oxygen consumption may lead to refractory VF and poor outcome. Effects of a single dose of esmolol in addition to epinephrine during CPR were investigated in a porcine model of VF with an underlying acute myocardial infarction (AMI). VF was ischemically induced in 16 pigs and left untreated for 12 min. During CPR, animals were randomized to receive epinephrine (30 μ g/kg) with either esmolol (0.5 mg/kg) or saline (control). Pigs were then observed up to 96 h. Coronary perfusion pressure (CPP) increased during CPR in the esmolol group compared to control (47 ± 21 vs. 24 ± 10 mmHg at min 5, $p < 0.05$). In both groups, 7 animals were successfully resuscitated and 4 survived up to 96 h. No significant differences were observed between groups in the total number of DFs

delivered prior to final resuscitation. Brain histology demonstrated reductions in cortical neuronal degeneration/necrosis (score 0.3 ± 0.5 vs. 1.3 ± 0.5 , $p < 0.05$) and hippocampal microglial activation (6 ± 3 vs. $22 \pm 4\%$, $p < 0.01$) in the esmolol group compared to control. Lower circulating levels of NSE were measured in esmolol animals compared to controls ($2 [1-3]$ vs. $21 [16-52]$ ng/mL, $p < 0.01$). In this preclinical model, $\beta 1$ -blockade during CPR did not facilitate VF termination but provided neuroprotection.

STUDIES ON THE WAVEFORM ANALYSIS AMSA:

- STUDY 2. AMSA TO GUIDE DEFIBRILLATION DURING CPR IN OHCA PATIENTS: A PILOT, RANDOMIZED CONTROLLED TRIAL (AMSA TRIAL)
- STUDY 3. PRECLINICAL FEASIBILITY OF REAL TIME AMSA MEASUREMENT DURING CPR USING A MODIFIED CLINICAL DEFIBRILLATOR
- STUDY 4. IDENTIFYING AN AMI DURING CPR IN A PRECLINICAL PORCINE MODEL OF VF

Current CPR guidelines recommend providing a short period of CC until the defibrillator is ready for rhythm analysis and DF delivery. CPR should be then immediately restarted and continued for 2 min until rhythm reanalysis is undertaken and another electrical shock given, if needed. However, this recommendation is based on limited published data. In fact, the timing of DF in relationship to CC and the priority of intervention, i.e. DF first or CC first, remain a subject of major interest. Real time VF waveform analysis has been proposed and advocated for several decades as a potential non-invasive guide to optimize DF during CPR. If optimal timing of DF delivery could be determined by a real-time VF waveform analysis, it would be possible to prevent the delivery of unsuccessful high energy electrical shocks and minimize post-resuscitation myocardial injury. Among the different waveform analysis algorithms, AMSA has been recognized as one of the most accurate predictors of DF success.

Despite evidence from numerous animal studies and retrospective analyses of human data, no prospective clinical investigations on real-time AMSA analysis during CPR have been conducted yet. Study 2 (AMSA trial) was a pilot multicenter randomized clinical trial reporting the first in-human use of an AMSA-guided DF strategy in OHCA patients. The aim of the study was to test the hypothesis that CPR guided by real-time AMSA analysis was feasible and could predict outcome of DF attempts. The study demonstrated the feasibility of measuring and reading AMSA in real-time during CPR in the out-of-hospital setting. Moreover, the present study provided clinical validation of the capability of AMSA to predict DF success and to be able to guide CPR. AMSA values, acquired for the first time during ongoing resuscitation in human patients, were confirmed to be significantly higher when the DF attempts led to VF termination and return of spontaneous circulation

(ROSC), compared to unsuccessful attempts. Indeed, AMSA appeared to be independently associated with DF success, providing further evidence for its utility as a valid tool to identify the optimal timing for DF delivery during CPR.

Currently, a major challenge to the routine use of waveform measures is that these measures are conventionally calculated during pauses in CPR because CCs cause electrical artefact in the electrocardiogram (ECG). Such interruptions generally contradict best-practice guidelines which call for minimally-interrupted CPR to support resuscitation. Interruption, in fact, reduces the period of vital myocardial perfusion and has been proven to yield sub-optimal outcome and greater post-resuscitation myocardial dysfunction. Moreover, in some special conditions, like transport of patients, the use of mechanical CPR (and continuous CCs) is widespread. Study 3 was an experimental study on a swine model of CA with underlying coronary occlusion. We measured AMSA in real time during mechanical CPR without any interrupting CCs, using for the first time a modified clinical defibrillator with an integrated real time AMSA calculator, that analysed the signal collected by the defibrillatory pads. Indeed, in this preclinical setting, real time AMSA measurement during CPR was feasible without pauses.

Evidence from animal and clinical retrospective studies indicates that VF waveform measures, in particular AMSA, are differentially affected by acute ischemia. Nevertheless, a well-defined cut-off value for clinical use could not be identified. Study 4 is a pilot study on a new experimental swine model of CA with underlying occlusion of different branches of the coronary arteries and continuous AMSA display measured by a modified defibrillator. The study demonstrated that in presence of Left Coronary Artery (LCA) occlusion, AMSA values were lower and presented a minor increase during CPR compared to non-ischemic CA. Interestingly, VF due to occlusion of Right Coronary Artery (RCA) affected AMSA values to a lesser extent, thus reinforcing the finding from previous studies, showing that AMSA values are different according to the localization of ST Segment Elevation Myocardial Infarction (STEMI) and lower in the leads adjacent to the ischemic area.

In conclusion, studies on the waveform analysis AMSA confirm the feasibility of a real time AMSA-guide CPR strategy in a real clinical scenario and suggest the potential application of this strategy also when mechanical CPR is employed, without CC pauses. For the first time, the predictive capability of AMSA has been prospectively confirmed in a clinical setting. Interestingly, AMSA emerged also as a potential tool to detect an underlying ischemia and its localization. On the whole, the strength of these studies is the novelty of data on AMSA and the consistency of evidences between the clinical and experimental settings, thus paving the way for a routinely use of AMSA during CPR.

2 ABBREVIATIONS

AMI	Acute Myocardial Infarction
AMSA	Amplitude Spectrum Area
aPTT	Activated Partial Thromboplastin Clotting Time
ATP	Adenosine Triphosphate
AUC	Area Under The Curve
CA	Cardiac Arrest
Ca ²⁺	Calcium Ion
CCs	Chest Compressions
CO	Cardiac Output
CPC	Cerebral Performance Category
CPP	Coronary Perfusion Pressure
CPR	Cardiopulmonary Resuscitation
DF	Defibrillation
DIC	Disseminated Intravascular Coagulation
ECG	Electrocardiogram
EMS	Emergency Medical Services
EtCO ₂	End-Tidal Carbon Dioxide
Eureca	European Registry Of Cardiac Arrest
FiO ₂	Fraction of inspired Oxygen
HR	Hazard Ratio
hs-cTnT	High-Specificity-Cardiac Troponin T
IL	Interleukin
K ⁺	Potassium Ions
LAD	Left anterior descending
LCA	Left Coronary Artery
LCx	Left Circumflex Coronary Artery
LMCA	Left Main Coronary Artery
LV	Left Ventricular
MI	Myocardial infarction

Na ⁺	Sodium Ions
NFK β	Nuclear Factor Kappa β
NPV	Negative Predictive Value
NSE	Neuronal Specific Enolase
OHCA	Out Of Hospital Cardiac Arrest
OR	Odds Ratio
PCAS	Post Cardiac Arrest Syndrome
PCO ₂	Partial Pressure Of Carbon Dioxide
PPV	Positive Predictive Value
PTI	Prothrombin Time Index
Q	Quartile
ROC	Receiver Operating Characteristic
ROS	Reactive Oxygen Species
ROSC	Return of Spontaneous Circulation
RR	Relative Risk
SD	Standard Deviation
SEM	Standard Error of the Mean
STEMI	ST Segment Elevation Myocardial Infarction
TNF α	Tumor Necrosis Factor α
Vs	Ventilations
VEGF	Vascular Endothelial Growth Factor
VF	Ventricular Fibrillation

3 INTRODUCTION

CA is a dramatic clinical event that can occur suddenly and often without premonitory signs. This condition is characterized by sudden loss of consciousness caused by the lack of cerebral blood flow, which occurs when the heart ceases to pump. CCs and early DF are the cornerstones of CPR in CA, while the only definitive treatment for VF remains prompt DF.

CA represents a leading cause of death in the western world. The European Registry of Cardiac Arrest (EuReCa), an international project of the European Resuscitation Council, provides the most comprehensive information on the epidemiology of CA in Europe (*Grasner 2016, Grasner 2020*). The reported incidence of CA varies greatly between countries, but also between regions within countries. In the EuReCa ONE study the incidence of out of hospital cardiac arrest (OHCA) confirmed by Emergency Medical Services (EMS) was estimated at 84 per 100,000 inhabitants per year, varying from 28 to 160. The estimated incidence of OHCA where resuscitation was attempted by EMS was 49 per 100,000 inhabitants, varying from 19 to 104. The follow-up study, EuReCa TWO, collected data for three months and reported OHCA confirmed by EMS to be 89 per 100,000 inhabitants per year, varying from 53 to 166, with resuscitation attempted by EMS reported as 56 per 100,000 inhabitants, varying from 27 to 91. However, likely there is a substantial underreporting of CA incidence. The number of reported OHCA in Europe has increased in recent years when compared to one or two decades ago. Whether these differences reflect an increased incidence or simply more comprehensive reporting is unclear; at least in part, it can be explained by improved case ascertainment methods and increased coverage by regional and national registries in recent years (*Grasner 2021*).

Despite major efforts to improve outcomes of CA, average survival rate remains dismal (approximately 8% at hospital discharge, varying from 0% to 18%). Though the initial success of CPR, in fact, the majority of victims die within 72 hr from hospital admission, due to what is now called “Post Cardiac Arrest Syndrome (PCAS)” (*Brown 1992, Nolan 2008, Peberdy 2010, Sasson 2010, Schenkenberger 1994*). Most prominent are post resuscitation myocardial failure, ischemic brain damage and processes related to the systemic ischemia/reperfusion response (*Nolan 2008*). Severe heart contractile failure has been implicated as one of the most important mechanism accounting for the early fatal outcome (*Gazmuri 2012, Laurent 2002, Tang 1993, van Alem 2003*). Long term morbidity and mortality after successful CPR, instead, largely depend on recovery of neurologic function (*Nolan 2008, Sandroni 2013 and 2013b*). Poor neurological outcomes are still common (50% with 33% in a persistent vegetative state) in countries where good prognostication and withdrawal of life sustaining treatment is not practiced (*Grasner 2021*).

In European countries where withdrawal of life sustaining treatment is routinely practiced, a good neurological outcome is seen in > 90% of patients (*Grasner 2021*). Most patients, however, are not able to return to work. Amongst survivors with a good neurological outcome, neuro-cognitive, fatigue and emotional problems are common and lead to a reduced quality of life. Patients and relatives may develop post-traumatic stress disorder (*Grasner 2021*).

The mechanisms responsible for post-CA myocardial and cerebral injury are not well understood, although several events have been described. The reintroduction of oxygenated blood after ROSC stimulates a sequence of complex actions that lead to acute inflammatory responses and release of reactive oxygen species (ROS), causing oxidative damage, cellular edema, cell membrane damage, calcium ion (Ca^{2+}) overload, mitochondrial dysfunction, and apoptosis (*Dezfulian 2007, Lebuffe 2003, Levraut 2003, Nolan 2008, Ouyang 1999, Polderman 2009*). Several other processes, including interactions between pleiotropic mediators, coagulation abnormalities, activation of the inflammatory cytokine cascade, chemokine upregulation and ultimately recruitment of inflammatory leukocytes and reactive astrogliosis have also been reported after CA and are major players in the final outcome (*Adrie 2002 and 2004 and 2005, Frangogiannis 1998, Meybohm 2009, Neumar 2008, Nolan 2008, Vakeva 1998*).

3.1 ETIOLOGY

CAUSES OF SUDDEN CARDIAC ARREST
Coronary heart disease <ul style="list-style-type: none">• ST-segment elevation• Other myocardial infarction• Unstable angina• Silent ischaemia
Electrical heart disease, often associated with SCD in the young <ul style="list-style-type: none">• Long QT-syndrome• Short QT syndrome• Brugada syndrome• Catecholaminergic Polymorphic Ventricular Tachycardia• Triadin knock-out syndrome• Arrhythmogenic bi-leaflet mitral valve prolapse• Drug or medication induced
Non-atherosclerotic coronary artery anomalies
Congenital heart disease <ul style="list-style-type: none">• Hypertrophic cardiomyopathy
Dilated cardiomyopathy
Valvular heart disease
Table 3.3.1. Causes of sudden cardiac death. <i>Adapted from Soar 2021.</i>

Coronary Heart Disease remains the most common cause of sudden cardiac death. Coronary Heart Disease accounts for approximately 80% of all sudden cardiac death while non-ischemic cardiomyopathies are responsible for another 10–15%.

Sudden cardiac death can occur in individuals with structural heart disease and in individuals without any structural heart disease, such as arrhythmic syndromes, including long-QT syndromes, short-QT syndromes, catecholaminergic polymorphic ventricular tachycardia and Brugada syndrome.

Hypertrophic cardiomyopathy is the most common cause of sudden cardiac death in adults younger than 35 years of age. In the young, inherited diseases, congenital heart disease, myocarditis and substance abuse are predominant causes (Figure 3.1.1) (*Soar 2021*).

3.1.1 Coronary heart disease

Coronary Heart Disease is associated with a marked increase in sudden cardiac death risk. Generally, sudden cardiac death occurs in patients with Coronary Heart Disease during or after myocardial infarction (MI), secondary to multi-vessel coronary artery disease, previous MI with myocardial scarring particularly during the first 30 days post-MI, and in those with ischemic cardiomyopathy and marked left ventricular (LV) systolic dysfunction. About two-thirds of all sudden cardiac death due to Coronary Heart Disease occur either as the first clinical manifestation of coronary artery disease or in

individuals with known coronary artery disease who were thought to be low risk based on current risk stratification schemes. Four main pathophysiologic substrates contribute to sudden cardiac death: transient ischemia, acute coronary syndrome, scar-related arrhythmia, and ischemic cardiomyopathies that produce potentially fatal arrhythmias such as VF, ventricular tachycardia, asystole, and bradycardia. With improvements in primary prevention and revascularization techniques, age-adjusted mortality related to Coronary Heart Disease has declined within the last five decades; however, the percentage of sudden cardiac death associated with Coronary Heart Disease has remained unchanged. This association suggests complex interactions between Coronary Heart Disease and triggering events such as ischemia, autonomic nervous system dysfunction, electrolyte imbalance or drug toxicity. Furthermore, individual genetic profiles add another layer of complexity. Additional factors, such as heart failure and LV hypertrophy predispose to ventricular arrhythmias. Cardiac electrophysiology studies can identify patients with Coronary Heart Disease at high versus low risk of sudden cardiac death, but the only indicator that has been identified to be consistently associated with an increased risk of sudden cardiac death in the setting of Coronary Heart Disease and LV dysfunction is the severe reduction of LV ejection fraction (*Kandala 2017, Soar 2021*).

3.2 POST CARDIAC ARREST SYNDROME

ROSC after CA is an unnatural pathophysiological state created by successful CPR. In the early 1970s, Dr. Vladimir Negovsky recognized that the pathology caused by complete, whole-body ischemia and reperfusion was unique in that it had a clearly definable cause, time course, and constellation of pathophysiological processes (Negovsky 1972 and 1988 and 1995). Negovsky named this state “post resuscitation disease”. Although appropriate at the time, the term “resuscitation” is now used more broadly to include treatment of various shock states in which circulation has not ceased. Moreover, the term “post resuscitation” implies that the act of resuscitation has ended. Negovsky stated that “a second, more complex phase of resuscitation begins when patients regain spontaneous circulation after CA” (Negovsky 1972), thus the term PCAS has been adopted.

The PCAS comprises post-CA hypoxic-ischaemic brain injury, myocardial dysfunction, the systemic ischaemia/reperfusion response, and the persistence of the precipitating pathology. The severity of this syndrome will vary with the duration and cause of CA. It may not occur at all if the CA is brief (Nolan 2021). Pathophysiology, clinical manifestations and potential treatments of PCAS are summarized in Table 3.2.1.

Significant myocardial dysfunction is common after CA but typically starts to recover by 2-3 days, although full recovery may take significantly longer. The whole-body ischaemia/reperfusion of CA, CPR and ROSC activates immune and coagulation pathways contributing to multiple organ failure and increasing the risk of infection. Thus, the post-cardiac arrest syndrome has many features in common with sepsis, including intravascular volume depletion, vasodilation, endothelial injury and abnormalities of the microcirculation. (Nolan 2021).

The mechanisms responsible for post-CA myocardial and cerebral injury are not well understood, although several events have been described. At cellular level, the CA-induced whole-body ischemia causes hypoxia, conversion to anaerobic metabolism, intracellular acidosis, adenosine triphosphate (ATP) depletion, ion pump failure, intracellular Ca^{2+} accumulation, and cellular and mitochondrial edema (Chalkias 2012, Adrie 2004, Neumar 2008, Reis 2017). At systemic level, release of catecholamines, tumor necrosis factor α (TNF α), interleukin (IL) 1 β , complement and polymorphonuclear leukocyte activation, endothelial damage with increased microvascular permeability, coagulation cascade activation, and polymorphonuclear release of ROS and cytokines (Chalkias, 2012, Adrie 2004, Lindner 1992, Neumar 2008, Reis 2017).

SYNDROME	PATHOPHYSIOLOGY	CLINICAL MANIFESTATION	POTENTIAL TREATMENTS
BRAIN INJURY	<ul style="list-style-type: none"> • Impaired cerebrovascular autoregulation • Cerebral edema (limited) • Postischemic neurodegeneration 	<ul style="list-style-type: none"> • Coma • Seizures • Myoclonus • Cognitive dysfunction • Persistent vegetative state • Secondary Parkinsonism • Cortical stroke • Spinal stroke • Brain death 	<ul style="list-style-type: none"> • Therapeutic hypothermia • Early hemodynamic optimization • Airway protection and mechanical ventilation • Seizure control • Controlled reoxygenation (Sao2 94% to 96%) • Supportive care
MYOCARDIAL DYSFUNCTION	<ul style="list-style-type: none"> • Global hypokinesis (myocardial stunning) • Acute coronary syndrome 	<ul style="list-style-type: none"> • Reduced cardiac output • Hypotension • Dysrhythmias • Cardiovascular collapse 	<ul style="list-style-type: none"> • Early revascularization of AMI • Early hemodynamic optimization • Intravenous fluid • Inotropes • Intra-Aortic Balloon Pump • Left Ventricular Assist Device • Extracorporeal Membrane Oxygenation
SYSTEMIC ISCHEMIA/REPERFUSION RESPONSE	<ul style="list-style-type: none"> • Systemic inflammatory response syndrome • Impaired vasoregulation • Increased coagulation • Adrenal suppression • Impaired tissue oxygen delivery and utilization 	<ul style="list-style-type: none"> • Ongoing tissue hypoxia/ischemia • Hypotension • Cardiovascular collapse • Pyrexia (fever) • Hyperglycemia • Multiorgan failure • Infection 	<ul style="list-style-type: none"> • Early hemodynamic optimization • Intravenous fluid • Vasopressors • High-volume hemofiltration • Temperature control • Glucose control • Antibiotics for documented infection
PERSISTENT PRECIPITATING PATHOLOGY	<ul style="list-style-type: none"> • Cardiovascular disease (AMI/ Acute Coronary Syndrome, cardiomyopathy) • Pulmonary disease (Chronic Obstructive Pulmonary Disease, asthma) • Central Nervous System disease (Cerebrovascular Accident) • Thromboembolic disease (Pulmonary Embolism) • Toxicological (overdose, poisoning) • Infection (sepsis, pneumonia) • Hypovolemia (hemorrhage, dehydration) 	<ul style="list-style-type: none"> • Specific to cause but complicated by concomitant PCAS 	<ul style="list-style-type: none"> • Disease-specific interventions guided by patient condition and concomitant PCAS

CPR results in partial restoration of organ perfusion and triggering of reperfusion injury mechanisms. Global reperfusion injury is further amplified by the subsequent ROSC, stimulating a sequence of complex actions that lead to acute inflammatory responses and release of ROS, causing oxidative damage, cellular edema, cell membrane damage, Ca^{2+} overload, mitochondrial dysfunction, and apoptosis (Dezfulian 2007, Lebuffe 2003, Levraut 2003, Madathil 2016 Nolan 2008, Ouyang 1999, Polderman 2009). At systemic level, activated polymorphonuclears and platelets interacting with an injured and dysfunctional endothelium induce widespread microvascular plugging termed as the “no-reflow” phenomenon (Chalkias 2012). Activated polymorphonuclears further boost the cytokine storm and

infiltrate damaged tissues causing cell death (*Adams 2006*). The ongoing endothelial injury further impairs microvascular permeability contributing to intravascular volume depletion, while the concurrent, immune cells' inducible NO synthase-related overproduction of NO promotes peripheral vasodilation (*Adrie 2002*). The inflammatory cascade is amplified by nuclear factor kappa β (NFK β) activation. Several other processes, including interactions between pleiotropic mediators, coagulation abnormalities, activation of the inflammatory cytokine cascade, chemokine upregulation and ultimately recruitment of inflammatory leukocytes and reactive astrogliosis have also been reported (*Adrie 2002 and 2004 and 2005, Frangogiannis 1998, Meybohm 2009, Neumar 2008, Nolan 2008, Vakeva 1998*). Furthermore, a potential ischemia/reperfusion injury-associated disruption of the intestinal mucosal barrier (*Chalkias 2016*) may cause acute increases of pathogen-associated molecular patterns such as endotoxins in the systemic circulation, with further amplification of the systemic inflammation, and predisposition to multiple organ failure and "endogenous immunosuppression" (*Kakihana 2016*).

Severe heart contractile failure has been implicated as one of the most important mechanism accounting for most deaths in the first three days (*Gazmuri 2012, Laurent 2002, Nolan2021, Tang 1993, van Alem 2003*) while, in many countries, withdrawal of life sustaining treatment based on the prognostication of severe hypoxic-ischaemic brain injury accounts for most of the later deaths. Among patients surviving to Intensive Care Unit admission but subsequently dying in-hospital, withdrawal of life sustaining treatment following prognostication of poor neurological outcome is the cause of death in approximately two-thirds of OHCA (*Nolan2021*)

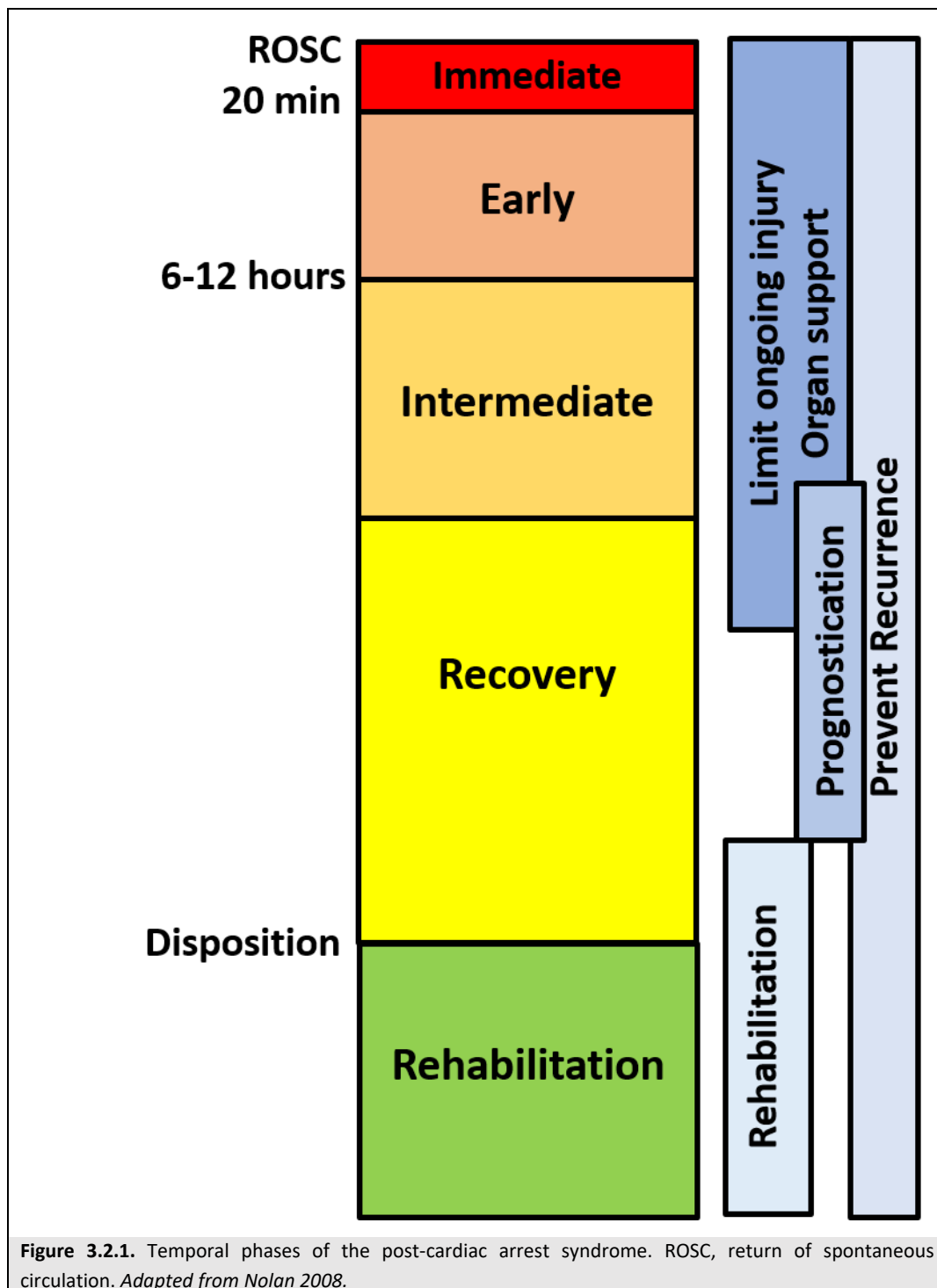
A more treatment-orientated approach has been proposed to define the phases of PCAS by time (Figure 3.2.1). Indeed, 4 phases are recognized: 1. the immediate post-arrest phase, including the first 20 min after ROSC; 2. the early post-arrest phase, defined as the period between 20 min and 6-12 hr after ROSC, when early interventions might be most effective; 3. The intermediate, between 6-12 and 72 hr, when injury pathways are still active and aggressive treatment is typically instituted; and 4. the period beyond 3 days after ROSC, considered the recovery phase when prognostication becomes more reliable and ultimate outcomes are more predictable (*Nolan 2008, Nolan 2021*).

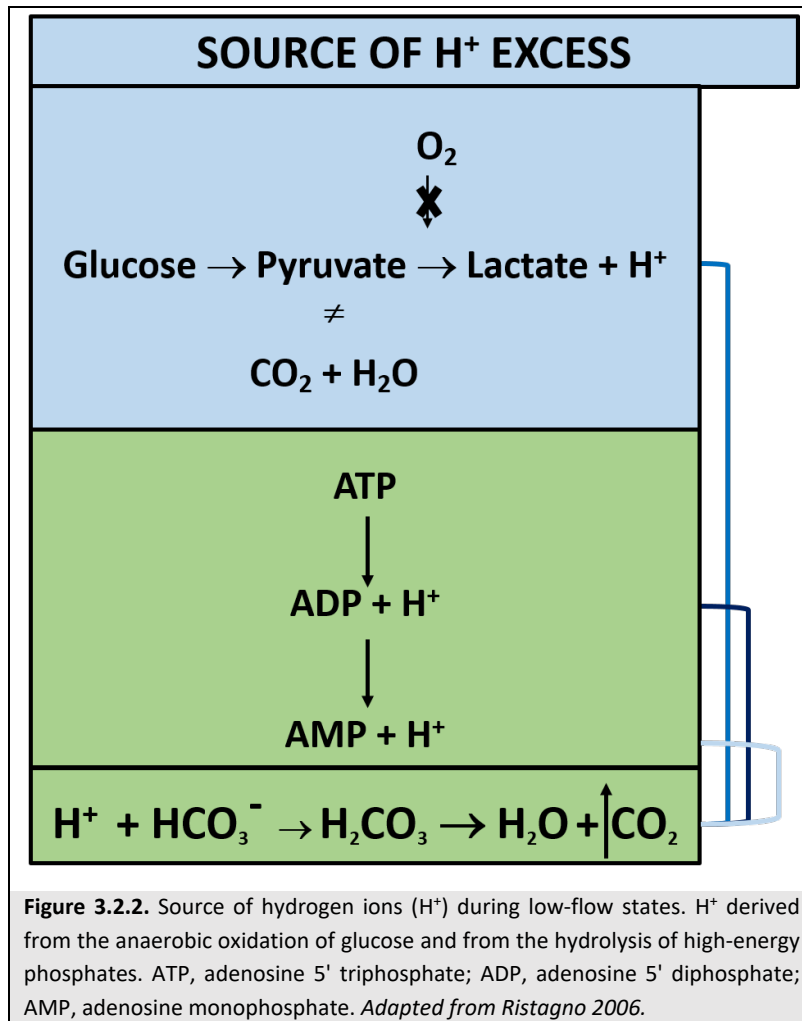
3.2.1 Post-cardiac arrest brain injury

Post CA brain injury manifests as coma, seizures, myoclonus, varying degrees of neurocognitive impairment and brain death. It is the responsible of death of the majority of patients after OHCA (*Lemiale 2013*).

The unique vulnerability of the brain is attributed to its limited tolerance of ischemia as well as its unique response to reperfusion. The mechanisms of brain injury triggered by CA and resuscitation are

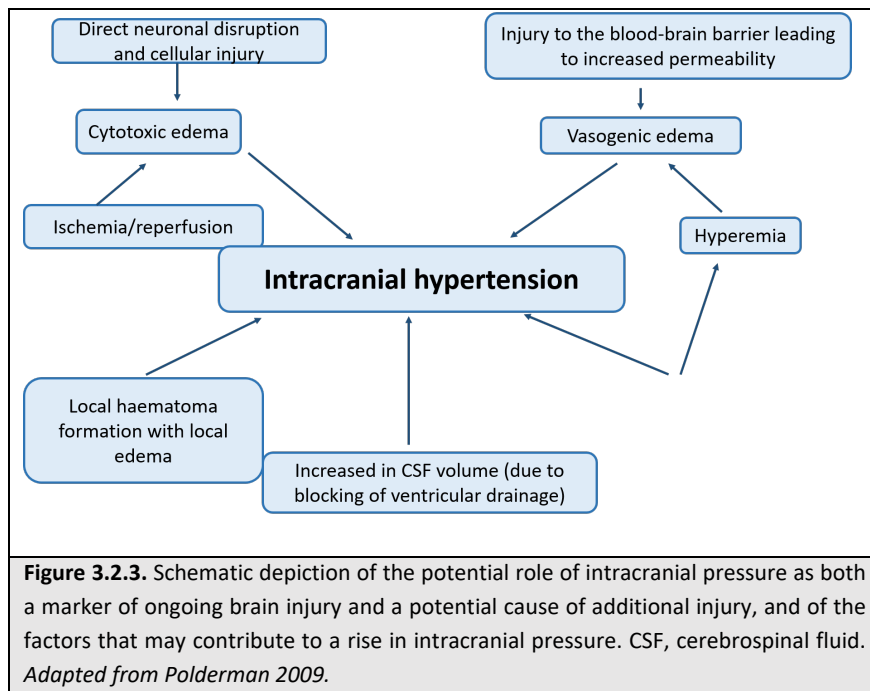
complex and include excitotoxicity, disrupted Ca^{2+} homeostasis, free radical formation, pathological protease cascades, and activation of cell death signaling pathways (Lipton 1999, Neumar 2000 and 2008, Nolan 2008, Polderman 2009). Both neuronal necrosis and apoptosis have been reported after CA. Histologically,





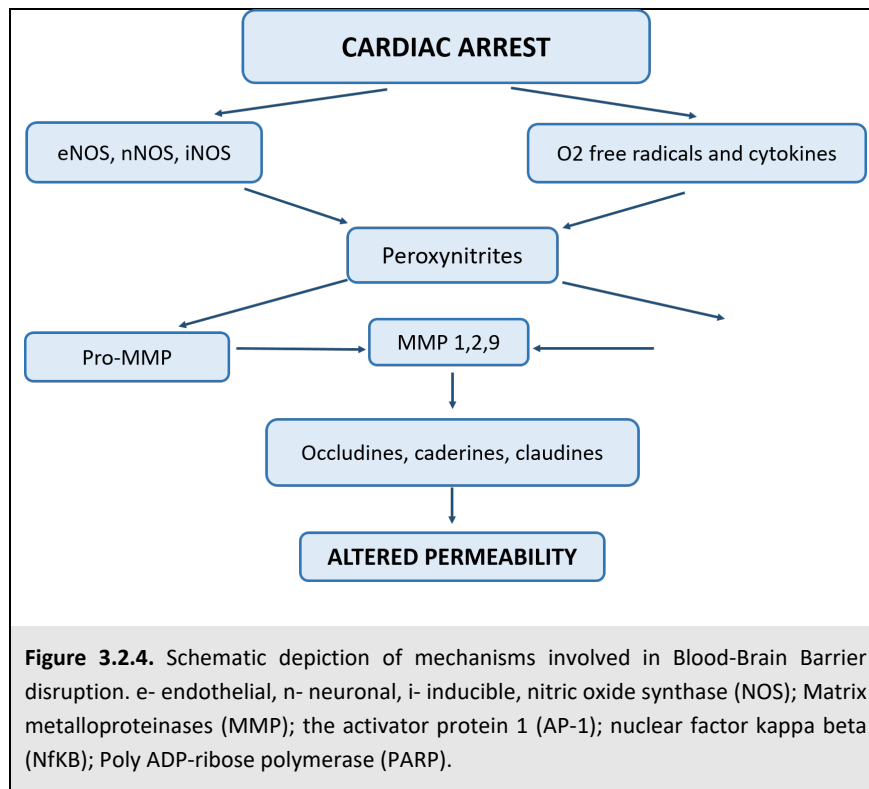
selectively vulnerable neuron subpopulations in the hippocampus, cortex, cerebellum, corpus striatum, and thalamus, degenerate over hours to days (Brierley 1973, Blomqvist 1985, Hossmann 2001, Neumar 2000, Nolan 2008, Polderman 2009, Pulsinelli 1985, Taraszewska 2002). Levels of high energy metabolites such as ATP and phosphocreatine decrease within seconds when oxygen supply to the brain is interrupted (Cavus 2006, Small 1999). The breakdown of ATP and the switch of intracellular metabolism to anaerobic glycolysis lead to an increase in intracellular levels of inorganic phosphate, lactate, and hydrogen ion, resulting in both intra- and extracellular acidosis (Figure 3.2.2).

Due to acidosis, the Blood-Brain Barrier of different brain areas breaks down, allowing for serum proteins to enter the brain microfluid environment (Figure 3.2.3) (Sharma 2011). Inflammatory cytokines and vascular endothelial growth factor (VEGF) (Kaur 2008), via release of NO (Fischer 1999) mediate decreased fluidity and integrity of cell membranes and increased vascular permeability of



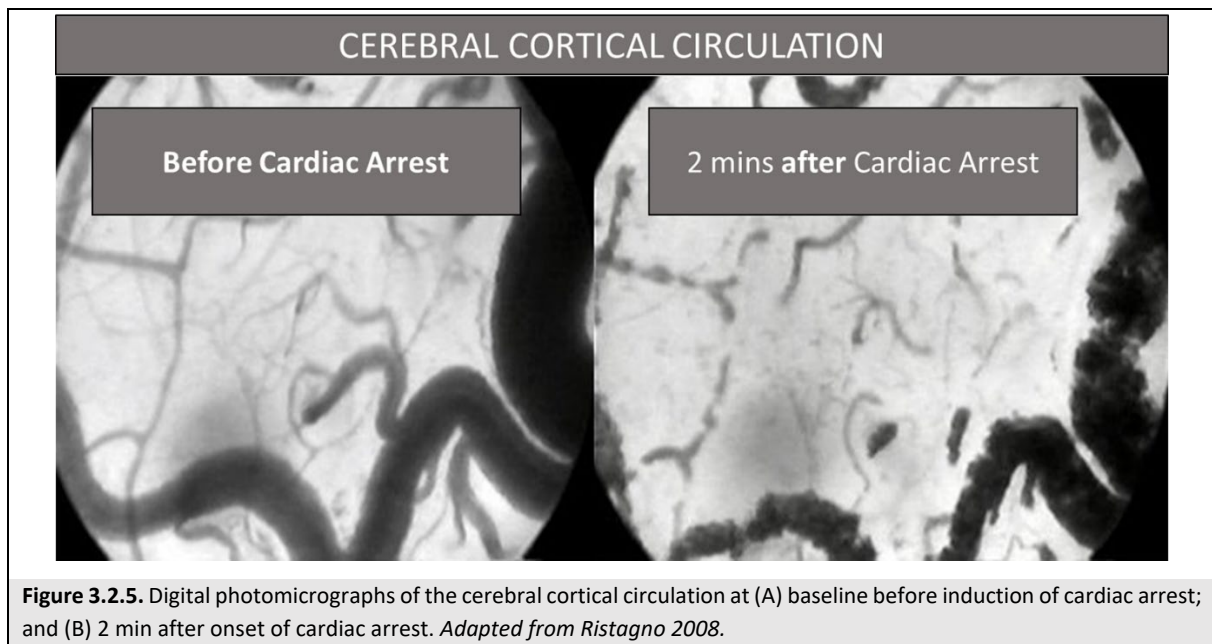
microvascular endothelial cells in the brain. More specifically, NO can interact with ROS producing peroxynitrite radicals, which activate matrix metalloproteinases (MMPs) that ultimately disrupt Blood-Brain Barrier junctions (figure 3.2.4). The passage of large molecules through the Blood-Brain Barrier enhances the passage of sodium ions (Na^+) and water from blood to brain compartment, altering the osmolality between them. These water and electrolyte changes following cell membrane damage and Blood-Brain Barrier breakdown result in cell swelling and brain edema formation. Brain edema contributes to the development of post CA intracranial hypertension, which further augments brain damage.

The disruption of Ca^{2+} homeostasis due to a progressive increase in cell membrane permeability and to the derangements of intracellular electrolytes represents another important mechanism of brain damage, due to failure of the ATP-dependent (sodium-potassium) $\text{Na}^+\text{-K}^+$ pumps and K^+ , Na^+ , and Ca^{2+} channels, leading to an additional influx of Ca^{2+} . Moreover, loss of ATP and acidosis inhibit the mechanisms that normally deal with excessive intracellular Ca^{2+} by sequestering Ca^{2+} from the cell, further aggravating intracellular Ca^{2+} overload. As a consequence, first, intracellular Ca^{2+} exerts cytotoxic effects leading to free radical production. Second, immediate early genes are activated and a depolarization of neuronal cell membranes occurs, with a release of large amounts of the excitatory neurotransmitter glutamate into the extracellular space (Neumar 2000, Polderman 2009, Siesjo 1989).



This leads to prolonged and excessive activation of membrane glutamate receptors, further stimulating Ca^{2+} influx through activation of Ca^{2+} channels in another vicious cycle. Under normal circumstances, neurons are exposed to only very brief pulses of glutamate; prolonged glutamate exposure induces a permanent state of hyperexcitability in the neurons (the excitotoxic cascade), which can lead to additional injury and cell death. In addition, the excess of in Ca^{2+} induces mitochondrial dysfunction, overwhelming the endogenous mitochondrial scavenging systems leading to mitochondrial dysfunction and cell death. Indeed, mitochondrial Ca^{2+} overload causes the induction of inner mitochondrial membrane permeability transition, which then leads to disruption of mitochondrial membrane integrity, irreversible oxidative damage, and the loss of ATP production, finally resulting in cell death (Polderman 2009).

A destructive process that is closely linked to but distinct from the mechanisms discussed above is the release of ROS following ischemia/reperfusion. Mediators such as superoxide, peroxynitrite, hydrogen peroxide, and hydroxyl radicals play an important role in determining whether injured cells will recover or die (Globus 1995 and 1995b, Novack 1996, Polderman 2009). Free radicals can oxidize and damage numerous cellular components. Although brain cells have various enzymatic and non-enzymatic antioxidant mechanisms that prevent this type of injury under normal circumstances, ROS production following



ischemia/reperfusion is so great that these defensive mechanisms are likely to be overwhelmed, leading to peroxidation of lipids, proteins, and nucleic acids.

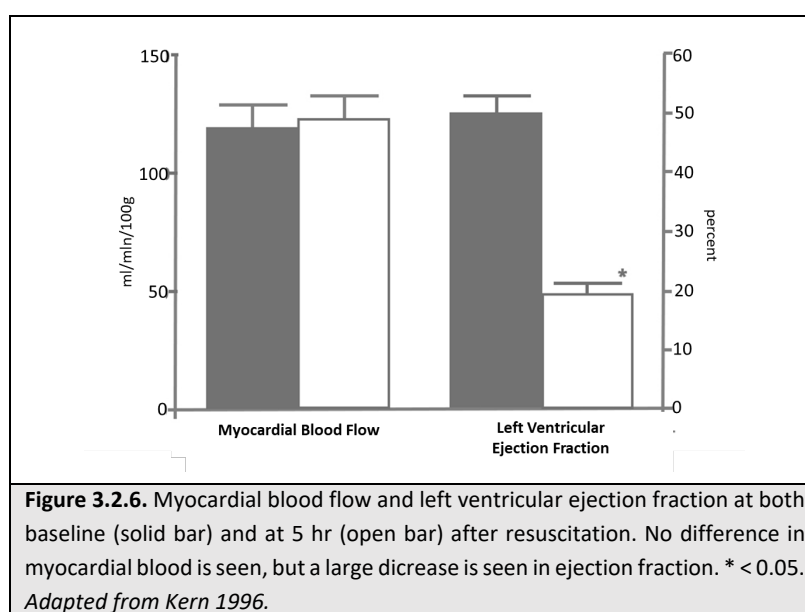
Post CA brain injury can also be followed by failure of cerebral microcirculation. During CA, in response to the stress of global ischemia, various cytokines are synthesized and released, resulting in activation of blood coagulation, platelets activation and decreased regional blood flow. Furthermore, with the onset of CPR, marked activation of blood coagulation occurs, which can lead to microthrombi, while the activated neutrophils and platelets accumulate in the microvasculature. This impaired reflow can cause persistent ischemia and small infarctions in some brain regions. The cerebral microvascular occlusion that causes no-reflow may further be compromised by the α_1 -adrenergic agonist of endogenous or exogenous adrenaline which reduces capillary blood flow (Figure 3.2.5) (Ristagno 2009). Other phenomena may be involved in cerebral perfusion disturbances, that include not only no-reflow events but also hyperemia episodes following ischemia: increased blood viscosity and perivascular edema, as well as possible down-regulation of NO synthesis, expression of endothelial adhesion molecules and generation of free radicals (Bottiger 1997, Donadello 2011, Hossmann 1993, Liachenko 2001, van Genderen 2012). Histologically, both neuronal necrosis and apoptosis have been reported after CA. Selectively vulnerable neuron subpopulations in the hippocampus, cortex, cerebellum, corpus striatum, and thalamus, degenerate over hours to days (Brierley 1973, Blomqvist 1985, Hossmann 2001, Neumar 2000, Nolan 2008, Polderman 2009, Pulsinelli 1985, Taraszewska 2002).

Beyond the initial reperfusion phase, several factors can potentially compromise cerebral oxygen delivery and possibly secondary injury in the hours to days after CA. These include hypotension,

hypoxemia, impaired cerebrovascular autoregulation, and brain edema. Furthermore, hyperglycemia is common in post-CA patients and is importantly associated with poor neurological outcome after CA (Calle 1989, Longstreth 1983 and 1984 and 1993, Mullner 1997, Skrifvars 2003).

3.2.2 Post-cardiac arrest myocardial dysfunction

Post-CA myocardial dysfunction contributes to the early deaths after resuscitation from CA (Herlitz 1995, Laurent 2002, Lavert 2004, Lemiale 2013, Neumar 2008, Nolan 2008,). Laboratory and clinical evidence, however, indicates that this phenomenon is both responsive to therapy and reversible (Cerchiari 1993, Hackenhaar 2014, Huang 2005, Kern 1996 and 1997, Laurent 2002, Nolan 2008, Ruiz-Bailén 2005). Immediately after ROSC, heart rate and blood pressure are extremely variable and this is mainly caused by a transient increase in myocardial and circulating catecholamines concentrations (Prengel 1992, Rivers 1994). Premature ventricular beats and episodes of ventricular tachycardia and VF commonly occur during the early minutes after resuscitation and account for early death. Furthermore, an overall condition of severe myocardial dysfunction, including variable degrees of systolic and diastolic dysfunction, is present (Babini 2018).



During this period with significant myocardial dysfunction, coronary blood flow however is not reduced, indicating a true stunning phenomenon rather than a permanent injury or infarction (Figure 3.2.6). Repetitive DFs are known to increase the severity of post-resuscitation myocardial dysfunction (Tang 2006). It has been reported that the longer was the duration of no-flow, the greater was the number of DF attempts and such a number of electrical countershocks was significantly related with the systolic dysfunction, represented by the LV ejection fraction impairment, and with the myocardial injury (i.e. high-specificity-cardiac troponin T (hs-cTnT) release) (Babini 2018).

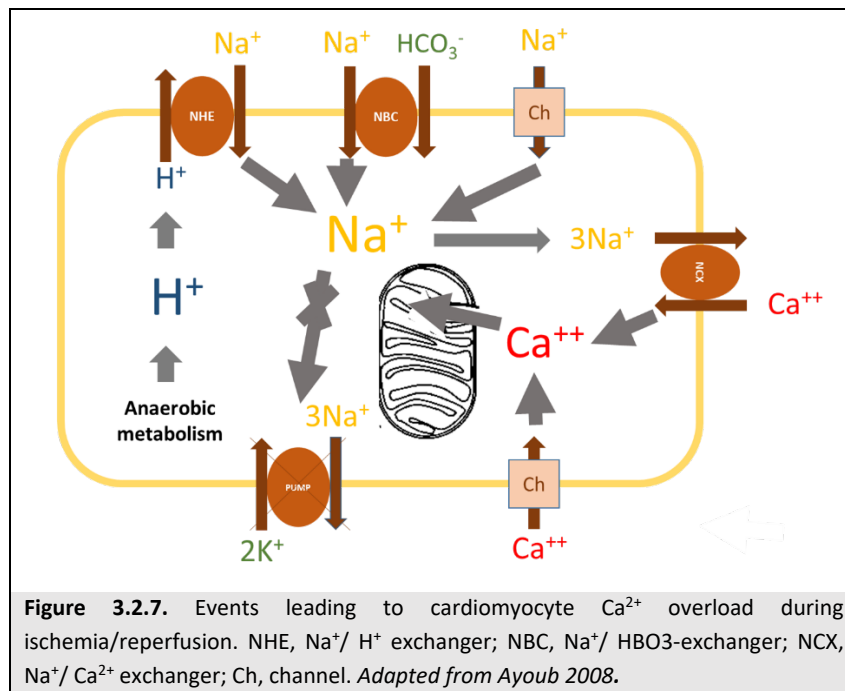
Hemodynamic Parameters	Interval From Onset of Cardiac Arrest to Measurement (h)						p Values [§]
	Intensive Care Unit Admission	Time 0	Time 1	Time 2	Time 3	Time 4	
	3.0(2.0–3.6)	6.8(4.3–7.3)	8.0(7.0–9.0)	12.0(11.0–13.5)	24.0(23.0–25.7)	67.0(52.0–72.0)	
Epinephrine perfusion (mg/h)	0	0	1.0 [†] (0–2.2)	1.3 [†] (0–2.0)	1.5 [†] (0–2.7)	0.4 [†] (0–1.6)	0.042
Heart rate (beats/min)	110 (89–123)	111 (91–124)	108 (97–125)	111 (98–128)	112 (101–125)	101 [*] (94–120)	0.215
Mean Arterial Pressure (mmHg)	87(75–103)	62 [†] (46–71)	79 [†] (69–102)	76 [†] (69–87)	80(71–89)	80(73–88)	0.04
Mean Pulmonary Arterial Pressure (mmHg)	-	-	28(22–32)	24 [†] (20–28)	24 [†] (20–27)	28(24–32)	0.005
Right Atrial Pressure (mmHg)	-	-	11(8–15)	10(8–13)	11(8–13)	12(9–15)	0.189
Pulmonary Occlusion Arterial Pressure (mmHg)	-	-	14(11–18)	12 [†] (10–15)	13(10–16)	14(10–18)	0.248
Cardiac Index (l/min x m ²)	-	-	2.1(1.4–2.9)	2.6 [†] (1.9–3.5)	3.2 [†] (2.7–4.2)	3.7 [*] (2.9–4.5)	< 0.001
Systemic Vascular Resistance Index (dynes x s/cm ⁵ x m ²)	-	-	2.9(1.9–4.7)	1.9 [†] (1.5–3.0)	1.7 [†] (1.3–2.0)	1.5 [†] (1.2–1.9)	< 0.001
Pulmonary Vascular Resistance Index (dynes x s/cm ⁵ x m ²)	-	-	438(339–593)	363 [†] (221–488)	261 [†] (183–346)	274 [*] (206–371)	< 0.001
Stroke Index (ml/m ²)	-	-	20.0(15.0–23.8)	22.5 [†] (18.4–32.1)	29.3 [†] (24.8–37.4)	35.3 [†] (28.5–42.1)	< 0.001
Left Ventricular Stroke Work (g x m/m ²)	-	-	23.8(19.3–31.0)	24.5(19.8–34.9)	33.3 [†] (25.0–43.1)	41.1 [†] (31.4–50.0)	< 0.001
Table 3.2.2. Hemodynamic data during the first 72 hours . Mean arterial pressure at admission and time 0 was determined by non invasive methods, and at times 1, 2, 3, and 4 by invasive monitoring. Data are presented as the median value (interquartile range). *p<0.05,†p<0.001,‡p<0.01 for all tests performed versus baseline. §The p value in the last column refers to non parametric analysis of variance (Kruskal-Wallis test). <i>Adapted from Laurent 2002.</i>							

In one series of 148 patients who underwent coronary angiography after CA, 49% of subjects had myocardial dysfunction manifested by tachycardia and elevated LV end-diastolic pressure, followed approximately 6 hr later by hypotension and low cardiac output (CO) (*Kern 1996, Laurent 2002*). This global dysfunction was transient, and full recovery occurred. In a swine model with no antecedent coronary or other LV dysfunction features, the time to recovery appeared to range between 24 and 48 hr. Several case series have described transient myocardial dysfunction after human CA. Cardiac index values reached their nadir at 8 hr after resuscitation, improved substantially by 24 hr, and almost uniformly returned to normal by 72 hr in patients who survived OHCA. This trend in arterial pressure, cardiac index and other hemodynamic parameters are described in Dr. Laurent's work (*Laurent 2002*), where clinical data over the 72 hr post CA are reported (Table 3.2.2).

Among the mechanisms underlying early post-resuscitation arrhythmia and myocardial dysfunction, cytosolic and mitochondrial Ca^{2+} overload following CA and CPR has been recognized as a determinant (*Ayoub 2008, Gazmuri 2012*). Ca^{2+} overload after CA is related to myocyte Na^+ content alteration. Under normoxic conditions the late Na^+ current (INaL) contributes very little to the total Na^+ content of the myocardial cell. However, during ischemia the INaL channel does not close properly. Under this condition the influx of Na^+ becomes substantial (*Kloner 2011*). Indeed, Na^+ influx through the late Na^+ channel appears to be the major contributor to the rise of cardiomyocyte intracellular Na^+ concentration observed during ischemia (*Zaza 2008*). It has been shown, in fact, that ischemia increases the amplitude of INaL in rat ventricular myocytes, from 50–100 pA up to 180–205 pA. Furthermore, following reperfusion, production of ROS is known to further increase INaL (*Ma 2005, Slezak 1995, Song 2006*).

In the setting of CA and CPR, main routes for cardiomyocyte Na^+ entry include the sodium-hydrogen exchanger isoform-1, the voltage-gated Na^+ channel, and the Na^+ -bicarbonate co-transporter. This cytosolic Na^+ accumulation, further augmented by the concurrent ischemia-induced Na^+ - K^+ -ATPase inability to extrude Na^+ , represents an important pathophysiological mechanism responsible for cell injury (*Wang 2007*). Cytosolic Na^+ causes, in fact, a subsequent increase in myocyte intracellular Ca^{2+} via the activity of Na^+ - Ca^{2+} exchanger (Figure 3.2.7) (*Ayoub 2008*).

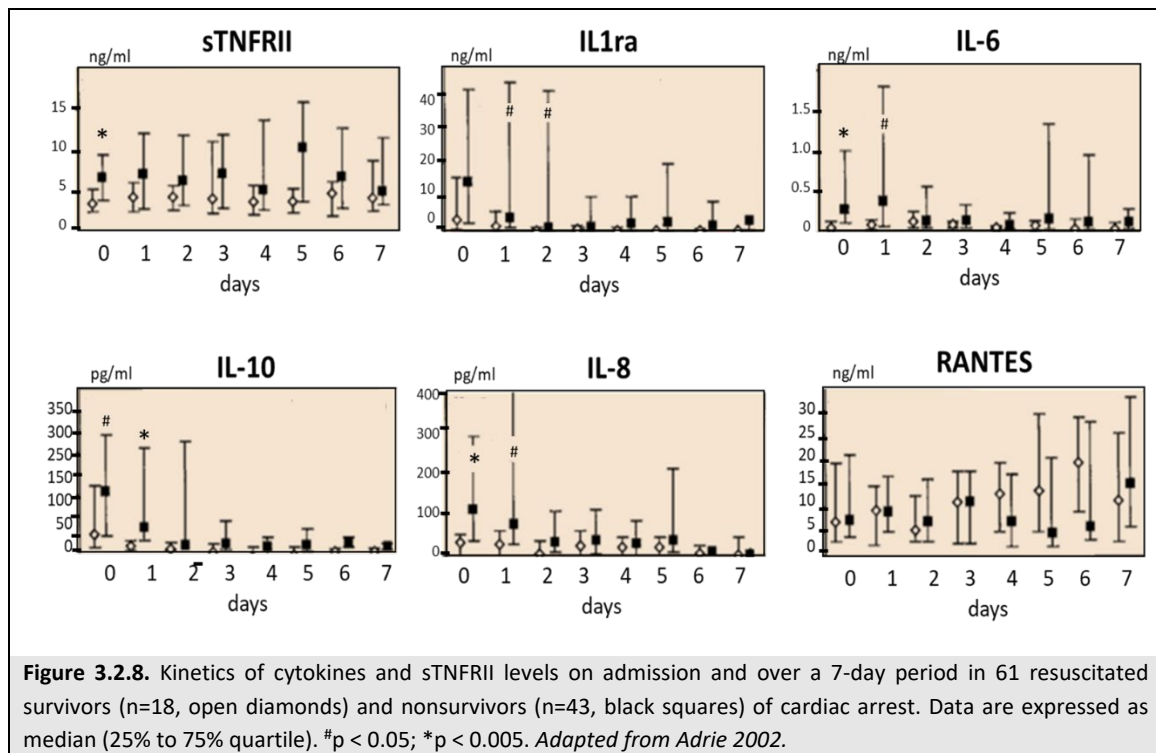
Post-resuscitation cytosolic Ca^{2+} accumulation in cardiomyocytes has, indeed, several deleterious consequences, including: electrical instability with ventricular arrhythmias early after resuscitation, i.e. premature ventricular complexes, ventricular tachycardia and VF; varying degrees of mechanical LV dysfunction that can compromise hemodynamic function, i.e. reduced contractility and increased diastolic tension; and mitochondrial dysfunction (*Ayoub 2008 and 2010, Gralinski 1996*).



Mitochondria are the major contributors in many cellular as well as extracellular regulatory functions that affect survival following an ischemic insult. In the setting of CA, mitochondria are thought to be progressively damaged during ischemia and further injured when reperfusion resumes. This leads to important alterations of the function of this organelle. Specifically, the dysfunction has been shown to be mainly associated with impaired complex activities that begin to deteriorate within the initial 15 min of ischemia. Nevertheless, ultrastructural changes of mitochondria during ischemia, including swelling, loss of matrix density and cristae disintegration, have been also demonstrated to correlate well with the duration of CA (Yeh 2009, Xu 2010). In addition to its bioenergetic function, mitochondria also participate in processes leading to cell death via necrosis or apoptosis. Various distinctive mechanisms have been identified including opening of the so called mitochondrial permeability transition pore (leading to collapse of proton motive force and uncoupling of respiration) (Halestrap 2004) and release of various pro-apoptotic proteins, including cytochrome c, apoptosis-inducing factor, Smac/DIABLO, endonuclease G, and a serine protease Omi/HtrA2 (Cai 1998, Green 1998, Radhakrishnan 2007 and 2009).

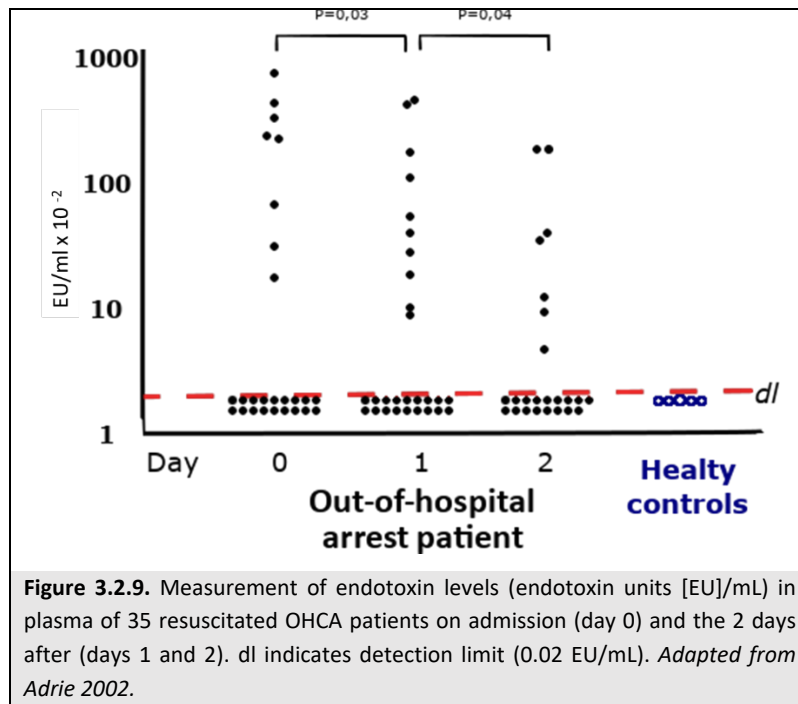
3.2.3 Post-cardiac arrest systemic inflammatory response

The whole-body ischemia/reperfusion that follows CA with associated oxygen debt causes, generalized activation of immunological and coagulation pathways, increasing the risk of multiple organ failure and infection (Adrie 2002 and 2004 and 2005, Adams 2006, Cerchiarri 1993b, Esmon 2003). As early as 3 hr after CA, blood concentrations of various cytokines, soluble receptors, and endotoxin increase, and the magnitude of



these changes are associated with outcome. More specifically, this inflammatory response includes endothelial activation, plasma cytokine elevation with deregulated cytokine production, presence of endotoxin in plasma, coagulation abnormalities, and adrenal dysfunction (Adrie 2002, Ristagno 2014, Nolan 2008, Peberdy 2010). Accordingly, this systemic inflammatory response brings evident similarities with sepsis and septic shock, and is generally described as a “sepsis-like” syndrome (Adrie 2002).

In details, soluble intercellular adhesion molecule-1, soluble vascular-cell adhesion molecule-1, and P- and E-selectins are increased during and after CPR, suggesting leucocyte activation or endothelial injury (Adrie 2002 and 2004, Gando 2000, Geppert 2000). Thus, altogether, the high levels of circulating cytokines, the presence of endotoxin in plasma, and the dysregulated production of cytokines found in CA patients resemble indeed the immunological profile of patients with sepsis (Figures 3.2.8 and 3.2.9) (Adrie 2002 and 2004).



Bro-Jeppesen showed how levels of IL-6 and IL-10 at baseline were significantly higher in non-survivors compared with survivors (Figures 3.2.10 and 3.2.11), whereas baseline levels of IL-1 β , IL-2, IL-4, IL-5, IL-9, IL-12, IL-13, TNF- α , interferon- γ , C reactive protein, and procalcitonin were similar in survivors and non-survivors at 30 days (Bro-Jeppesen 2015).

Activation of blood coagulation without inadequate activation of endogenous fibrinolysis is an important pathophysiological mechanism that may contribute to microcirculatory reperfusion disorders (Adrie 2005, Böttiger 1995). As shown in Dr. Adrie's work, at admission, 67 resuscitated patients showed a systemic inflammatory response with increased IL-6 and coagulation activity (thrombin-antithrombin complex), reduced anticoagulation (antithrombin, protein C, and protein S), activated fibrinolysis (plasmin-antiplasmin complex), and, in some cases, inhibited fibrinolysis (increased plasminogen activator inhibitor-1 with a peak on day 1). These abnormalities were more severe in patients who died within two days and were most severe in patients dying from early refractory shock. Protein C and S levels were low compared to healthy volunteers (Table 3.2.3 and figure 3.2.12) and discriminated CA survivors from non-survivors. Furthermore, a subgroup of patients had a transient increase in plasma-activated protein C at admission followed by undetectable levels. This, along with an increase in soluble thrombomodulin over time, suggested a secondary endothelial injury and dysfunction of the protein C anticoagulant pathway similar to that observed in severe sepsis. Intravascular fibrin formation and microthromboses are distributed throughout the entire microcirculation.

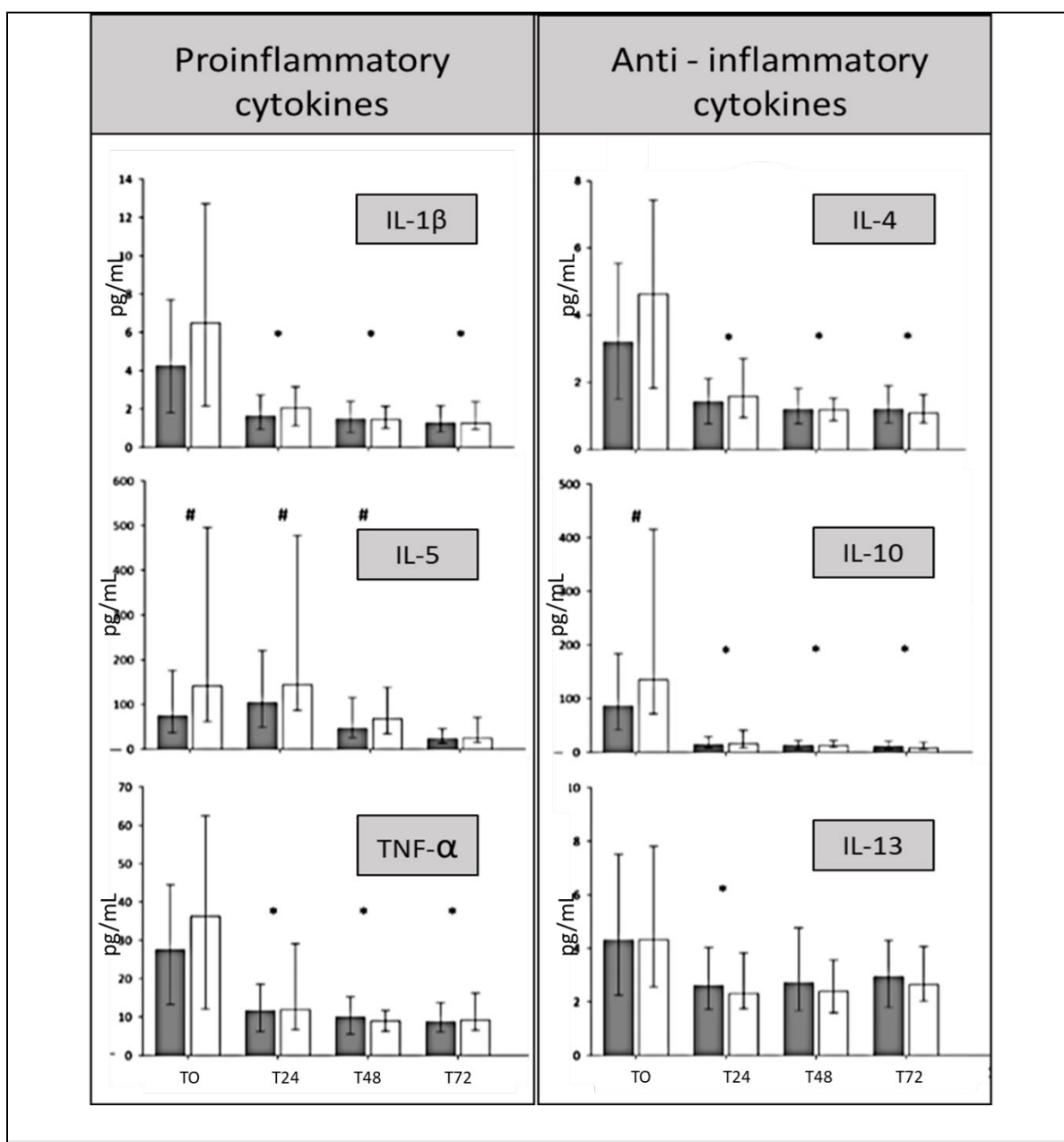
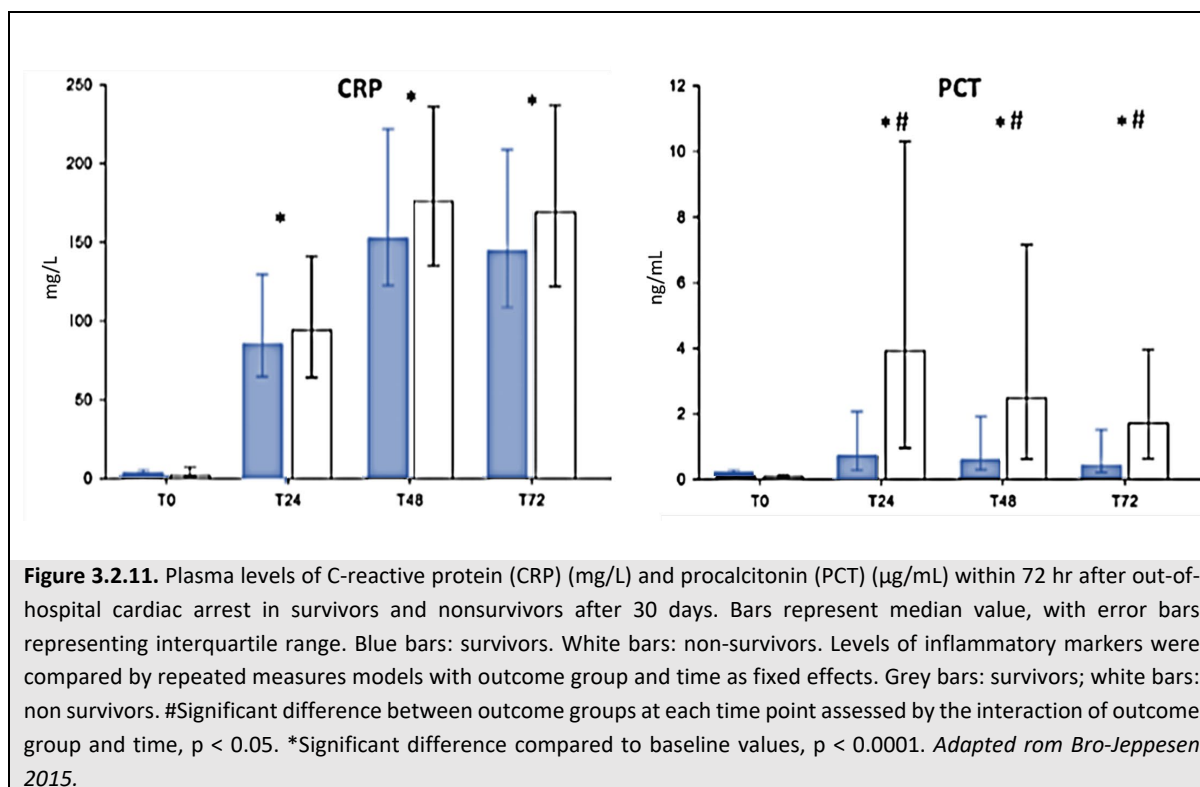


Figure 3.2.10. Plasma levels (pg/mL) within 72 hr after out-of-hospital cardiac arrest of selected proinflammatory cytokines—interleukin (IL)-1 β , IL-6, and tumor necrosis factor (TNF)- α and anti-inflammatory cytokines—IL-4, IL-10, IL-13 (B) in survivors and nonsurvivors after 30 days. Bars represent median value, with error bars representing interquartile range. Levels of inflammatory markers were compared by repeated measures models with outcome group and time as fixed effects. #Significant difference between outcome group at each time point was assessed by the interaction of outcome group and time, $p < 0.05$. *Significant difference compared to baseline values, $p < 0.0001$. Adapted from Bro-Jeppesen 2015.

Gando et al. was among the first studying coagulation during and after CPR, finding massive fibrin generation especially in the first 24 hr in 63 OHCA patients (Gando 1997). Similarly, increased levels of thrombin-antithrombin complexes were observed by Hostler et al. in patients affected by OHCA (Hostler 2007). Increased activation of blood coagulation without inadequate activation of endogenous fibrinolysis represents one of the main pathophysiological mechanisms involved in PCAS. Indeed, this

leads to disseminated intravascular coagulation (DIC), which clinically manifests as obstruction of microcirculation and multiple organ dysfunction. In particular, thrombotic occlusion in the brain vessels due to DIC causes the “no-reflow phenomenon” responsible of the microcirculatory failure occurring after CA and CPR. Altered coagulation in patients with PCAS is characterized by tissue factor-dependent coagulation, which is accelerated by impaired anticoagulant mechanisms, including antithrombin, protein C, thrombomodulin, and tissue factor pathway inhibitor (Wada 2017).



Gando et al. was among the first studying coagulation during and after CPR, finding massive fibrin generation especially in the first 24 hr in 63 OHCA patients (Gando 1997). Similarly, increased levels of thrombin-antithrombin complexes were observed by Hostler et al. in patients affected by OHCA (Hostler 2007). Increased activation of blood coagulation without inadequate activation of endogenous fibrinolysis represents one of the main pathophysiological mechanisms involved in PCAS. Indeed, this leads to disseminated intravascular coagulation (DIC), which clinically manifests as obstruction of microcirculation and multiple organ dysfunction. In particular, thrombotic occlusion in the brain vessels due to DIC causes the “no-reflow phenomenon” responsible of the microcirculatory failure occurring after CA and CPR. Altered coagulation in patients with PCAS is characterized by tissue factor-dependent coagulation, which is accelerated by impaired anticoagulant mechanisms, including antithrombin, protein C, thrombomodulin, and tissue factor pathway inhibitor (Wada 2017).

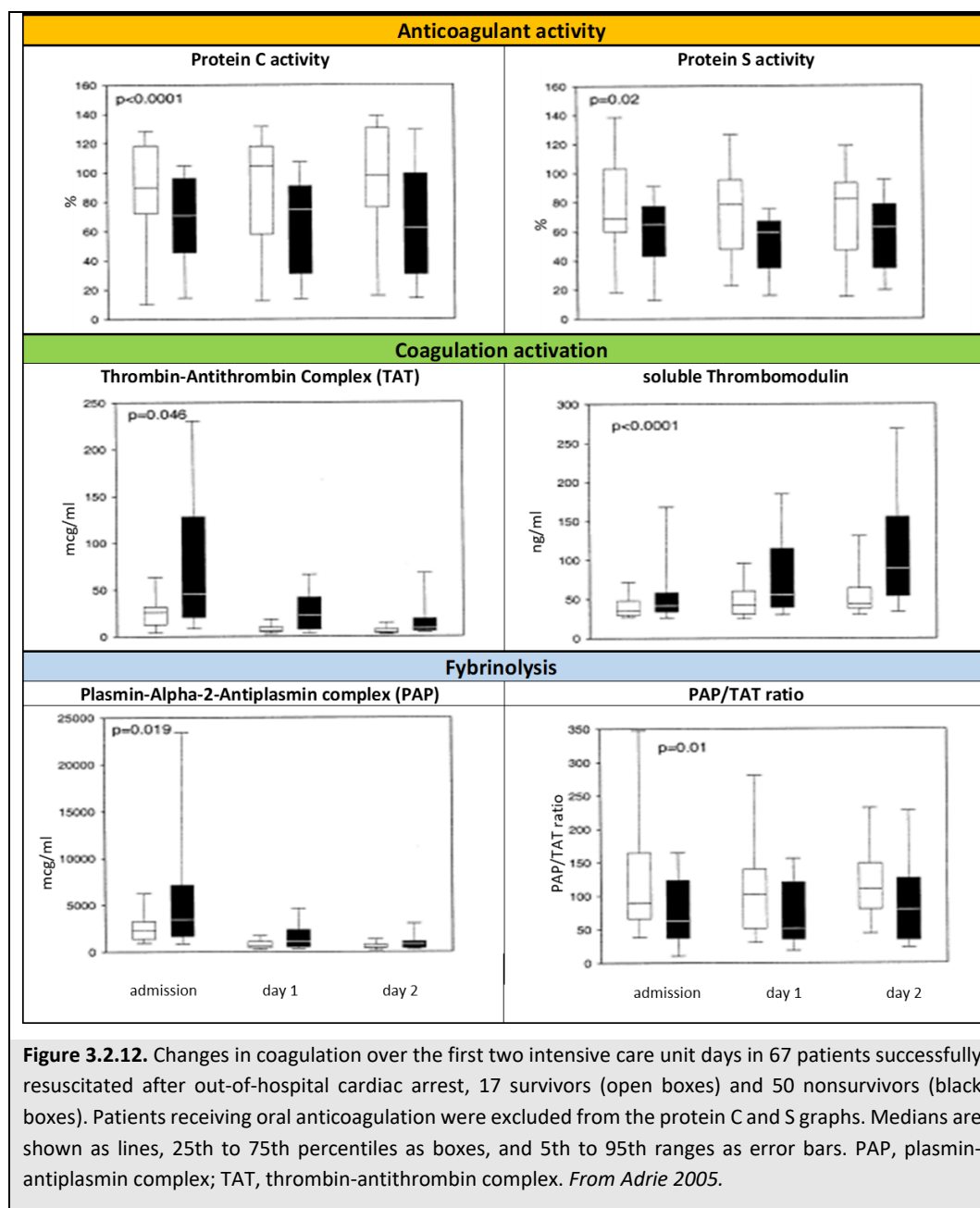
Parameters	Healthy Volunteers (n=10)	Severe sepsis (n=12)	Cardiac arrest			P value
			ICU admission (n = 67)	Day 1 (n=59)	Day 2 (n=50)	
White blood cell count (x10 ⁹ /l)	7.2 (6.7-7.8)	12 (7.3-30)	14.5 (11.3-18.7)	15.1 (10.3-21)	13.1 (9.6-17-1)	0.0001
Hematocrit	42 (42-44)	32 (30-35)	42 (39-46)	42 (37-45)	36 (35-40)	0.0001
Platelets (x10 ⁹ /l)	255 (223-304)	168 (92-213)	215 (176-280)	192 (155-262)	151 (117-190)	0.0001
sTM (ng/ml)	45 (40-53)	100 (70-123)	40 (32-56)	53 (36-89)	59 (40-119)	0.0001
AT (%)	107 (107-110)	51 (41-139)	88 (74-99)	88 (78-95)	82 (70-101)	0.003
D-dimer (mcg/ml)	0.25 (0.22-0.35)	4 (3.5-7)	9 (2.6-20)	3.7 (2-15)	2.2 (1.1 – 4)	0.0001
APTT (s)	39 (36-41)	67 (55-71)	43.8 (36-54)	54.6 (41-70)	59.8 (45-74)	0.01
TAT complex (mcg/ml)	1.8 (1.8-2.1)	9.7 (6-15)	36.2 (14.8-122)	11.9 (6.7-32.6)	7.6 (4.7-13.3)	0.0001
PAP complex (mcg/ml)	441 (289-554)	528 (450-740)	2,754 (1,654-4,576)	899 (450-1,749)	607 (415-996)	0.0001
PAI1 (AU/ml)	7.5 (5.7-10)	37 (24-86)	22.5 (7.3-43)	40.1 (22-86)	25 (15-40)	0.04

Table 3.2.3. Coagulation Parameters in Healthy Volunteers (Negative Control Group), Patients With Septic Shock (Positive Control Group), and Patients Admitted After Successfully Resuscitated Out-Of-Hospital Cardiac Arrest. Data are expressed as median (interquartile ranges). p values are for comparisons between healthy volunteers, septic patients, and cardiac arrest patients at admission. sTM, Soluble thrombomodulin; AT, Antithrombin; APTT, Activated partial thromboplastin time; TAT, Thrombin-antithrombin complex; PAP, Plasmin-antiplasmin complex; PAI-1, Plasminogen activator inhibitor-1. *Adapted from Adrie 2005.*

Wada et al published data about DIC in OHCA patients with ROSC and found that 208 out of 388 patients (54%) were in DIC status within 24 hr after CA. In their study, DIC patients experienced a worse outcome compared to non-DIC patients and DIC was found to be an independent predictor of mortality (Wada 2016). Similarly, Kim et al. analyzed patients with ROSC after OHCA and found a prevalence of DIC of 33%; moreover, the DIC Score was an independent predictor of poor outcome and early mortality risk (Kim 2013). The prognostic value of DIC score was confirmed by Ono et al who studied 315 OHCA patients with successful ROSC, and found that, except for fibrinogen level, all coagulation variables, fibrinolytic variables, and DIC score were associated with neurological outcomes (Ono 2017). Lee et al confirmed these findings, studying 317 CA patients after ROSC: DIC score was a significant predictor for poor neurologic outcome and 6-months mortality (Lee 2017).

We have described the coagulation derangements in a population with refractory CA undergoing extracorporeal-CPR showing a high prevalence of severe bleeding, with 73% of patients transfused with a high amount of blood products in the first 24 hr. (Ruggeri 2019) Further studies should be dedicated to the interaction between the massive coagulation derangements and the antiplatelet therapy that part of these patients receive, having coronary occlusion as the reason for the CA. Many authors suggest a possible implication of different coagulative profiles, in terms of profibrinolytic or antifibrinolytic profile, in the prognosis of patients with CA. Viersen et al performed rotational

thromboelastometry test at emergency department admission in 30 OHCA patients and found that a substantial part of them (53%) developed hyperfibrinolysis is in association with markers of



hypoperfusion (Viersen 2012). Schochl et al studied coagulation in 53 OHCA patients, through rotational thromboelastometry in blood samples taken out of hospital: prothrombin time index (PTI), activated partial thromboplastin clotting time (aPTT) and extrinsically activated test (EXTEM) Clotting Time (CT) revealed significant differences between ROSC and non-ROSC patients. Hyperfibrinolysis according to rotational thromboelastometry test results was very common (35,8%) (Schöchl 2013). Wada et al recently published that among DIC patients, hyperfibrinolysis was associated with a worse outcome and that lactate levels predicted hyperfibrinolysis (Wada 2016) Interestingly, hyperfibrinolysis seemed to be the

coagulative profile after unsuccessful resuscitation, in organ donors after circulatory determination of death (*Vendrell 2015*).

Finally, the stress of total body ischemia/reperfusion affects adrenal function. Relative adrenal insufficiency is common following CA and seems to be related to the severity of the ischemic insult (*Kim 2011*). Although an increased plasma cortisol level occurs in many patients after OHCA, relative adrenal insufficiency, defined as failure to respond to corticotrophin, is common (*Hekimian 2004, Schultz 1993*).

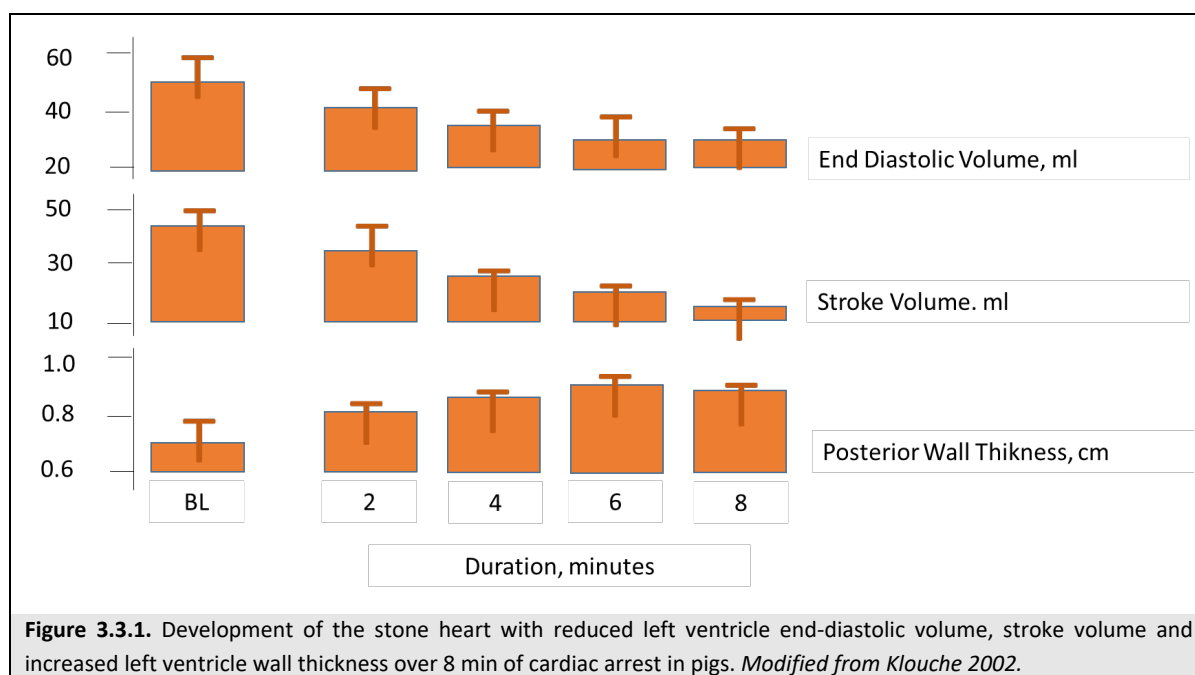
3.3 CPR AND DEFIBRILLATION

At the initial heart rhythm analysis during CPR, about 25–30% of OHCA are due to VF (*Agarwal 2009, Cobb 2002, Nolan 2010, Rea 2004, Ringh 2009, Travers 2010, Vaillancourt 2007*). It is likely that many more victims have VF or rapid ventricular tachycardia at the time of collapse but, by the time the first ECG is recorded the rhythm has deteriorated to asystole. When the rhythm is recorded soon after collapse, in particular by an on-site automated external defibrillator, the proportion of patients in VF can be as high as 65% (*Nolan 2010, Travers 2010*).

DF by electrical counter-shock represents the treatment of choice for this otherwise lethal arrhythmia. Electrical DF refers to the passage across the myocardium of an electrical current of sufficient magnitude to depolarize a critical mass of myocardium and to enable restoration of coordinated electrical activity. Indeed, successful DF is defined as the termination of fibrillation or, more precisely, the absence of VF/ventricular tachycardia within 5 sec after the shock delivery; however, the goal of attempted DF is to restore spontaneous circulation (*Deakin 2005 and 2010, Link 2010*). ROSC occurs rarely after initial DFs such that up to 75% of shock attempts fail to restore an organized rhythm (*Ristagno 2013, Ristagno 2015*). The probability of successful DF diminishes rapidly over time. For every min that passes between collapse and DF, survival rates from witnessed VF CA decrease by 7% to 10% if no CPR is provided.

VF is, in fact, characterized by three time-sensitive electrophysiological phases, including 1) the electrical phase of 0-4 min, 2) the circulatory phase of 4-10 min and 3) the metabolic phase of > 10 min. During the electrical phase, immediate DF is likely to be successful. As ischemia progresses, the success of attempted DF diminishes without CPR. This phase is characterized by transition to slow VF wavelets during accumulation of ischemic metabolites in the myocardium. Slow VF is often resistant to DF because there is no longer an excitable gap to interrupt the re-entry that sustains VF. The failure of DF to succeed in slow VF can be attributed to re-entry and recurrence of VF. In the metabolic phase, there is much less likelihood to achieve successful ROSC (*Weisfeldt 2002*).

During CA, coronary blood flow ceases, accounting for a progressive and severe energy imbalance. Intra-myocardial hypercarbic acidosis is associated with depletion of high energy phosphates and



correspondingly severe global myocardial ischemia (Johnson 1995, Kern 1990). The ischemic LV becomes contracted ushering in the “stone heart” characterized by reduced LV end-diastolic volume, stroke volume and increased LV wall thickness (Klouche 2000 and 2002). After the onset of contracture, the probability of successful DF becomes remote (Figure 3.3.1).

Early CPR, with partial restoration of CPP and myocardial blood flow, delays onset of ischemic myocardial injury and facilitates DF (Deshmukh 1989). When bystander CPR is provided, the decrease in survival rates is more gradual and averages 3% to 4% per min from collapse to DF attempt (Deakin 2005, Larsen 1993, Link 2010, Valenzuela 1997, Waalewijn 2001).

Accordingly, major factors contributing to the poor outcome after CA include delays in CPR, ineffective and frequently interrupted CCs, and limited access to, or delayed DF (Iwami 2012, Valenzuela 2000, Wik 2005). Thus, high-quality CCs with minimal pre and peri-shock pauses are strongly recommended to ameliorate myocardial metabolic status, increase the probability of DF success and improve post-CA myocardial function and survival (Cheskes 2014, Eftestøl 2002).

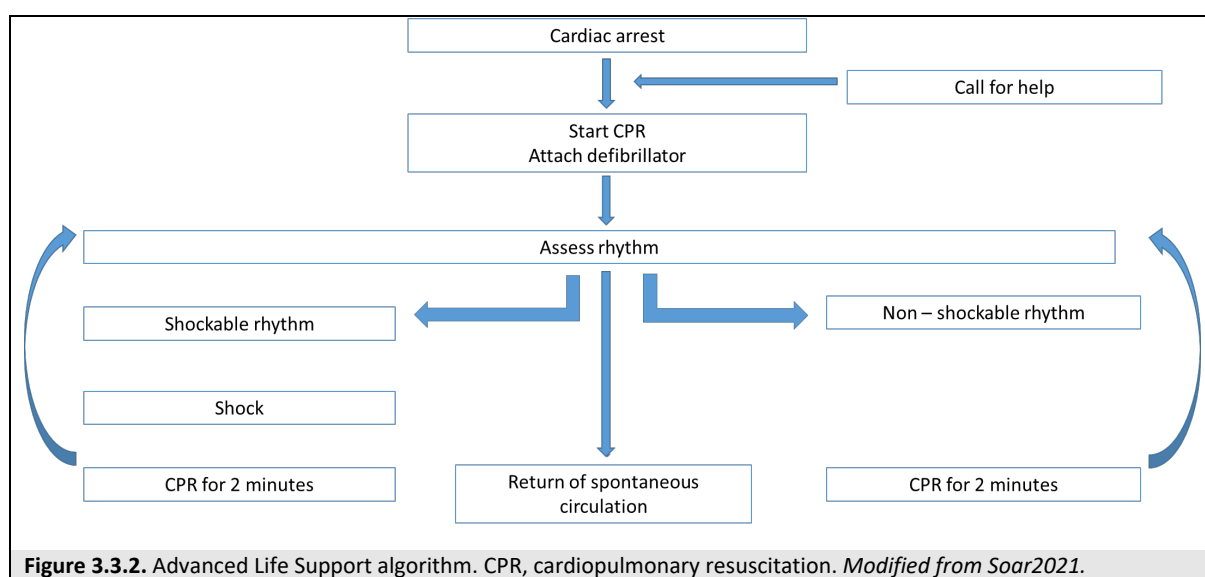
Community programs of lay bystander CPR and automated external defibrillator use improve outcome from OHCA (Soar 2021). The rate of bystander CPR varies between and within countries (average 58%, range 13%-83%) and the use of automated external defibrillators remains low in Europe (average 28%, range 3.8%-59%). 80% of European countries provide dispatch assisted CPR (Soar 2021).

The effectiveness of CCs in relation to the timing of DF has been a subject of major interest because it is difficult to determine the priority of CPR interventions (i.e. DF first or CC first). The 2005 guidelines recommended an initial interval of CC prior to DF, especially when the duration of untreated CA exceeded 4 min (*Wik 2005, AHA guidelines 2005*). In fact, previous randomised clinical trials had demonstrated the potential of a CPR-first strategy to improve CA survival, mainly when the response time was longer than 4–5 min (*Coob 1999, Wik 2003*).

Nevertheless, the subsequent guidelines highlighted the insufficient evidence to support or refute CPR before DF and called again for early DF as soon a defibrillator was available (*Baker 2008, Deakin 2010, Jacobs 2005, Link 2010, Huang 2014*). Subsequent DF has been recommended to be attempted on a time based protocol, i.e. after every 2 min cycle of CC (*Deakin 2010, Link 2010*).

The current algorithm suggested by Guidelines, however, may lead to futile DF attempts and unnecessary CC interruptions, potentially creating worse outcome (Figure 3.3.2) (*Cheskes 2011, Snyder 2004, Steen 2003, Xie 1997, Yu 2002*). The timing of DF is even more difficult to be chosen in the instance of recurrence of VF (*Shanmugasundaram 2012*). In addition, the severity of post resuscitation myocardial dysfunction and survival has been recognized to be related, in part, to the magnitude of the total electrical energy delivered with DF (*Osswald 1994, Tang 2004 and 2006, Xie 1997*). Indeed, increasing the DF energy produced significant reductions in survival rate, cardiac index, and LV function. Better survival and post resuscitation myocardial function have been observed when lower DF energies were used (*Tang 1999 and 2004, Xie 1997*).

However, the onset time of VF is rarely known, especially in the out-of-hospital setting, making it difficult to determine the priority of CPR intervention based on the duration of the untreated CA. There is also insufficient knowledge about the optimal duration of the CC interval prior to DF. The decision whether to interrupt CC to deliver a DF is therefore difficult. ECG analysis of the VF waveform might represent the best noninvasive decision guide (*Callaway 2005*).



3.3.1 Monitoring effectiveness of CC and predicting DF success

The evidence is secure that the quality of CC is a major determinant of successful resuscitation (Abella 2005, Gallagher 1995, Idris 2012, Vaillancourt 2011, Van Hoeyweghen 1993, Wik 1994 and 2005). Existing and established predictors of good quality CPR and thereby successful resuscitation include CPP (Deshmukh 1989, Paradis 1990, Sanders 1985 and 1985b, Yu 2002), and end-tidal carbon dioxide (etCO₂) (Falk 1988, Lah 2011, Heradstveit 2012, Kolar 2008, Weil 1985).

Blood flows generated by CC are dependent on the pressure gradient between the aortic and the venous pressures (Andreka 2006). CPP, defined as the difference between simultaneously measured minimal aortic pressure and right atrial pressure during compression diastole (Kette 1991, Gazmuri 1996, Tang 1993 and 1999), is highly correlated with coronary blood flow during cardiac resuscitation and is currently recognized as the best single indicator of the likelihood of successful DF and ROSC (Niemann 1985, Paradis 1990, Povoas 2000). Based on both experimental and clinical observations, ROSC can be predicted when CPP is maintained above 15 mmHg during CC (Kern 1988, Niemann 1985, Paradis 1990).

Resuscitative strategies that increase CPP, including high quality CC (Ristagno 2007, Wik 1996) as well as the use of vasopressors (Lewis 1969, Mentzelopoulos 2013, Olasveengen 2012), have been therefore supported and considered more effective in restoring spontaneous circulation. Although the importance of blood pressure during CPR is clear, invasive measurements, including aortic and right atrial pressure are only available or feasible at the time of resuscitation in a small minority of patients, especially in the pre-hospital settings.

EtCO₂ is the partial pressure of carbon dioxide (pCO₂) measured at the end of expiration. It reflects CO, tissue perfusion and pulmonary blood flow, as well as the ventilation minute volume. Carbon dioxide

is produced in perfused tissues by aerobic metabolism, transported by the venous system to the right side of the heart and pumped to the lungs by the right ventricle, where it is removed by alveolar ventilation. Under condition of CA and CPR, the CO is usually less than one-third of normal and pulmonary flow and etCO_2 are consequently dramatically reduced. EtCO_2 is therefore an indirect measurement of pulmonary blood flow and CO produced by CCs (Falk 1988, Weil 1985). EtCO_2 is highly correlated with CPP during CPR, and may thereby serve as a non-invasive surrogate of CPP (Gudipati 1988, von Planta 1989).

During CPR, waveform capnography enables a continuous, non-invasive measurement of pCO_2 in the exhaled air. In the typical capnogram, the etCO_2 recorded at the end of the plateau phase best reflects the alveolar pCO_2 . EtCO_2 is most reliable when the patient's trachea is intubated, but it can also be used with a supraglottic airways or bag mask.

EtCO_2 has emerged as a valuable tool for monitoring the effectiveness of CCs during CPR (Falk 1988, Garnett 1987, Neumar 2010, Ristagno 2007, Weil 1985), nevertheless whether this can be used to guide care and improve outcome in clinical practice requires further study. (Sheak 2015, Soar 2021)

Failure to achieve an etCO_2 value >10 mmHg during CPR is associated with a poor outcome in observational studies (Levine 1997, Paiva 2018, Sutton 2016). When etCO_2 exceeds the threshold level of approximately 10 to 15 mmHg during CPR, greater likelihood of successful ROSC has been reported (Cantineau 1996, Grmec 2001, Neumar 2010). However, values of etCO_2 during CPR depend on several factors including the timing of measurement (initial vs. final, (Kolar 2008, Poppe 2019) cause of CA, (Grmec 2003, Heradstveit 2012) CC quality (Hamrick 2014) ventilation rate and volume (Gazmuri 2012b) presence of airway closure during CPR (Grieco 2019) and the use of adrenaline, which causes significant decrease in etCO_2 by increasing pulmonary shunting (Callaham 1992, Hardig 2016, Tang 1991).

In general, etCO_2 tends to decrease during CPR in patients in whom resuscitation is unsuccessful and tends to increase in those who go on to achieve ROSC (Kolar 2008, Poppe 2019). For this reason, etCO_2 trends might be more appropriate than point values for predicting ROSC during CPR (Paiva 2018). However, evidence on this is still limited (Brinkrolf 2018). Studies assessing the prognostic value of etCO_2 have not been blinded, which may have caused a self-fulfilling prophecy. For this reason, although an $\text{etCO}_2 > 10$ mmHg measured after tracheal intubation or after 20 min of CPR may be a predictor of ROSC or survival to discharge, using etCO_2 threshold values alone as a mortality predictor or for the decision to stop a resuscitation attempt is not recommended by current Guidelines (Soar 2021).

In addition, etCO_2 may also provide the earliest clinical evidence of ROSC (Falk 1988, Neumar 2010). When ROSC occurs, etCO_2 may increase up to three times above the values during CPR (Garnett 1987). Capnography may therefore help detect ROSC during resuscitation and avoid unnecessary CC or

adrenaline in a patient with ROSC. However, no specific threshold for the increase in etCO₂ has been identified for reliable diagnosis of ROSC. The increase in etCO₂ can start several minutes before a palpable pulse is detected (*Lui 2016, Pokorna 2010, Sandroni 2016*).

3.4 ROLE OF EPINEPHRINE

Initial pharmacological interventions during CPR are directed to raise CPP by increasing peripheral vascular resistance, with the intent to improve the chances for ROSC (*Angelos 2008, Panchal 2020, Paradis 1990*).

Thus, epinephrine has been the recommended adrenergic agent during CPR for more than 50 years, although its efficacy in improving CA outcome has not been unanimously demonstrated (*Gräsner 2020, Jacobs 2011, Olasveengen 2012, Panchal 2020, Perkins 2018*). A recent large randomized controlled trial confirmed the benefits of epinephrine on ROSC and survival to hospital discharge, while no effects on survival with favorable neurological outcome were reported (*Perkins 2018*).

The primary vasopressor efficacy of epinephrine is due to its α -adrenergic effects on vascular smooth muscle, which cause peripheral vasoconstriction during CPR. However, epinephrine also has potent β 1-adrenergic agonist actions, which increase myocardial oxygen utilization, failing to improve the balance between oxygen supply and demand (*Tang 1995, Ditchey 1988, Livesay 1978*). This detrimental effect may worsen post-CA myocardial dysfunction and increase the sensitivity of the myocardium to arrhythmias, leading to refractory VF (*Tang 1995; Jingjun 2009*).

3.4.1 Potential role of β 1-adrenergic blockade during CPR

A recent metanalysis anticipated potential beneficial effects of esmolol, an ultrashort-acting β 1-blocker, on short and long-term outcome in CA patients with refractory VF (*Gottlieb 2020*).

In animal studies on CA, β 1-adrenergic blockade with esmolol administered with epinephrine during CPR has been shown to reduce myocardial dysfunction and to increase the rate of ROSC with fewer DFs and survival, when compared to epinephrine alone (*Cammarata 2004, Killingsworth 2004, Theochari 2008, Zhang 2013*). Nevertheless, all these investigations were conducted in models of electrically induced VF in normally perfused hearts until CA. Recently, administration of esmolol, during veno-arterial extracorporeal membrane oxygenation resuscitation failed to demonstrate a clear cardio-protective effect or improvement in outcome in an ischemically-induced CA (*Karlsen 2019*).

Thus, the beneficial effects of esmolol administration during CPR in preventing the adverse β 1-adrenergic effects of the epinephrine should also be confirmed in the case of a CA due to ischemic origin, i.e. due to acute MI (AMI).

3.5 VENTRICULAR FIBRILLATION WAVEFORM ANALYSIS TO PREDICT OUTCOME

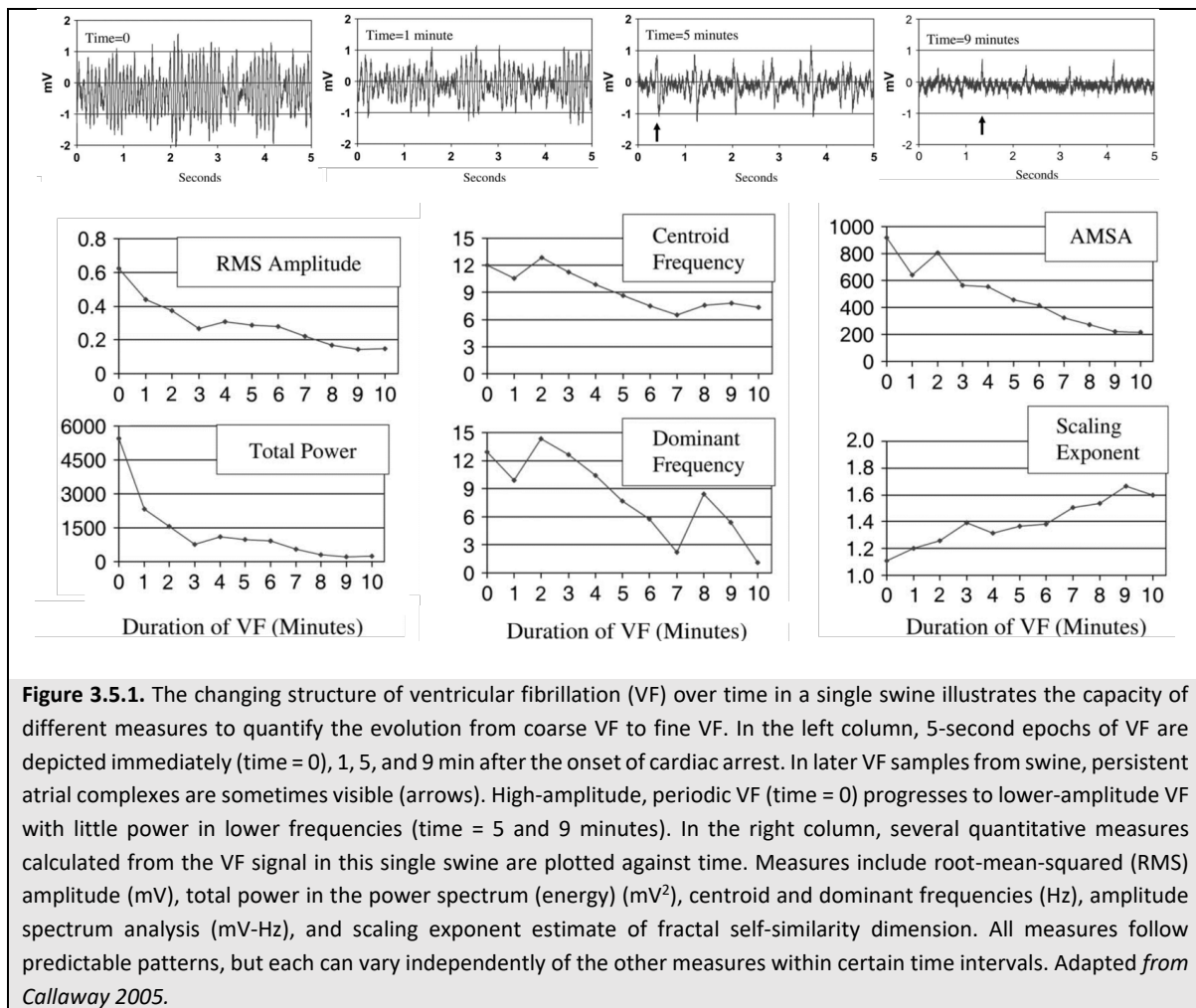
Current rhythm analysis and shock timing is standardized to 2-min intervals. This timing may not be optimal across all patients to maximize benefit from shock, given individual differences in CA etiology and physiology. Such heterogeneity suggests opportunity to improve outcome if shock administration could be tailored and timed to individual physiologic measures. The optimal timing of DF could be determined by evaluating the probability of shock outcome. If the shock attempt has a high likelihood of DF success, an electrical shock should be prompted and delivered. Otherwise, unnecessary shocks should be avoided and alternate therapy such as CPR, especially high-quality CC, eventually with medications, should be utilized. Ideally, the optimal DF strategy should identify the priority of CPR treatment (CCs or DF) for each patient; minimize CCs interruptions; speed up the delivery of early effective DF; and reduce the number of ineffective shocks. These goals may be achieved through new available algorithm for ECG and VF waveform analysis during CPR.

Although the decreasing organization of VF over time was described both electrocardiographically and visually decades ago (*Wiggers 1953*), recent studies have examined quantitative electrocardiographic analysis during CA (Figure 3.5.1) (*Callaway 2005*). All of these studies seek to provide quantitative confirmation of the common clinical experience that the amplitude and structure of the VF waveform decreases with increasing ischemia duration, and this decrease in VF structure is associated with decreased likelihood of successful DF or resuscitation (*Callaway 2005*).

3.5.1 Analyses of ECG features during VF and CPR

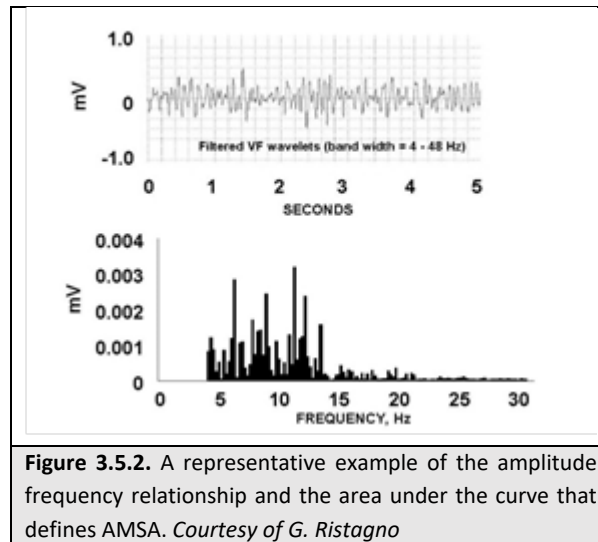
The search for a reliable indicator of successful DF obtained from the analyses of ECG features has begun more than 30 years ago. The initial approaches to ECG analysis included measurements of VF amplitude and frequency (*Brown 1991*). To improve sensitivity and specificity of the ECG predictors for ROSC, more sophisticated methods of VF waveform analyses were introduced and investigated.

Earlier investigations using ECG focused on “amplitude or voltage” of VF wavelets as a predictor of the likelihood of successful DF. VF voltage, or signal amplitude, is defined as the maximum peak-to-trough VF amplitude in a given time window of the ECG signal (*Noc 1999*). Mean VF voltage is the average of VF voltage over the same time interval. It was observed that VF amplitude declines over time and greater amplitudes were associated with correspondingly greater success of DF (*Callahan 1993, Dalzell 1991*,



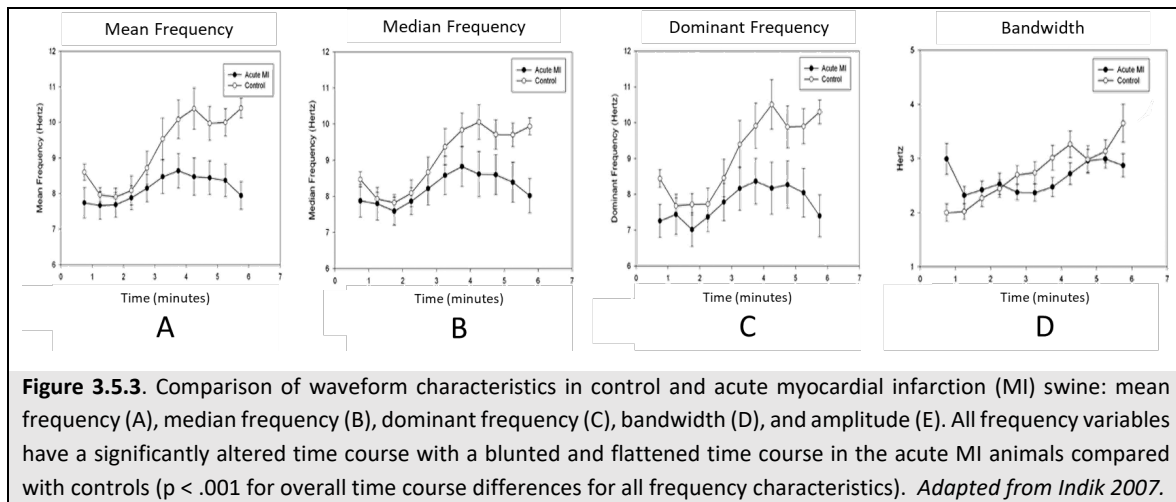
Noc 1994, Strohmenger 1996, Stults 1987, Weaver 1985). Several studies have shown that this ECG feature reflects vital organ blood flow and specifically myocardial blood flow and energy metabolism (Brown 1989, Dalzell 1991, Noc 1999, Strohmenger 1997, Weaver 1985). Weaver et al. (Weaver 1985) observed that patients in which the VF amplitude was greater than 0.2 mV had a significantly greater likelihood of resuscitation. The observation that DF success rate is higher during the initial period of CA, where “coarse VF” with an amplitude greater than 0.2 mV is present, while success of DF is greatly reduced at the stage of “fine VF”, has finally evolved to extensive quantitative analysis of ECG waveform. VF voltage appeared not only as a predictor of ROSC but it also affirmed its utility as indicator of VF duration from collapse.

Subsequently, it was realized that other parameters could be computed utilizing fast Fourier Transform analyses in a selected ECG interval, including VF median frequency, peak power frequency, edge frequency, and spectral flatness measure. The starting point for all these calculations was the “power spectrum”, defined as the square of Fourier amplitudes (Figure 3.5.2).



Brown et al. (Brown 1991) developed a technique that analyzed VF voltage and VF frequency such to obtain the so called VF “median frequency” (Brown 1991, Strohmenger 1994). The median frequency represents the frequency at which half of the power of the spectrum is above and half below. In a porcine model of VF and CPR, a median frequency of more than 9.14 Hz had 100% sensitivity and 92% specificity in predicting the success of a DF attempt. Frequency analysis of VF wavelets and, specifically, median frequency was also correlated with CPP in animal models as well as human victims and therefore it became the preferred ECG feature to be used as predictor of outcome (Brown 1989 and 1991 and 1996, Carlisle 1990, Martin 1991, Monsieurs 1998, Stewart 1992, Strohmenger 1996 and 1997). In addition, this parameter appeared as a more accurate indicator for estimating the duration of untreated VF, compared to the earlier VF amplitude (Brown 1989 and 1993, Dzwonczyk 1990, Martin 1991).

Recently, in the pursuit of a more optimal ECG feature prognosticator, several studies focused on the changes and differences of VF waveform features in relationship to the pathophysiology of CA. Specifically, investigators focused on the differences between VF as resultant of an ischemic heart disease, which represents the main cause of sudden death, and VF electrically induced, which represents the main experimental model employed in laboratories (Niemann 2007, Wang 2007b). The balloon occlusion of one branch of coronary artery represents a valid method to reproduce, in the experimental settings, the common cause of human CA. The distribution of the coronary artery blood supply in the swine is, in fact, very similar to that of humans. Minimal pre-existing collateral vessels are present and therefore a total occlusion of one of the branches of the coronary arteries tree can produce massive MI with a consequent mortality rate which could reach 30% (Babini 2018, Hughes 2003,

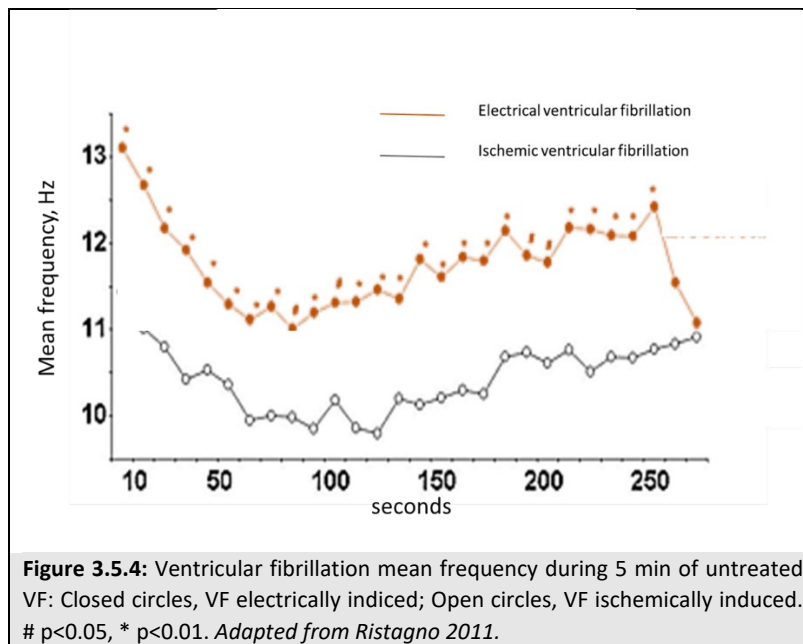


Swindle 1986, Maxwell 1987, Ristagno 2007). On the whole, animal studies showed lower frequency characteristics underlying AMI is present, even lower than animals with a previous MI (Indik 2006 and 2008, Jacobson 2000)

Indik et al. (Indik 2007) induced VF in swine in which AMI followed ligation of the left anterior descending coronary artery (LAD). The study revealed that VF features, such as median, mean, or dominant frequency and bandwidth were significantly reduced compared with those derived from a VF electrically induced (Figure 3.5.3).

In a porcine model of ischemic induced CA, by acute occlusion of the LAD, Ristagno et al. (Ristagno 2007b and 2011) have confirmed lower mean VF frequency in comparison to the electrical induced VF (Figure 3.5.4).

Although VF features might be different in relationship to the cause of CA, in the ischemic model of VF ECG features continuously changed during resuscitative maneuvers. In particular, VF amplitude and Mean Frequency increased during CC and such increases correlated with successful DF (Ristagno 2008b and 2008c and 2011). These observations provided evidence that ECG predictors of outcome were, at least in part, related to the mechanism by which VF evolved.



3.5.2 Overview of principal waveform analyses

VF measures can be divided into three general categories: measures of the waveform amplitude (Weaver 1985), frequency-based measures (e.g., with Fourier or wavelet transforms (Watson 2004), and measures of the degree to which the waveform differs from random noise (nonlinear or chaos analyses) (Callaway 2001). Combinations of these analyses have been employed in a few other studies (Callaway 2005, Eftestøl 2000) (Table 3.5.1).

Predictors obtained from **time domain** describe the characteristics of waveform amplitudes, phases or voltages (Callaway 2005, Endoh 2011, Joar 2007, Neurauter 2007, Weaver 1985). Unluckily, time domain methods are affected by other factors: interference, body size/composition, skin resistance, size and position of electrodes, lead ways, and recording conditions.

The **frequency domain** features describe the frequency component characteristics of VF waveform (Brown 1996, Eftestøl 2000 and 2001, Endoh 2011, Goto 2003, Gundersen 2008, Hamprecht 2001, Indik 2008, Martin 1991, Neurauter 2007, Stewart 1992, Strohmenger 1997, Watson 2005). Techniques to quantify the component frequencies of the VF signal have employed Fourier and wavelet analyses as well as novel numerical techniques.

Fourier Transform consists of splitting a short segment of the VF waveform into small subunits and then expressing each of these as the sum of multiple simpler waves of a given amplitude and frequency, obtaining the so called “power spectrum”.

Time domain	
Peak-to-peak amplitude (PPA)	Difference between the maximum and minimum recorded VF voltage within a given window
Mean amplitude	Average amplitude of the waveform
Median slope and mean slope (mns)	Average steepness of the waveform. They reflect both the amplitude and frequency information of VF
Root mean squared (RMS)	Square root of the mean of the squares of all the amplitudes
Signal integral	Sum of the absolute amplitude in a certain time interval
Frequency domain	
Peak power frequency (PF) or dominant frequency (DF)	Highest peak in the resulting power spectral density (PSD)
Energy	Sum of the single power values of the PSD
Maximum power	Maximum value of PSD
Power spectrum area (PSA)	Sum of contributing frequencies weighted by the absolute values of the PSD of the VF signal
Centroid power	Power coordinate of the center of the spectral mass
Centroid frequency (CF)	Frequency coordinate of the center of the spectral mass
Median frequency (MDF)	Mean of all of the contributing frequencies weighted by the power at each frequency
Amplitude spectrum area(AMSA)	Describes the amplitude-weighted mean frequency
Time-frequency domain	
Wavelet-based peak power frequency	Highest peak in the resulting wavelet transform
Wavelet-based energy	Sum of the single power values of the wavelet transform
Cardioversion outcome prediction (COP)	Wavelet-entropy marker. Metric of the temporal behavior of the signal.
Wavelet synchrosqueezed transform	Provides a detailed time-frequency representation from which instantaneous frequency trends can be extracted accurately
Nonlinear measures of randomness	
Scaling exponent	Estimate of the fractal self-similarity dimension
Hurst exponent	A measure of long term memory of time series
Irregularity	Direct indicator of chaotic behaviour
The logarithm of the absolute correlations (LAC)	Quantifies how individual parts of a signal are self-similar at different points along its length.
Detrended fluctuation analysis (DFA)	Statistical self-affinity of VF waveform

Table 3.5.1. Principal waveform analysis. VF, ventricular fibrillation.

In FTT, the original signal is analyzed in epochs (e.g., 5 or 10 seconds at a time) and combined with a sinusoidal function. Different techniques differ only in the selection of the test function: the power spectrum is the square of the FTT of the signal, while in wavelet transform, the original function is convolved with a periodic function that is itself time-window gated, providing concomitant spectral and temporal information (**Time-frequency domain**) (Box 2008, Martin 1991, Watson 2004 and 2005). Frequency domain features are robust and less affected by external factors than the time-domain features.

Although VF appears to be comprised of random electrical activity, several investigators have examined whether VF is a chaotic process. A chaotic signal is one that is not periodic (repeating like a sine wave) but that still has underlying structure. In contrast, a random signal would have no

underlying structure aside from its amplitude and power spectrum (e.g., white noise). Because the electrocardiographic signal is related to complex, but not random, physiologic processes occurring in the fibrillating heart, it seems self-evident that there should be some chaotic features of the VF signal. Early debates about whether this chaotic nature can be measured have largely settled in favor of some chaotic features for VF. Many statistics exist for quantifying the degree of organization in a chaotic signal, including at least fractal self-similarity dimension, D , which is directly related to the Hurst exponent, H , by $D = 2 - H$ (Callaway 2001, Jagric 2007, Jalife 1996, Lin 2010, Panfilov 1998, Podbregar 2003, Rodriguez 2009, Sherman 2008). The non-linear dynamic methods, however, are sensitive to the noise and interference.

Numerous studies have been performed retrospectively in a clinical setting, on different predictors of DF success (Table 3.5.2). Freese et al. performed a multicenter, double-blind, randomized study, enrolling OHCA patients in 2 urban EMS systems treated with automated external defibrillators using either a VF waveform analysis algorithm or the standard shock-first protocol. In the waveform analysis algorithm, a 4.5 s segment of ECG free of artefact was selected from the presenting VF rhythm and analyzed with a proprietary software program identical to that implemented in the commercial FR2 automated external defibrillator as SMART CPRTM (Philips Medical Systems). The program calculates the ECG “line-length”, yielding a measure that reflects the amplitude, rate and complexity of the ECG. This VF score showed a sensitivity >80% and a specificity >60% with respect to the probability of achieving ROSC in a previous small retrospective study (Snyder 2007). The VF waveform analysis used a predefined threshold value below which ROSC was unlikely with immediate DF, allowing selective treatment with a 2-minute interval of CPR before initial DF. Unluckily, no immediate or long-term survival benefit was noted for either treatment algorithm (Freese 2013).

The use of combined measures is emerging as a promising research field (Bender 2021, Coult 2018 and 2019, He 2015, Shandilya 2016). For instance, in a retrospective study on VF segments from 692 patients, logistic models combining waveform analysis measures, AMSA and Median Slope, with prior return of organized rhythm improved prediction of shock success during CPR (Coult 2018). The use of support vector machine applied to VF segments during CCs seems another useful tool to improve the prediction of survival (Coult 2019). A novel technique combining wavelet synchrosqueezed transform and decision-tree classifier (machine learning) was associated with high accuracy in classifying different types of VF waveform (e.g., primary vs. asphyxia-associated) showing a potential application in guiding the resuscitative intervention (Bender 2021).

Study	VF feature	Patients (no.)	Sensitivity	Specificity	Outcome
Time domain					
Weaver 1985	PPA	394	97	23	Survival
Dalzell 1991	Amplitude	70	NA	NA	ROOR
Stewart 1992	PPA	41	54	98	ROSC
Callaham 1993	PPA	265	54	98	Survival
Brown 1996	Average Peak	55	100	47	ROSC
Strohmenger 1997	Amplitude	154	NA	NA	ROOR
Monsieurs 1998	Max-min	100	70	70	Survival
Strohmenger 2001	Amplitude	89	92	42	ROSC
Callaway 2001	RMS	75	NA	NA	Survival
Hamprecht 2001	Power	54	59	52	ROSC
Podbregar 2003	MAX-MIN ENERGY	47	100	97	ROOR
Neurauter 2007	MdS	197	95	53	ROSC
Neurauter 2008	MdS	192	95	50	ROSC
Shanmugasundarama 2012	Slope	44	83	70	ROSC
Coult 2018	MdS	208	NA	NA	ROOR
Ristagno 2015	Signal Integral	2447	AUC 0.842 (0.824–0.859)		ROOR
		860	AUC 0.736 (0.702–0.771)		Survival
Frequency domain					
Stewart 1992	Dominant	56	NA	NA	ROSC
Martin 1991	Centroid	7	NA	NA	ROSC
Brown 1996	Centroid; Dominant	55	100	47	ROSC
Strohmenger 1997	MdF; Dominant; Edge Frequency	154	NA	NA	ROOR
Monsieurs 1998	Crossing	100	70	70	Survival
Eftestol 2000	Centroid; dominant spectral flatness	156	92	42	ROSC
Strohmenger 2001	Centroid; Dominant	89	92	42	ROSC
Hamprecht 2001	Dominant; energy	54	59	52	ROSC
Goto 2003	Centroid	47	77	90	Survival
Watson 2004	Entropy	NA	91	60	ROSC
Watson 2005-2006	COP	110	97	63	ROSC
Box 2008	COP	54	100	60	ROSC
Endoh 2011	CF	152	77	63	ROSC
Ristagno 2015	Peak frequency	2447	AUC 0.695 (0.672–0.719)		ROOR
		860	AUC 0.637 (0.598–0.675))		Survival
	MdF	2447	AUC 0.625 (0.600–0.650)		ROOR
		860	AUC 0.596 (0.558–0.637)		Survival
	Mean Frequency	2447	AUC 0.523 (0.497–0.550)		ROOR
		860	AUC 0.511 (0.470–0.551)		Survival
Callaway 2001	ScE	75	NA	NA	Survival
Podbregar 2003	Hurst exponent	47	100	97	ROOR
Lin 2010	DFA (DFA α 2)	155	61	63	ROSC
Combination Measures					
Eftestøl 2001	Combination of CF and Energy	156	91	36	ROSC
Podbregar 2003	Maximal amplitude and Hurst exponent	47	100	97	ROOR
Jekova 2004	Multiple paramenters	84	62	80	ROSC
Coult 2018	AMSA + prior ROOR	692	AUC with CPR 0.73 [0.70-0.76] AUC wth CPR 0.76 [0.72-0.79]		ROOR
	MdS + prior ROOR		AUCwith CPR 0.74 [0.71-0.77] AUC wth CPR 0.76 [0.72-0.79]		ROOR
Shandilya 2016	Multiple Domain Integrative	153	AUC 78.8%		ROOR
Table 3.5.2. Principal clinical studies of waveform analysis of ventricular fibrillation (AMSA not included). VF, ventricular fibrillation; PPA, peak-to-peak amplitude; RMS, root mean square; MdS, median slope; MdF, median frequency; COP, cardioversion outcome prediction; CF, centroid frequency; ScE, scaling exponent; DFA, detrended fluctuation analysis; AMSA, amplitude spectrum aream ROOR, return of organized rhythm, ROSC, return of spontaneous circulation.					

3.5.3 Evolution of Amplitude spectrum area (AMSA)

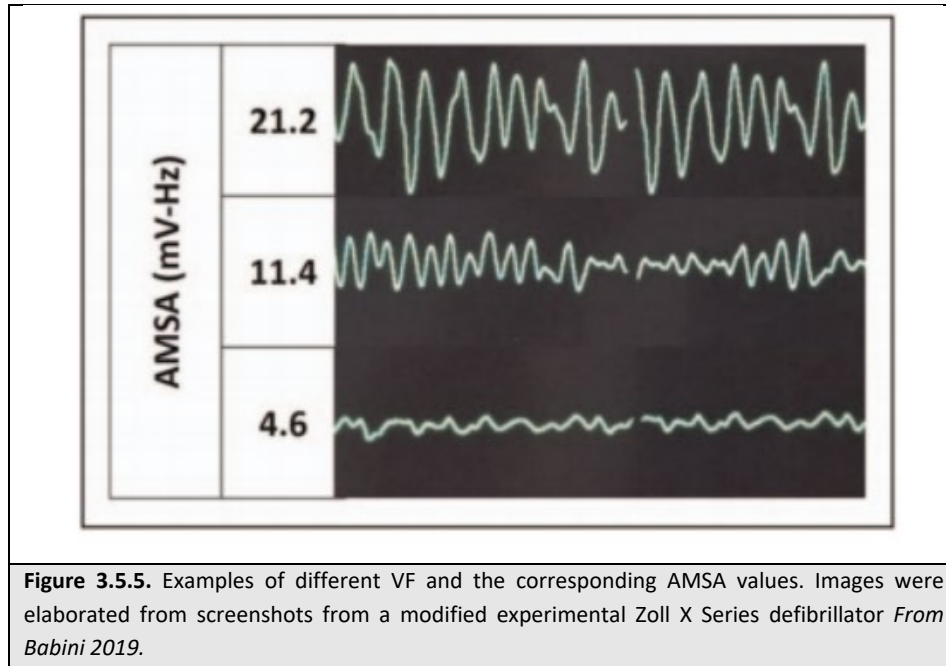
The need for ECG analyses and prediction for successful DF escalated following the introduction of automated external defibrillators. Initial efforts focused on the ECG indicator widely investigated at that time and specifically evaluated the possibility of VF amplitude to predict resuscitability in a rodent model of CA and CPR. Increases in CPP during CCs were associated with concomitant increases in VF voltage and greater VF voltages were observed in successfully resuscitated animals. Moreover, greater VF voltages after initiation of cardiac resuscitation were associated with increases in myocardial creatine phosphate, and significant decreases in lactate content. Accordingly, increases in VF voltage during cardiac resuscitation reflected increases in myocardial perfusion and favorable changes in myocardial energy metabolism with consequent greater success of CPR (*Noc 1994*). In a porcine model of CA and CPR, successfully resuscitated animals had significantly greater CPP, dominant VF amplitude, mean VF amplitude, and dominant VF frequency. No animals were resuscitated if CPP was <8 mm Hg, dominant amplitude <0.48 mV, mean amplitude <0.25 mV, or dominant frequency <9.9 Hz, independently of the duration of untreated VF. However, DF attempts uniformly failed when mean amplitude was below the threshold level even though dominant frequency would have predicted otherwise. Efforts to obtain a better predictor led to the “defibrillator predictor” in which mean amplitude and dominant frequency were combined.

Utilizing stepwise multiple regression analysis, the investigators identified a single numerical score which was established as a DF predictor and was represented by the following equation (*Noc 1999*):

$$\text{Defibrillator Predictor} = 3.60 - 4.85 * \text{mean VF amplitude} - 0.06 * \text{VF dominant frequency}.$$

This predictor served as an objective noninvasive measure on par with that of CPP for predicting the success of DF. DFs were unsuccessful if the combination of mean amplitude and dominant frequency did not exceed a specific threshold value. Unfortunately, positive predictive value (PPV) was still suboptimal, being 20%.

Drs. Pernat and Povoas (*Pernat 2001, Povoas 2000 and 2002*), continuing the earlier studies, finally introduced the new DF outcome predictor, namely AMSA (Figure 3.5.5). This ECG-derived parameter was obtained from conventional scalar limb ECG leads, continuously monitored during uninterrupted CC.



The electrocardiographic signal was sampled and recorded at a frequency of 300 Hz. The amplitude spectrum was obtained by Fourier Transform of the ECG scalar signal. AMSA was then calculated from the resulting amplitude frequency spectrum according to the following equation:

$$\text{AMSA} = \sum A_i \times F_i$$

where A_i is the amplitude at the i th frequency F_i .

To minimize low-frequency artefacts produced by CC and to exclude the electrical interference of ambient noise at frequencies greater than 48 Hz, the analyses were performed between the frequencies of 4 and 48 Hz.

In an initial study, Dr. Povoas (*Povoas 2000*) investigated CPP, obtained from arterial and right atrial pressure and VF mean amplitude, Mean Frequency, and AMSA, obtained from ECG recordings in 55 domestic pigs during CPR. From these measurements, threshold values for ROSC were obtained and subsequently validated in another 10 animals. CPP and mean amplitude each had PPVs of 100% but negative predictive values (NPVs) of only 44% and 22%, respectively. Mean Frequency predicted successful DF with a PPV of 75% but a NPV of only 30%. AMSA yielded a better combination of PPV and NPVs of 86% and 85%, respectively. Among the exciting and impressive results obtained with this new ECG parameter, the high NPV was of special note since the investigators realized that AMSA was able to minimize repetitive and ineffective electrical shocks during CPR.

During the same period, Dr. Pernat confirmed these results, demonstrating the capability of AMSA to optimize the timing of DF (*Pernat 2001*). In a porcine model of CA and resuscitation, AMSA was highly

correlated with CPP levels during CPR and AMSA, similarly to CPP, was significantly greater in animals that were resuscitated compared to those that were not. In no instances a perfusing rhythm was restored when AMSA was <21.0 mV-Hz. The AMSA value of 21 mV-Hz predicted restoration of perfusing rhythm with sensitivity and specificity above 90%. The NPV of AMSA was 95% and statistically equivalent to that of CPP, mean amplitude, and Mean Frequency. However, the PPV, was greatly improved with AMSA, namely 78% in contrast to the lower predictive values yielded by CPP, mean amplitude, and Mean Frequency, which were below 40%.

One year later, Dr. Povoas (*Povoas 2002*) further investigated the real time application of AMSA in a porcine model of CA. The investigators confirmed that an AMSA value of 21 mV-Hz had a NPV of 96% and a PPV of 78%. An AMSA value of 21 mV-Hz or greater predicted restoration of a perfusing rhythm in 7 of 8 instances and AMSA of 20 mV-Hz or less correctly predicted failure of electrical resuscitation in 24 of 26 instances.

The progressive increases in AMSA observed before successful resuscitation further demonstrated that AMSA had the potential of providing an objective guide allowing for better quality control of CPR. Failure to increase AMSA values to near threshold levels prognosticated failure of DF.

These initial empirical trials identified AMSA as a good predictor for guiding the DF attempt. Subsequent validation studies confirmed that AMSA had impressively higher specificity and PPV compared with the other predictors, maintaining sensitivity and NPV comparable to CPP, mean amplitude, and Mean Frequency. More importantly, AMSA was not invalidated by artefacts resulting from CC fulfilling the goal of a predictor that would allow for uninterrupted CC during ECG analyses. AMSA was well correlated with CPP, which is widely recognized as the gold standard for predicting the success of DF. Yet, CPP was robust only for negative prediction. It is the specificity and the PPV, which are assured by AMSA that are more likely to minimize the adverse effects of repetitive high energy shocks during CPR and the resulting post-resuscitation myocardial dysfunction. Generally, in multiple observational studies, higher AMSA has been associated with higher rates of termination of VF and ROSC, while lower values predicted failure of resuscitation efforts (*Babini 2019, Indik 2014 and 2015*). Despite the research for other waveform analysis measures has continued over the years, AMSA was confirmed as one of the most predictive measures of shock success, not only in experimental settings (*Yang 2019*) but also when analyzing retrospective data (*He 2015*).

Aiello et al. recently developed an AMSA-driven DF protocol and showed in a swine model of non-ischemic VF to be more effective than the current guidelines-driven protocol (*Aiello 2017*). The AMSA-driven protocol required fewer shocks to achieve ROSC with successful survival at 240 minutes, resulting in less myocardial dysfunction. In a subsequent work, the same group tested in addition an

AMSA-driven shocks and epinephrine protocol, based on the fact that assessing real-time the metabolic state of the myocardium during VF through AMSA could help guide the delivery of resuscitation interventions like shock, identifying myocardial “readiness” for successful DF, and epinephrine, when there is a need to increase myocardial perfusion based on the AMSA level. Both protocols, to guide shocks or shocks and epinephrine, resulted in less postresuscitation myocardial dysfunction and better survival, attributed to with less electrical and adrenergic myocardial burdens, despite the rate of ROSC was not affected (*Aiello 2021*).

3.5.4 Applicability of AMSA to a clinical scenario

The subsequent step in the evolution of AMSA as an indicator of effectiveness of intervention and to guide DF was the confirmation of its efficacy in clinical settings. The first confirmation of the capability of AMSA to predict success of DF and ROSC in a clinical scenario was reported by Young et al. (*Young 2004*) in the late 2004. This study was a retrospective analysis of ECG traces, representing lead 2 equivalent recordings, on 108 DF attempts on 46 victims of CA due to VF during OHCA. An AMSA value of 13 mV-Hz predicted successful DF, with a sensitivity of 91% and a specificity of 94%. This data represented the first evidence of the capability to extend the predictive value of AMSA to human patients.

In 2008, Ristagno et al. (*Ristagno 2008b*) analyzed a new database including episodes of VF or ventricular tachycardia with DF attempts, obtained from human victims of OHCA. ECGs were recorded from automated external defibrillators which provided escalating biphasic shocks in the sequence, 120 – 150 – 200 Joules. AMSA was confirmed as a valid tool to predict the likelihood that any electrical shock would have restored a perfusing rhythm during CPR in 90 OHCA patients. The analysis was performed on a 4.1 second interval of ECG recordings immediately preceding the delivery of the DF. For purpose of this study, the outcome of the shock was defined as successful if DF restored an organized rhythm with heart rate ≥ 40 beats/min commencing within the 1 min post shock period. Outcome was considered not successful if VF, ventricular tachycardia (heart rate > 150 beats/min), asystole or pulseless electrical activity, with pauses > 5 sec, occurred after DF. AMSA values were significantly greater in successful DF, compared to unsuccessful one, 16 mV-Hz and 7 mV-Hz respectively. A threshold value of AMSA of 12 mV-Hz was able to predict the success of each DF attempt with a sensitivity of 91% and a specificity of 97%. The PPV, which refers to the proportion of the shocks that were correctly predicted to restore a perfusing rhythm, was 95%. The NPV, which instead refers to the proportion of the shocks that were predicted to fail and actually failed to restore a perfusing rhythm, was 97%. The results of this study were consistent with the previous retrospective analysis (*Young 2004*). Of particular interest was the fact that although different models of defibrillators were employed in

the two studies, the results were consistent. This was therefore a further confirmation that AMSA represented an excellent predictor of DF success, and this capability was independent from the defibrillatory energies and waveforms utilized. In a recent study including 267 CPR sequences from 77 victims of OHCA, Dr. Eftestøl and colleagues (*Eftestøl 2004*) confirmed AMSA as one of the most powerful predictors of success of DF.

Ristagno et al. further studied the capability of AMSA to predict the success of DF analyzing ECG data, including 1260 DFs, obtained from 609 CA patients due to VF. AMSA sensitivity, specificity, accuracy, and PPV and NPV for predicting DF success were calculated, together with receiver operating characteristic (ROC) curves. AMSA was significantly higher prior to a successful DF than prior to an unsuccessful DF (15.6 ± 0.6 vs. 7.97 ± 0.2 mV-Hz, $p < 0.0001$). Intersection of sensitivity, specificity and accuracy curves identified a threshold AMSA of 10 mV-Hz to predict DF success with a balanced sensitivity, specificity and accuracy of almost 80%. Higher AMSA thresholds were associated with further increases in accuracy, specificity and PPV. AMSA of 17 mV-Hz predicted DF success in two third of instances (PPV of 67%). Low AMSA, instead, predicted unsuccessful DFs with high sensitivity and NPV >97%. Area under the ROC curve was 0.84. CC depth affected AMSA value. In 303 patients with CC depth data collected with an accelerometer, changes in AMSA were analyzed in relationship to CC depth. When depth was <1.75 in., AMSA decreased for consecutive DFs, while it increased when the depth was >1.75 in. ($p < 0.05$) (*Ristagno 2013*).

More recently, the same group evaluated the ability of AMSA to predict DF outcome retrospectively in a large derivation-validation study on out-of-hospital VFs. AMSA was validated as an accurate predictor of DF and long-term survival (*Ristagno 2015*). See section 1.5.10.

Recently, retrospective studies included AMSA derived measures such as delta AMSA in order to further increase the prediction capability. Schoene et al. studied the course of AMSA during resuscitation and how this course is related to outcome, evaluating 390 OHCA patients. Until the third shock, AMSA measured before the shock was strongly associated with favorable neurologic survival. The median change in AMSA was 0.24 - 0.21; a positive median change in AMSA between shocks was associated with favorable neurologic survival (*Schoene 2014*). Nakagawa et al. developed an equation to predict ROSC, where the change in AMSA (Δ AMSA) was added to AMSA measured immediately before the first shock. They retrospectively investigated 285 VF patients given prehospital electric shocks. Both AMSA and Δ AMSA were independent factors influencing ROSC induction by electric shock. Area Under the Curve (AUC) for predicting ROSC was 0.851 for AMSA and 0.891 for AMSA + Δ AMSA (*Nakagawa 2017*). Thannhauser et al. focused on the predictive capability of AMSA not only in the early phase of resuscitation, but also in the late shocks. Interestingly, they demonstrated that the association

between AMSA and Δ AMSA (current AMSA/AMSA relative to the latest shock) with shock success differed between the early and late phase of resuscitation. In fact, restricted to the first few shocks, the associations between AMSA, Δ AMSA and shock success was confirmed. Contrastingly, in the later phase of resuscitation, Δ AMSA showed no association. The observed association between AMSA-values and shock success in this later phase were less consistent (*Thannhauser 2019*). Principal studies on AMSA are reported in Table 3.5.3.

In the pediatric population, Raymond et al. characterized AMSA during CA and found that pre-shock AMSA was not associated with termination of VF, whereas average AMSA had a trend to significance for association in ROSC, but not 24-hour survival or survival to hospital discharge (*Raymond 2021*).

AUTHOR	POPULATION	AMSA (mV-Hz, for DF success or failure) & PREDICTIVE PERFORMANCE			ENDPOINTS	MAIN FINDINGS
Coult et al. 2017	OHCA n=692	CCs-	6.00 [4.02-7.97] vs. 3.74 [2.21-5.27]	AUC: 0.71 OR: 1.31 [1.21-1.42]	ROOR	AMSA was significantly higher in successful defibrillations. Prior ROOR, AMSA improved the prediction of shock success during CPR
		CCs+	7.15 [4.95-9.35] vs. 5.21 [3.26-7.16]	AUC: 0.60 OR: 1.22 [1.14-1.31]		
Dumas et al. 2019	OHCA n=716	Univariate OR: 1.31 [1.24-1.37] Multivariate OR: 1.27 [1.20-1.34]			Survival	Higher Charleson Comorbidities Index was associated with lower AMSA and reduced chance of survival
Coult et al. 2019	OHCA n=1151	CCs-		AUC: 0.73 [0.71-0.76]	ROOR	Waveform analysis prognostic performance was reduced during CCs. AMSA performed as one of the best single-feature predictor of CA outcome The use of combined measures allowed for diagnostic performance to increase
		CCs+		AUC: 0.67 [0.64-0.70]		
		CCs-		AUC: 0.72 [0.70-0.75]	ROSC	
		CCs+		AUC: 0.71 [0.67-0.74]		
		CCs-		AUC: 0.75 [0.73-0.78]	Survival	
		CCs+		AUC: 0.72 [0.69-0.75]		
Frigerio et al. 2020	OHCA n=112		10.8 [8.07-14.19] vs. 6.9 [4.7-11.3]	AUC: 0.68 [0.65-0.72] Se: 82.7 [70.9-88.4] Sp: 55.1 [47.0-65.9]	ROOR	AMSA and ETCO ₂ predicted defibrillation success and ROSC; however, they were correlated only in patients who achieved ROSC
			13.3 [10.6-16.7] vs. 8.4 [5.7-12.5]	AUC: 0.74 [0.71-0.78] Se: 82.7 [75.2-88.4] Sp: 65.0 [60.9-69.4]	ROSC	
Chicote et al. 2019	OHCA n=214			AUC 0.75 [0.72-0.75] Se: 79.8 [71.4-85.5] Sp: 63.2 [58.5-71.6]	ROOR	AMSA and ETCO ₂ predicted shock success; however, the predictivity of ETCO ₂ was restricted to first defibrillations only
Thannhauser et al. 2019	OHCA n=139	All shocks	9.7 [7.0-14.0] vs. 7.5 [5.3-11.1]		ROOR	AMSA related to defibrillation success. Increase in AMSA during early phase of resuscitation (first 3 shocks) was associated with defibrillation success and increased predictivity of AMSA absolute value
		Early shocks	11.3 [7.8-15.9] vs. 8.1 [5.1-11.1]			
		Late shocks	8.6 [6.0-12.3] vs. 6.8 [5.5-11.0]			
Coult et al. 2021	OHCA n=1151	CCs-		AUC: 0.74 [0.71-0.76]	ROOR	AMSA predictivity was inferior during chest compression. The use of a novel prognostic algorithm improved significantly the prediction of defibrillation success regardless of on-going CPR
		CCs+		AUC: 0.66 [0.63-0.69]		
		CCs-		AUC: 0.74 [0.71-0.76]	Survival	
		CCs+		AUC: 0.70 [0.67-0.73]		

Firoozabadi et al. 2013	OHCA n=116				AUC: 0.83 Se (with a Sp of 90%): 39% Sp (with a Se of 90%): 61%	ROSC	Various VF features correctly predicted defibrillations success. AMSA was in the first six features ranked by AUC
Howe et al. 2014	OHCA & IHCA n=41				AUC: 0.78	ROOR	AMSA was a good predictor of defibrillation success
Coult et al. 2016	OHCA n=442				AUC: 0.77 [0.73-0.82] AUC: 0.72 [0.67-0.77]	ROOR Survival	AMSA predicted accurately rhythm and clinical outcomes using VF epochs as short as 0.8 s (compared to 5 s)
Nakagawa et al. 2017	OHCA n=285	First DFs	13.4 ± 6.4 vs. 8.0 ± 5.8		AUC: 0.851 [0.797-0.906]	ROSC	An algorithm including AMSA and AMSA variation between first and second shock, increased the predictive performance
Indik et al. 2014	OHCA n=89		First defibrillation Average AMSA		1.036 [1.004-1.069] 1.058 [1.020-1.097]	ROSC	Both AMSA measured before the first shock and the average of AMSA over shocks was highly predictive of outcome; however the latter approach showed greater predictive performance
			First defibrillation Average AMSA		1.058 [1.021-1.098] 1.076 [1.033-1.121]	Hospital admission	
			First defibrillation Average AMSA		1.061 [1.029-1.112] 1.070 [1.029-1.112]	Hospital discharge	
Ristagno et al. 2013	OHCA n=609	All DF	15.6 ± 0.6 vs. 7.9 ± 0.2		AUC: 0.84	ROOR	AMSA value correlated with depth of CCs AMSA < 7 mV·Hz predicted shock failure with a NPV 97% AMSA>17 mV·Hz predicted shock success with a PPV 67% for all defibrillations and PPV 60% for the first defibrillation
		First DF	15.7 ± 0.9 vs. 8.7 ± 0.3		AUC: 0.80		
		Subsequent DFs	15.5 ± 0.8 vs. 7.9 ± 0.2		AUC: 0.87		
		Refractory VF	12.7 ± 1.0 vs. 7.0 ± 0.2		AUC: 0.81		
		Recurrent VF	16.8 ± 1.0 vs. 13.8 ± 1.8		AUC: 0.65		
Ristagno et al. 2015	OHCA n=1617	All DFs First DF unadjusted	OR: 1.33 [1.20-1.37] OR: 1.33 [1.28-1.38]		AUC: 0.89 AUC: 0.89	ROOR	AMSA was validated in a large derivation-validation study as an accurate predictor of defibrillation success and long-term survival. Proposed thresholds: Defibrillation failure: 6.5 mV·Hz (NPV 98% and Se 97%); Defibrillation success: 15.5 mV·Hz (PPV>84% and Sp 97%)
		Last shock	11.7 ± 5.3 vs. 7.4 ± 4.1	Relative risk adjusted: 1.22 [1.17-1.26] AUC: 0.692		ROSC	
		Last shock	12.6 ± 5.3 vs. 10.8 ± 5.1	1.05 [1.02-1.10]		Hospital discharge	
		Last shock	13.1 ± 5.3 vs. 10.6 ± 5.2	1.06 [1.03-1.10]		6-month survival	
		Last shock	13.1 ± 5.1 vs. 10.8 ± 5.3	1.06 [1.03-1.10]		1-year survival	

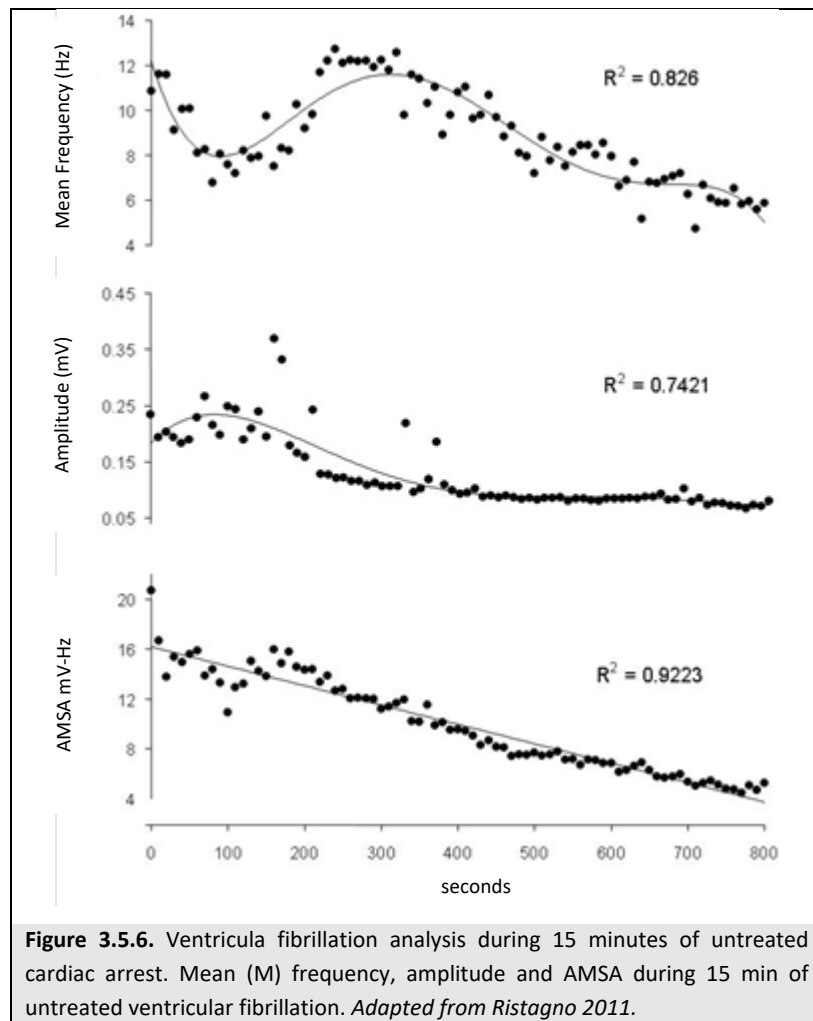
Table 3.5.3: Principal studies on AMSA. OH, out-of-hospital; IH, in-hospital; CA, cardiac arrest; CCs, chest compressions; CCs+, analysis during CCs; CCs-, analysis without CCs; ROOR, return of organized rhythm; ROSC, return of spontaneous circulation; PPV, predictive positive value; NPV, negative predictive value; Sp, specificity, Sn, sensitivity; AUC, area under the curve. *Adapted from Babini 2019.*

3.5.5 CPR quality and duration of untreated VF

Quality of CC is a major issue for CPR success (*Brower 2015, Cheskes 2014, Gallagher 1995, Vaillancourt 2011, Van Hoeyweghen 1993, Wik 1994*). Li et al. have investigated the possibility of assessing the quality of CPR, and especially of CC depth, utilizing AMSA. In a porcine model of VF and CPR, animals were randomized to either optimal or suboptimal CC depth after onset of VF. Optimal depth of mechanical compression was defined as a decrease of 25% in anterior posterior diameter of the chest during compression. Suboptimal compression was defined as a decrease of 17.5% in anterior posterior diameter. All animals had ROSC after optimal compressions. This contrasted with suboptimal compressions after which none of the animals had ROSC. AMSA, once again has been proven to be, like CPP, predictive of outcome. The calculated AMSA values during CPR and immediately prior to the DF attempt were significantly greater after optimal CCs, in contrast to the sub-optimal ones. In that experimental setting, the quality of CCs was closely related to the AMSA value and in turn, to the likelihood of ROSC. Like threshold value of CPP, AMSA threshold value was achieved contingent on the depth of compressions such that AMSA increased progressively during CC and predicted the likelihood of successful DF. AMSA therefore was confirmed to serve also as an indicator of effective CC, as well as a tool for guiding DF delivery. The extension of the AMSA measurement to guide the quality of CC was explained as the capability to restore the electrical robustness of the myocardium through restoring threshold level of coronary blood flow (*Li 2008*).

A recent study including a large number of OHCA patients, showed a correlation between bystander CPR and more robust initial VF waveform measures at the EMS arrival. VF waveform analysis and in particular AMSA mediated up to one-half of the survival benefit associated with bystander CPR, suggesting that much of the survival benefit conferred by bystander CPR may be a result of improvement to the myocardium (*Bessen 2021*).

Similar to AMSA, other physiological measures have been proposed as CCs quality parameters during CPR (*Sutton 2016*), for example the etCO_2 (*Savastano 2017, Chicote 2019*). In a retrospective analysis, both AMSA and etCO_2 were independent predictors of shock success and ROSC (*Frigerio 2021*). However, AMSA was superior to etCO_2 as a single-feature predictor of shock success and ROSC (AUC for shock success: 0.68 vs. 0.59; AUC for ROSC 0.74 vs. 0.56). Of note, AMSA and etCO_2 correlated only in case of ROSC. A plausible explanation is that AMSA increases when myocardial perfusion increases (*Yang 2019*), while etCO_2 increase when pulmonary and systemic perfusion increase (*Shibutani 1994*).

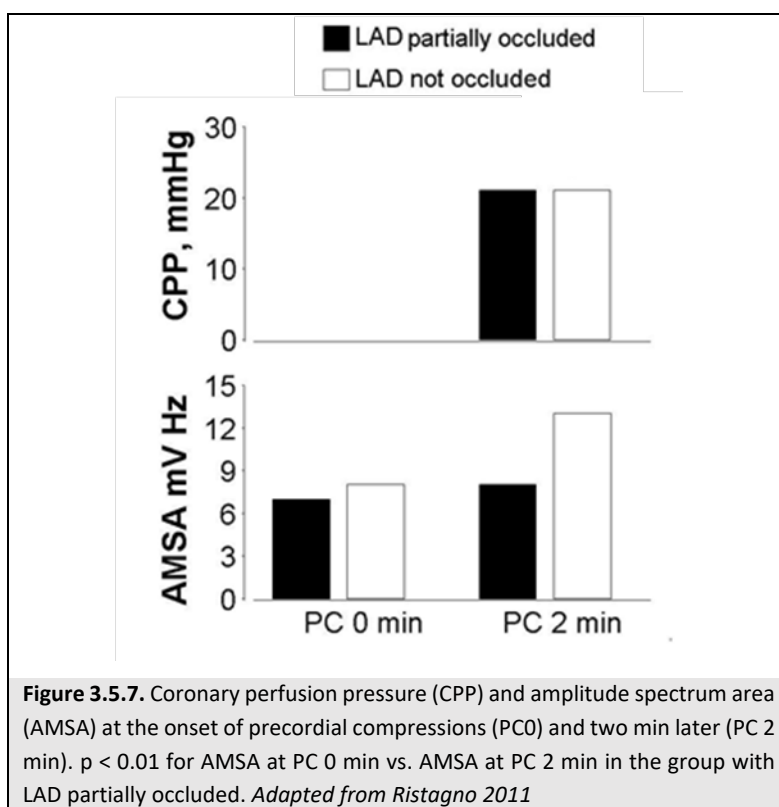


Effective CCs improves both myocardial and systemic perfusion, causing an increase in both AMSA and etCO_2 . Pathological conditions such as ongoing coronary occlusion or aortic root dissection, excluding part of the myocardium from the systemic circulation, may dissociate the correlation between AMSA and etCO_2 , thus reducing the capability of the etCO_2 to predict DF success (Frigerio 2021, Ristagno 2007).

Beside the quality of CC, AMSA might also be useful for retrieving the duration of untreated VF in the case of unwitnessed CA (Niemann 1992, Ristagno 2011). In nine domestic male pigs, VF was induced and left untreated for 15 min (Ristagno 2011). AMSA, more than VF amplitude and frequency, was highly correlated with the downtime of VF and decreased over time, as shown in Figure 3.5.6.

Significantly lower AMSA was observed after 3 min of untreated VF. Following the 4th min of VF, AMSA values decreased more rapidly. More recently, in a study aimed at investigating the validation of Spectral Energy to guide DF in a porcine model of CA and compare it with AMSA, AMSA was confirmed to gradually decay during untreated VF, and after the application of CPR and epinephrine, significantly increase in animals which were later successfully defibrillated (AMSA AUC for first DF success 0.76-0.81) (Yang 2019).

3.5.6 CA with underlying myocardial ischemia



Myocardial ischemia and reperfusion have been involved in the triggering of malignant ventricular dysrhythmias (Ouyang 1981, Qin 2002) and both the duration and the severity of myocardial ischemia play important roles in developing myocardial cell damage (Reimer 1979).

Indeed, Ristagno et al. have earlier described that AMSA was superior to CPP as indicator of return to a perfusing rhythm following DF, under condition of partial occlusion of the LAD (Ristagno 2007b). In a porcine model of CA and resuscitation, a partial occlusion of the LAD, which was approximately 75% of the internal lumen, was maintained during CPR. During CC, CPP increased and exceeded threshold value for successful resuscitation. AMSA however, was significantly lower in the animals in which the partial occlusion of the LAD was maintained during CPR (Figure 3.5.7). This was reflected by the greater number of electrical shocks required to terminate VF with lesser success of resuscitation. CPP is in fact, an indirect indicator of myocardial flow produced by CC and represents a gradient pressure between aorta and right atrium. This gradient can be maintained even in the presence of occlusion of the coronary tree. AMSA, which is instead related to myocardial blood flow and metabolism, has been shown to substantially decrease when the myocardial perfusion is truly reduced (Ristagno 2011).

Capability of ECG predictors, i.e. AMSA and its slope, in the presence of AMI was further tested in a porcine model of CA with or without AMI. Untreated VF duration and AMI were independent predictors of ROSC following VF CA and AMSA and slope were able to predict ROSC (*Indik 2011*). However, the evidences about the capability of AMSA to predict ROSC in the presence of coronary occlusion are not consistently demonstrated in other studies (*Indik 2008 and 2009*).

AMI seems to result in lower AMSA values also when OHCA were analysed (*Hulleman 2017, Olasveengen 2009, Thannhauser 2020*) although evidences are contradictory (*Hidano 2016*). Potentially, localization of AMI could play a role in the effects of AMI on the waveform analysis (*Bonnes 2015, Indik 2008, Nas 2021*).

Previous MI seem to lower AMSA in the majority of studies. In a very large study in which multiple VF waveform analyses were tested as predictors of DF success and outcome from OHCA, AMSA was lower for patients with a previous MI (*Ristagno 2015*). Hulleman et al. found effect of previous MI on AMSA only in the subgroup of patients with STEMI. A previous MI was associated with lower AMSA (*Hulleman 2017*). Bonnes et al. found that waveform was markedly lower in the leads adjacent to the area of infarction. In the leads corresponding with the infarct localisation, the bandwidth was broader as well, indicating less organised VF (*Bonnes 2015*).

3.5.7 AMSA and patient's characteristics and medications

Little is known about other patient characteristics that may influence the VF waveform (*Bonnes 2017, Kern 1990*). Chronic health diseases may directly affect myocardial substrate availability and reduce the chance of survival from CA. The presence of a history of previous MI or congestive heart failure reduce VF frequencies (*Indik 2011, Olasveengen 2009*), while older age, male sex, and diabetes mellitus are known to decrease AMSA (*Ristagno 2015*). In a retrospective analysis of 716 CA patients, the number of comorbidities expressed as Charleson Comorbidities Index was an independent predictor of survival at discharge in a multivariable logistic regression model (*Dumas 2019*). When AMSA was included in the model, both AMSA and Charleson Comorbidities Index were both independent predictors of survival (*Dumas 2019*).

Patients with chronic comorbidities frequently receive multiple medications, including cardiovascular drugs, that may modify myocardial conductivity and metabolic status, thus affecting the VF waveform and the predictivity of AMSA. In a multivariable logistic regression analysis, cardiovascular drugs were generally not associated with AMSA, particularly when chronic comorbidities were included in the model (*Hulleman 2020*). On the other hand, VF frequencies are known to be reduced by the use of beta-blockers (*Sherman 2012*), while antihypertensive drugs, instead, seem to increase AMSA (*Ristagno 2015*). Interestingly, the use of K⁺-sparing diuretics remained an independent predictor of reduced AMSA. Hyperkalaemia is a well known side effect of K⁺-sparing agents and greater extracellular K⁺ levels reduce the DF threshold; however, whether higher K⁺

concentration relates to lower AMSA is unclear (*Hulleman 2020*). In two studies, the most important predictors of AMSA values were the CA characteristics (e.g., age, response time, witnessed CA, cardiac cause) (*Dumas 2019, Hulleman 2020*). Salcido et al. investigated the relationship between AMSA, Median Slope, and centroid frequency and the intra-resuscitation antiarrhythmic drugs amiodarone, lidocaine, and placebo (secondary analysis of the ROC ALPS trial). AMSA and Median Slope measures of the first available VF were associated with rearrest case status, while Median Slope and centroid frequency, but not AMSA, were associated with ALPS treatment group (*Salcido 2018*).

AMSA seems to be higher in patients with increased LV mass, while LV diameter does not affect AMSA (*Bonnes 2017*).

3.5.8 Artefacts

A major challenge to the routine use of waveform measures to help guide care is that these measures are conventionally calculated during pauses in CPR because CC cause electrical artefact in the ECG (*Affatato 2016, Fitzgibbon 2002, Li 2009, Ruiz de Gauna 2014*,). Such interruptions generally contradict best-practice guidelines which call for minimally-interrupted CPR to support resuscitation. Interruption, in fact, reduces the period of vital myocardial perfusion and has been proven to yield sub-optimal outcome and greater post-resuscitation myocardial dysfunction (*Feneley 1988, Sato 1997*).

At present, several filters and algorithms to reduce and eliminate ECG artefacts and noise due to CCs, or ambient interferences have been developed and successfully used (*Berger 2007, Gong 2013, Li 2008b and 2012, Lo 2013, Noc 1999, Pernat 2001, Povoas 2000 and 2002, Strohmenger 1996 and 1997, Zuo 2021*). The filtered ECG signals or CPR-artefact-free ECG signals presented better results than the ECG signals with CPR artefacts (*Neurauter 2008*).

A preprocessing step is usually employed to obtain the 'pure' ECG signal before the waveform analysis, including a notch filter to remove alternating current interference at 50-60 Hz, a high-pass filter to remove baseline drifting and CPR artefact, and a low-pass filter to remove the myographic noise (*Amann 2010, Granegger 2011, Irusta 2009, Ruiz 2010, Werther 2012*).

Only recently, a pilot investigation of Median Slope and AMSA waveform measures during CCs measured and confirmed the expected reduction in prognostic performance compared with compression-free analysis (*Coult 2018*). These results were confirmed by the same group in a larger study, that described the decline of predictive performance of individual waveform measures declined during CPR (Table 3.5.4) (*Coult 2019*).

Nevertheless, since AMSA is computed from the product of each frequency and its magnitude, this measure increasingly emphasizes higher-frequency content and, consequently, may still be relatively better-suited to evaluate VF during CC as it inherently ignores some CPR artefact. In fact, the fundamental frequency of CCs is approximately 2 Hz, while VF frequencies are primarily between 3 and 8 Hz.

WAVEFORM MEASURE	TYPE	SURVIVAL WITH CCS	SURVIVAL WITHOUT CCS	ROSC WITH CCS	ROSC WITHOUT CCS	ROOR WITH CCS	ROOR WITHOUT CCS
Support vector machine	Combination	0.75 [0.72–0.78]*	0.75 [0.73–0.78]*	0.72 [0.69–0.75]*	0.72 [0.70–0.75]*	0.70 [0.67–0.73]*	0.75 [0.72–0.77]*
Neural network	Combination	0.74 [0.71–0.77]	0.75 [0.73–0.78]	0.71 [0.68–0.74]†	0.72 [0.69–0.75]	0.69 [0.66–0.72]	0.74 [0.72–0.77]
Logistic regression	Combination	0.73 [0.70–0.76]	0.74 [0.71–0.77]†	0.71 [0.68–0.74]	0.71 [0.69–0.74]	0.69 [0.66–0.72]	0.73 [0.70–0.76]†
Wavelet energy	Frequency	0.73 [0.70–0.76]†	0.75 [0.73–0.78]	0.71 [0.68–0.74]	0.73 [0.70–0.76]	0.68 [0.65–0.71]†	0.74 [0.71–0.76]†
Amplitude spectrum area	Frequency	0.72 [0.69–0.75]†	0.75 [0.73–0.78]	0.71 [0.67–0.74]†	0.72 [0.70–0.75]	0.67 [0.64–0.70]‡	0.73 [0.71–0.76]†
Median slope	Time-domain	0.69 [0.67–0.72]‡	0.73 [0.71–0.76]‡	0.68 [0.65–0.72]‡	0.72 [0.69–0.75]	0.66 [0.63–0.69]‡	0.74 [0.72–0.77]
Centroid frequency	Frequency	0.68 [0.65–0.71]‡	0.71 [0.69–0.74]‡	0.66 [0.63–0.69]‡	0.69 [0.66–0.71]†	0.63 [0.60–0.67]‡	0.68 [0.65–0.70]‡
Peak frequency	Frequency	0.64 [0.61–0.67]‡	0.71 [0.68–0.74]‡	0.64 [0.61–0.67]‡	0.67 [0.64–0.70]‡	0.61 [0.58–0.64]‡	0.67 [0.64–0.70]‡
Signal integral	Time-domain	0.63 [0.60–0.66]‡	0.69 [0.67–0.72]‡	0.62 [0.59–0.66]‡	0.70 [0.67–0.73]‡	0.60 [0.56–0.63]‡	0.73 [0.70–0.76]†
Peak amplitude	Time-domain	0.59 [0.56–0.63]‡	0.65 [0.62–0.68]‡	0.60 [0.56–0.63]‡	0.66 [0.63–0.69]‡	0.59 [0.55–0.62]‡	0.70 [0.67–0.73]‡
Mean amplitude	Time-domain	0.58 [0.55–0.61]‡	0.65 [0.62–0.68]‡	0.58 [0.55–0.62]‡	0.67 [0.64–0.70]‡	0.57 [0.53–0.60]‡	0.71 [0.68–0.74]‡
Root mean square amplitude	Time-domain	0.58 [0.55–0.62]‡	0.65 [0.62–0.68]‡	0.58 [0.55–0.62]‡	0.66 [0.63–0.70]‡	0.57 [0.53–0.60]‡	0.71 [0.68–0.74]‡

Table 3.5.4. AUC Values for Waveform Measure Prediction of Outcomes. Area under receiver operating characteristic curve (AUC) values presented as AUC [95% CI] sorted by AUC for predicting survival with chest compressions (CCs). *Support vector machine AUC (column referent). †Significant AUC difference vs. column referent by the DeLong method ($p < 0.05$, 2-sided). ‡Significant AUC difference vs. column referent by the DeLong method with Bonferroni correction ($p < 0.0019$, 2-sided). ROSC, return of spontaneous circulation; ROOR, return of organized rhythm. *Adapted from Coult 2019*

Zuo et al introduced an algorithm to estimate AMSA during CPR by assessing the VF signal quality based solely on the surface ECG waveform recorded from automated external defibrillators, demonstrating that CC-corrupted low quality VF signals can be correctly identified and that AMSA can be reliably estimated from the VF signals both during ongoing CC and during CC pause. Furthermore, the method was validated by preserving the predictive performance of DF success in patients with presenting shockable rhythms (Zuo 2021).

Studies have investigated combination measures, with the rationale that machine learning models (eg, neural networks or support vector machines) could optimally combine information from individual measures that quantify different aspects of the VF waveform combination, in order to improve the prediction capability of the analysis and applying it also during CC with a sufficient high performance (He 2015, Howe 2014, Neurauter 2007). Despite in general combination measures did not demonstrate a clear advantage over individual measures, Coult et al. described a promising combination model—the support vector machine—that

improved prediction of survival during CCs to the point of achieving performance similar to the highest performance without CCs (Coult 2019).

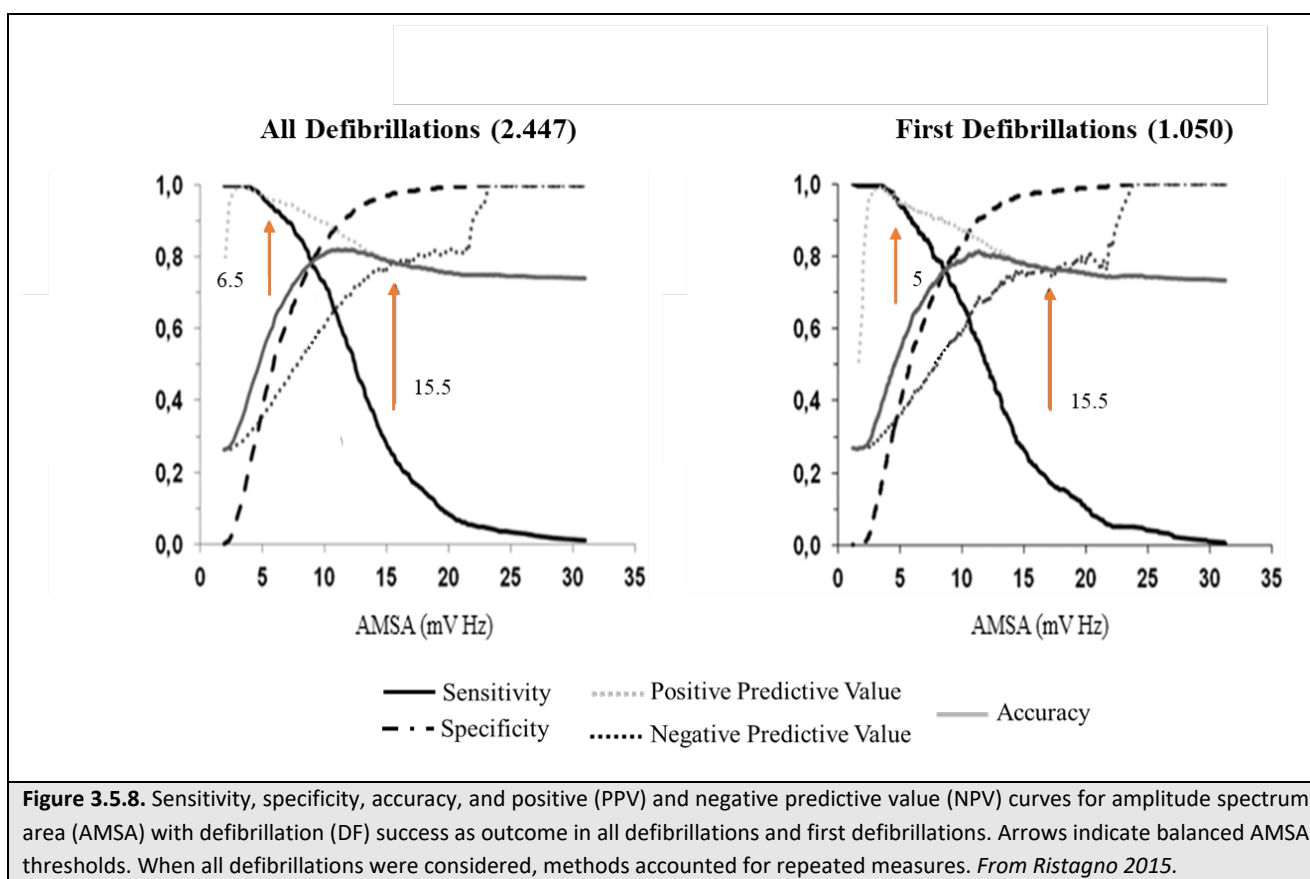
Another possible approach to overcome the problem, could be the use of short CPR-free segment. In fact, compared to epoch length of 5 seconds, the prognostic ability of AMSA declined significantly at epoch lengths of 0.2 s for predicting return of organized rhythm (AUC = 0.74, $p = 0.03$) and at lengths ≤ 0.6 s for predicting neurologically intact survival (AUC = 0.70, $p = 0.04$). For lengths decreasing from 5.0 to 0.8 s, AMSA performance did not differ significantly from the reference for either outcome. These results are consistent with our physiological understanding of VF as the median frequency of VF is approximately 3–6 cycles per second. Epochs on the order of 1 s would generally include multiple VF cycles from which to derive waveform measures (Coult 2016). Nonetheless, even these brief interruptions are logistically challenging to coordinate, and would not support continuous VF waveform assessment during CPR

3.5.9 Guideline statement on “Ventricular Fibrillation Waveform Analysis”

2010: There is evidence that VF waveforms change over time. Several retrospective case series, animal studies, and theoretical models suggest that it is possible to predict, with varying reliability, the success of attempted DF by analyzing the VF waveform. However, there are currently no prospective studies that have identified optimal waveforms and/or timing. The value of VF waveform analysis to guide DF management is uncertain (Class IIb, LOE C) (Deakin 2010, Link 2010).

2015: It is possible to predict, with varying reliability, the success of DF from the fibrillation waveform. If optimal DF waveforms and the optimal timing of shock delivery can be determined in prospective studies, it should be possible to prevent the delivery of unsuccessful high energy shocks and minimise myocardial injury. This technology is under active development and investigation but current sensitivity and specificity is insufficient to enable introduction of VF waveform analysis into clinical practice (Soar 2015).

2021: It is possible to predict, with varying reliability, the success of DF from the fibrillation waveform. If optimal DF waveforms and the optimal timing of shock delivery can be determined in prospective studies, it should be possible to prevent the delivery of unsuccessful high energy shocks and minimise myocardial injury. This technology is under active development and investigation, but current sensitivity and specificity are insufficient to enable introduction of VF waveform analysis into clinical practice. Although one large RCT and 20 observational studies published since the 2010 guidelines review have shown promise and some improvements in this technology, there remains insufficient evidence to support routine use of VF waveform analysis to guide the optimal timing for a shock attempt (Soar 2021).



3.5.10 Development of an AMSA guided resuscitation strategy with a two-thresholds approach

More recently, the ability of AMSA to predict DF outcome was retrospectively validated in a large database of out-of-hospital VFs, by a derivation/validation approach. ECG data were obtained from CAs occurring in 9 city-areas in Lombardia Region, Italy. A database, including 2.447 DF attempts from 1.050 patients, was used as derivation group, while an additional database, including 1.386 DF attempts from 567 patients, served as validation group. Higher AMSA was associated with successful DF, with an unadjusted odds ratio (OR) of 1.33 (95% CI, 1.20-1.37) for all DFs and 1.33 (95% CI, 1.28-1.38) for first DF attempts. From the derivation group, the following AMSA thresholds were identified: ≥ 15.5 mV-Hz for DF success; and < 6.5 mV-Hz for DF failure. In the validation database, $\text{AMSA} \geq 15.5$ mV-Hz predicted DF success with a PPV of 84%, while $\text{AMSA} < 6.5$ mV-Hz predicted DF failure with a NPV $> 98\%$. Area under the ROC curve for DF outcome prediction was 0.861 (Figure 3.5.8) (Ristagno 2015).

3.6 THE SWINE MODEL OF CA

The pathophysiological complexities of CA and CPR challenge the development of animal models that accurately replicate the clinical situation. Reliable preclinical models of CA and resuscitation are essential to decipher the injury mechanisms and develop treatments to increase survival and improve quality of life after CA. Many experimental animal preparations have been developed, nevertheless porcine models offer several important advantages over other species, and outcomes in this large animal are readily translated to the clinical setting (*Cherry 2015, Ristagno 2013*).

Several attributes make the domestic pig an ideal model for CA research:

- a large mammal, the pig accommodates extensive instrumentation for blood sampling, monitoring of intravascular and intracardiac pressures, ECG and intravenous administration of medications and experimental treatments;
- pigs tolerate invasive surgical procedures and rapidly regain consciousness after anesthesia;
- heart rate, blood pressure, and serum chemistries of pigs and humans are very similar
- pigs have sufficient blood volume to permit collection of multiple arterial and venous samples for analyses of blood gases and serum chemistry;
- neurological examinations have been developed to evaluate neurobehavioral function in pigs
- the pig's large chest accommodates forceful precordial chest compressions and application of transthoracic defibrillatory pads of electrical energies similar to those used clinically
- pigs have the largest brains among the commonly studied laboratory animals, which provides ample tissue for extensive biochemical and histological analyses of specific brain subregions.

An impressive variety of swine cardiac arrest models are reported in the literature and the protocols chosen for each experimental phase can profoundly influence outcome (*Cherry 2015*).

The most common method of inducing VF is the application of an electrical current to the right ventricular endocardium in a closed-chest preparation. Typically, a pacing wire is introduced into the external jugular vein and advanced into the right ventricle. While the wire is in contact with the right ventricular endocardium, a rapid train of impulses is transmitted which, within seconds, initiates VF. An important advantage of this method is the well-defined and reproducible time of VF onset (*Indik 2006*).

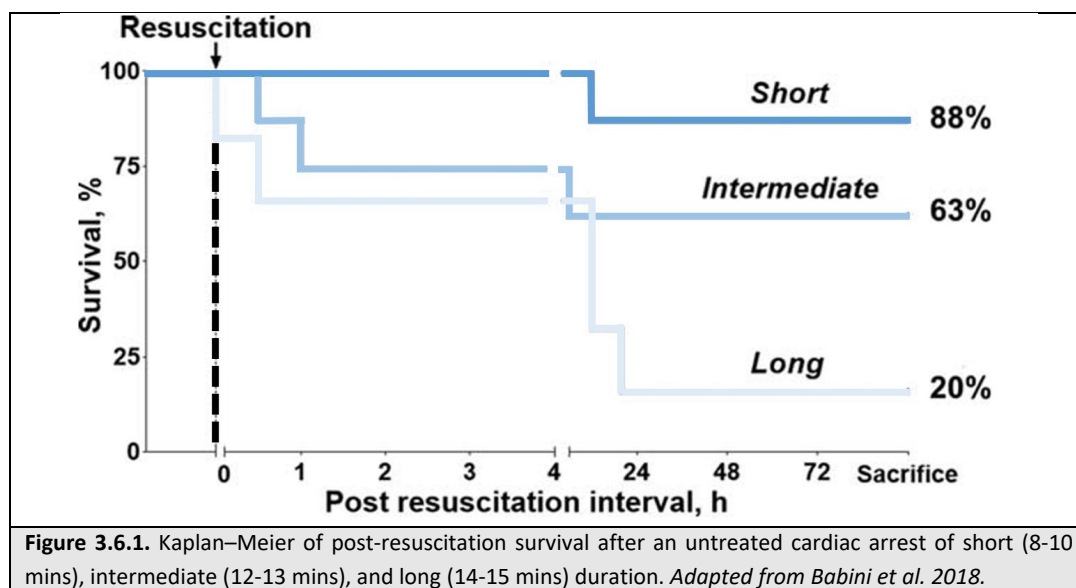
In order to replicate the most common cause of CA, porcine models of ischemia-induced VF are available, affording ready translation of results to clinical settings. Porcine myocardium lacks significant coronary collateral vessels (*Sahni 2008*), so the ischemia imposed by occlusion of a major coronary artery, e.g., the LAD coronary artery, is sufficiently severe to initiate VF within several minutes of occlusion. Coronary occlusions may be imposed by introducing a balloon occluder with the aid of fluoroscopy into the target vessel and

produces typical ECG changes. Ventricular fibrillation typically ensues within 5-10 min of coronary occlusion. Because the onset of cardiac arrest is delayed to a variable extent while the artery is occluded, the severity of myocardial injury may vary considerably among experiments. The number and intensity of the DFs required to restore sinus rhythm is greater in porcine models of ischemically-induced vs electrically-induced arrest, as is the incidence of post-resuscitation ventricular premature beats and recurrence of VF (*Cherry 2015, Indik 2006, Ristagno 2007b*).

A pivotal aspect in the porcine model of CA is the duration of untreated CA before resuscitation; as the more the interval is prolonged, the less survival and good neurological recovery become achievable (*Babini 2018*), as described in Figure 3.6.1. Then, CPR can be administered by a pneumatic, piston-driven device (e.g. Lucas device), ensuring consistency of frequency and depth of compressions across experiments or, alternatively, precordial compressions can be administered manually (*Magliocca 2015*). The duration of CPR before DF varies among different models, as well as the administration and dosage of a systemic vasoconstrictor.

Unluckily the criteria for the definition of resuscitation outcome, defibrillation success and ROSC, present differences among the models, making difficult the comparison between results. Moreover, the criteria for abandoning futile resuscitation efforts should be defined.

In conclusion, published reports show the domestic pig to be a suitable large animal model of CA, being responsive to CPR, DFs and medications, and yielding extensive information to foster advances in clinical treatment of CA (*Cherry 2015*).



4 AIM OF THE STUDIES

The present thesis includes both experimental and clinical studies directed to improve the outcome of patients affected by CA using a pharmacological and an electrophysiological approach.

First, we performed a pharmacological study directed to investigate experimentally the role of β 1-blockade during CPR, and then we performed a series of studies evaluating prospectively the feasibility of a real time VF waveform analysis, namely AMSA, to guide resuscitation and to potentially diagnose an underlying cardiac ischemia during VF.

Both the studies therefore concurred to the same goal of identify new tools to improve resuscitation.

4.1 STUDY 1: EFFECTS OF ESMOLOL DURING CPR TO REDUCE THE TOTAL NUMBER OF DEFIBRILLATIONS NEEDED TO TERMINATE VF IN A PORCINE MODEL OF CA WITH AN UNDERLYING AMI

The aim of this study was to investigate the effects of a single dose of esmolol, compared to placebo, in addition to epinephrine during CPR in a preclinical porcine model of CA with an underlying AMI (*Babini 2018, Fumagalli 2020, Ristagno 2014*). A decrease in the total number of DFs needed to terminate VF with esmolol compared with placebo was hypothesized.

4.2 STUDY 2: AMSA TO GUIDE DEFIBRILLATION DURING CPR IN OHCA PATIENTS: A PILOT, RANDOMIZED CONTROLLED TRIAL (AMSA TRIAL)

AMSA trial was a pilot multicenter randomized clinical trial reporting the first in-human use of an AMSA-guided DF strategy in OHCA patients. The aim of the study was to test the hypothesis that a CPR guided by real-time AMSA analysis was feasible and could predict outcome of DFs attempts.

4.3 STUDY 3: PRECLINICAL FEASIBILITY OF REAL TIME AMSA MEASUREMENT DURING CPR USING A MODIFIED CLINICAL DEFIBRILLATOR

The aim of this study was to investigate the role of AMSA measured in real time during mechanical CPR and without CC pauses, as predictor of shock success and CC quality in a porcine model of CA with an underlying AMI.

4.4 STUDY 4: IDENTIFYING AN AMI DURING CPR IN A PRECLINICAL PORCINE MODEL OF VF

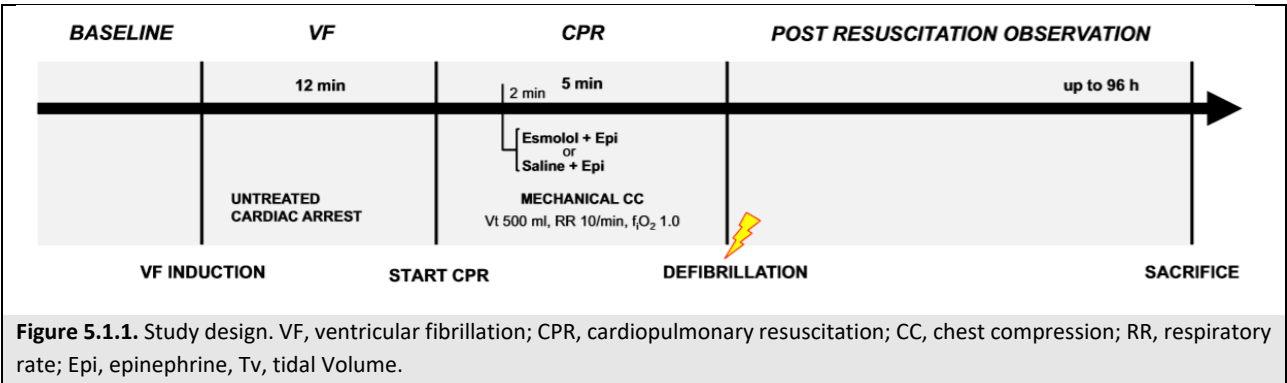
The aim of the study was to investigate, in a clinically relevant porcine model of CA, the potential additional role of AMSA in identifying an underlying AMI and its localization during VF and CPR.

5 STUDY 1. EFFECTS OF ESMOLOL DURING CPR TO REDUCE THE TOTAL NUMBER OF DEFIBRILLATIONS NEEDED TO TERMINATE VF IN A PORCINE MODEL OF CA WITH AN UNDERLYING AMI

5.1 METHODS

5.1.1 Study design

This was a randomized, placebo-controlled experimental study investigating the effects of esmolol (Brevibloc, Baxter, IL, USA) compared to placebo (saline, NaCl 0.9%) in addition to epinephrine during CPR in a porcine ischemic CA model. The study design is detailed in Figure 5.1.1.



5.1.2 Ethical considerations

Procedures involving animals and their care were in compliance with national (D.L. n. 116, G.U., suppl. 40, 18 February 1992, Circolare no. 8, G.U., 14 Luglio 1994) and international laws and policies (EEC Council Directive 86/609, OJL 358, 1, December 12, 1987; Guide for the Care and Use of Laboratory Animals, US National Research Council, 1996). Approval of the study was obtained by the University of Milan Institutional review board committee and Governmental Institution (Italian Ministry of Health: approval no. 72/2014-PR) (Ruggeri 2021). The study was reported in accordance with the ARRIVE (Animal Research: Reporting of In Vivo Experiments) guidelines.

5.1.3 Animal preparation

Sixteen healthy male domestic pigs (39±0.5 kg), adult (4-6 months of age) were fasted the night before the experiment except for free access to water. Anesthesia was induced by intramuscular injection of ketamine (20 mg/kg) followed by intravenous administration of propofol (2 mg/kg) and sufentanyl (0.3 µg/kg) through

an ear vein access. Anesthesia was then maintained by continuous intravenous infusion of propofol (4–8 mg/kg/h) and sufentanyl (0.3 µg/kg/h). A cuffed tracheal tube was placed, and animals were mechanically ventilated with a tidal volume of 15 mL/kg and Fraction of inspired Oxygen (FiO₂) of 0.21. Respiratory frequency was adjusted to maintain the etCO₂ between 35 and 40 mmHg, monitored with an infrared capnometer (*Babini 2018, Fumagalli 2020, Ristagno 2014*). To measure aortic pressure, a fluid-filled 7F catheter was advanced from the right femoral artery into the thoracic aorta. For measurements of right atrial pressure, core temperature, and LV CO, a 7F pentalumen thermodilution catheter was advanced from the right femoral vein into the pulmonary artery. Conventional pressure transducers were used (MedexTransStar, Monsey, NY). MI was induced in a closed-chest preparation by intraluminal occlusion of the LAD coronary artery (*Babini 2018, Fumagalli 2020, Ristagno 2014*). Briefly, a 6F balloon-tipped catheter was inserted from the right common carotid artery and advanced into the aorta and then into the LAD, beyond the first diagonal branch, with the aid of image intensification and confirmed by injection of radiographic contrast media. For inducing VF, a 5F pacing catheter was advanced from the right jugular vein into the right ventricle. The position of all catheters was confirmed by characteristic pressure morphology and/or fluoroscopy. A frontal plane ECG was recorded.

5.1.4 Experimental procedure

Fifteen min prior to inducing CA, animals were randomized by the sealed envelope method to receive at min 2 of CPR one of the following intravenous treatments in addition to epinephrine (30 µg/kg): (1) esmolol 0.5 mg/kg; or (2) equivalent volume of normal saline (control).

After baseline measurements, the LAD catheter balloon was then inflated with 0.7 mL of air to occlude the flow, as previously described (*Babini 2018, Fumagalli 2020, Ristagno 2014*). If VF did not occur spontaneously after 10 min, CA was induced with 1 to 2 mA alternating current delivered to the right ventricle endocardium. Ventilation was discontinued after the onset of VF. After 12 min of untreated VF, CPR, including CCs with the LUCAS 2 (PhysioControl Inc, Lund, Sweden) and ventilation with oxygen (tidal volume of 500 mL, 10 breaths/min), was initiated. At min 2 of CPR, animals received central venous bolus administration of either esmolol or saline, immediately followed by epinephrine. After 5 min of CPR, DF was attempted with a single biphasic 150-J shock, using an MRx defibrillator (Philips Medical Systems, Andover, MA). If ROSC was not achieved, CPR was resumed and continued for 1 min before a subsequent DF. Additional doses of adrenaline were administered at min 7 and 12 of CPR. The resuscitation maneuvers were continued until successful ROSC or for a maximum of 15 min. ROSC was defined as the restoration of an organized cardiac rhythm with a mean arterial pressure of more than 60 mmHg. After that, if VF reoccurred, it was treated by immediate DF. Immediately after resuscitation, the LAD catheter correct placement was reconfirmed by fluoroscopy (*Babini 2018*). After successful resuscitation, anesthesia was maintained, and animals were invasively monitored for 4 h. Forty-five min after resuscitation, the LAD catheter was withdrawn. Temperature of the animals was maintained at 38 °C±0.5 °C during the whole experiment. After 4 hs, catheters were removed,

wounds were repaired, and the animals were extubated and returned to their cages. Analgesia with butorphanol (0.1 mg/kg) was administered by intramuscular injection. At the end of the 96 h post-resuscitation observational period, animals were sacrificed painlessly with an intravenous injection of 150 mg/kg sodium thiopental, and heart and brain were harvested for histology.

5.1.5 Measurements

Hemodynamics, etCO_2 , and ECG were recorded continuously on a personal computer-based acquisition system (WinDaq DATAQ Instruments Inc, Akron, OH). CPP was computed from the differences in time-coincident diastolic aortic pressure and right atrial pressure. CO was measured by thermodilution technique (COM-2; Baxter International Inc, Deerfield, IL). Arterial blood gases were assessed with an i-STAT System (Abbott Laboratories, Princeton, NJ). Plasma hs-cTnT and serum neuronal specific enolase (NSE) were measured with electrochemiluminescence assays (Roche Diagnostics Italia, Monza, Italy).

As previously described (*Babini 2018, Fumagalli 2020, Ristagno 2014*), neurologic recovery was assessed with the Neurologic Alertness Score, ranging from 100 (normal) to 0 (brain death), and with the swine Neurologic Deficit Score, ranging from 0 (normal) to 400 (brain death). Finally, the functional recovery was evaluated before the sacrifice according to Overall Performance Categories as follows: 1=normal, 2=slight disability, 3=severe disability, 4=coma, and 5=brain death or death. Outcome was defined as poor when Overall Performance Categories was ≥ 3 . Scores were assessed by veterinarians blinded to treatment.

At sacrifice, the brains were carefully removed from the skulls and fixed in 4% buffered formalin. Standardized 5-mm coronal slices were taken. The hippocampal CA1 sector and the cortex were chosen as regions of interest and were paraffin embedded. Five-micrometer-thick sections were then obtained and stained with hematoxylin–eosin. The proportion of neuronal loss and degeneration/necrosis (shrunken neurons with deeply acidophilic cytoplasm and pyknotic nucleus) was quantified as absent (0), rare (1), few (2), and numerous (3). Immunohistochemistry with antibody against microglia-specific ionized calcium-binding adaptor molecule 1 (Iba1) was used to detect reactive microglia activation. The evaluation was performed in the pyramidal CA1 layer of the hippocampus. Three fields, corresponding to an area of 0.3 mm² each, were chosen among the most positively stained (hot spots) and photographed. Digital photographs of Iba1-immunostained sections were analyzed with a semiautomated counting software (ImageJ analysis program <http://rsb.info.nih.gov/ij/>). The area of reactive microglia was expressed as the relative area of intensity of Iba-1 staining, over the area of the layer of pyramidal cells, expressed as percentage. An experienced pathologist, blinded to treatment, performed the assessments. Myocardial infarct was assessed by tetrazolium chloride staining. The LV was sliced into 5-mm-thick transverse sections, which were incubated (20 min) in a Tetrazolium Chloride solution and then transferred to 4% formalin overnight before

image analysis. Infarct size was reported as the percentage of Tetrazolium Chloride -negative area relative to LV area (*Babini 2018, Fumagalli 2020, Ristagno 2014*).

5.1.6 Statistical analyses

One sample Kolmogorov–Smirnov Z test was used to confirm the normal distribution of the data. Categorical variables were presented as proportion, while continuous variables as mean \pm SEM or median [Quartile (Q) 1-3], as appropriate. Differences in clinical characteristics according to experimental group (control vs. esmolol) were compared by the Fisher's exact test for categorical variables; T test or nonparametric Mann–Whitney U test was adopted for continuous variables. Two-way ANOVA was used to assess the treatment effect over time in the overall population for hemodynamics and the biomarkers (hs-cTnT, NSE) which were considered in base 10 logarithm transformed. Sidak's post hoc correction for multiple comparisons was used for the comparison between groups at each time point. The sample size was estimated on the total number of DFs delivered prior to final resuscitation. From our data from a previous study (*Ristagno 2014*), assuming a reduction of DFs prior to resuscitation of at least 80% in the esmolol group compared to the control one, 8 animals per group would have been needed to have a power=0.8 ($\alpha=0.05$, 2-sided). A value of $p < 0.05$ was considered significant. Data analyses were performed using GraphPad Prism (version 7.02 for Windows, GraphPad, Software, USA).

5.2 RESULTS

No significant differences in hemodynamics, etCO₂, CO, and arterial blood gases were observed between the 2 groups at baseline (Table 5.2.1).

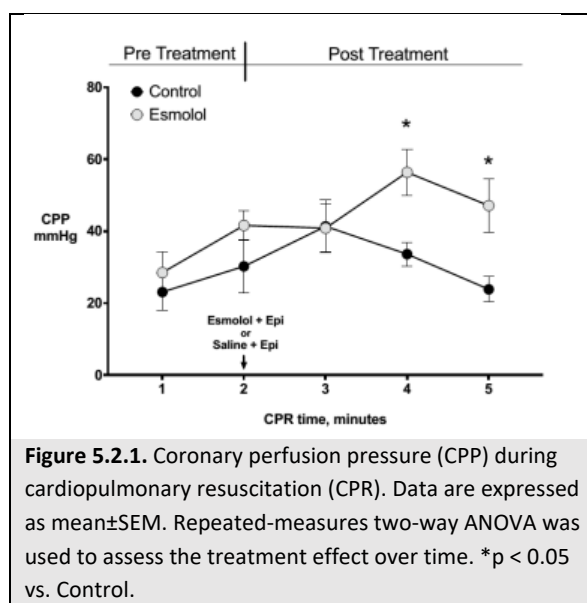
	Control n=8	Esmolol n=8	p value
Heart Rate, beat/min			
BL	98 ± 11	90 ± 8	0.56
PR1	190 ± 10	143 ± 11	0.02
PR2	171 ± 10	135 ± 12	0.05
PR3	167 ± 20	116 ± 13	0.05
PR4	153 ± 19	108 ± 13	0.08
Systolic Arterial Pressure, mmHg			
BL	116 ± 3	117 ± 4	0.82
PR1	102 ± 5	104 ± 8	0.84
PR2	101 ± 5	109 ± 6	0.37
PR3	96 ± 3	110 ± 7	0.11
PR4	93 ± 6	120 ± 4	0.004
Mean arterial pressure, mmHg			
BL	97 ± 4	99 ± 4	0.73
PR1	76 ± 4	86 ± 8	0.25
PR2	83 ± 6	95 ± 5	0.14
PR3	79 ± 6	93 ± 6	0.13
PR4	76 ± 4	103 ± 5	0.002
Diastolic Arterial Pressure, mmHg			
BL	84 ± 3	83 ± 5	0.89
PR1	62 ± 3	75 ± 7	0.13
PR2	72 ± 5	86 ± 5	0.08
PR3	68 ± 6	83 ± 6	0.12
PR4	63 ± 4	93 ± 5	0.001
Right Atrial Pressure, mmHg			
BL	6 ± 1	6 ± 1	0.75
PR1	9 ± 1	6 ± 1	0.11
PR2	8 ± 1	7 ± 1	0.31
PR3	7 ± 1	7 ± 1	0.47
PR4	8 ± 1	6 ± 1	0.21
Mean Pulmonary Artery Pressure, mmHg			
BL	18 ± 2	19 ± 1	0.62
PR1	21 ± 2	20 ± 2	0.65
PR2	19 ± 2	20 ± 2	0.97
PR3	12 ± 1	21 ± 1	0.30
PR4	20 ± 1	21 ± 1	0.67
Pulmonary Capillary Wedge Pressure, mmHg			
BL	10 ± 1	8 ± 1	0.40
PR1	11 ± 2	9 ± 1	0.30
PR2	10 ± 1	8 ± 0	0.18
PR3	11 ± 1	11 ± 1	0.90

PR4	11 ± 1	10 ± 1	0.40
LV Cardiac Output, L/min			
BL	4 ± 0	4 ± 0	0.32
PR1	4 ± 0	4 ± 0	0.85
PR2	3 ± 0	3 ± 0	0.39
PR3	3 ± 0	3 ± 0	0.1
PR4	3 ± 0	3 ± 0	0.47
Stroke volume, ml			
BL	46 ± 4	45 ± 5	0.82
PR1	19 ± 2	25 ± 4	0.20
PR2	19 ± 2	22 ± 2	0.45
PR3	18 ± 4	26 ± 4	0.18
PR4	20 ± 3	33 ± 6	0.09
pH			
BL	7.48 ± 0	7.47 ± 0	0.79
PR2	7.34 ± 0	7.38 ± 0	0.41
PR4	7.40 ± 0	7.41 ± 0	0.70
PaCO₂, mmHg			
BL	38 ± 1	37 ± 1	0.35
PR2	40 ± 1	40 ± 1	0.90
PR4	40 ± 0	41 ± 2	0.77
PaO₂, mmHg			
BL	78 ± 6	79 ± 5	0.93
PR2	111 ± 8	109 ± 9	0.90
PR4	103 ± 13	111 ± 11	0.63
BE, mmol/L			
BL	5 ± 2	3 ± 1	0.45
PR2	-3 ± 2	-2 ± 1	0.54
PR4	1 ± 2	2 ± 2	0.71
HCO₃, mmol/L			
BL	29 ± 1	27 ± 1	0.36
PR2	22 ± 2	25 ± 2	0.36
PR4	25 ± 2	26 ± 1	0.68
Table 6.1.1. Hemodynamics and arterial blood gas analysis. Data are expressed as mean ± SEM. p values refer to Sidak's post hoc correction for multiple comparisons. BL, baseline; PR post-resuscitation hours; LV, left ventricle; PaO ₂ , arterial partial pressure of oxygen; PaCO ₂ , arterial partial pressure of carbon dioxide; BE, base excess. <i>From Ruggeri 2021</i>			

Seven animals in each group were successfully resuscitated. No significant differences were observed between groups in the duration of CPR, in the number of recurrent VFs within 15 min post-ROSC, and in the total number of DFs delivered prior to final resuscitation (Table 6.1.2).

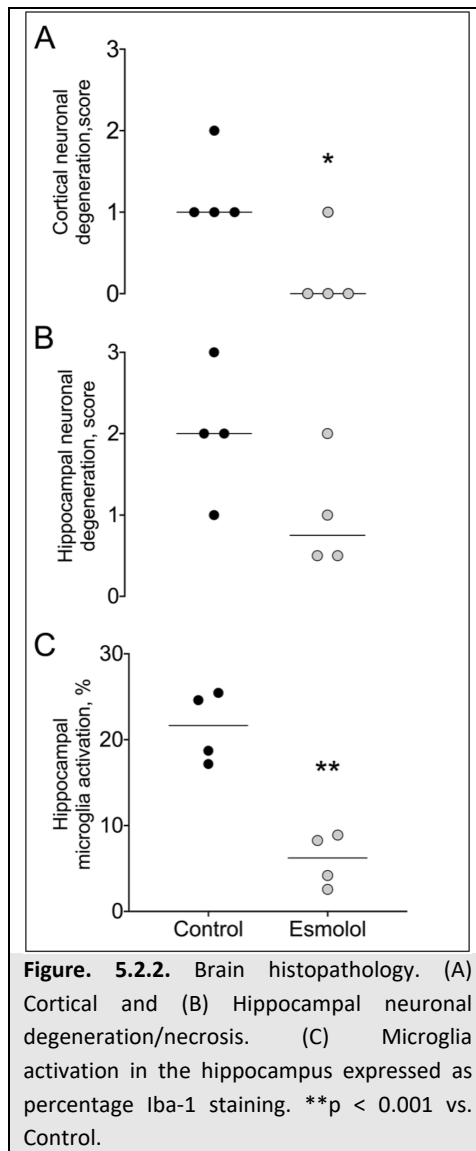
	Control n=8	Esmolol n=8	p value
Defibrillations to ROSC, n	2 [1-2]	1 [1-1.5]	0.43
Recurrent VFs within 15 min post ROSC, n	7 [0.5-19.5]	0 [0-9]	0.29
Duration of CPR prior to ROSC, s	320 [300-62]	304 [301.5-307]	0.88
Total defibrillations delivered to final resuscitation, n	8 [2-29]	7 [1-12]	0.28
Successful resuscitation, n	7/8	7/8	> 0.99
96h survival, n	4/7	4/7	> 0.99
96h survival with good OPC score, n	2/7	3/7	> 0.99
NAS			
24 h	63 [38-88]	63 [21-100]	> 0.99
48 h	76 [50-100]	70 [30-100]	0.60
72 h	76 [53-96]	100 [40-100]	0.90
NDS			
24 h	116 ± 38	119 ± 53	0.97
48 h	65 ± 18	103 ± 50	0.56
72 h	60 ± 35	79 ± 56	0.79

Table 6.1.2. Resuscitation outcome. Data are expressed as median and interquartile range or mean±SEM. ROSC, return to spontaneous circulation; CPR, cardiopulmonary resuscitation; OPC, Overall performance category (OPC was defined good when=1–2); NAS, Neurological Alertness Score; NDS, Neuronal Deficit Score. *From Ruggeri 2021*



During the initial 2 min of CPR, CPP was equivalent in the 2 groups. However, following treatment administration, CPP was significantly higher in the esmolol group compared to the control one ($p < 0.05$, Figure 5.2.1).

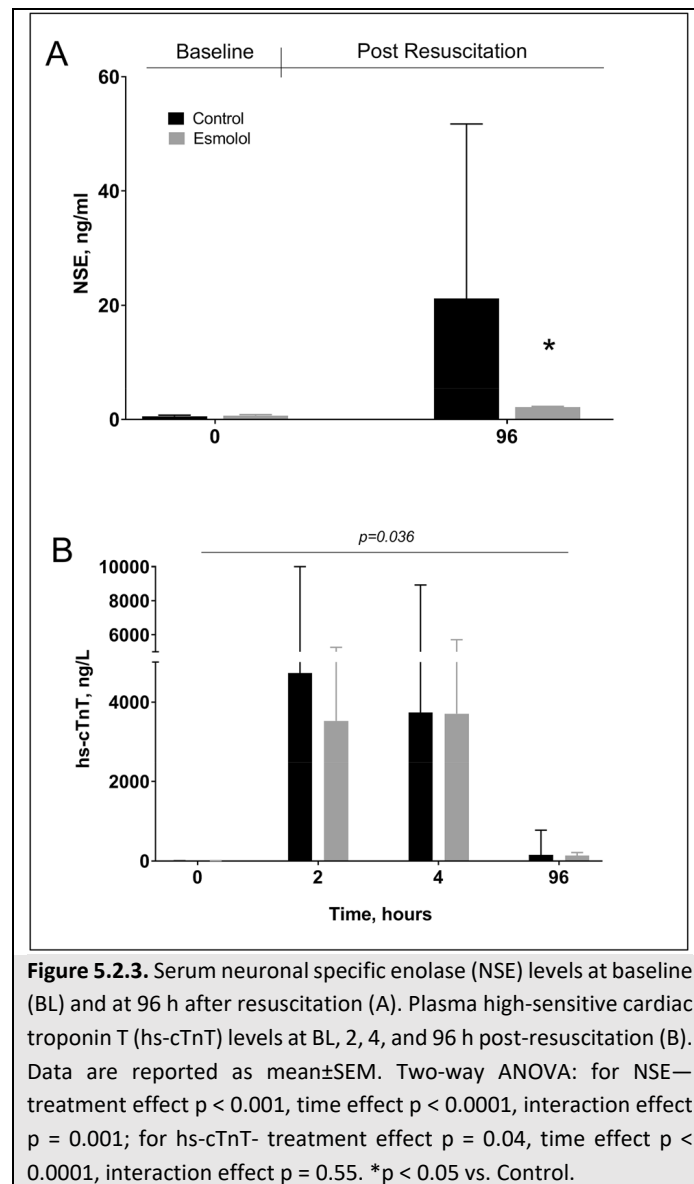
Post-resuscitation heart rate was lower in the esmolol group compared to the control group, with a significant reduction at 1 h after resuscitation ($p = 0.02$, Table 6.1.1). This was associated with significantly higher systolic, mean, and diastolic arterial pressures in animals treated with esmolol compared to those receiving placebo (Table 6.1.1). No differences in post-resuscitation pulmonary hemodynamics and cardiac function parameters were observed between the 2 groups, although a trend towards a higher stroke volume was observed in the esmolol group compared to the control one 4 h after resuscitation ($p = 0.09$, Table 6.6.1).



There were no differences between groups in the number of animals that survived up to 96 h, and in good neurological recovery, although a trend in favor of esmolol was observed (43% vs. 29%, Table 6.1.2). Brain histology showed a significant reduction in cortical neuronal degeneration/necrosis in the esmolol group compared to the control one (mean score 0.3 vs. 1.3, $p = 0.03$, Figure 5.2.2a), while only a trend was present in the hippocampal region (mean score 1 vs. 2, $p = 0.11$, Figure 5.2.2b). A marked reduction of microglial

activation in the hippocampus was also observed after treatment with esmolol compared to control (mean % 6 vs. 2, $p < 0.001$, Figure 5.2.2c).

Significantly lower circulating levels of NSE were measured in esmolol animals compared to controls at 96 h after resuscitation (median 2.2 vs. 21, $p < 0.0001$, Figure 5.2.3a). Plasmatic levels of hs-cTnT were lower in the esmolol group compared to the control one up to 96 h after resuscitation (Figure 5.2.3b, $p = 0.04$). However, macroscopic anatomy of the heart showed similar LV infarct size between the 2 groups (13% vs. 9%, $p = 0.23$).



5.3 DISCUSSION

5.3.1 Main findings

This experimental study demonstrated that in a porcine model of ischemically induced CA, esmolol administration together with epinephrine during CPR reduced neurological injury, as represented by less neuronal degeneration, microglial activation, and lower circulating levels of NSE, compared to placebo with epinephrine. Esmolol in addition to epinephrine during CPR also accounted for a higher CPP compared to saline plus epinephrine and prevented post-resuscitation tachycardia and arterial hypotension. No effects on long term functional outcome were observed. However, the primary endpoint of the study was not demonstrated, as no difference in the number of DFs needed to resuscitation was detected between the groups.

5.3.2 VF termination

The beneficial effects of esmolol in terminating VF have been reported in small retrospective case series including CA patients with refractory VF, indicating that β 1-blockade should be considered in this setting prior to cessation of resuscitative efforts (*Driver 2014, Lee 2016*). This was not the case in our study, in which neuroprotection represented the main result after administration of esmolol during CPR.

5.3.3 Neuroprotection

Neuroprotection with reduced hippocampal neuronal degeneration and smaller cortical infarct size by esmolol compared to control has been previously described after transient focal ischemia in rats (*Goyagi 2012; Goyagi 2012b*). Our group has also previously reported that epinephrine reduced cerebral cortical microvascular blood flow increasing the severity of cerebral ischemia during CPR in pigs, while β -blockade, in association with an α -1 adrenergic antagonist, reverted this detrimental effect (*Ristagno 2009*). More recently, in a porcine model of prolonged VF, a bolus of esmolol during CPR has been proven to alleviate the impairment of cerebral microcirculation caused by the administration of epinephrine and to improve neurological outcome, in comparison to epinephrine alone (*Li 2019*). Indeed, the density of perfused vessel was higher in esmolol-treated animals with a preserved morphology of brain endothelial cells, which appeared disrupted by epinephrine (*Li 2019*). Thus, a better cortical microcirculation after esmolol may be hypothesized and likely accounted for the markedly reduced neuronal degeneration/necrosis together with neuroinflammation and NSE release observed in our study. Unfortunately, neuroprotection by combination of esmolol and epinephrine was observed only on histopathology and circulating biomarkers, while no effect on long term neurological recovery was found. One reason might be the relatively small sample of animals, attributable to many resuscitated pigs (42%) dying in the first days after resuscitation. These early deaths, while reinforcing

the clinical relevance of this model of CA with an underlying AMI, obscured the neurological outcome in the dead animals. Although the same mortality rate was observed in both groups, if animals died due to the AMI, as it may be extrapolated by the greater hs-cTnT release in the control group, or due to a more severe brain damage, cannot be clarified.

Another possible explanation for the neuroprotective effect of β 1-blockade observed during CPR might be the higher CPP recorded after esmolol administration compared to placebo, which might have accounted for a higher cerebral perfusion and consequent prevention of neuronal injury. Previous experimental CPR studies showed the same increase in CPP starting 1 min after esmolol administration and maintained throughout resuscitation compared to placebo (*Cammarata 2004; Ringgaard 2019*). Esmolol would likely decrease the oxygen requirements of the myocardium during VF, further exacerbated by epinephrine, and thereby minimize global ischemic injury and ATP content reduction. This might mitigate the evolution towards the condition of stone heart, consequently improving left ventricle compliance and stroke volume generated by chest compression and ultimately CPP, compared to epinephrine alone (*Tang 1995; Klouche 2002*). We also observed that post-resuscitation tachycardia and arterial hypotension were prevented by esmolol, likely contributing to a better post-ROSC cerebral perfusion, further preserving the brain.

5.3.4 Cardioprotection

Multiple studies in models of electrically induced VF demonstrated that esmolol given during CPR seemed to modulate the electrical properties of the myocardium and intracellular calcium handling, which contributed to the reduction in the occurrence of recurrent and resistant VFs and to a better post-resuscitation myocardial function (*Tang 1995, Jingjun 2009; Theochari 2008; Killingsworth 2004*). Whether the cardioprotective effect of esmolol is still maintained in the instance of ischemically induced CA remains yet to be elucidated. Indeed, no improvement in CO or reduction of myocardial infarct size has been observed after a single dose of esmolol prior to adrenaline compared to placebo in a recent study employing an ischemic CA pig model with extracorporeal resuscitation (*Karlsen 2019*). In our model, myocardial protection was suggested by the reduced levels of circulating hs-cTnT observed after beta-blocked administration compared to the use of placebo. However, LV infarct size was similar in the two groups and VF was not terminated by a lower number of DFs in esmolol-treated animals compared to controls, as initially hypothesized.

5.3.5 Limitations

Whether starting a continuous infusion of esmolol after the initial bolus or first ROSC would have been more effective in preventing recurrency of VF and achieving sustained ROSC than the single bolus remains unknown. Nevertheless, the single bolus injection strategy was chosen for its high translational and practical application in the clinical out-of-hospital settings.

Other limitations should be acknowledged. Firstly, this was a purely descriptive study. Indeed, earlier experimental studies have already compared epinephrine with other different vasopressor treatments during CPR, i.e. noradrenaline, vasopressin, epinephrine associated with selective/non-selective beta blockers, amines with predominant α -1 adrenergic actions, α -2 adrenergic agonists, consistently reporting the greater myocardial oxygen consumption after epinephrine as the main mechanisms accounting for post-resuscitation myocardial dysfunction and anticipating more optimal vasopressor interventions (*Tang 1995, Cammarata 2004, Zhang 2013, Brown 1986; Pellis 2003, Klouche 2003, Prengel 2005, Lindner 1990*). Unfortunately, among the above interventions, those investigated clinically, i.e. norepinephrine and vasopressin, failed to improve outcome compared to epinephrine (*Callahan 1992, Soar 2019*). More specifically, esmolol administered with epinephrine during CPR has been consistently shown to reduce myocardial dysfunction and to increase the rate of ROSC in contrast to epinephrine alone in the electrically induced VF, and mechanisms have been already described (*Cammarata 2004, Theochari 2008, Killingsworth 2004, Zhang 2013*). Thus, the present study was designed to confirm these beneficial effects of esmolol when added to epinephrine in a model of ischemically induced CA, while concurrent comparison with other vasopressors was not replicated. Secondly, since the original endpoint of this study was VF termination and not neurological outcome, no measures of cerebral perfusion pressure or carotid blood flow or regional brain oxygenation were planned to directly investigate and/ or provide specific mechanistic insights of neuroprotection. Nevertheless, earlier studies have already described improved cerebral perfusion when β -blockade was associated with epinephrine during CPR (*Ristagno 2009, Li 2019*). Thirdly, since the sample size was calculated considering the above primary endpoint, although the experimental model reproduced a clinically relevant condition with ischemic VF and a prolonged no-flow time, the number of animals in each group was not powered to detect a significant difference in long-term neurological outcomes. Fourthly, we are aware that the optimal hemodynamics usually observed in models of CPR performed in the laboratory, i.e. high CPP values after a prolonged untreated CA, can be hardly reproduced during a clinical resuscitation.

Finally, post-resuscitation myocardial function was not directly assessed, i.e. through echocardiography; however, data on heart rate, hemodynamics, stroke volume, and circulating biomarkers confirm evidence of cardioprotection.

6 STUDY 2. AMSA TO GUIDE DEFIBRILLATION DURING CPR IN OHCA PATIENTS: A PILOT, RANDOMIZED CONTROLLED TRIAL (AMSA TRIAL)

6.1 METHODS

6.1.1 Study design

AMSA trial was originally designed as a phase III multicenter, open-label, efficacy, randomized, controlled clinical trial in OHCA, registered with ClinicalTrials.gov, NCT03237910. A total of 388 patients were planned to be enrolled by the EMS of Milan and Monza (SOREU Metropolitana, Azienda Regionale Emergenza Urgenza – AREU, Milan), and Bologna (Maggiore Hospital, AUSL, Bologna) in Italy. Espoo EMS, Helsinki, Finland, also joined the trial in January 2020, but did not enroll patients. The protocol was approved centrally by the Ethic Committee AREA 2 Milano, Fondazione IRCCS Cà Granda Ospedale Maggiore Policlinico, Milan, Italy (approval n. 772-2020) and then by the Ethics Committees in each participating Center. The use of an investigational modified X-Series defibrillator, ZOLL Med. Corp. Chelmsford, USA, was notified to the Italian Ministry of Health, according to National regulations. The trial qualified for exception from informed consent under emergency circumstances. A deferred written consent was then obtained from each patient who survived and regained mental capacity or from a legal surrogate, depending on the circumstances. A Data and Safety Monitoring Board was appointed.

The trial formally started on November 2018 with the training of the EMS personnel. Patients' enrolment was then planned to start on April 1st, 2019, but it was deferred till October 1st, 2019, because the AMSA-equipped defibrillators underwent an urgent software update by ZOLL Med. Corp. Headquarter in the US, due to an internal error alert evidenced in some device during the regular morning test. On February 20th, 2020, enrolment was then stopped till August 2020 due to the first COVID-19 pandemic wave that hit the Northern Italy (*Grasselli JAMA 2020*). In September 2020, the EMS teams underwent a retraining on the trial protocol to restart the study in October 2020; however, a second COVID-19 pandemic wave started in October and lasted till June 2021. Thus, on July 27th, 2021, the Steering Committee formally decided to stop the study due to low rate recruitment. AMSA trial therefore become a pilot study reporting the first in-human use of real-time AMSA analysis to guide CPR.

6.1.2 Patient population

All adult patients (age ≥ 18 years old) with an OHCA of presumably cardiac etiology and with a presenting shockable rhythm, i.e. VF or pulseless ventricular tachycardia, were eligible for inclusion. Exclusion criteria included age < 18 years, CA with a presenting non-shockable rhythm, traumatic CA, CA from a presumably non-cardiac cause, presumable irreversible death or known terminal illness, pregnancy, DF delivered by an automated external defibrillator prior to EMS arrival, enrolment in another clinical or device trial within the previous 30 days, refused informed consent to the use of data.

6.1.3 Randomization

The interventions, i.e. AMSA-CPR or standard-CPR were assigned randomly to each EMS team, using a centrally generated randomization plan. The randomization was balanced in every center by a stratified scheme. The assignment of intervention followed a complete crossover design, so that each EMS team was switched from one intervention to the other according to a predefined 3-month period. EMS teams were assigned to the intervention with AMSA- or standard-CPR in a 1:1 ratio. Upon arrival to the OHCA scene, the physician of the EMS team verified inclusion and exclusion criteria and eligibility for the study and was responsible for enrolment. Randomization scheduled was generated at the Coordinating Center, Istituto di Ricerche Farmacologiche Mario Negri, IRCCS, Milan, Italy.

6.1.4 Real-time AMSA analysis

An X-Series defibrillator (ZOLL Med. Corp., MA, USA) with a new software capable to measure and display AMSA values in real-time, was used for the trial. Beside AMSA, the X-Series units monitored all other patient vital signs, as a regular X-Series device. The “OneStep CPR electrodes” (ZOLL Med. Corp., MA, USA) were employed for the study (Figure 6.1.1). These defibrillatory pads presented an acceleration sensor that located between the rescuer's hands and the patient's lower sternum monitored rate and depth of CCs (Figure 6.1.2, 6.1.3).

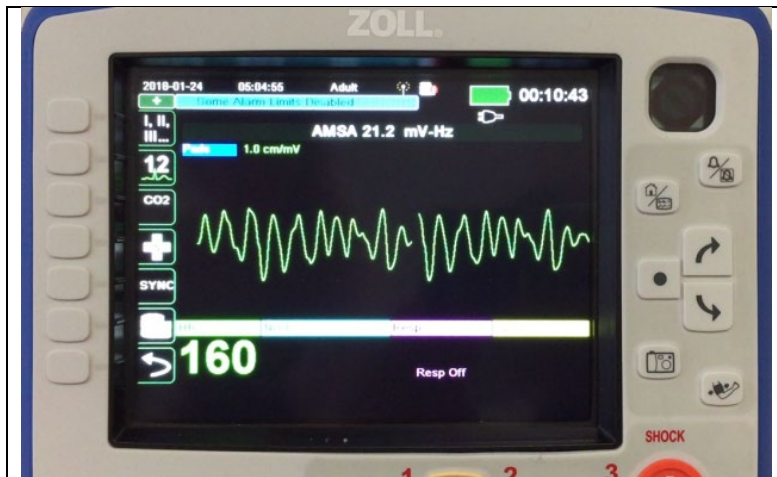


Figure 6.1.1. Zoll X Series Defibrillator displaying the AMSA value on the screen.



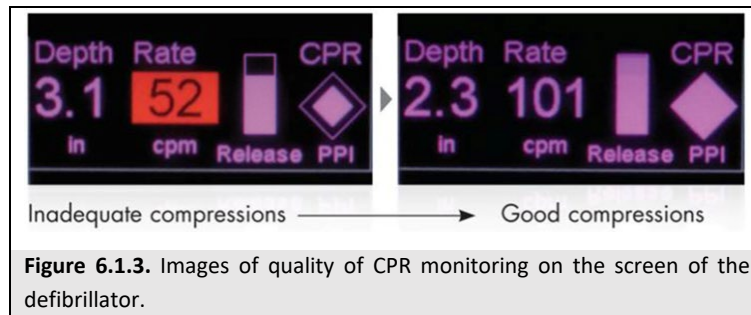
Figure 6.1.2. Defibrillatory pads.

AMSA calculation was performed in real-time by a built-in software, which acquired the ECG signal from the defibrillatory pads and displayed the value continuously, as shown in Figure 6.1.1.

The VF waveform analysis required an artefact-free signal and thus it was performed during the hands-off interval for delivering of 2 ventilations (Vs). For this reason, CPR was performed with a CC:V ratio of 30:2, even in the presence of an established advanced airway. Thus, through the accelerometer sensor located in the defibrillatory pads, the software recognized pauses in CC and started AMSA analysis on a 512-point window (2.05 sec), such that AMSA value was displayed on the defibrillator screen in approximately 3 sec. ECG signals were processed in real-time using the algorithm previously published (Ristagno 2015). Briefly, a 2-Hz high-pass filter was employed to minimize low-frequency artefacts and a 48-Hz low-pass filter to remove interference of ambient noise at higher frequencies. ECG signals were then converted from a time to a frequency domain by fast Fourier Transform. A Tukey Fourier Transform window was used to reduce edge effects.

AMSA was calculated as the sum of the products of individual frequencies and their amplitudes: $AMSA = \sum A_i \cdot F_i$, where A_i represented the amplitude at i th frequency F_i .

The AMSA defibrillator was used in both study groups, but the AMSA analysis algorithm was turned on only in the AMSA group, while the standard-CPR arm used the defibrillator as a regular X-Series. After each case, the defibrillator data, including CPR, quality feedback, defibrillation recordings, and AMSA values, if the AMSA algorithm was activated, were downloaded and stored in a centralized ECG biobank to be reviewed and analyzed.



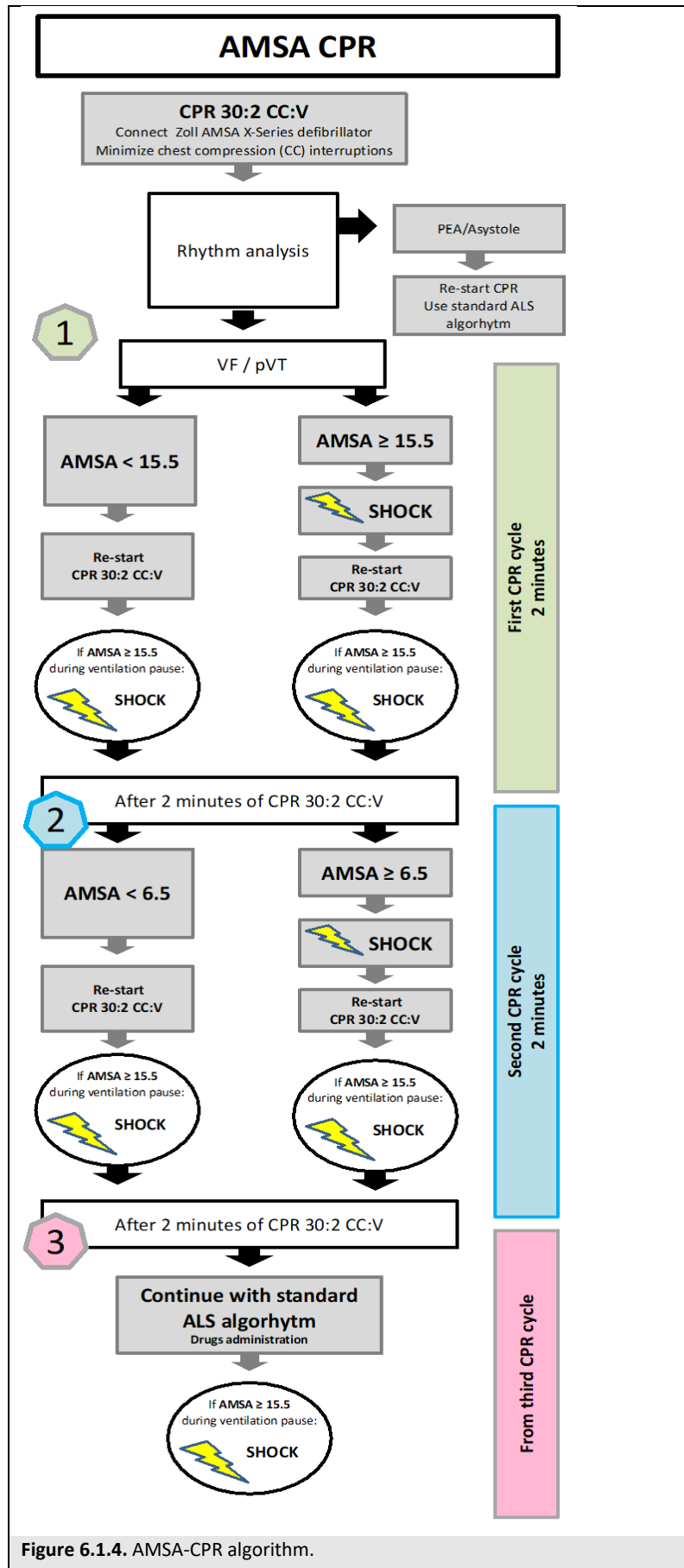


Figure 6.1.4. AMSA-CPR algorithm.

6.1.5 Trial interventions

The interventional protocol applied in the AMSA-CPR group is detailed in Figure 6.1.4. Upon arrival to the CA victim, the EMS rescuers started CCs while the defibrillatory pads were applied and the AMSA defibrillator switched on. The first AMSA value was then read on the defibrillator screen (Figure 6.1.1) and: if AMSA was ≥ 15.5 mV-Hz, an immediate DF was attempted, followed by CPR for 2 min, with a CC:V of 30:2; if AMSA was < 15.5 mV-Hz, DF was not attempted while CPR (with a 30:2 CC:V) was performed for 2 min. After completion of the first 2-min CPR cycle, AMSA was read again and: if it was ≤ 6.5 mV-Hz, the DF was not attempted, and CPR continued for an additional 2-min cycle; if AMSA was > 6.5 mV-Hz, an immediate DF attempt was delivered, followed by a 2-min CPR cycle.

After completion of the second 2-min CPR cycle and till the end of the resuscitative intervention, CPR was then continued based on standard 2015 European Resuscitation Council guidelines (a DF attempt every 2-min CPR cycles). During the whole resuscitation period, AMSA was measured during pauses for ventilations (Vs) (every 30 CC, approximately every 20-25 sec) and in case it was ≥ 15.5 mV-Hz an immediate DF attempt was anticipated, prior to complete the 2-min cycle (Figure 6.1.4).

In the Standard-CPR arm, the DF was delivered based on the 2015 European Resuscitation Council CPR guidelines (*Soar 2015*): an immediate DF when the defibrillator was ready and then a subsequent attempt at the end of each 2-min CPR cycle, with a 30:2 CC:V ratio.

In both groups, rescuers received real-time feedback on the quality of CC and Vs. CPR drugs for shockable rhythms, i.e. adrenaline and amiodarone, were given based on 2015 European Resuscitation Council guidelines, i.e. at the beginning of the 3rd CPR cycle and repeated accordingly to recommendations (*Soar 2015*). All patients who survived to hospital admission were admitted to Intensive Care Unit and received post-resuscitation care accordingly to local standards of care, based on European Resuscitation Council guidelines (*Nolan 2015*). Long-term survival was evaluated through a telephone interview by a qualified evaluator, together with neurological recovery by cerebral performance category (CPC 1: a return to normal cerebral function and normal living; CPC 2: cerebral disability but sufficient function for independent activities of daily living; CPC 3: severe disability, limited cognition, inability to carry out independent existence; CPC 4: coma; CPC 5: death or brain death).

6.1.6 Selected AMSA threshold for defibrillation delivery decision

AMSA decisional thresholds, i.e. ≥ 15.5 mV-Hz to prompt for early DF and < 6.5 mV-Hz to refuse DF in favour of CPR, were chosen based on an earlier retrospective study conducted by our group in a large clinical database of OHCA (*Ristagno 2015*). More specifically, an ECG database including 2.447 DF attempts from 1.050 patients, was used as derivation group, while an additional database, including 1.386 DF attempts from 567 patients, served as validation group. The following AMSA thresholds were identified in the validation group:

≥ 15.5 mV-Hz predicted DF success with a PPV of 84%, while AMSA < 6.5 mV-Hz predicted DF failure with a NPV of 98%.

6.1.7 EMS training

From November 7th, 2018, to February 28th, 2019, physicians and nurses of the Advanced Life Support teams in Milan, Monza, and Bologna EMS underwent a training program, including frontal lessons and hands-on workshops with simulated scenario on the mannikin, to familiarize with the AMSA-defibrillator and to gain confidence with the AMSA interventional protocol. More specifically, training focused on: correct defibrillatory pads position; correct hands placement in order to minimize artefacts on the ECG; capability to read AMSA values during pauses for Vs; recognizing AMSA threshold values and corresponding CPR manoeuvres; protocol algorithm. A training booklet, together with flowcharts and tutorial videos were also created and were available for the EMS personnel (Figure 6.1.5). In Milan and Monza EMS, 50 training courses were organized for a total of 278 rescuers, including both physicians and nurses; in Bologna 20 courses were organized for a total of 123 rescuers, both physicians and nurses, for 5 Advanced Life Support vehicles. After the end of the training period, EMS teams employed the AMSA-defibrillators (with the AMSA algorithm disabled) for a month (from March 1st, 2020, to March 31st, 2020) as device for all the rescue missions, to familiarize with the use of this device, prior to start patients' enrollment. After enrollment started, retraining sessions were organized every 3 months, i.e. prior to the next randomization block. Espoo EMS teams underwent the same training program as above from January 2020, then stopped for trial discontinuation. Two training courses were organized and 20 rescuers, including physicians and paramedics, for 2 Advanced Life Support vehicles were trained.

6.1.8 Outcomes

The former primary efficacy outcome of the trial was termination of VF/pulseless ventricular tachycardia with achievement of ROSC. Secondary outcomes included: number of DF attempts and duration of CPR prior to ROSC; hs-cTnT; short-term and long-term survival with good neurological function at 1 and 6 months; effects of CPR quality on AMSA.

Assuming an incidence of the primary endpoint of 35% in a historical cohort (*Ristagno 2015*), a sample size of 194 patients per group would have been required for the study to have 80% power to detect a 14% absolute improvement (resulting in an endpoint frequency of 49% in the AMSA group) with a two-sided α level of 5%.

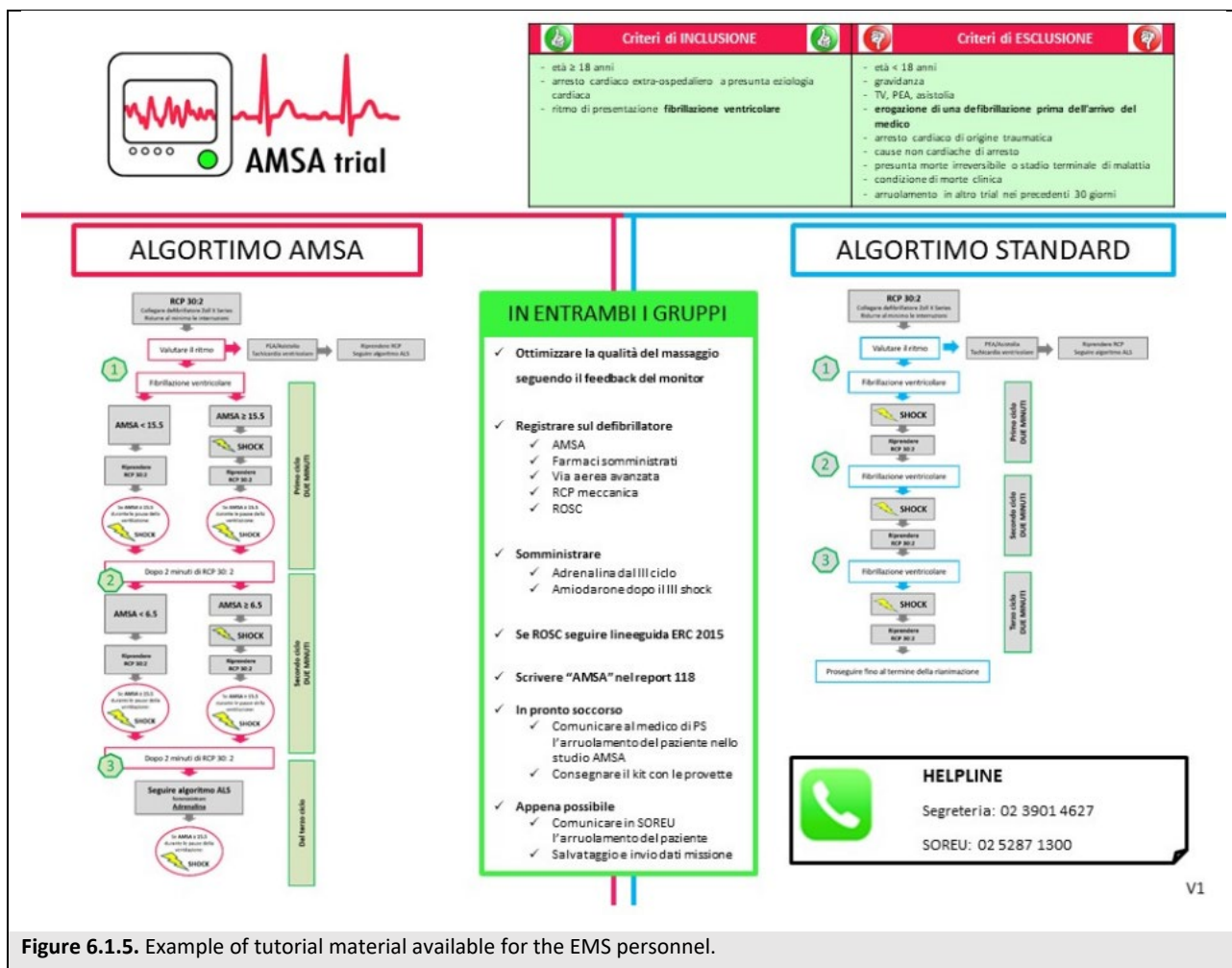


Figure 6.1.5. Example of tutorial material available for the EMS personnel.

Due to the early discontinuation of the trial, the study enrolled only 31 patients (8% of the calculated sample size) and thus was underpowered to show difference between the treatment groups and to demonstrate the above endpoints. Thus, AMSA trial turned into a pilot multicenter randomized clinical study reporting the first-time human use of a real-time AMSA analysis during CPR in OHCA patients. The main aim of the study was redirected into testing the hypothesis that a real-time AMSA analysis during CPR was feasible and might predict the success of DF.

DF outcome was defined according to established criteria (Ristagno 2013 and 2015) as "DF Success" if DF restored an organized rhythm with heart rate ≥ 40 bpm, potentially associated with ROSC, commencing within 60 sec after DF and as "DF Failure" if any other rhythm, including VF/ventricular tachycardia and asystole or low heart rate < 40 bpm, occurred. "Any ROSC" was defined as any documented ROSC in the absence of ongoing CC (Gräsner 2020). "Sustained ROSC" was achieved when the spontaneous circulation was maintained up to 20 min and/or till hospital admission. Long-term outcomes included survival to hospital discharge and at 1 and 6 months. Favourable neurological outcome was defined as a CPC score of 1-2.

Information to assess the outcomes were entered by investigators into a secure web-based Case Report Form Research Electronic Data Capture - REDCap software, <https://redcap.marionegri.it>.

6.1.9 Statistical analyses

The main analyses have been performed according to an intention-to-treat approach. Descriptive statistics were reported as counts and percentages for categorical variables and as mean with standard deviation (SD) or median with Q1 to Q3 for continuous variables and counting processes. Normal distribution of data was investigated.

Comparison between groups, AMSA-CPR vs. Standard-CPR, was performed by one-way ANOVA for continuous variables or Fisher exact test for categorical ones. Comparisons between mean AMSA values for DF outcome were performed with the use of regression methods that accounted for the correlation between repeated measures for each patient, whereas comparisons for the other outcomes (sustained ROSC and survival until hospital discharge and 1 and 6 months after CA) were performed with the t test or ANOVA.

Logistic regression was used to investigate the association between AMSA and the different outcomes, i.e. DF outcome (with repeated measure adjustment when all DFs were considered) and sustained ROSC, while Cox regression models were used for survival at hospital discharge, survival at 6 months. AMSA was included separately in the model as continuous variable. Unadjusted and adjusted relative risks (RR), with the corresponding 95% CI, are reported: OR for logistic models and Hazard Ratio (HR) for Cox regression models respectively. The estimates were adjusted for age and gender, EMS arrival time, and presence of STEMI.

The discriminatory ability of AMSA was measured as AUC with the use of DF success (with repeated-measures adjustment for all DFs) and sustained ROSC as outcomes. AUC with 95% CI and p values for difference from chance (AUC=0.5) are reported.

The sensitivity, defined as the capability of AMSA to identify a DF success, was calculated as the number of correctly predicted successful DFs divided by the total number of successful DFs.

The specificity, which referred to the capability of AMSA to identify a DF failure, was calculated as the number of correctly predicted unsuccessful DFs divided by total number of unsuccessful DFs. PPV referred to the proportion of DFs predicted by AMSA to be successful and that actually were successful. NPV represented the proportion of DFs that were predicted by AMSA to be not successful and that actually failed. The accuracy was calculated as the proportion of true results (both true positively predicted successful DFs and true negatively predicted unsuccessful DFs) in the population. Finally, sensitivity, specificity, PPV, NPV and accuracy curves were computed to evaluate threshold values of AMSA.

A P value of less than 0.05 was considered to indicate statistical significance. All statistical analyses were performed using SPSS version 27.

6.2 RESULTS

6.2.1 Study Population

A total of 31 patients were enrolled in the trial, 19 randomized to AMSA-CPR and 12 to standard-CPR. Baseline characteristics, CPR interventions, and outcomes were similar between the two groups and are summarized in Table 6.2.1.

	Total n=31	AMSA-CPR n=19	Standard-CPR n=12
Gender, male n (%)	24 (77)	15 (79)	9 (75)
Age, yr	65 ± 13	63 ± 15	67 ± 8
Pre-arrest CPC 1, n (%)	30 (100)	18 (100)	12 (100)
STEMI, n/tot (%)	12/19 (63)	7/9 (78)	5/10 (50)
NSTEMI, n/tot (%)	4/19 (21)	1/9 (11)	3/10 (30)
No, n/tot (%)	3/19 (16)	1/9 (11)	2/10 (20)
Successful PCI, n/tot (%)	13/19 (68)	7/9 (78)	6/10 (60)
Witnessed cardiac arrest, n (%)			
Yes, lay bystander	22 (71)	13 (68)	9 (75)
Yes, EMS	7 (23)	4 (21)	3 (25)
No	2 (7)	2 (11)	0
Bystander CPR before EMS arrival, n (%)			
Yes, complete	4 (13)	3 (16)	1 (8)
Yes, compressions only	15 (48)	8 (42)	7 (58)
No	10 (32)	6 (32)	4 (33)
Unknown	2 (7)	2 (11)	0
EMS arrival time, min	9 ± 3	10 ± 2	9 ± 4
CPR duration to sustained ROSC, min	18 ± 14	23 ± 16	14 ± 12
Number of defibrillation attempts, n	3.9 ± 3.8	4.7 ± 4.4	2.7 ± 2.4
Chest compression depth, cm	4.8 ± 1.3	4.6 ± 0.9	5.0 ± 1.8
Chest compression rate, CC/min	125 ± 14	128 ± 15	120 ± 13
Chest compression fraction, (%)	69 ± 19	73 ± 10	62 ± 28
Patients receiving adrenaline, n (%)	22 (71)	15 (79)	7 (58)
Patients receiving amiodarone, n (%)	17 (55)	14 (74)	3 (25) *
Sustained ROSC, n (%)	18 (58)	9 (53)	9 (75)
Survival to hospital discharge, n (%)	14 (45)	8 (42)	6 (50)
1-month survival, n (%)	14 (45)	8 (42)	6 (50)
6-month survival, n (%)	13 (42)	7 (37)	6 (50)
6-month survival with CPC 1-2, n (%)	12 (39)	6 (31)	6 (50)

Table 6.2.1. Population characteristics and outcomes. * $p \leq 0.05$ vs. AMSA CPR. CPC, Cerebral Performance Category; STEMI, ST Segment Elevation Myocardial Infarction; NSTEMI, non ST Segment Elevation Myocardial Infarction; PCI, Percutaneous Coronary Intervention; EMS, Emergency Medical Services; CPR, Cardiopulmonary Resuscitation; ROSC, Return of spontaneous Circulation.

Seventy-seven percent of patients were male with a mean age of 65 years, and in 63% of the 19 patients admitted alive to the hospital, a STEMI was present. Ninety-four percent of CAs were witnessed, 71% by a lay bystander, while 23% directly by the EMS. Bystander CPR was performed in 61% before EMS arrival at the CA scene, which averaged 9 min from the emergency call. No differences between AMSA- and standard-CPR groups were observed.

Patients received CPR for an average of 18 min prior to sustained ROSC. A mean of 4 DF attempts were delivered for each patient, over the resuscitation intervention, with no differences between groups. No differences in CPR quality, i.e. CC depth, rate and fraction, and in administration of adrenaline, were reported between the two groups. More patients in the AMSA group received amiodarone during CPR, compared to those in the standard-CPR arm ($p < 0.05$, Table 6.2.1).

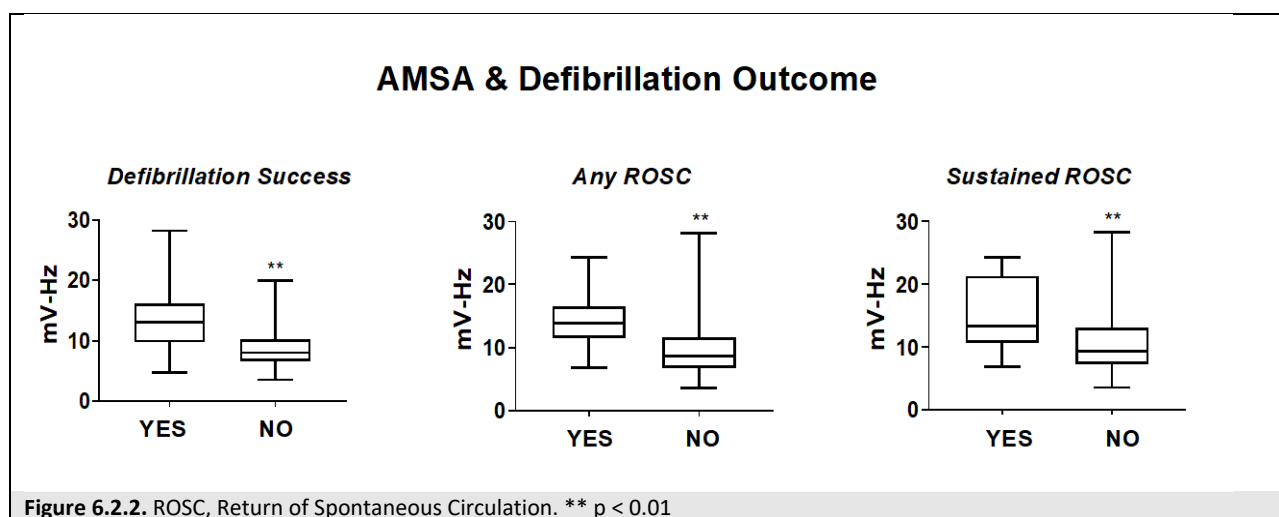
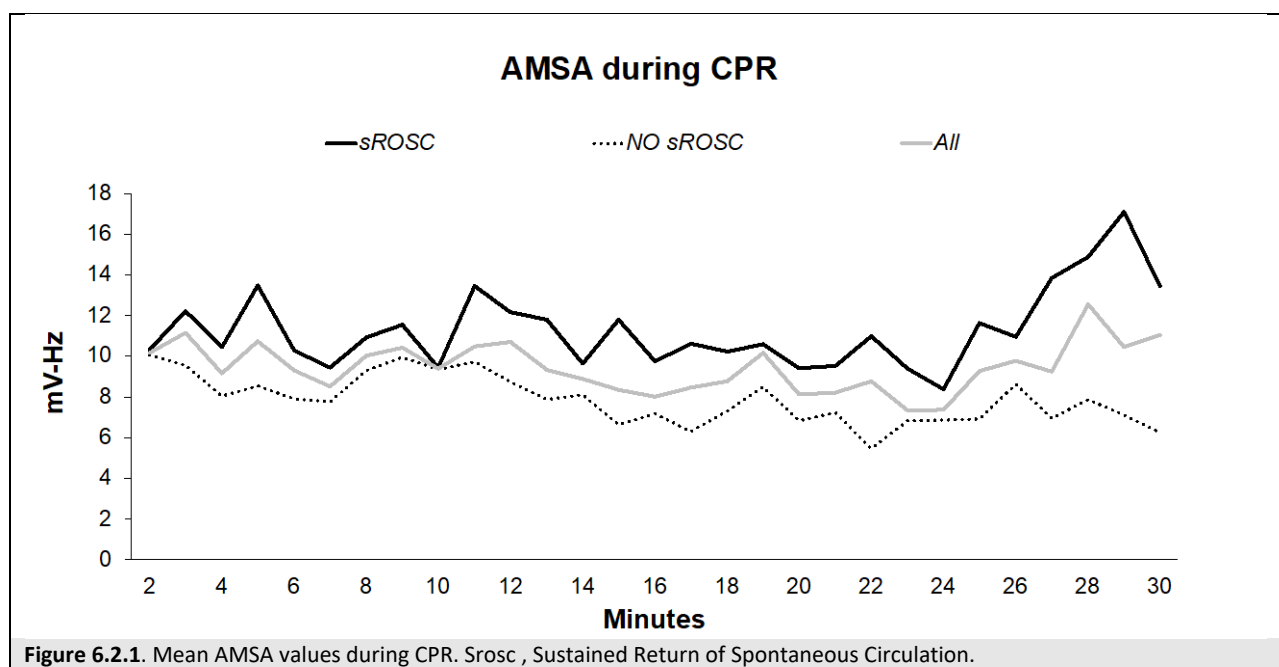
6.2.2 Overall defibrillation and clinical outcomes

A total of 121 DFs were attempted in the 31 patients enrolled, 89 in the AMSA-CPR and 32 in the standard-CPR group. No differences in DF outcomes were observed between the 2 groups. Sustained ROSC was achieved in 58% of patients and 1-month survival was 45%. Thirty-nine percent of patients were alive at 6 months with a good neurological recovery. No differences in short and long-term outcomes were observed between AMSA-CPR and standard-CPR groups (Table 6.2.1).

6.2.3 AMSA and defibrillation outcomes

The following analyses were performed in the 19 patients enrolled to AMSA-CPR, in whom AMSA was measured real-time during resuscitation and a total of 86 DFs were delivered. Mean AMSA was 9.5 ± 1.2 mV-Hz during the first 30 min of resuscitation. AMSA values over time are represented in Figure 6.2.1. Higher values of AMSA were observed in patients who achieved sustained ROSC, in whom AMSA increased during CPR, compared to those who were not resuscitated, in whom AMSA decreased overtime (Figure 6.2.1).

AMSA was significantly higher before a successful DF than a failing one ($p < 0.01$, Figure 6.2.2). DFs leading to any ROSC and sustained ROSC also presented an AMSA significantly higher compared to that measured prior to DF attempts with poor outcomes ($p < 0.01$, Figure 6.2.2).



The AUC values for association of AMSA with DF success and sustained ROSC were 0.78 (95%CI, 0.69-0.89; $p < 0.01$) and 0.75 (95%CI, 0.59-0.90; $p < 0.05$), respectively. Higher AMSA was significantly associated with DF success, any ROSC, and sustained ROSC, with an unadjusted OR respectively of 1.31 (95% CI, 1.14–1.52, for 1 mV-Hz increase), 1.26 (95%CI, 1.08-1.49, for 1 mV-Hz increase), and 1.18 (95%CI, 1.04-1.35, for 1 mV-Hz increase), as detailed in Table 6.2.2. In the multivariable logistic regression analyses, after adjustment for age, gender, EMS arrival time, and presence of STEMI, higher AMSA values remained significantly associated with DF success, with an OR of 1.23 (95%CI, 1.06-1.45, for 1 mV-Hz increase, Table 6.2.2). AMSA was not associated with long-term outcomes (HR for poor outcome, i.e. CPC 3-5: 0.65 95%CI 0.25-1.71, for 1 mV-Hz increase).

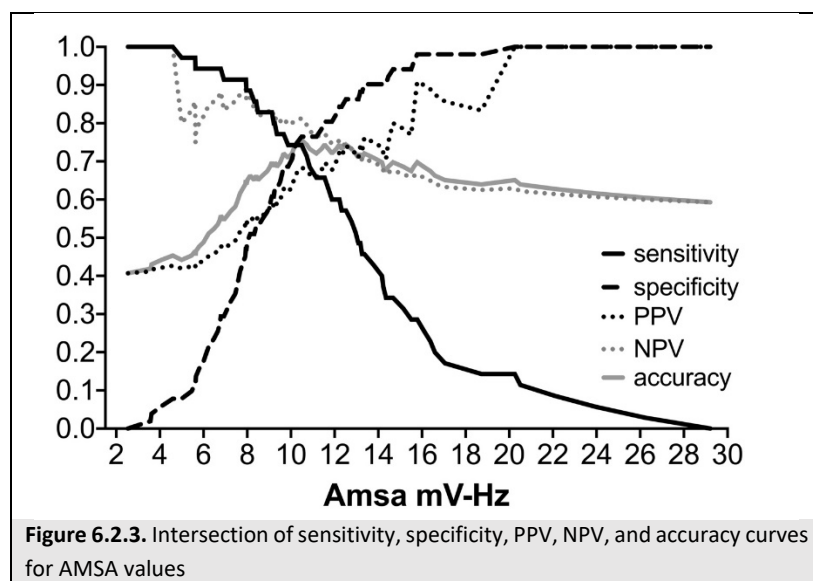
		OR	95% CI
<i>Defibrillation Success</i>			
Univariate	AMSA	1.31**	1.14 - 1.52
Multivariate	AMSA	1.23**	1.06 - 1.45
	Male	0.52	0.08 - 3.41
	Age	1.07	0.97 - 1.19
	EMS arrival time	0.77	0.59 - 1.03
	STEMI	0.60	0.01 - 30.5
<i>Any ROSC</i>			
Univariate	AMSA	1.26**	1.07 - 1.49
Multivariate	AMSA	1.13	0.88 - 1.45
	Male	0.44	0.03 - 6.55
	Age	1.05	0.99 - 1.11
	EMS arrival time	0.69	0.45 - 1.08
	STEMI	0.54	0.07 - 4.36
<i>Sustained ROSC</i>			
Univariate	AMSA	1.18	1.04 - 1.35
Multivariate	AMSA	1.07	0.93 - 1.23
	Male	0.18	0.01 - 2.94
	Age	1.07	0.99 - 1.15
	EMS arrival time	0.77	0.46 - 1.28
	STEMI	0.29	0.02- 5.08
Table 6.2.2. Logistic regression analyses for AMSA and defibrillation outcomes. OR Odds ratio; AMSA Amplitude Spectrum Area; EMS, Emergency Medical System; STEMI, ST Segment Elevation Myocardial Infarction. For 1 mV-Hz AMSA increase; ** p ≤ 0.01.			

DF success and any ROSC were significantly more frequent when DFs were attempted with AMSA ≥ 15.5 mV-Hz, compared to those performed with AMSA value < 15.5 mV-Hz (Table 6.2.3). Defibrillating for an AMSA ≥ 15.5 mV-Hz led to a successful DF in 77% of instances (Table 6.2.3). Thus, this preselected threshold accounted for a PPV of 0.77, with a specificity of 0.94 (Figure 6.2.3). When DFs were attempted with an AMSA < 6.5 mV-Hz, successful DF were significantly less frequent compared to DF attempts for an AMSA ≥ 6.5 mV-Hz (14% vs. 46%, $p < 0.05$). Defibrillating for an AMSA < 6.5 mV-Hz led to a DF failure in 86% of instance (Table 6.2.3). Thus, this preselected threshold accounted for a NPV of 0.86, with a sensitivity of 0.94 (Figure 6.2.3). None of the DFs delivered for an AMSA < 6.5 mV-Hz led to any ROSC and sustained ROSC (Table 6.2.3).

	AMSA < 15.5 mV-Hz n=73	AMSA ≥ 15.5 mV-Hz n=13
DF Success, n (%)	25 (34)	10 (77) **
Any ROSC, n (%)	15 (21)	7 (54) *
Sustained ROSC, n (%)	7 (10)	3 (23)
	AMSA < 6.5 mV-Hz n=14	AMSA ≥ 6.5 mV-Hz n=72
DF Success, n (%)	2 (14)	33 (46) *
Any ROSC, n (%)	0	22 (31) *
Sustained ROSC, n (%)	0	10 (14)

Table 6.2.3. AMSA values and defibrillation outcome. AMSA Amplitude Spectrum Area; DF, defibrillation; ROSC, Return of spontaneous circulation. * $p \leq 0.05$

With the use of the intersection of sensitivity, specificity, and accuracy curves, an AMSA threshold of 10.2 mV-Hz provided a balanced sensitivity, specificity, and accuracy of 0.74, with a PPV of 0.67 and a NPV of 0.81 for DF success in all attempts (Figure 6.2.3). An AMSA threshold of 15.6 mV-Hz instead provided a balanced accuracy and PPV of 0.83 for DF success, with a specificity of 0.96. Higher AMSA thresholds were associated with further increases in PPV and specificity, i.e. AMSA > 20.2 mV-Hz led to a PPV of 1). For lower AMSA thresholds, the majority of unsuccessful DFs were correctly predicted with high sensitivity and NPV, i.e. an AMSA < 4.5 mV-Hz yielded a NPV of 1 (Figure 6.2.3).



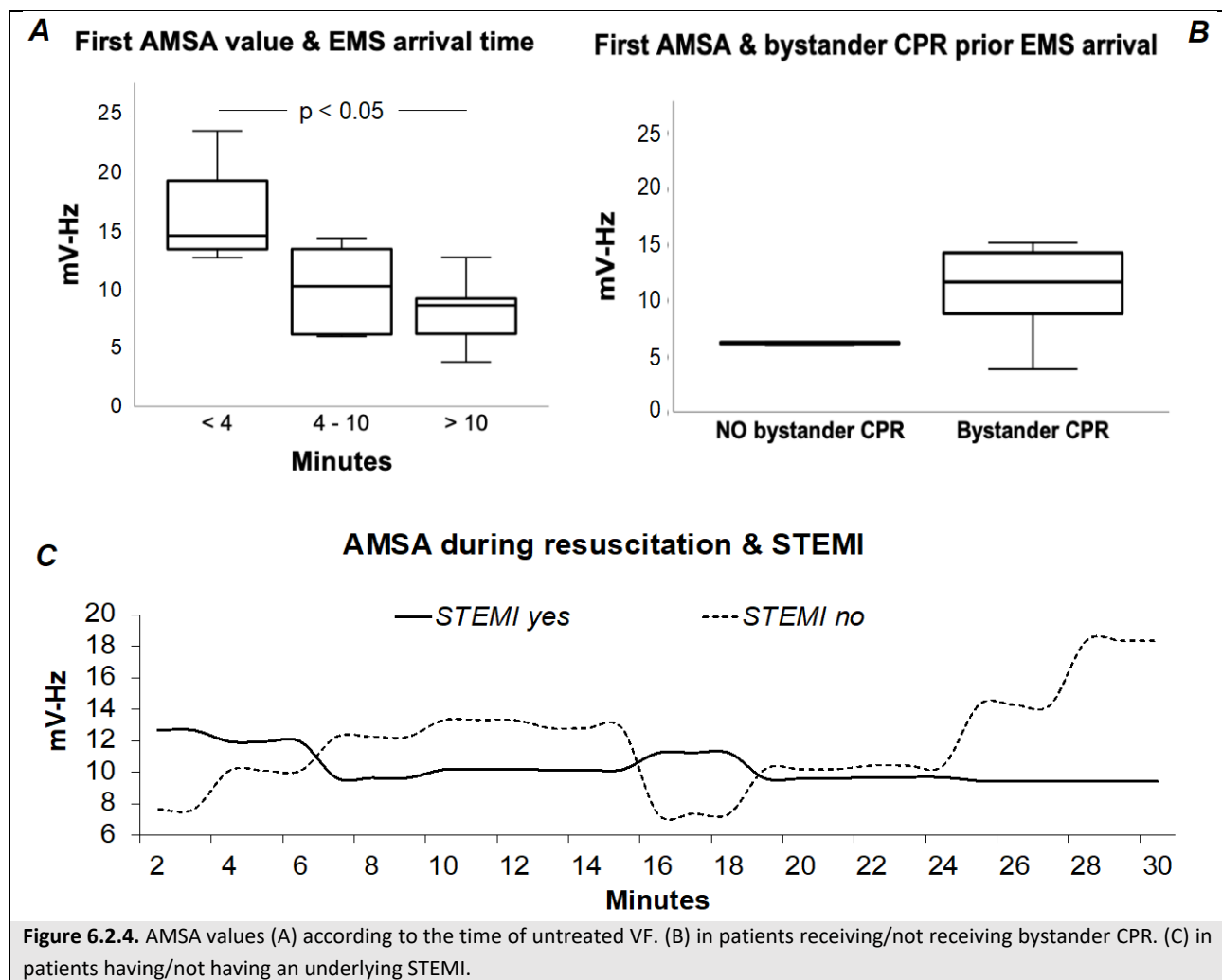
6.2.4 AMSA and resuscitation interventions and STEMI

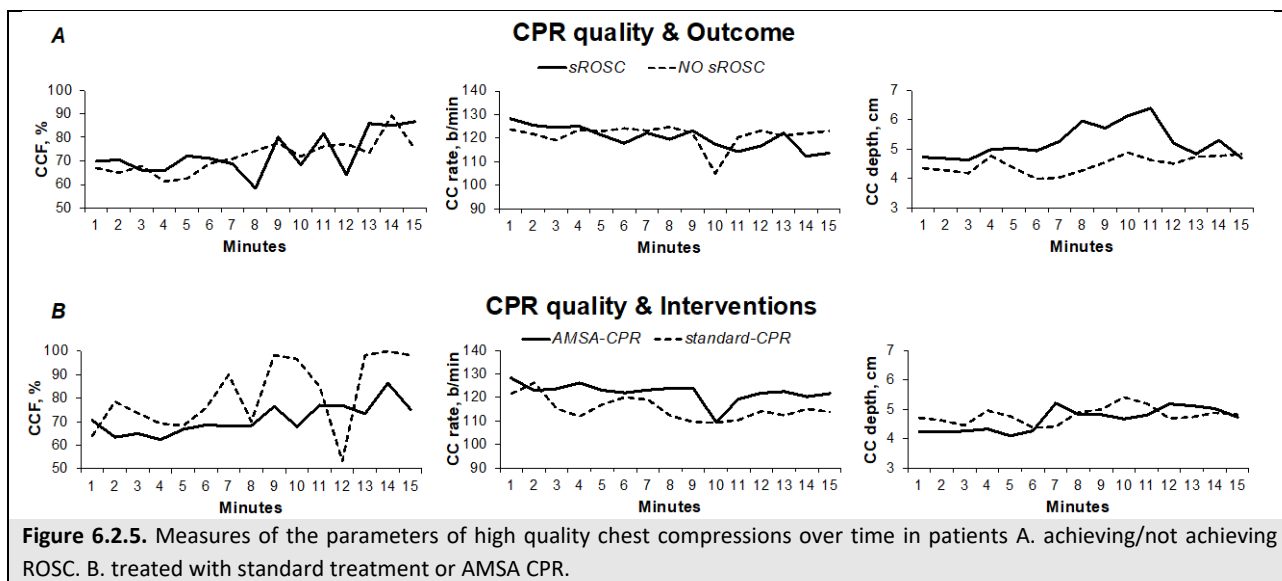
Interval between EMS call and arrival on the scene affected first AMSA values measured when the defibrillator was applied. Indeed, AMSA decreased during the min of untreated CA, with a steep decrease from 16.4 to 10.1 mV-Hz, after the initial 4 min ($p < 0.05$, Figure 6.2.4A).

Similarly, CPR performed prior to EMS arrival affected first AMSA measured. In patients who received bystander CPR prior to EMS arrival, AMSA values were more than double compared to those measured in patients who did not receive bystander CPR (Figure 6.2.4B).

Seven patients in the AMSA group were diagnosed with a STEMI at hospital arrival (Table 6.2.1). Compared with patients without STEMI, initial AMSA values at the beginning of CPR were higher when a STEMI was present (Figure 6.2.4C). However, during CPR, while AMSA increased in patients without a STEMI, it decreased overtime when a STEMI was present (Figure 6.2.4C).

CPR quality, i.e. CC depth, rate and CCF, were similar in the two groups (p not significant, Table 6.2.1 and Figure 6.2.5A). CPR quality was also similar for patients achieving sustained ROSC, compared to those who did not (p not significant, Figure 6.2.5B).





6.3 DISCUSSION

6.3.1 Main findings

Study 2 was a pilot multicenter randomized controlled trial, reported first-ever the prospective clinical application of an AMSA-guided CPR algorithm. It demonstrated the feasibility of measuring and reading AMSA in real-time during CPR in the out-of-hospital setting. Moreover, the present study provided a clinical validation of the capability of AMSA to predict DF success and to be able to guide CPR. AMSA values, acquired for the first time during ongoing resuscitation in human patients, were confirmed to be significantly higher when the DF attempts led to VF termination and ROSC, compared to unsuccessful attempts. Indeed, AMSA appeared to be independently associated with DF success, further emerging as a valid tool to identify the optimal timing for DF delivery during CPR.

6.3.2 Prediction of successful defibrillation

In study 2, an AMSA value ≥ 15.5 mV-Hz prompted for early DF, while a value < 6.5 mV-Hz refused DF in favour of CPR. These AMSA decisional thresholds were derived from an earlier large retrospective study in which VF traces from 1667 OHCA patients were analysed post-hoc and AMSA calculated using a derivation/validation design approach (*Ristagno 2015*). In that study, an AMSA value of 9 mV-Hz was able to predict DF outcome with a balanced sensitivity, specificity, and accuracy of 0.78. However, it appeared clear the need for using 2 different threshold values to improve accuracy in DF prediction: a lower value able to predict DF failure with the highest NPV, and a higher value able to predict a DF success with the highest PPV. Thus, an AMSA ≥ 15.5 mV-Hz predicted DF success with a PPV ranging between 0.78-0.84 (in the derivation and validation groups, respectively), while AMSA < 6.5 mV-Hz predicted DF failure with a NPV of 0.95-0.98. Although AMSA trial enrolled only 19 patients in the AMSA arm, for a total of 86 DF delivered, it confirmed the predicting capability of the above thresholds. Indeed, AMSA ≥ 15.5 mV-Hz showed a PPV of 0.77, while AMSA < 6.5 a NPV of 0.86. (*Ristagno 2013 and 2015*).

Thus, this study prospectively confirmed the value of an AMSA guided-CPR based on 2 decisional thresholds to achieve high accuracy in DF success prediction. More importantly, data acquired represent a solid base to design an AMSA-two trial with optimized thresholds. The decision of interrupting CC to attempt a DF might be limited to instances when the highest probability of success is expected, i.e. when a PPV of at least 0.8 is warranted. DF may be delivered as initial intervention or during CC even before completion of a regular 2-min cycle, when AMSA reaches the threshold of 16 mV-Hz, that in our study accounted for a PPV stably > 0.8 . In the presence of a very low AMSA, the likelihood of delivering a successful DF is low and CC therefore might be performed until AMSA is deemed to be favourable for a DF, minimizing interruptions in CPR and delivery

of unnecessary shocks. A threshold < 6.5 mV-Hz, as we selected in our study, led to a 14% of successful DF, although no patients receiving a DF with an AMSA value below this threshold ultimately achieved ROSC. However, an $AMSA \leq 4.5$ mV-Hz showed a NPV of 1 and thus it could be safely employed to refuse a DF throughout the resuscitation intervention and not limited to only the first 2 CPR cycles, as we did in AMSA trial, in order to avoid the ethical concern of not delivering a treatment at all in those patients with a stable low AMSA. Thus, in designing a new trial, the following AMSA thresholds are suggested: ≥ 16 mV-Hz to prompt for early DF and ≤ 4.5 mV-Hz to refuse DF in favour of CPR.

6.3.3 AMSA during untreated VF and high -quality CPR

In study 2, of interest was the relationship observed between the EMS arrival time from the emergency call and the first AMSA measured. AMSA decreased significantly during the interval of untreated CA, with a steep decrease from 16.4 to 10.1 mV-Hz after the initial 4 min, as electrophysiological evidence of the progressive increase of myocardial ischemia, moving from the “electrical” phase to the “circulatory” phase of VF (*Weisfeldt 2002, Salcido 2009*). This is further supported by the higher first AMSA values measured in patients who received bystander CPR prior to EMS arrival compared to those without, as result of a CC-generated coronary blood flow that maintained the myocardial energy state (*Aiello 2021*). Consistently, in the experimental setting of study 3 and 4, VF was left untreated for 12 min and a decrease in AMSA values could be noted.

These findings may be of additional importance in the view of using real-time AMSA analysis not only to optimize DF delivery, but also as a surrogate of the duration of untreated CA and indicator of the vital status of the myocardium.

In earlier studies AMSA has appeared to carry the additional promise of being able to monitor the effectiveness of CC. In a porcine model, in which animals were randomized to optimal or suboptimal CC depth, AMSA thresholds achieved were contingent on the depth of compressions (*Li 2008*). Similarly, in a retrospective analysis of ECG traces from 609 OHCA, AMSA decreased between consecutive shocks during shallow CC, while it increased when CC was of greater depth (*Ristagno 2013*).

In AMSA trial, however, no relationship between CC quality and AMSA values was observed. This can be explained in different ways; first, the low number of patients enrolled in the AMSA group did not allow to identify any effect of CPR quality on AMSA. Second, overall CPR quality, in terms of depth and rate, was similar in the whole population, thus not allowing for a clear impact on AMSA. Finally, in the light of the results of studies 3 and 4, where mechanical CPR was employed, not only the CC quality, but also the presence of an underlying cardiac ischemia affects the changes of AMSA values in response to CPR. More than half of patients of study 2 presented a STEMI and this might have affected AMSA values even in the presence of an adequate CC quality.

6.3.4 Feasibility of AMSA reading during CPR

Interruption of CC for ECG analyses has been usually required in order to analyse VF with reduced artefacts, and calculate AMSA.

In study 2, AMSA was calculated during pauses in CC to deliver 2 Vs. The 4 sec necessary to deliver the 2 Vs based on current guidelines (*Olasveengen 2020*) were longer enough to have AMSA measured and showed on the defibrillator screen. A CPR with a 30:2 CC:V algorithm was therefore needed for an AMSA-guided CPR, even in the presence of an advanced airway. Despite initial concerns, this approach, led to similar survival and favorable neurologic outcome, when compared to continuous CC with asynchronized Vs, in a population of more than 23.000 OHCA's (*Nichol 2015*).

6.3.5 Implications

In study 2, for the first time AMSA has been used prospectively in human patients during ongoing resuscitation manoeuvres. The study showed the feasibility of a real-time AMSA guided CPR and confirmed the ability of AMSA to predict the success of DF in the real clinical scenario. Further, considering all the information derived from this pilot trial, a larger trial can be planned, with optimized AMSA thresholds. Finally, these results are of strong value because they were derived from a randomized controlled trial conducted in 3 different cities.

6.3.6 Limitations

We recognize important limitations of this study. First, AMSA trial was discontinued for no patients' enrolment and thus only a small number of OHCA's were included, making the study not powered to demonstrate differences between AMSA-guided CPR vs. standard-CPR in terms of outcome. Nevertheless, it represents the first report of a prospective clinical application of AMSA during OHCA. The small number of patients was probably the reason why in this study an association between AMSA and long-term outcome was not observed, as previously reported (*Ristagno 2015, Schoene 2014*). Third, Post-DF asystole or pulseless electric activity were not included in the definition of successful DF because, although they may be considered a successful termination of VF, they are not associated with ROSC (*Ristagno 2015*). The criterion we used to define successful DF, therefore, reflected not only VF termination but also the quality of the resulting rhythm and thus offered a more effective identification and discrimination of clinically useful DF outcome predictors. Nevertheless, to overcome the limitation of defining successful DF based on the ECG tracing, in this pilot study the relationship between the last DF attempt and sustained ROSC was evaluated.

Another possible limitation of the study is that the calculation of absolute AMSA values by the defibrillator can be subject to electrode placement (*Thannhauser 2021, Indik 2008*). From studies with both laypersons and

professionals it is known that pad misplacement is common in clinical practice, resulting in variations in bipolar lead recording (*Heames 2018, Bodtker 2018, Nurmi 2004*). However, during the training phase of ASMA trial, the correct pads placement was explained and verified by the researchers during mannequin simulations. Therefore, misplacement of the pads during the trial is deemed unlikely. Nevertheless, variability due to presence of AMI and myocardial mass (*Bonnes 2017*) could have played a role. Of note, this study confirmed the capability of AMSA to predict the success of DF in a real clinical scenario including all the possible variabilities in patients and resuscitation management.

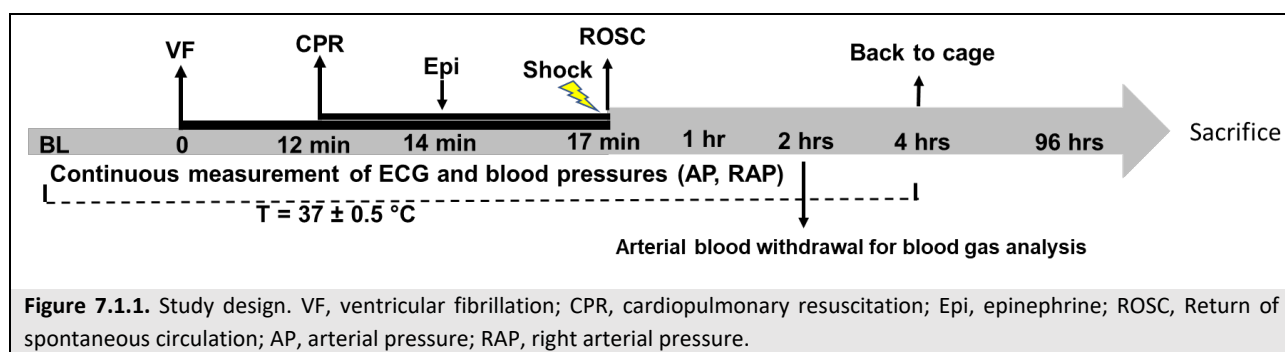
Due to the strict inclusion criteria, i.e. shockable rhythm with no DF delivered by bystanders or BLS rescue teams prior to arrival of Advanced Life Support ones, the enrolment had been already planned to be slow and for that new centres were under recruitment in Italy and in Europe, i.e. Espoo EMS. However, in February 2020, just 4 months after the trial kick off, the first patient was diagnosed with COVID-19 in Italy and since then, an increasing number of cases was recorded in Lombardy, and subsequently throughout the Country, with a high pressure on the healthcare system and on EMSs (*Trentini 2021*). Due to the recurrence of subsequent pandemics waves with no burden relief on the EMS, the trail was discontinued for the impossibility to enrol patients. Indeed, the COVID-19 pandemics affected the system-of-care of OHCA with longer EMS arrival time, reductions in shockable rhythms and ultimately worse outcomes (*Scquizzato 2020*). AMSA trial was therefore underpowered to demonstrate differences between AMSA-guided vs. standard-CPR. Nevertheless, this pilot trial remains of high importance since a real-time AMSA analysis was finally used in the clinical scenario, testing prospectively AMSA capability to predict DF outcome and guide CPR, in response to a specific knowledge gap claimed in 2015 CPR guidelines and reinforced in 2021 (*Soar 2015 and 2021*). The prospective use of AMSA confirmed this predictor to be independently associated with DF success. These results are even stronger if we consider that they have been achieved with a small number of patients, i.e. only 19 with an AMSA evaluated, and in a multicentre randomized controlled trial.

7 STUDY 3. PRECLINICAL FEASIBILITY OF REAL TIME AMSA MEASUREMENT DURING CPR USING A MODIFIED CLINICAL DEFIBRILLATOR

7.1 METHODS

7.1.1 Study design

This was prospective observational, experimental study investigating the feasibility of real-time AMSA monitoring during mechanical CPR without CC interruptions. The study design is detailed in figure 7.1.1.



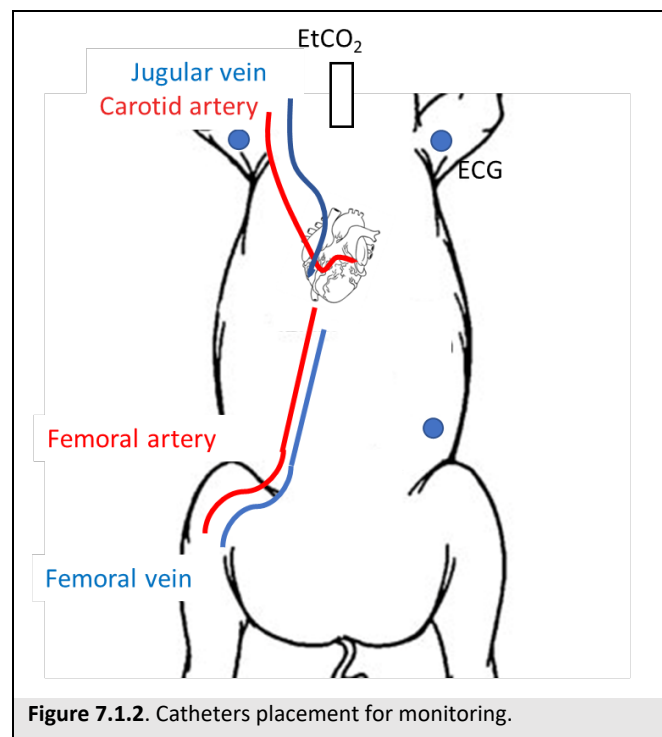
7.1.2 Ethical considerations

Procedures involving animals and their care were in compliance with national (D.L. n. 116, G.U., suppl. 40, 18 February 1992, Circolare no. 8, G.U., 14 Luglio 1994) and international laws and policies (EEC Council Directive 86/609, OJL 358, 1, December 12, 1987; Guide for the Care and Use of Laboratory Animals, US National Research Council, 1996). Approval of the study was obtained by the University of Milan Institutional review board committee and Governmental Institution (Italian Ministry of Health: approval no. 657/2020-PR). The study is reported in accordance with the ARRIVE (Animal Research: Reporting of In Vivo Experiments) guidelines.

7.1.3 Animal preparation

Fourteen healthy male domestic pigs, adult (4-6 months of age), were fasted the night before the experiment except for free access to water. Anesthesia was induced by intramuscular injection of ketamine (20 mg/kg) followed by intravenous administration of propofol (2 mg/kg) and sufentanyl (0.3 µg/kg) through an ear vein access. Anesthesia was then maintained by continuous intravenous infusion of propofol (4–8 mg/kg/h) and

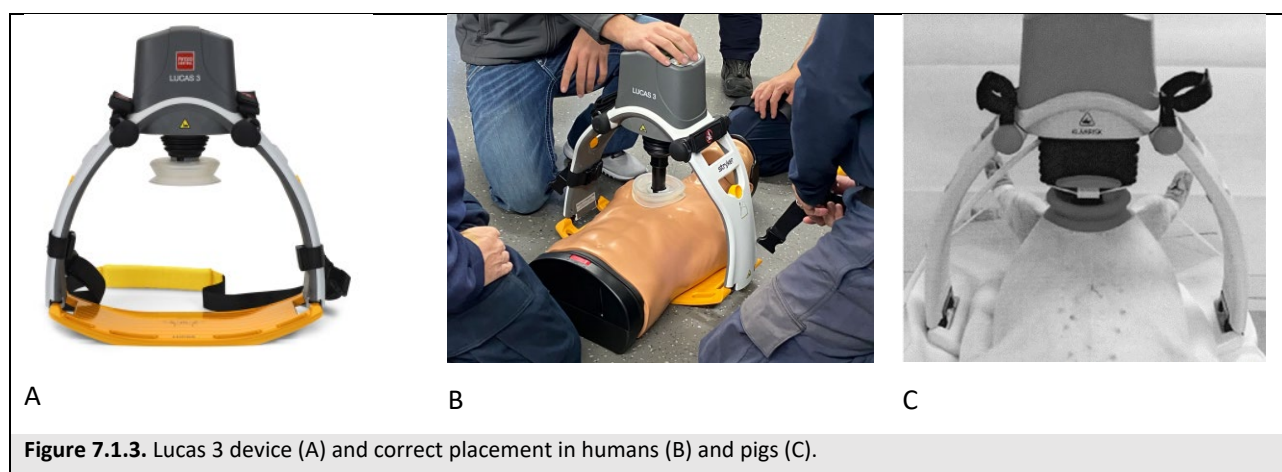
sufentanyl (0.3 µg/kg/h). A cuffed tracheal tube was placed, and animals were mechanically ventilated with a tidal volume of 15 mL/kg and FiO₂ of 0.21. Respiratory frequency was adjusted to maintain the etCO₂ between 35 and 40 mmHg, monitored with an infrared capnometer (Babini 2018, Fumagalli 2020, Ristagno 2014). To measure aortic pressure, a fluid-filled 7F catheter was advanced from the right femoral artery into the thoracic aorta. For measurements of right atrial pressure, core temperature, a 7F pentalumens thermodilution catheter was advanced from the right femoral vein into the pulmonary artery. Conventional pressure transducers were used (MedexTransStar, Monsey, NY) (Figure 7.1.2).



MI was induced in a closed-chest preparation by intraluminal occlusion of the LAD coronary artery (Babini 2018, Fumagalli 2020, Ristagno 2014). Briefly, a 6F balloon-tipped catheter was inserted from the right common carotid artery and advanced into the aorta and then into the LAD, beyond the first diagonal branch, with the aid of image intensification and confirmed by injection of radiographic contrast media. For inducing VF, a 5F pacing catheter was advanced from the right jugular vein into the right ventricle. The position of all catheters was confirmed by characteristic pressure morphology and/or fluoroscopy. A frontal plane ECG was recorded. The defibrillator used was a CE approved defibrillator, X-Series, ZOLL Med. Corp., MA, USA <http://www.zoll.com/medical-products/defibrillators/x-series/EMS/>. The defibrillatory pads “OneStep CPR electrodes” were used after removal of the sensor for CPR quality, with the purpose to not interfere with the AMSA calculation process.

7.1.4 Experimental procedure

After baseline measurements, the LAD catheter balloon was then inflated with 0.7 mL of air to occlude the flow, as previously described (Babini 2018, Fumagalli 2020, Ristagno 2014). If VF did not occur spontaneously after 10 min, CA was induced with 1 to 2 mA AC current delivered to the right ventricle endocardium. Ventilation was discontinued after the onset of VF. After 12 min of untreated VF, CPR, including CCs with the LUCAS 3.0 device (Stryker) (Figure 7.1.3) and ventilation with oxygen (tidal volume of 500 mL, 10 breaths/min), was initiated. At min 2 of CPR, animals received central venous bolus administration of epinephrine. After 5 min of CPR, DF was attempted with a single biphasic 150-J shock. If ROSC was not achieved, CPR was resumed and continued for 1 min before a subsequent DF. The resuscitation maneuvers were continued until successful ROSC or for a maximum of 15 min. ROSC was defined as the restoration of an organized cardiac rhythm with a mean arterial pressure of more than 60 mmHg. After that, if VF reoccurred, it was treated by immediate DF. Immediately after resuscitation, the LAD catheter correct placement was reconfirmed by fluoroscopy (Babini 2018).



7.1.5 Measurements

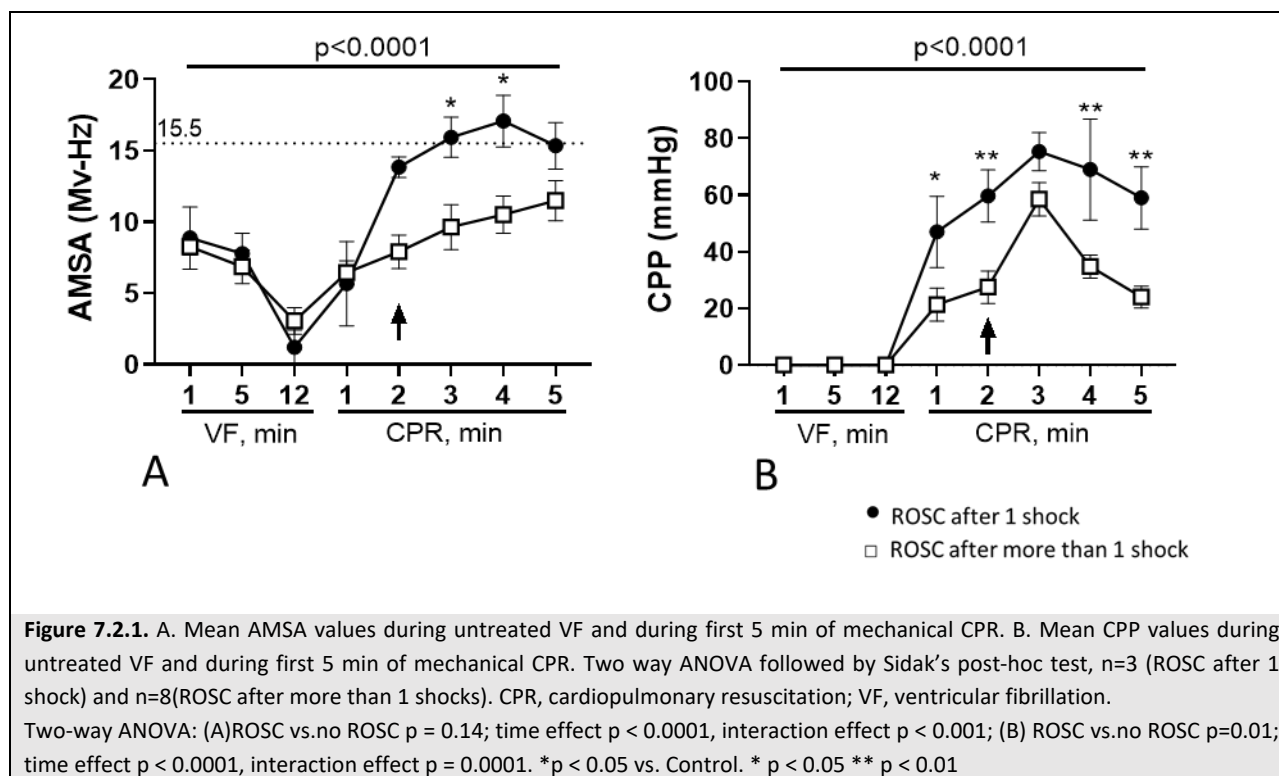
Hemodynamics, etCO_2 , and ECG were recorded continuously on a personal computer-based acquisition system (WinDaq DATAQ Instruments Inc, Akron, OH). CPP was computed from the differences in time-coincident diastolic aortic pressure and right atrial pressure. Arterial blood gases were assessed with an i-STAT System (Abbott Laboratories, Princeton, NJ). AMSA calculation was performed in real-time by a built-in software in the X-Series defibrillator, which acquired the ECG signal from the defibrillatory pads and displayed the AMSA values continuously. As the modified Zoll defibrillator is normally set to start AMSA calculation only when CCs are not detected by the pads “OneStep CPR electrodes”, in order to have a continuous AMSA calculation, the sensor for CPR quality was removed from the pads and the pads were placed in a latero-lateral position in the chest of the animal, to avoid CC-related artefacts on the VF waveform.

The ECG analysis was performed continuously on a 512-point window (2.05 sec). ECG signals were processed with the use of a 2-Hz high-pass filter to minimize low-frequency artefacts produced by CC and a 48-Hz low-pass filter to remove interference of ambient noise at higher frequencies. Analog ECG signals were converted from a time to a frequency domain by fast Fourier Transform. A Tukey fast Fourier Transform window was used to reduce edge effects. AMSA was calculated as the sum of the products of individual frequencies and their amplitudes: $AMSA = \sum A_i \cdot F_i$, where A_i represents the amplitude at i th frequency F_i .

7.1.6 Statistical analysis

Categorical variables were presented as proportion, while continuous variables as mean \pm standard error of the mean (SEM). One sample Kolmogorov–Smirnov Z test is used to confirm normal distribution of the data. Differences in clinical characteristics according to experimental group were compared by the Fisher’s exact test for categorical variables; T test or nonparametric Mann–Whitney U test was adopted for continuous variables. For comparisons of time-based variables, repeated measures analysis of variance (ANOVA) is used. For comparisons between groups at the given time points, one-way ANOVA with Tukey’s multiple comparison is used for normally distributed variables, while Kruskal-Wallis test with Dunn’s multiple comparison is used for not normally distributed variables. Spearman test is performed for the non-parametric variable correlation analyses.

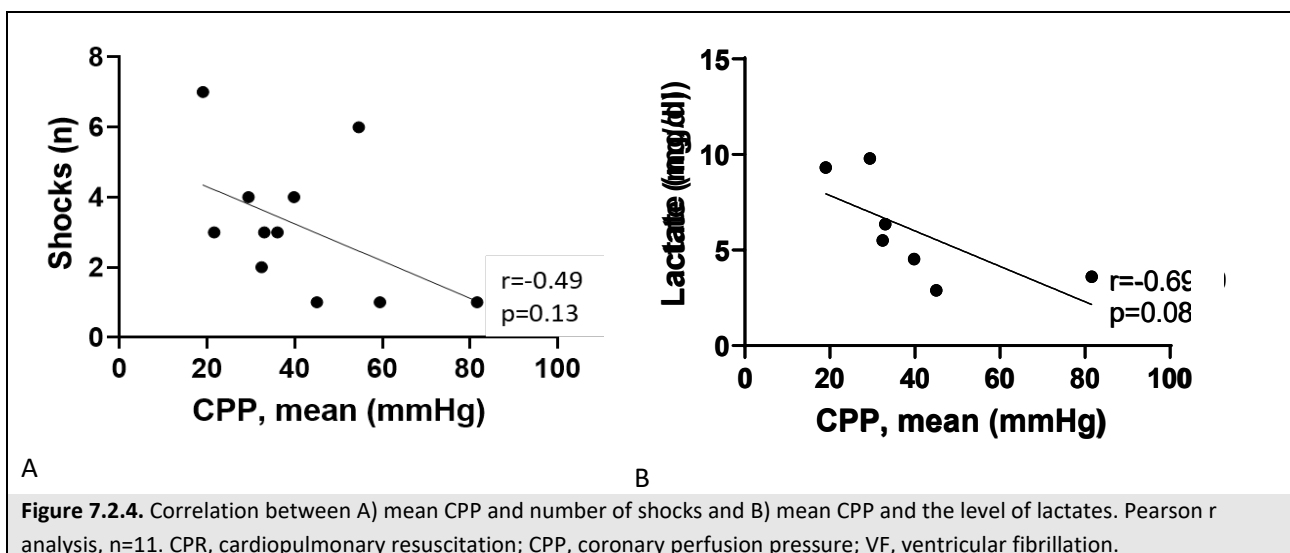
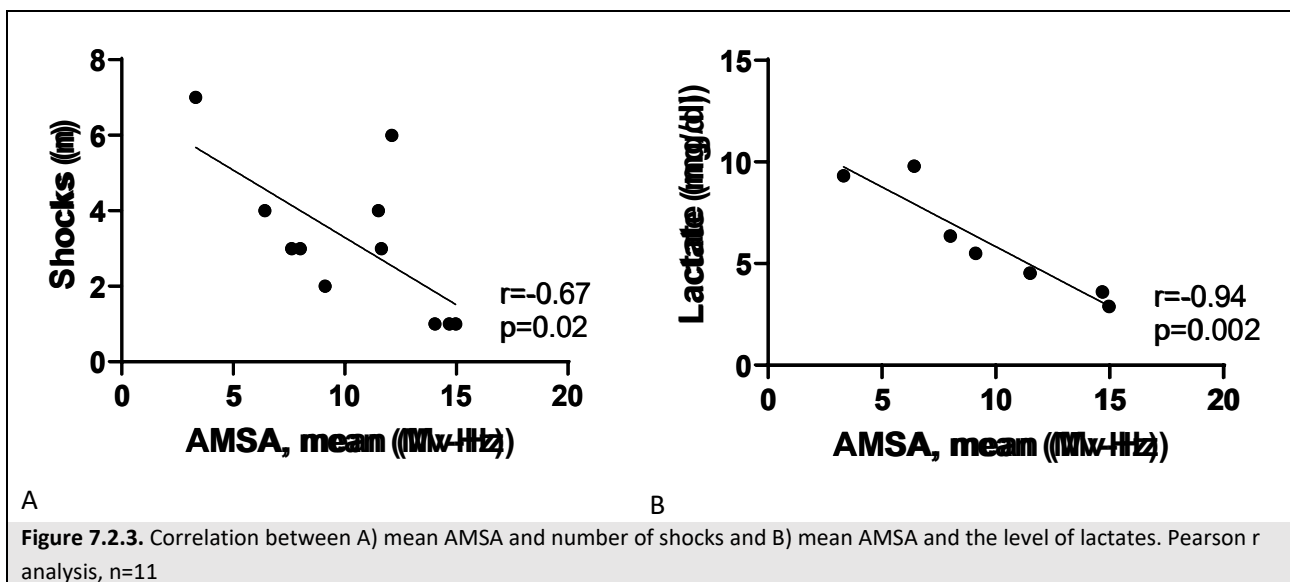
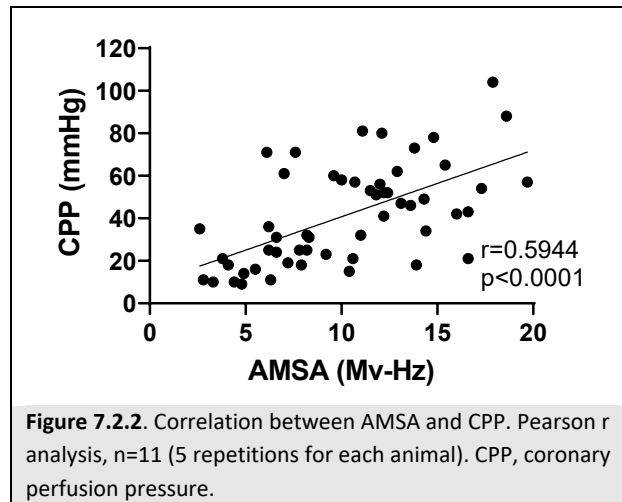
7.2 RESULTS



Fourteen animals were included in the study (mean body weight: 41.4 ± 5.3 kg). Three (21%) animals had successful DFs with ROSC after the first shock, 8 (57%) had ROSC after more than 1 shock (on average 4 shocks), while 3 (21%) animals had no ROSC. AMSA values were displayed continuously during mechanical CPR.

Mean AMSA increased during CPR in all animals, and was higher during resuscitation in animals having ROSC after the first shock, compared to animals in which resuscitation required more than one shock, although the difference was not significant. CPP increased during CPR and was significantly related with the success of DF ($p=0.01$, Figure 7.2.1).

CPP and AMSA presented a strong correlation ($r 0.59$, $p < 0.0001$) as shown in Figure 7.2.2. AMSA values showed a significant inverse correlation with the number of DF attempts ($p = 0.02$), (Figure 7.2.3A) while on the contrary CPP did not present any significant correlation with the number of DFs (Figure 7.2.4A). Similarly, lactates were strongly associated with AMSA values ($p < 0.01$) but not with CPP significantly (Figures 7.2.3B and 7.2.4B).



7.3 DISCUSSION

7.3.1 Main findings

In this study on a preclinical model of ischemic CA, we measured AMSA in real time during mechanical CPR without interrupting CCs, using for the first time a modified clinical device and simulating a real clinical use of this predictive tool. Indeed, in this preclinical setting, real time AMSA measurement during CPR was feasible.

7.3.2 Feasibility of AMSA reading during mechanical CPR

Mechanical CPR is widely employed during CPR and in particular in circumstances when manual CPR is deemed suboptimal, like transport (*Magliocca 2020*). Study 3 shows the potential feasibility of an AMSA guided resuscitation strategy also when mechanical CPR is applied. In fact, we measured AMSA in real time during mechanical CC in a swine model of CA, without any interruptions, using a modified defibrillator for experimental use. In order to reduce the interference due to chest compressions, the defibrillatory pads, that collected the VF signal to analyse AMSA, were placed in a latero-lateral position. The defibrillatory pads were applied after removal of the sensor for CPR quality, such to have a continuous AMSA measurement. AMSA was confirmed a good predictor of DF success, presenting a good correlation with the CPP, with the number of shocks and the lactate levels. Previous studies confirmed the prediction capability of AMSA also when it was measured during CC, despite lower AUC were reported compared to AMSA measured from artefacts-free ECG (*Coult 2019*). Unfortunately, in this study no comparison with AMSA analysis during CC pauses were possible. Remarkably, to our knowledge this is the first study reporting prospectively AMSA calculation in real time during CC.

7.3.3 Implications

In study 3, we showed for the first time the feasibility of a real time AMSA evaluation during mechanical chest compressions without CPR interruptions. The study shows the potential application of an AMSA guided resuscitation strategy also during continuous CCs without pauses.

7.3.4 Limitations

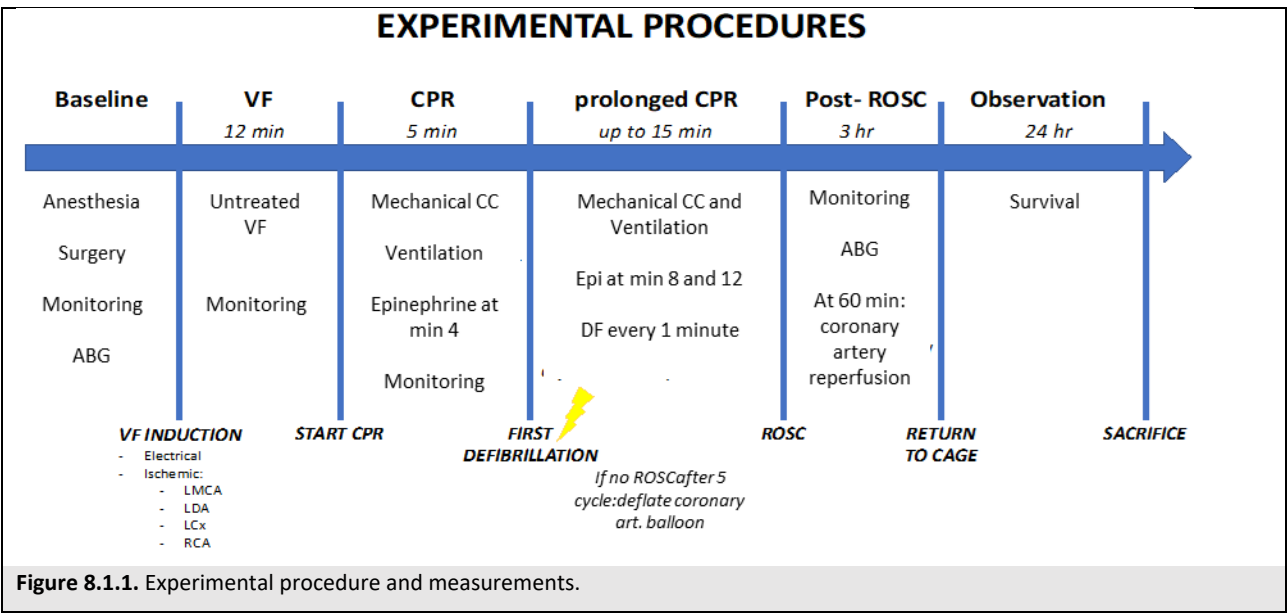
This study has several limitations. To understand the effect of continuous CC in corruption of the signal of the analysed ECG segment, a control group with AMSA analysed during CC pause could have given more information. Moreover, artefacts typical of a real clinical CPR scenario, i.e. transport, have been not investigated. The small number of animals limited the statistical analyses.

8 STUDY 4. IDENTIFYING AN AMI DURING CPR IN A PRECLINICAL PORCINE MODEL OF VF

8.1 METHODS

8.1.1 Study Design

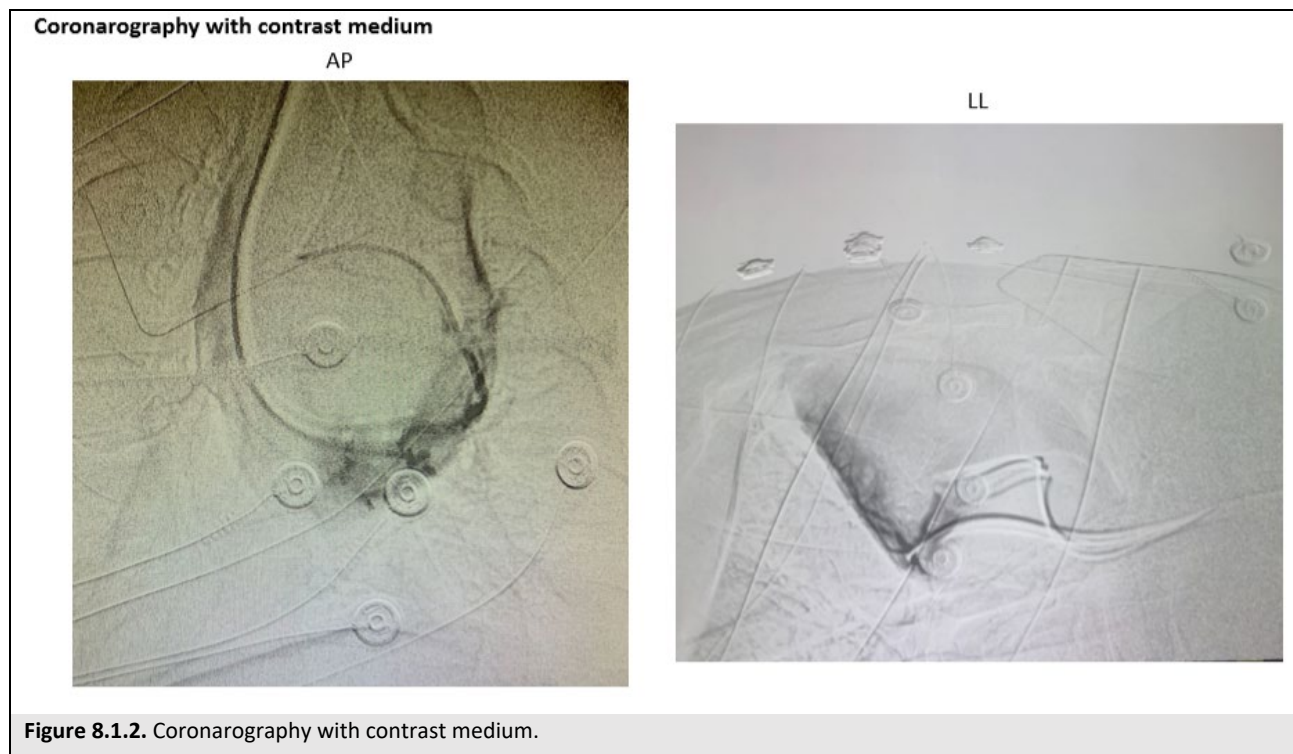
This was a prospective observational, experimental study in a swine model of CA, investigating the role of AMSA in the early diagnosis of an underlying AMI with different coronary arteries occlusion. The study design is detailed in figure 8.1.1.



8.1.2 Ethical considerations

Procedures involving animals and their care were in compliance with national (D.L. n. 116, G.U., suppl. 40, 18 February 1992, Circolare no. 8, G.U., 14 Luglio 1994) and international laws and policies (EEC Council Directive 86/609, OJL 358, 1, December 12, 1987; Guide for the Care and Use of Laboratory Animals, US National Research Council, 1996). Approval of the study was obtained by the University of Milan Institutional review board committee and Governmental Institution (Italian Ministry of Health: approval no. 1129/2020-PR). The study is reported in accordance with the ARRIVE (Animal Research: Reporting of In Vivo Experiments) guidelines.

8.1.3 Animal preparation



Eighteen male domestic pigs, adult (4-6 months of age), were fasted the night before experiment except for free water access. Anesthesia was induced by intramuscular injection of ketamine (20 mg/kg) followed by intravenous administration of propofol (2 mg/kg) and sufentanyl (0.3 µg/kg) through an ear vein access. Anesthesia was then maintained by continuous intravenous infusion of propofol (4-8 mg/kg/h) and sufentanyl (0.3 µg/kg/h). A cuffed tracheal tube was placed, and animals were mechanically ventilated with a tidal volume of 15 mL/kg and FiO₂ of 0.21. Respiratory frequency was adjusted to maintain the etCO₂ between 35 and 40 mmHg, monitored with an infrared capnometer. For measurement of aortic pressure, a fluid-filled 7F catheter was advanced from the right femoral artery into the thoracic aorta. For measurements of right atrial pressure, core temperature, and CO, a 7F pentalumens thermodilution catheter was advanced from the right femoral vein into the pulmonary artery. Conventional pressure transducers are used (MLT0699, AdInstruments, UK).

Frontal plane ECG was recorded. AMI was induced in a closed-chest preparation by intraluminal occlusion of one of the following coronary arteries: 1. the left main coronary artery (LMCA or proximal left coronary LC Prox); 2. the LAD coronary artery (between the first and the second diagonal branch); 2. the left circumflex coronary artery (LCx); 3. the right coronary artery (RCA). Specifically, a 5F balloon-tipped catheter was inserted from the right common carotid artery and advanced into the aorta and then into the coronary artery tree, with the aid of image intensification and confirmed by injection of radiographic contrast media (Figure 8.1.2).

For inducing VF, a 5F pacing catheter was advanced from the right jugular vein into the right ventricle.

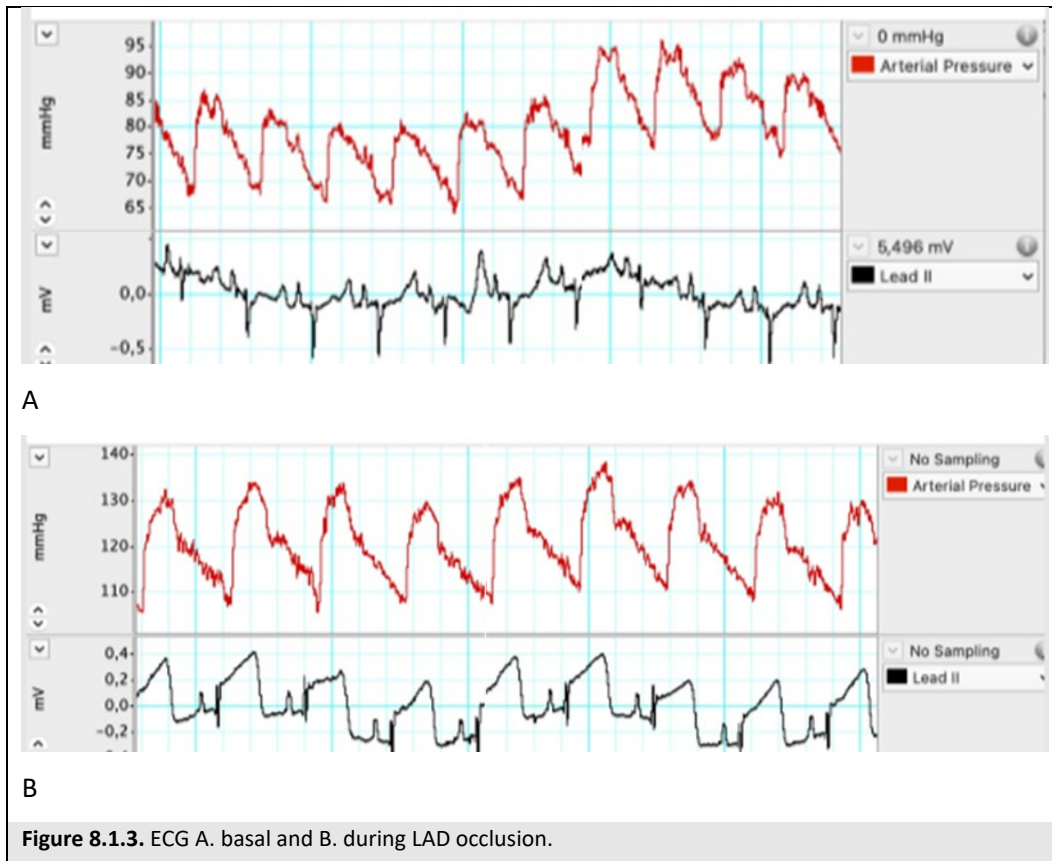


Figure 8.1.3. ECG A. basal and B. during LAD occlusion.

Data were acquired continuously from baseline, through coronary occlusion, VF and CPR, and post-resuscitation with the aid of a Powerlab, ADInstruments, as shown in figure 8.1.3.

To acquire a clean ECG trace to calculate AMSA, CPR was stopped for 5 sec during each minute of CCs (from sec 45 to sec 50), as shown in figure 8.1.4.

Blood gas analysis was performed at baseline and 2 hr and 24 hr post-resuscitation.

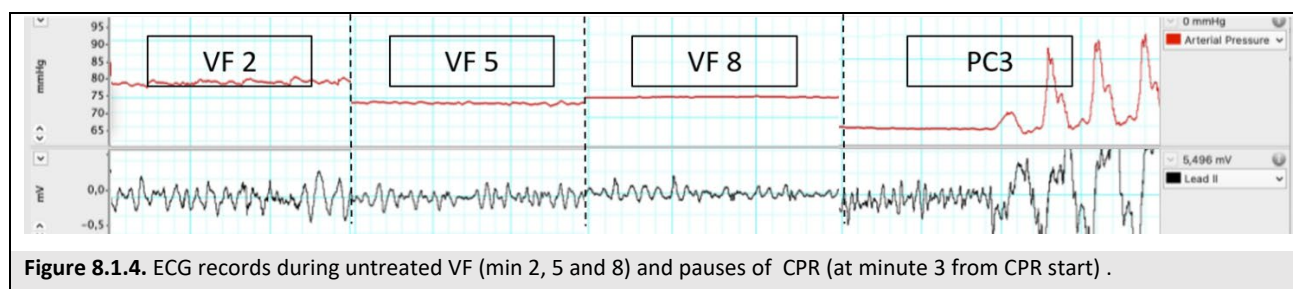


Figure 8.1.4. ECG records during untreated VF (min 2, 5 and 8) and pauses of CPR (at minute 3 from CPR start) .

8.1.4 Experimental design

After recording of baseline measurement, the balloon of the coronary artery catheter was inflated with 0.8 mL of air to occlude the flow. Occlusion was confirmed by the rapid occurrence of progressive electrocardiographic ST segment modification. If VF did not occur spontaneously, after an hr of artery occlusion, it was electrically induced with 1 to 2 mA alternating current delivered to the endocardium of the right ventricle. Ventilation was discontinued after onset of VF. After 12 min of untreated VF, CPR, including

CCs with the LUCAS 3 (PhysioControl Inc, Lund, Sweden) and ventilation with oxygen (tidal volume of 500 mL, 10 breaths/min), was initiated (coronary artery balloon still inflated).

During CPR, at the end of every min a pause of 6 sec in CC is observed to obtain artefact-free ECG to measure AMSA. After 4 min of CPR, a blood gas analysis is performed. After 5 min of CPR, DF was attempted with a single biphasic 200-J shock, using an X-Series defibrillator (ZOLL Med. Corp., USA). If resuscitation was not achieved, CPR was resumed and continued for 1 min before a subsequent DF. If after five additional 1-min cycles, ROSC was not achieved, the coronary artery balloon was deflated and CPR continued. Adrenaline (1 mg) was administered via the right atrium after 4, 8, and 12 min of CPR. The resuscitation procedures were continued until resuscitation or for a maximum of 16 min. If VF reoccurred, it was treated by immediate DF. Immediately after resuscitation, the coronary artery occlusion balloon and the catheter correct placement was reconfirmed by fluoroscopy. After successful resuscitation, anesthesia was maintained, and animals were monitored during the subsequent 3 hr. Two hr after coronary occlusion the coronary artery balloon was deflated, and the catheter withdrawn.

Temperature of the animals was maintained at $38^{\circ}\text{C} \pm 0.5^{\circ}\text{C}$ during the whole experiment. After 3 hr, catheters were removed, wounds were repaired, and the animals were extubated and returned to their cages. At the end of the 24-h post-resuscitation observation period, animals were sacrificed painlessly. Autopsy was performed routinely for potential injuries due to CPR or obfuscating disease.

8.1.5 Measurements

EtCO₂ and AMSA were measured and recorded by X-Series ZOLL defibrillator. More specifically, AMSA analysis was performed during hands-off time on a 512-point window (2.05 sec) ending 0.5 second before DF. AMSA was calculated as the sum of the products of individual frequencies and their amplitudes: $\text{AMSA} = \sum A_i \cdot F_i$, where A_i represents the amplitude at i th frequency F_i . Recorded ECG signals were also processed with the use of a 2-Hz high-pass filter to minimize low-frequency artefacts produced by CC and a 48-Hz low-pass filter to remove interference of ambient noise at higher frequencies. Analog ECG signals were digitized and converted from a time to a frequency domain by fast Fourier Transform. A Tukey Fourier Transform window is used to reduce edge effects.

Arterial blood gases, including also lactates, were assessed with the i-STAT System (Abbott Laboratories, Princeton, NJ).

8.1.6 Endpoints of the study

The primary endpoint was the identification of an AMI during CPR for VF CA, through analysis of AMSA.

The secondary endpoints included: identification of the AMI localization during CPR; ROSC; need for revascularization to achieve ROSC; duration of CPR and number of DFs prior to ROSC; post-resuscitation malignant arrhythmia.

8.1.7 Statistical analysis

Categorical variables were presented as proportion, while continuous variables as mean \pm SEM. One sample Kolmogorov–Smirnov Z test is used to confirm normal distribution of the data. Differences in clinical characteristics according to experimental group were compared by the Fisher’s exact test for categorical variables; T test or nonparametric Mann–Whitney U test was adopted for continuous variables. For comparisons of time-based variables, repeated measures analysis of variance (ANOVA) is used. For comparisons between groups at the given time points, one-way ANOVA with Tukey’s multiple comparison is used for normally distributed variables, while Kruskal-Wallis test with Dunn’s multiple comparison is used for not normally distributed variables.

8.2 RESULTS

A total of 15 pigs were studied (weight: 40.8 ± 3.3 kg). Of these, the first was a pilot study to test the initial setting. The other 14 animals were randomized to one of the 5 study groups, as reported in Table 6.4.1.

VF occurred spontaneously after coronary occlusion in all the animals in the LAD and in the proximal left coronary artery (LC Prox or LMCA) group, in 2/3 of animals in the LCx, and in none in the RCA group. In 50% of animals in the LAD and in all pigs in the LCx group, the coronary artery needed to be reperfused in order to achieve ROSC. Animals in the LCx and the LC Prox groups needed a higher number of DFs to achieve sustained ROSC/resuscitation. Almost all the animals were successfully resuscitated (87%), however 50% of resuscitated animals died during the initial 24 hr (Table 6.4.1).

Baseline and post-resuscitation hemodynamics and blood gases are summarized in Table 6.4.2. AMI animals showed lower mean arterial pressure and higher pulmonary artery pressure in the PR period, compared to no AMI animals; greater signs of heart failure and lung congestion (higher pulmonary artery pressure) were observed in the LAD and RCA groups.

Group	n	VF Spontaneously	Reperfusion during CPR	ROSC	Defibrillations	24h survival
No AMI	4	0/4	0/4	4/4	15±2	2/4
-LAD	4	4/4	2/4	3/4	12±2	2/4
-LCx	3	2/3	1/3	2/3	20±18	1/2
-RCA	2	0/2	1/2	2/2	10±6	0/2
-LC Prox	2	2/2	2/2	2/2	43±33	1/2

Table 6.4.1. CPR data and outcomes.

In the overall population, AMSA values decreased over time during untreated VF and increased during CPR (figure 8.2.1). AMSA mean values were significantly higher in animals reaching ROSC compared to animals that died ($p = 0.04$, Figure 8.2.2)

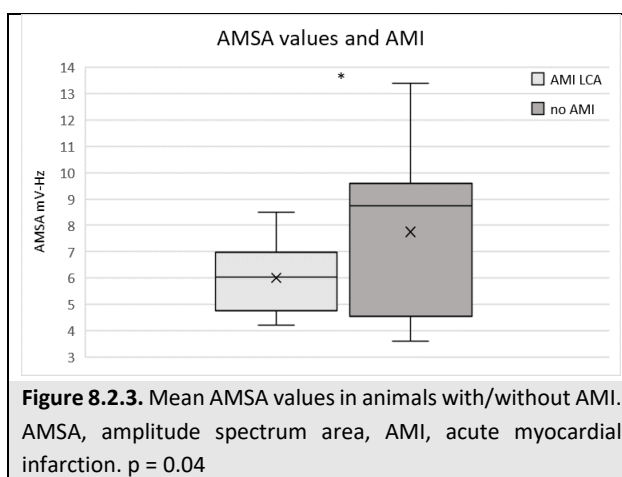
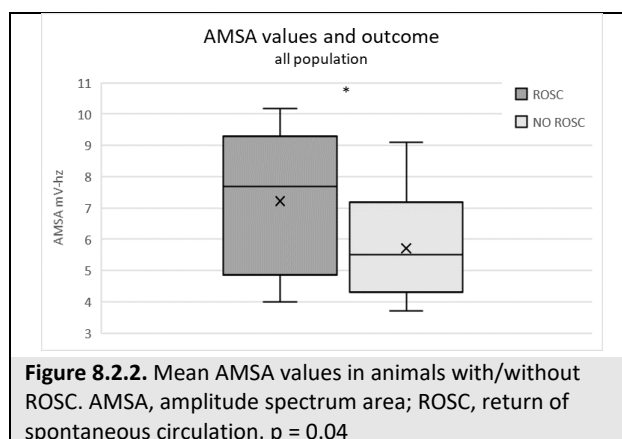
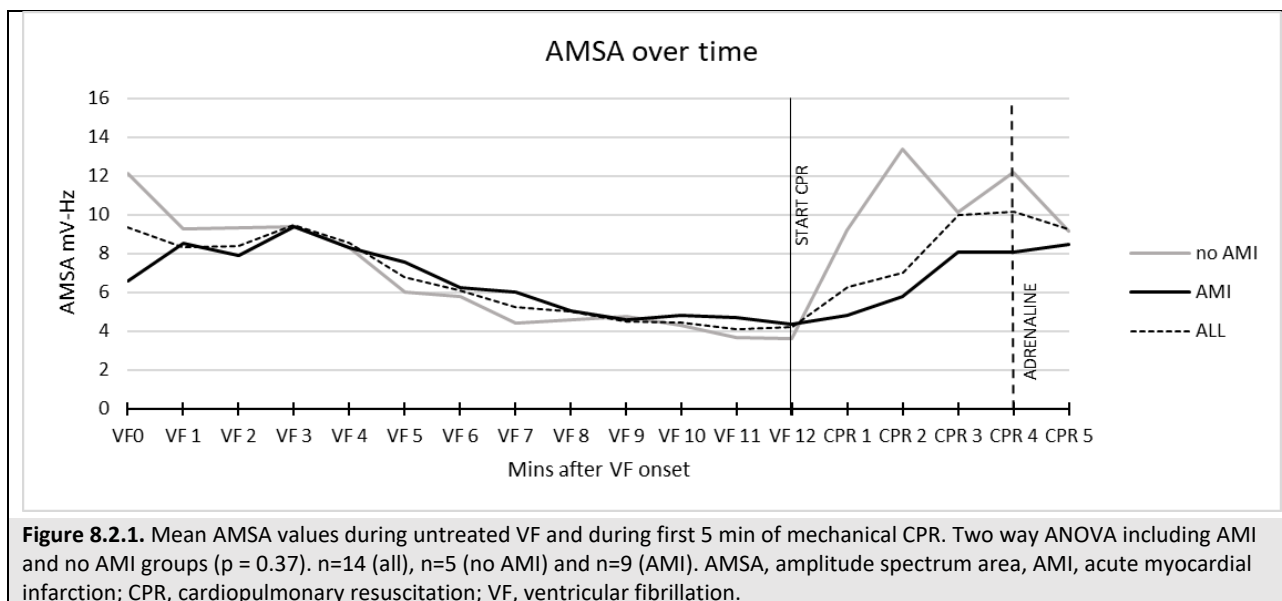
When analyzing separately animals with/without underlying AMI, mean AMSA values were significantly higher in no AMI group compared to AMI group ($p = 0.04$) (figure 8.2.3). Animals without AMI presented a higher increase in AMSA values during CPR compared to AMI group, although not significant ($p = 0.37$, Figure 8.2.1).

When analyzing AMSA values according to the coronary artery involved, a significant different trend could be noticed in the groups ($p = 0.02$). In particular, LAD and LCx occlusion group showed minor AMSA increase in response to CPR, while RCA group showed a greater increase in AMSA values after CPR, similar to the no

AMI group (Figure 8.2.4 and 8.2.5). This was more evident when analyzing the average increment (Δ AMSA) of AMSA values after 3 min of CPR ($p = 0.008$, Figure 8.2.6). When analyzing Δ AMSA during CPR (difference between AMSA at minute 5 and AMSA at minute 3), the difference between the groups was not significant.

Group	HR b/min	MAP mmHg	RAP mmHg	PAP mmHg	CO L/min
No AMI					
BL	114 \pm 24	113 \pm 13	6 \pm 1	26 \pm 6	3.6 \pm 0.6
PR 1hr	173 \pm 41	85 \pm 42	7 \pm 2	25 \pm 3	2.3 \pm 0.7
PR 2hr	192 \pm 16	84 \pm 40	6 \pm 1	30 \pm 6	2.2 \pm 0.4
PR 3hr	172 \pm 55	94 \pm 20	5 \pm 2	26 \pm 3	2.2 \pm 0.4
LAD					
BL	117 \pm 29	106 \pm 13	5 \pm 2	28 \pm 3	3.5 \pm 0.2
PR 1hr	192 \pm 13	68 \pm 13	8 \pm 3	30 \pm 10	2.2 \pm 0.4
PR 2hr	136 \pm 52	61 \pm 20	8 \pm 2	33 \pm 9	1.7 \pm 0.4
PR 3hr	193 \pm 13	98 \pm 7	12 \pm 5	33 \pm 18	1.9 \pm 0.1
LCx					
BL	91 \pm 12	115 \pm 7	7 \pm 1	28 \pm 1	3.2 \pm 0.4
PR 1hr	150	94	7	34	2
PR 2hr	159	42	6	38	1.5
PR 3hr	174	90	6	35	1.6
RCA					
BL	94 \pm 23	109 \pm 27	6 \pm 2	24 \pm 2	3.8 \pm 1.2
PR 1hr	131 \pm 110	100 \pm 30	10 \pm 2	31 \pm 4	2.7 \pm 1.2
PR 2hr	209 \pm 11	91 \pm 33	17 \pm 1	45 \pm 5	2
PR 3hr	196 \pm 24	87 \pm 7	12 \pm 7	43 \pm 1	2.4 \pm 0.6
LC Prox					
BL	86 \pm 5	114 \pm 1	7 \pm 4	29 \pm 8	3.5 \pm 0.1
PR 1hr	171	65	4	22	3.1
PR 2hr	158	97	6	29	2.1
PR 3hr	-	-	-	-	-

Table 6.4.2. Hemodynamics. HR, heart rate, MAP, mean arterial pressure; RAP right arterial pressure, PAP, pulmonary arterial pressure; CO, cardiac output; AMI, acute myocardial infarction; BL, baseline; LAD, left descending artery; LCx, Left Circumflex; PR, post resuscitation.



When analyzing only the group with left coronary occlusion, AMSA was higher in animals reaching ROSC but the difference was not significant ($p = 0.41$) (Figure 8.2.7)

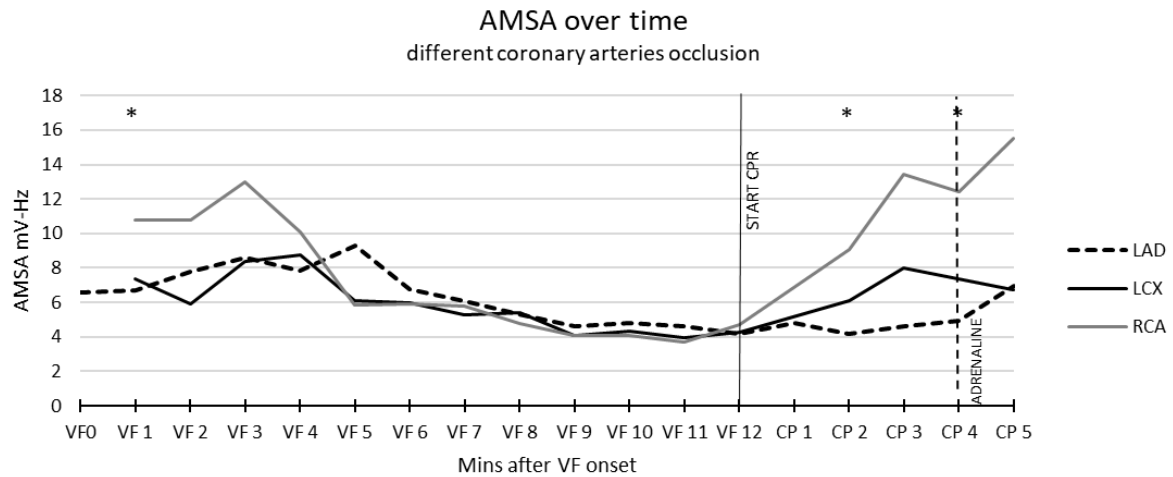


Figure 8.2.4. Mean AMSA values during untreated VF and during first 5 min of mechanical CPR. Two way ANOVA ($p = 0.02$). AMSA, amplitude spectrum area; LAD, left anterior descending; LCx, left circumflex coronary artery; CPR, cardiopulmonary resuscitation; RCA right coronary artery; VF, ventricular fibrillation. * $p < 0.05$ LAD vs. RCA

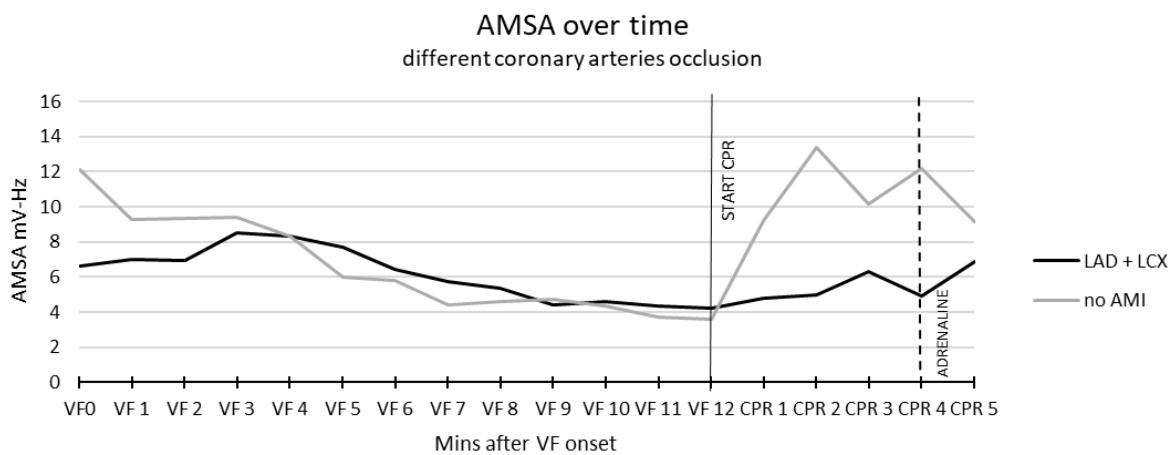
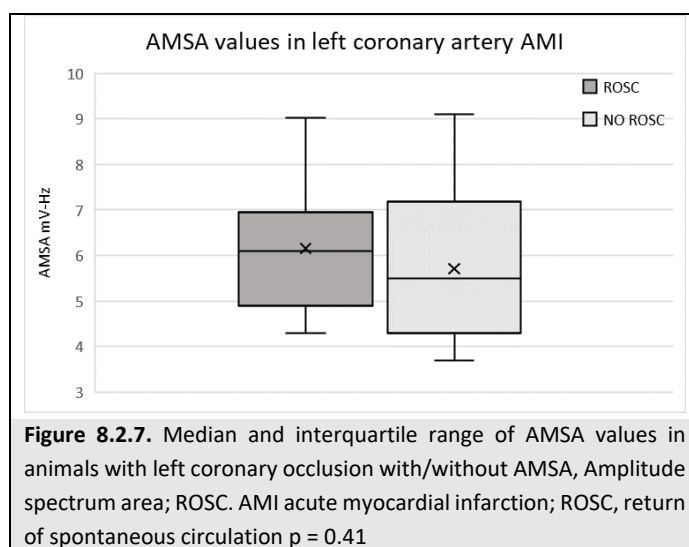
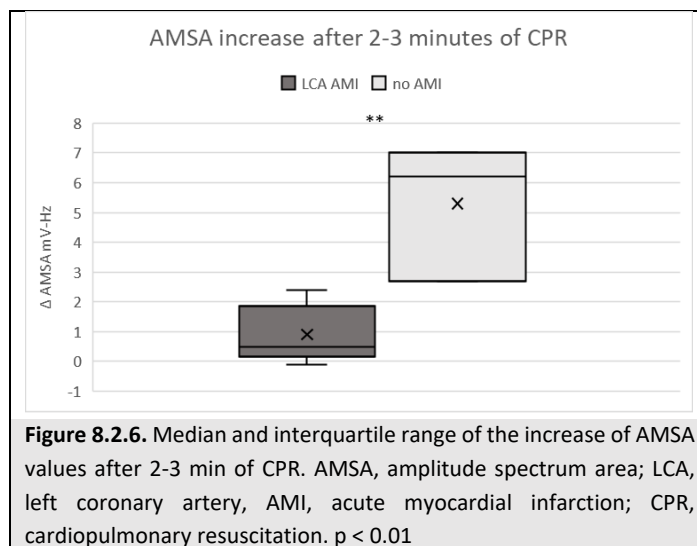


Figure 8.2.5. Mean AMSA values during untreated VF and during first 5 min of mechanical CPR. Two way ANOVA ($p = 0.03$). AMSA, amplitude spectrum area; LAD, left anterior descending; LCx, left circumflex coronary artery; CPR, cardiopulmonary resuscitation; VF, ventricular fibrillation.



8.3

8.3 DISCUSSION

8.3.1 Main findings

From this pilot study on a new experimental swine model of CA with underlying occlusion of different branches of the coronary arteries and continuous AMSA display measured by a modified defibrillator, we demonstrated that in presence of LCA occlusion, AMSA values were lower and presented a minor increase during CPR compared to non-ischemic CA. VF due to occlusion of RCA affected AMSA values to a lesser extent, thus potentially allowing for AMI identification.

8.3.2 AMSA and underlying AMI

Currently, there are no diagnostic tools to distinguish between ischemic or not ischemic etiology of CA during active resuscitation. Notably, acute coronary occlusions are more prevalent in shock-resistant VF-patients (requiring more than 3 shocks) compared to patients without and there is an association between increasing numbers of shocks and a higher likelihood of acute coronary occlusion. Shock-resistant VF-patients have lower 24-h survival rate and survival to discharge compared to patients without shock resistant VF (*Nas 2021*). Thus, a real-time appreciation of the CA etiology could have implications for resuscitation therapy.

Evidence from animal studies indicates that VF waveform measures, in particular AMSA, are differentially affected by acute ischemia, as these waveform measures may differ at the outset or over the course of resuscitation (*Ristagno 2011, Indik 2011*). Nevertheless, retrospective clinical studies report controversial results. In fact, a retrospective clinical study including 101 patients, showed that ischemic heart disease alters VF waveform characteristics, including AMSA. In this study, acute ischemic events seemed to have a larger impact on VF characteristics than chronic ischemic disease and heart failure. However, a well-defined cut-off value for clinical use could not be identified, thus limiting the application of VF waveform analysis as a diagnostic tool in the clinical setting (*Olasveengen 2009*). A subsequent clinical study of out-of-hospital VF, comparing STEMI, nSTEMI, and non-ischemic causes of CA did not observe differences according to etiology classifications across a host of waveform measures, including AMSA, prior to the initial shock or in the change of measure between the first and second shock (*Hidano 2016*). Only recently, a large retrospective study showed significantly lower AMSA values in case of underlying STEMI (*Thannhauser 2021*).

In the clinical study 2, a different trend in AMSA values overtime was observed in patients who presented a STEMI compared to those without. Interestingly, in patients with STEMI, AMSA decreased overtime during ongoing CPR, despite an initial high value, while it increased in patients without STEMI.

The initial high AMSA in STEMI patients can be explained because more than half of this patients were already connected to the defibrillator and monitored by EMS for a suspected STEMI when VF occurred. The initial AMSA measured was therefore high, because coincident with onset of CA. However, later on even if CPR was performed, the myocardium was not well perfused due to a coronary occlusion, resulting in decreases of AMSA, as demonstrated experimentally (*Ristagno 2007, Indik 2011*).

In study 4, animals with an underlying AMI presented lower mean AMSA values, in line with other preclinical and clinical studies (*Ristagno 2007, Indik 2011, Thannhauser 2022*). Of more importance, AMI animals presented a minor increase of AMSA values during the first 3 min of mechanical CPR compared to animals without AMI. Notably, after the steep increase in AMSA values characterizing the first 3 min of CPR, AMSA values seemed to remain stable. This trend can be also appreciated, even if to a lesser extent, observing clinical data. In our view, the initial increase of AMSA in response to CPR is the key concept for the possible role of AMSA in the detection of an underlying ischemia. In fact, after untreated VF and global ischemia of the heart, the myocardial perfusion provided by high quality CC translates in stable high values of AMSA (*Gazmouri 2016*), while on the contrary, myocardial perfusion is incomplete in the presence of coronary occlusion, and thus AMSA values increase to a minor extent and remain stably low. Further studies are necessary to clarify if the prediction capability of AMSA is maintained in case of underlying AMI, (*Ristagno 2007, Indik 2011*) as our data do not provide a clear contribution to address the issue. In fact, in study 3 and 4, where a LCA occlusion was present, AMSA presented higher values in animals reaching ROSC compared to animals that did not have ROSC, but the difference was not significant.

Confirmative studies are needed to support the potential application of real-time AMSA analysis for early identification of the underlying arrest cause, nevertheless, study 2 and 4 reinforce the future perspective of an early diagnosis of underlying ischemia during VF.

8.3.2.1 Localization of AMI

In study 4, we obtained spontaneous VF after occlusion of different branches of the coronary arteries in a swine model of CA and recorder continuous AMSA through a modified defibrillator. Thanks to this model of ischemic CA with different coronaries involved, we could notice that the difference in AMSA values between AMI and non-AMI were more marked when analysing only LCA group. In fact, AMSA values in animals with a RCA occlusion seemed to be more similar those in the no-AMI group. A possible interpretation for this observation, is the defibrillatory pads placement on the thorax. In fact, VF is analyzed by the defibrillator in order to obtain AMSA values, from the defibrillatory pads, which are in a position resembling a Lead II using frontal electrodes. Thus, the defibrillator analyses VF to obtain AMSA values, based on an ECG trace that reflects in pigs the electrical status of the LV.

The impact of ECG recording direction on AMSA has been studied in a recent large retrospective trial analysing ECG records during ICD implantation testing (*Nas 2021*). On average, authors found absolute AMSA-values to be markedly lower in lead I than in lead II, with a mean difference of 22%, in line with previous data (*Indik 2008*). While AMSA-values were observed to be almost equal in the low category (<6.5 mVHz), AMSA in lead I was markedly lower than in lead II in the high category (>15.5 mVHz).

In the swine model of study 4, LCA occlusion produced a change in the lead II records, that corresponds to the record analyzed with the defibrillatory pads to obtain AMSA. In fact, as the LCA is occluded and the myocardial not perfused during CPR, the VF signal captured by the pads, which are close to the ischemic region, is of lower amplitude and frequency, thus measuring lower ASMA values. On the other side, in the swine model, RCA occlusion produces a change in ECG record that is "far" from lead II, and the VF signal read by the pads has high AMSA values as it comes from myocardium that is perfused during CPR, having no coronary occlusion. Further experiments are necessary to understand the implications of which ECG trace is analysed for AMSA calculation, in order to detect all the possible localizations of cardiac ischemia. A possible role could be played by orthogonal ECG electrodes, which have the advantage not to interfere with CCs during CPR.

Study 4 reinforces the finding from previous studies, showing that AMSA values are different according to the localization of STEMI (*Nas 2021*), and lower in the leads adjacent to the ischemic area (*Bonnes 2015*). Data encourages future studies about the role of AMSA, analysed using different ECG leads, in order to detect an underlying ischemia and rapidly predispose for early revascularization strategies.

8.3.3 Implications

In study 4, we set up a swine model with different localization of AMI, with continuous AMSA calculation. In this model, preliminary data not only confirmed lower values of AMSA in the presence of AMI, more relevant when the infarct localization was close to the ECG lead read by the defibrillatory pads, but also described a significant lower increase of AMSA values in response to CPR in the presence of AMI.

8.3.4 Limitations

This study has several limitations. A greater number of animals per group is needed to acquire solid results and perform a valid statistical analysis. Notably, in this study a relevant difference in the sample size of the groups of animals can be noted; however, since the reproducibility of the non-ischemic model of CA is well described in literature (*Cherry 2015*), in our view the results are not affected by the low number of CA animals without underlying ischemia. On the contrary, the presence of a similar

trend in AMSA values in animals with an underlying ischemia, represents a strength of this study, being the variability in the extent of the ischemic area expected based of previous evidences (*Cherry 2015*), although not measured in this study. ECG monitoring, including orthogonal traces, could help in defining the AMI localization. Other instrumental analysis, like cardiac echography, biomarkers as hs-cTnT and NT-proANP, and histological samples would help in finding the correlation between VF waveform analysis and the extension of the ischemic area.

9 CONCLUSIONS

The studies provided new evidences in the field of CA with potential implications the therapeutic strategies.

In **study 1**, β 1-blockade during CPR did not facilitate VF termination but provided neuroprotection. Indeed, esmolol administration together with epinephrine during CPR accounted for a reduction of neurological injury as represented by less neuronal degeneration and microglial activation, and lower levels of NSE compared to the control treatment with saline plus epinephrine.

Studies on the waveform analysis AMSA confirm the feasibility of a real time AMSA-guide CPR strategy in a real clinical scenario (**study 2**) and suggest the potential application of this strategy also when mechanical CPR is employed (experimental **study 3**). For the first time, the predictive capability of AMSA has been prospectively confirmed in a clinical setting (**study 2**). Interestingly, AMSA emerged also as a potential tool to detect an underlying ischemia and its localisation (**study 4**). On the whole, the strength of these study is the novelty of data on AMSA and the consistency of evidences between the clinical and experimental setting, paving the way for a routinely use of AMSA during CPR. Larger clinical studies are however needed to confirm the results presented in this thesis.

10 REFERENCES

A

- Abella BS, Sandbo N, Alvarado JP, et al. Quality of cardiopulmonary resuscitation during in-hospital cardiac arrest. *JAMA* 2005; 293:305-310
- Adams JA. Endothelium and cardiopulmonary resuscitation. *Crit Care Med* 2006;34:S458-S465
- Adrie C, Adib-Conquy M, Laurent I, et al. Successful cardiopulmonary resuscitation after cardiac arrest as a “sepsis-like” syndrome. *Circulation* 2002; 106:562–568
- Adrie C, Laurent I, Monchi M, et al. Postresuscitation disease after cardiac arrest: a sepsis-like syndrome? *Curr Opin Crit Care* 2004; 10:208-212
- Adrie C, Monchi M, Laurent I, et al. Coagulopathy after successful cardiopulmonary resuscitation following cardiac arrest: implication of the protein C anticoagulant pathway. *J Am Coll Cardiol* 2005; 46:21-28
- Affatato R, Li Y, Ristagno G. See through ECG technology during cardiopulmonary resuscitation to analyze rhythm and predict defibrillation outcome. *Curr Opin Crit Care* 2016;22:199-205.
- Agarwal DA, Hess EP, Atkinson EJ, White RD. Ventricular fibrillation in Rochester, Minnesota: experience over 18 years. *Resuscitation* 2009; 80:1253–1258
- Aiello S, Perez M, Cogan C, et al. Real-Time Ventricular Fibrillation Amplitude-Spectral Area Analysis to Guide Timing of Shock Delivery Improves Defibrillation Efficacy During Cardiopulmonary Resuscitation in Swine. *J Am Heart Assoc* 2017; 6:e006749
- Aiello SR, Mendelson JB, Baetiong A, et al. Targeted Delivery of Electrical Shocks and Epinephrine, Guided by Ventricular Fibrillation Amplitude Spectral Area, Reduces Electrical and Adrenergic Myocardial Burden, Improving Survival in Swine. *J Am Heart Assoc* 2021;10:e023956
- Amann A, Klotz A, Niederklapfer T, et al. Reduction of CPR artifacts in the ventricular fibrillation ECG by coherent line removal. *BioMedical Engineering* 2010; 9:1-15
- American Heart Association guidelines for cardiopulmonary resuscitation and emergency cardiovascular care 2005: part 4. Adult basic life support. *Circulation* 2005; 112:IV-19 –IV-34
- Anderson RJ, Jinadasa SP, Hsu L. Shock subtypes by left ventricular ejection fraction following out-of-hospital cardiac arrest. *Crit Care* 2018;22(1):162
- Andreka P, Frenneaux MP. Haemodynamics of cardiac arrest and resuscitation. *Curr Opin Crit Care* 2006; 12:198-203

- Angelos MG, Butke RL, Panchal AR, et al. Cardiovascular response to epinephrine varies with increasing duration of cardiac arrest. *Resuscitation* 2008;77:101-10
- Ayoub IM, Kolarova J, Gazmuri RJ. Cariporide given during resuscitation promotes return of electrically stable and mechanically competent cardiac activity. *Resuscitation* 2010; 81:106-110
- Ayoub IM, Radhakrishnan J, Gazmuri RJ. Targeting Mitochondria for Resuscitation from Cardiac Arrest. *Crit Care Med* 2008; 36:S440–S446

B

- Babini G, Grassi L, Russo I. Duration of Untreated Cardiac Arrest and Clinical Relevance of Animal Experiments: The Relationship Between the "No-Flow" Duration and the Severity of Post-Cardiac Arrest Syndrome in a Porcine Model. *Shock* 2018;49:205-212
- Babini G, Ruggeri L, Ristagno G. Optimizing defibrillation during cardiac arrest. *Curr Opin Crit Care* 2021;27(3):246-254
- Baker PW, Conway J, Cotton C, et al. Defibrillation or cardiopulmonary resuscitation first for patients with out-of-hospital cardiac arrests found by paramedics to be in ventricular fibrillation? A randomised control trial. *Resuscitation* 2008; 79:424–431
- Bender D, Morgan RW, Nadkarni VM, et al. MLWAVE: A novel algorithm to classify primary versus secondary asphyxia-associated ventricular fibrillation. *Resusc Plus* 2021;5:100052
- Berger RD, Palazzolo J, Halperin H. Rhythm discrimination during uninterrupted CPR using motion artifact reduction system. *Resuscitation* 2007; 75:145-152
- Bessen B, Coult J, Blackwood J. Insights From the Ventricular Fibrillation Waveform Into the Mechanism of Survival Benefit From Bystander Cardiopulmonary Resuscitation. *J Am Heart Assoc* 2021; 10:e020825
- Blomqvist P, Wieloch T. Ischemic brain damage in rats following cardiac arrest using a long-term recovery model. *J Cereb Blood Flow Metab* 1985;5:420-431
- Bodtker H, Rosendahl D. Correct AED electrode placement is rarely achieved by laypersons when attaching AED electrodes to a human thorax. *Resuscitation* 2018;127:e12-3
- Bonnes JL, Thannhauser J, Hermans MC et al. Ventricular fibrillation waveform characteristics differ according to the presence of a previous myocardial infarction: A surface ECG study in ICD-patients. *Resuscitation* 2015; 96:239-45
- Bonnes JL, Thannhauser J, Nas J, et al. Ventricular fibrillation waveform characteristics of the surface ECG: Impact of the left ventricular diameter and mass. *Resuscitation* 2017 ;115:82-89
- Bottiger BW, Krumnikl JJ, Gass P, et al. The cerebral 'no-reflow' phenomenon after cardiac arrest in rats influence of low-flow reperfusion. *Resuscitation* 1997;34:79-87

- Böttiger BW, Motsch J, Böhrer H, et al. Activation of blood coagulation after cardiac arrest is not balanced adequately by activation of endogenous fibrinolysis. *Circulation* 1995; 92:2572–2578
- Box M, Watson J, Addison P, et al. Shock outcome prediction before and after CPR: A comparative study of manual and automated active compression-decompression CPR. *Resuscitation* 2008; 78:265-274
- Brierley JB, Meldrum BS, Brown AW. The threshold and neuropathology of cerebral “anoxic-ischemic” cell change. *Arch Neurol* 1973;29:367-374
- Brinkrolf P, Borowski M, Metelmann C, et al. Predicting ROSC in out-of-hospital cardiac arrest using expiratory carbon dioxide concentration: Is trend-detection instead of absolute threshold values the key? *Resuscitation* 2018;122: 19-24
- Bro-Jeppesen J, Annborn M, Hassager C, et al. Hemodynamics and vasopressor support during targeted temperature management at 33 degrees C Versus 36 degrees C after out-of-hospital cardiac arrest: a post hoc study of the target temperature management trial. *Critical care medicine* 2015;43:318-27
- Brouwer TF, Walker RG, Chapman FW et al. Association Between Chest Compression Interruptions and Clinical Outcomes of Ventricular Fibrillation Out-of-Hospital Cardiac Arrest. *Circulation* 2015; 132):1030-7
- Brown CG, Birinyi F, Werman HA et al. The comparative effects of epinephrine versus phenylephrine on regional cerebral blood flow during cardiopulmonary resuscitation. *Resuscitation* 1986;14:171–183
- Brown CG, Dzwonczyk R, Werman HA, et al. Estimating the duration of ventricular fibrillation. *Ann Emerg Med* 1989; 18:1181–1185
- Brown CG, Griffith RF, Van Ligten P, et al. Median frequency: a new parameter for predicting defibrillation success rate. *Ann Emerg Med* 1991; 20:787–789
- Brown CG, Martin DR, Pepe PE, et al. A comparison of standard-dose and high-dose epinephrine in cardiac arrest outside the hospital. The Multicenter High-Dose Epinephrine Study Group. *N Engl J Med* 1992;327:1051-5
- Brown CG, Dzwonczyk R, Martin DR. Physiologic measurement of ventricular fibrillation ECG signal: Estimating the duration of ventricular fibrillation. *Ann Emerg Med* 1993; 22:70-74
- Brown CG, Dzwonczyk R. Signal analysis of the human electrocardiogram during ventricular fibrillation: Frequency and amplitude parameters as predictors of successful countershock. *Ann Emerg Med* 1996; 27:184–188

C

- Cai J, Yang J, Jones DP. Mitochondrial control of apoptosis: the role of cytochrome c. *Biochim Biophys Acta* 1998; 1366:139-149
- Callaham M, Barton C, Matthay M. Effect of epinephrine on the ability of end-tidal carbon dioxide readings to predict initial resuscitation from cardiac arrest. *Crit Care Med* 1992;20:337-43
- Callaham M, Barton C, Matthay M. Effect of epinephrine on the ability of end-tidal carbon dioxide readings to predict initial resuscitation from cardiac arrest. *Crit Care Med* 1992;20:337-43
- Callaham M, Braun O, Valentine W, et al. Prehospital cardiac arrest treated by urban first-responders; profile of patient response and prediction of outcome by ventricular fibrillation waveform. *Ann Emerg Med* 1993; 22:1664-1667
- Callaham M, Madsen CD, Barton CW et al. A randomized clinical trial of high-dose epinephrine and norepinephrine vs standard-dose epinephrine in prehospital cardiac arrest. *JAMA* 1992;268:2667–2672
- Callaway CW, Menegazzi JJ. Waveform analysis of ventricular fibrillation to predict defibrillation. *Curr Opin Crit Care* 2005; 11:192-199
- Callaway CW, Sherman LD, Mosesso VN Jr, et al. Scaling exponent predicts defibrillation success for out-of-hospital ventricular fibrillation cardiac arrest. *Circulation* 2001; 103:1656–1661
- Calle PA, Buylaert WA, Vanhaute OA. Glycemia in the postresuscitation period. The Cerebral Resuscitation Study Group. *Resuscitation* 1989; 17:S181-S188
- Cammarata G, Weil MH, Sun S, et al. Beta1-adrenergic blockade during cardiopulmonary resuscitation improves survival. *Crit Care Med* 2004;32:S440–S443
- Cantineau JP, Lambert Y, Merckx P, et al. End-tidal carbon dioxide during cardiopulmonary resuscitation in humans presenting mostly with asystole: a predictor of outcome. *Crit Care Med* 1996; 24:791–796
- Carlisle EJ, Allen JD, Kernohan WG, et al. Fourier analysis of ventricular fibrillation of varied aetiology. *Eur Heart J* 1990; 11:173–181
- Cavus E, Bein B, Dorges V, et al. Brain tissue oxygen pressure and cerebral metabolism in an animal model of cardiac arrest and cardiopulmonary resuscitation. *Resuscitation* 2006, 71, 97–1
- Cerchiari EL, Safar P, Klein E, et al. Cardiovascular function and neurologic outcome after cardiac arrest in dogs: the cardiovascular post-resuscitation syndrome. *Resuscitation* 1993; 25:9-33
- Cerchiari EL, Safar P, Klein E, et al. Visceral, hematologic and bacteriologic changes and neurologic outcome after cardiac arrest in dogs. The visceral post-resuscitation syndrome. *Resuscitation* 1993b; 25:119-136

- Chalkias A, Scheetz MH, Gulati A, et al. Periarrest intestinal bacterial translocation and resuscitation outcome. *J Crit Care* 2016;31:217–20
- Chalkias A, Xanthos T. Pathophysiology and pathogenesis of post-resuscitation myocardial stunning. *Heart Fail Rev* 2012; 17:117–28.
-
- Cherry BH, Nguyen AQ, Hollrah RA et al. Modeling cardiac arrest and resuscitation in the domestic pig. *World J Crit Care Med* 2015;4:1-12
- Cheskes S, Schmicker RH, Christenson J, et al. Perishock pause: an independent predictor of survival from out-of-hospital shockable cardiac arrest. *Circulation* 2011; 124:58-66
- Cheskes S, Schmicker RH, Verbeek PR, et al. The impact of peri-shock pause on survival from out-of-hospital shockable cardiac arrest during the Resuscitation Outcomes Consortium PRIMED trial. *Resuscitation* 2014;85:336-42
- Chicote B, Aramendi E, Irueta U et al. Value of capnography to predict defibrillation success in out-of-hospital cardiac arrest. *Resuscitation* 2019; 138:74-81
- Cobb LA, Fahrenbruch CE, Olsufka M, et al. Changing incidence of out-of-hospital ventricular fibrillation, 1980–2000. *JAMA* 2002; 288:3008–3013
- Cobb LA, Fahrenbruch CE, Walsh TR, et al. Influence of cardiopulmonary resuscitation prior to defibrillation in patients with out-of-hospital ventricular fibrillation. *JAMA* 1999; 281:1182-8
- Coob L, Fahrenbruch C, Walsh T, et al. Influence of cardiopulmonary resuscitation prior to defibrillation in patients with out-of-hospital ventricular fibrillation. *JAMA* 1999; 281:1182–1188
- Coult J, Sherman L, Kwok H et al. Short ECG segments predict defibrillation outcome using quantitative waveform measures. *Resuscitation* 2016;109:16-20
- Coult J, Kwok H, Sherman L, et al. Ventricular fibrillation waveform measures combined with prior shock outcome predict defibrillation success during cardiopulmonary resuscitation. *J Electrocardiol* 2018;51:99-106
- Coult J, Blackwood J, Sherman L, et al. Ventricular Fibrillation Waveform Analysis During Chest Compressions to Predict Survival From Cardiac Arrest. *Circ Arrhythm Electrophysiol.* 2019;12:e006924

D

- Dalzell GW, Adgey AA. Determinants of successful transthoracic defibrillation and outcome in ventricular fibrillation. *Br Heart J* 1991; 65:311-316

- Deakin CD, Nolan JP. *European Resuscitation Council Guidelines for Resuscitation 2005: Section 3. Electrical therapies: Automated external defibrillators, defibrillation, cardioversion and pacing. Resuscitation 2005; 1:S25–S37*
- Deakin CD, Nolan JP, Sunde K, et al. *European Resuscitation Council Guidelines for Resuscitation 2010 Section 3. Electrical therapies: automated external defibrillators, defibrillation, cardioversion and pacing. Resuscitation 2010; 81:1293-1304*
- Deshmukh HG, Weil MH, Gudipati CV, et al. *Mechanism of blood flow generated by precordial compression during CPR, I: studies on closed chest precordial compression. Chest 1989; 95:1092-1099*
- Dezfulian C, Raat N, Shiva S, et al. *Role of the anion nitrite in ischemia-reperfusion cytoprotection and therapeutics. Cardiovasc Res 2007 15;75:327-38*
- Ditchey RV, Lindenfeld J. *Failure of epinephrine to improve the balance between myocardial oxygen supply and demand during closed-chest resuscitation in dogs. Circulation 1988;78:382–389*
- Donadello K, Favory R, Salgado-Ribeiro D, et al. *Sublingual and muscular microcirculatory alterations after cardiac arrest: A pilot study. Resuscitation 2011;82:690–695*
- Driver BE, Debaty G, Plummer DW, et al. *Use of esmolol after failure of standard cardiopulmonary resuscitation to treat patients with refractory ventricular fibrillation. Resuscitation. 2014;85:1337–1341*
- Dumas F, Coult J, Blackwood J, et al. *The association of chronic health status and survival following ventricular fibrillation cardiac arrest: investigation of a primary myocardial mechanism. Resuscitation 2019; 137:190–196*
- Dzwonczyk R, Brown CG, Werman HA. *The median frequency of ECG during ventricular fibrillation: Its use in an algorithm for estimating the duration of cardiac arrest. IEEE Trans Biomed Engng 1990; 37:640-646*

E

- Eftestøl T, Sunde K, Aase S, et al. *"Probability of successful defibrillation" as a monitor during CPR in out-of-hospital cardiac arrested patients. Resuscitation 2001; 48:245-254*
- Eftestøl T, Sunde K, Aase SO, et al. *Predicting outcome of defibrillation by spectral characterization and nonparametric classification of ventricular fibrillation in patients with out-of-hospital cardiac arrest. Circulation 2000; 102:1523–1529*
- Eftestøl T, Sunde K, Steen PA et al. *Effects of interrupting precordial compressions on the calculated probability of defibrillation success during out-of-hospital cardiac arrest. Circulation 2002;105:2270-3*

- Eftestøl T, Wik L, Sunde K, Steen PA. Effects of cardiopulmonary resuscitation on predictors of ventricular fibrillation defibrillation success during out-of-hospital cardiac arrest. *Circulation* 2004; 110:10-15
- Endoh H, Hida S, Oohashi S, et al. Prompt prediction of successful defibrillation from 1-s ventricular fibrillation waveform in patients with out-of-hospital sudden cardiac arrest. *J Anesth* 2011; 25:34-41
- Esmon CT. Coagulation and inflammation. *J Endotoxin Res* 2003; 9:192-198
- Ewy GA, Zuercher M, Hilwig RW, et al. Improved neurological outcome with continuous chest compressions compared with 30:2 compressions-to-ventilations cardiopulmonary resuscitation in a realistic swine model of out-of-hospital cardiac arrest. *Circulation* 2007;116:2525-30

F

- Falk JL, Rackow EC, Weil MH. End-tidal carbon dioxide concentration during cardiopulmonary resuscitation. *N Engl J Med* 1988; 318:607-611
- Feneley MP, Maier GW, Kern KB, et al. Influence of compression rate on initial success of resuscitation and 24 hour survival after prolonged manual cardiopulmonary resuscitation in dogs. *Circulation* 1988; 77:240–250
- Firoozabadi R, Nakagawa M, Helfenbein ED, Babaeizadeh S. Predicting defibrillation success in sudden cardiac arrest patients. *Journal of Electro-cardiology*. 2013;46:473–9
- Fischer S, Clauss M, Wiesnet M, et al. Hypoxia induces permeability in brain microvessel endothelial cells via VEGF and NO. *Am J Physiol* 1999; 276:C812–C820
- Fitzgibbon E, Berger R, Tsitlik J, et al. Determination of the noise source in the electrocardiogram during cardiopulmonary resuscitation. *Crit Care Med* 2002;30:S148-53
- Frangogiannis NG, Youker KA, Rossen RD, et al. Cytokines and the microcirculation in ischemia and reperfusion. *J Mol Cell Cardiol* 1998; 30:2567-2576
- Freese JP, Jorgenson DB, Liu PY, et al. Waveform analysis-guided treatment versus a standard shock-first protocol for the treatment of out-of-hospital cardiac arrest presenting in ventricular fibrillation: results of an international randomized, controlled trial. *Circulation* 2013;128:995-1002
- Frigerio L, Baldi E, Aramendi E. End-tidal carbon dioxide (ETCO₂) and ventricular fibrillation amplitude spectral area (AMSA) for shock outcome prediction in out-of-hospital cardiac arrest. Are they two sides of the same coin? *Resuscitation* 2021; 160:142-149
- Fumagalli F, Olivari D, Boccardo A, et al. Ventilation With Argon Improves Survival With Good Neurological Recovery After Prolonged Untreated Cardiac Arrest in Pigs. *J Am Heart Assoc* 2020;9:e016494

- Fumagalli F, Silver AE, Tan Q et al. Cardiac rhythm analysis during ongoing cardiopulmonary resuscitation using the Analysis During Compressions with Fast Reconfirmation technology. *Heart Rhythm* 2018;15(2):248-255

G

- Gallagher EJ, Lombardi G, Gennis P. Effectiveness of bystander cardiopulmonary resuscitation and survival following out-of-hospital cardiac arrest. *JAMA* 1995; 274:1922–1925
- Gando S, Kameue T, Nanzaki S, et al. Massive fibrin formation with consecutive impairment of fibrinolysis in patients with out-of-hospital cardiac arrest. *Thromb Haemost* 1997; 77:278–282
- Gando S, Kameue T, Nanzaki S, et al. Platelet activation with massive formation of thromboxane A2 during and after cardiopulmonary resuscitation. *Intensive Care Med* 1997b; 23:71–76
- Gando S, Nanzaki S, Morimoto Y, et al. Out-of-hospital cardiac arrest increases soluble vascular endothelial adhesion molecules and neutrophil elastase associated with endothelial injury. *Intensive Care Med* 2000; 26:38-44
- Garnett RA, Ornato JP, Gonzales ER, et al. End tidal carbon dioxide monitoring during cardiopulmonary resuscitation. *JAMA* 1987; 257:512-515
- Gazmuri RJ, Ayoub IM, Radhakrishnan J. Clinically plausible hyperventilation does not exert adverse hemodynamic effects during CPR but markedly reduces end-tidal PCO₂. *Resuscitation* 2012b;83:259-64
- Gazmuri RJ, Radhakrishnan J. Protecting mitochondrial bioenergetic function during resuscitation from cardiac arrest. *Crit Care Clin* 2012;28(2):245-70
- Gazmuri RJ, Weil MH, Bisera J, et al. Myocardial dysfunction after successful resuscitation from cardiac arrest. *Crit Care Med* 1996; 24:992-1000
- Gazmuri RJ, Kaufman CL, Baetiong A, et al. Ventricular Fibrillation Waveform Changes during Controlled Coronary Perfusion Using Extracorporeal Circulation in a Swine Model. *PLoS One*. 2016;11:e0161166
- Geppert A, Zorn G, Karth GD, et al. Soluble selectins and the systemic inflammatory response syndrome after successful cardiopulmonary resuscitation. *Crit Care Med* 2000; 28:2360-2365
- Globus MY-T, Alonso O, Dietrich WD, et al. Glutamate release and free radical production following brain injury: Effects of posttraumatic hypothermia. *J Neurochem* 1995; 65:1704–1711
- Globus MY-T, Busto R, Lin B, et al. Detection of free radical activity during transient global ischemia and recirculation: Effects of intra-ischemic brain temperature modulation. *J Neurochem* 1995b; 65:1250–1256

- Gong Y, Chen B, Li Y. A review of the performance of artifact filtering algorithms for cardiopulmonary resuscitation. *J Healthc Eng* 2013; 4:185-202
- Goto Y, Suzuki I, Inaba H. Frequency of ventricular fibrillation as predictor of one-year survival from out-of-hospital cardiac arrests. *Am J Cardiol* 2003; 92:457-459
- Gottlieb M, Dyer S, Peksa GD. Beta-blockade for the treatment of cardiac arrest due to ventricular fibrillation or pulseless ventricular tachycardia: a systematic review and meta-analysis. *Resuscitation* 2020; 146:118–125
- Goyagi T, Horiguchi T, Nishikawa T, et al. Neuroprotective effects of selective beta-1 adrenoceptor antagonist landilol and esmolol on transient forebrain ischemia in rats: a dose-response study. *Brain. Res* 2012;1461:96–101
- Goyagi T, Tobe Y, Nishikawa T. Long-term and spatial memory effects of selective β_1 -antagonists after transient focal ischemia in rats. *Br. J. Anaesth* 2012b;109:399–406
- Gralinski MR, Chi L, Park JL, et al. Protective effects of ranolazine on ventricular fibrillation induced by activation of the ATP-dependent potassium channel in the rabbit heart. *J Cardiovasc Pharmacol Ther* 1996; 1:141–148
- Granegger M, Werther T, Gilly H. Use of independent component analysis for reducing CPR artefacts in human emergency ECGs. *Resuscitation* 2011; 82:79-84
- Gräsner JT, Lefering R, Koster RW, et al. EuReCa ONE-27 Nations, ONE Europe, ONE Registry: A prospective one month analysis of out-of-hospital cardiac arrest outcomes in 27 countries in Europe. *Resuscitation* 2016;105:188-95
- Gräsner JT, Wnent J, Herlitz J, et al. Survival after out-of-hospital cardiac arrest in Europe - Results of the EuReCa TWO study. *Resuscitation* 2020;148:218-226
- Gräsner JT, Herlitz J, Tjelmeland IBM, et al. European Resuscitation Council Guidelines 2021: Epidemiology of cardiac arrest in Europe. *Resuscitation* 2021;161:61-79
- Green DR, Reed JC. Mitochondria and apoptosis. *Science* 1998; 281:1309-1312
- Grieco DL, J Brochard L, Drouet A. Intrathoracic Airway Closure Impacts CO₂ Signal and Delivered Ventilation during Cardiopulmonary Resuscitation. *Am J Respir Crit Care Med* 2019;199(6):728-737.
- Grieco DL, L JB, Drouet A, et al. Intrathoracic Airway Closure Impacts CO₂ Signal and Delivered Ventilation during Cardiopulmonary Resuscitation. *Am J Respir Crit Care Med* 2019;199:728-37
- Grmec S, Klemen P. Does the end-tidal carbon dioxide (EtCO₂) concentration have prognostic value during out-of hospital cardiac arrest? *Eur J Emerg Med* 2001; 8:263–269
- Grmec S, Lah K, Tusek-Bunc K. Difference in end-tidal CO₂ between asphyxia cardiac arrest and ventricular fibrillation/pulseless ventricular tachycardia cardiac arrest in the prehospital setting. *Crit Care* 2003;7:R139-44

- Gudipati CV, Weil MH, Bisera J, et al. Expired carbon dioxide: A noninvasive monitor of cardiopulmonary resuscitation. *Circulation* 1988; 77:234–239
- Gundersen K, Kvaløy J, Kramer-Johansen J, et al. Identifying approaches to improve the accuracy of shock outcome prediction for out-of-hospital cardiac arrest. *Resuscitation* 2008; 76:279-284

H

- Hackenhaar FS, Fumagalli F, Li Volti G, et al. Relationship between post-cardiac arrest myocardial oxidative stress and myocardial dysfunction in the rat. *J Biomed Sci* 2014 19;21:70
- Halestrap AP, Clarke SJ, Javadov SA. Mitochondrial permeability transition pore opening during myocardial reperfusion--a target for cardioprotection. *Cardiovasc Res* 2004; 61:372-385
- Hamprecht F, Jost D, Rüttimann M, et al. Preliminary results on the prediction of countershock success with fibrillation power. *Resuscitation* 2001; 50:297-299
- Hamrick JL, Hamrick JT, Lee JK, et al. Efficacy of chest compressions directed by end-tidal CO₂ feedback in a pediatric resuscitation model of basic life support. *J Am Heart Assoc* 2014;3:e000450
- Hardig BM, Götberg M, Rundgren M. Physiologic effect of repeated adrenaline (epinephrine) doses during cardiopulmonary resuscitation in the cath lab setting: A randomised porcine study. *Resuscitation* 2016;101:77-83
- He M, Gong Y, Li Y, et al. Combining multiple ECG features does not improve prediction of defibrillation outcome compared to single features in a large population of out-of-hospital cardiac arrests. *Crit Care* 2015;19:425
- Heames RM, Sado D, Deakin CD. Do doctors position defibrillation paddles correctly? Observational study. *BMJ* 2001;322:1393-4
- Hekimian G, Baugnon T, Thuong M, et al. Cortisol levels and adrenal reserve after successful cardiac arrest resuscitation. *Shock* 2004; 22:116-119
- Heradstveit BE, Sunde K, Sunde GA, et al. Factors complicating interpretation of capnography during advanced life support in cardiac arrest--a clinical retrospective study in 575 patients. *Resuscitation* 2012; 83:813-818
- Heradstveit BE, Sunde K, Sunde GA. Factors complicating interpretation of capnography during advanced life support in cardiac arrest--a clinical retrospective study in 575 patients. *Resuscitation* 2012;83(7):813-8
- Herlitz J, Ekström L, Wennerblom B, et al. Hospital mortality after out-of-hospital cardiac arrest among patients found in ventricular fibrillation. *Resuscitation* 1995; 29:11-21
- Hidano D, Coult J, Blackwood J, et al. Ventricular fibrillation waveform measures and the etiology of cardiac arrest. *Resuscitation* 2016; 109:71-75

- Hossmann KA, Oschlies U, Schwindt W, et al. Electron microscopic investigation of rat brain after brief cardiac arrest. *Acta Neuropathol (Berl)* 2001; 101:101-113
- Hossmann KA. Ischemia-mediated neuronal injury. *Resuscitation* 1993; 26:225-235
- Hostler D, Callaway CW, Newman DH, et al. Thrombin-antithrombin appearance in out-of-hospital cardiac arrest. *Prehosp Emerg Care* 2007;11(1):9-13
- Howe A, Escalona OJ, Di Maio R et al. A support vector machine for predicting defibrillation outcomes from waveform metrics. *Resuscitation*. 2014; 85:343-349
- Huang L, Weil MH, Tang W, et al. Comparison between dobutamine and levosimendan for management of postresuscitation myocardial dysfunction. *Crit Care Med* 2005; 33:487–491
- Huang Y, He Q, Yang LJ, et al. Cardiopulmonary resuscitation (CPR) plus delayed defibrillation versus immediate defibrillation for out-of-hospital cardiac arrest. *Cochrane Database Syst Rev* 2014;2014:CD009803
- Hughes GC, Post MJ, Simons M, et al. Translational physiology: porcine models of human coronary artery disease: implications for preclinical trials of therapeutic angiogenesis. *J Appl Physiol* (1985) 2003; 94:1689-701
- Hulleman M, Salcido DD, Menegazzi JJ, et al. Predictive value of amplitude spectrum area of ventricular fibrillation waveform in patients with acute or previous myocardial infarction in out-of-hospital cardiac arrest. *Resuscitation*. 2017; 120:125-131
- Hulleman M, Salcido DD, Menegazzi JJ, et al. Ventricular fibrillation waveform characteristics in out-of-hospital cardiac arrest and cardiovascular medication use. *Resuscitation* 2020; 151:173-180

|

- Idris AH, Guffey D, Aufderheide TP, et al. Relationship between chest compression rates and outcomes from cardiac arrest. *Circulation* 2012; 125:3004-3012
- Indik JH, Donnerstein RL, Kern KB, et al. Ventricular fibrillation waveform characteristics are different in ischemic heart failure compared with structurally normal hearts. *Resuscitation* 2006; 69:471-7
- Indik JH, Donnerstein RL, Berg RA, et al. Ventricular fibrillation frequency characteristics are altered in acute myocardial infarction. *Crit Care Med* 2007; 35:1133–1138
- Indik JH, Peters CM, Donnerstein RL, et al. Direction of signal recording affects waveform characteristics of ventricular fibrillation in humans undergoing defibrillation testing during ICD implantation. *Resuscitation* 2008; 78:38-45

- Indik JH, Shanmugasundaram M, Allen D, et al. Predictors of resuscitation outcome in a swine model of VF cardiac arrest: A comparison of VF duration, presence of acute myocardial infarction and VF waveform. *Resuscitation* 2009; 80:1420-1423
- Indik JH, Allen D, Gura M, et al. Utility of the ventricular fibrillation waveform to predict a return of spontaneous circulation and distinguish acute from post myocardial infarction or normal Swine in ventricular fibrillation cardiac arrest. *Circ Arrhythm Electrophysiol* 2011;4(3):337-43
- Indik JH, Conover Z, McGovern M, et al. Association of amplitude spectral area of the ventricular fibrillation waveform with survival of out-of-hospital ventricular fibrillation cardiac arrest. *J Am Coll Cardiol*. 2014; 64:1362-9
- Indik JH, Conover Z, McGovern M, et al. Amplitude-spectral area and chest compression release velocity independently predict hospital discharge and good neurological outcome in ventricular fibrillation out-of-hospital cardiac arrest. *Resuscitation*. 2015; 92:122-8
- Indik JH, Peters CM, Donnerstein RL, et al. Direction of signal recording affects waveform characteristics of ventricular fibrillation in humans undergoing defibrillation testing during ICD implantation. *Resuscitation* 2008; 78:38-45
- Irusta U, Ruiz JU, de Gauna SR, et al. A Least Mean-Square Filter for the Estimation of the Cardiopulmonary Resuscitation Artifact Based on the Frequency of the Compressions. *Ieee T Bio-Med Eng* 2009; 56:1052-1062
- Isasi I, Irusta U, Aramendi E, et al. Rhythm Analysis during Cardiopulmonary Resuscitation Using Convolutional Neural Networks. *Entropy (Basel)*. 2020;22:595
- Iwami T, Kitamura T, Kawamura T, et al. Chest compression-only cardiopulmonary resuscitation for out-of-hospital cardiac arrest with public-access defibrillation: a nationwide cohort study. *Circulation* 2012; 126:2844-2851

J

- Jacobs IG, Finn JC, Jelinek GA, et al. Effect of adrenaline on survival in out-of-hospital cardiac arrest: a randomised double-blind placebo-controlled trial. *Resuscitation* 2011;82:1138–1143
- Jacobs IG, Finn JC, Oxeir HF, et al. CPR before defibrillation in out-of-hospital cardiac arrest: a randomized trial. *Emerg Med Australas* 2005; 17:39–45
- Jagric T, Marhl M, Stajer D, et al. Irregularity test for very short electrocardiogram (ECG) signals as a method for predicting a successful defibrillation in patients with ventricular fibrillation. *Translational Research* 2007; 149:145-151
- Jalife J, Gray R. Drifting vortices of electrical waves underlie ventricular fibrillation in the rabbit heart. *Acta Physiol Scand* 1996; 157:123-131

- Jekova I, Mougeolle F, Valance A. Defibrillation shock success estimation by a set of six parameters derived from the electrocardiogram. *Physiol Meas* 2004; 25:1179-1188
- Jingjun L, Yan Z, Weijie DZ, et al. Effect and mechanism of esmolol given during cardiopulmonary resuscitation in a porcine ventricular fibrillation model. *Resuscitation* 2009;80:1052–1059
- Joar EJ, Jo K, Kjetil S. Shock outcome is related to prior rhythm and duration of ventricular fibrillation. *Resuscitation* 2007; 75:60-67
- Johnson BA, Weil MH, Tang W, et al. Mechanisms of myocardial hypercarbic acidosis during cardiac arrest. *J Appl Physiol* 1995; 78:1579-1584

K

- Kakihana Y, Ito T, Nakahara M, et al. Sepsis-induced myocardial dysfunction: pathophysiology and management. *J Intensive Care* 2016;4: 22
- Kandala J, Oommen C, Kern KB. Sudden cardiac death. *Br Med Bull* 2017; 122(1):5-15
- Karlsen H, Bergan HA, Halvorsen et al. Esmolol for cardioprotection during resuscitation with adrenaline in an ischaemic porcine cardiac arrest model. *Intensive Care Med Exp* 2019;7:65
- Kaur C, Ling EA. Blood brain barrier in hypoxic-ischemic conditions. *Curr Neurovasc Res* 2008; 5:71-81
- Kern KB, Ewy GA, Voorhees WD, et al. Myocardial perfusion pressure: a predictor of 24-hour survival during prolonged cardiac arrest in dogs. *Resuscitation* 1988; 16:241–250
- Kern KB, Garewal HS, Sanders AB, et al. Depletion of myocardial adenosine triphosphate during prolonged untreated ventricular fibrillation: effect on defibrillation success. *Resuscitation* 1990; 20:221-222
- Kern KB, Hilwig RW, Berg RA, et al. Postresuscitation left ventricular systolic and diastolic dysfunction: treatment with dobutamine. *Circulation* 1997; 95:2610–2613
- Kern KB, Hilwig RW, Rhee KH, et al. Myocardial dysfunction after resuscitation from cardiac arrest: an example of global myocardial stunning. *J Am Coll Cardiol* 1996; 28:232–240
- Kette F, Weil MH, Gazmuri RJ. Buffer solutions may compromise cardiac resuscitation by reducing coronary perfusion pressure. *JAMA* 1991; 266:2121-2126
- Killingsworth CR, Wei CC, Dell'Italia LJ et al. Short-acting beta-adrenergic antagonist esmolol given at reperfusion improves survival after prolonged ventricular fibrillation. *Circulation* 2004;109:2469-74
- Kim J, Kim K, Lee JH, et al. Prognostic implication of initial coagulopathy in out-of-hospital cardiac arrest. *Resuscitation* 2013;84:48-53

- Kim JJ, Hyun SY, Hwang SY, et al. Hormonal responses upon return of spontaneous circulation after cardiac arrest: a retrospective cohort study. *Crit Care*. 2011;15:R53
- Kloner RA, Dow JS, Bhandari A. The Antianginal Agent Ranolazine is a Potent Antiarrhythmic Agent that Reduces Ventricular Arrhythmias: Through a Mechanism Favoring Inhibition of Late Sodium Channel. *Cardiovascular Therapeutics* 2011;29:e36–e41
- Klouche K, Weil MH, Sun S et al. Echo-Doppler observations during cardiac arrest and cardiopulmonary resuscitation. *Crit Care Med* 2000; 28: N212-N213
- Klouche K, Weil MH, Sun S, et al. A comparison of alpha-methylnorepinephrine, vasopressin and epinephrine for cardiac resuscitation. *Resuscitation* 2003;57:93-100
- Klouche K, Weil MH, Sun S, et al. Evolution of the Stone Heart After Prolonged Cardiac Arrest. *Chest* 2002; 122:1006-1011
- Kolar M, Krizmaric M, Klemen P, et al. Partial pressure of end-tidal carbon dioxide successful predicts cardiopulmonary resuscitation in the field: a prospective observational study. *Crit Care* 2008;12:R115

L

- Lah K, Križmarić M, Grmec S. The dynamic pattern of end-tidal carbon dioxide during cardiopulmonary resuscitation: difference between asphyxial cardiac arrest and ventricular fibrillation/pulseless ventricular tachycardia cardiac arrest. *Crit Care* 2011; 15:R13
- Larsen MP, Eisenberg MS, Cummins RO, et al. Predicting survival from out-of-hospital cardiac arrest: a graphic model. *Ann Emerg Med* 1993; 22:1652–1658
- Laurent I, Monchi M, Chiche JD, et al. Reversible myocardial dysfunction in survivors of out-of-hospital cardiac arrest. *J Am Coll Cardiol* 2002;40(12):2110-6
- Laver S, Farrow C, Turner D, et al. Mode of death after admission to an intensive care unit following cardiac arrest. *Intensive Care Med* 2004;30:2126–2128
- Lebuffe G, Schumacker PT, Shao ZH, et al. ROS and NO trigger early preconditioning: relationship to mitochondrial KATP channel. *Am J Physiol Heart Circ Physiol* 2003;284:H299-308
- Lee YH, Lee KJ, Min YH, et al. Refractory ventricular fibrillation treated with esmolol. *Resuscitation*. 2016;107:150–155
- Lee DH, Lee BK, Jeung KW, et al. Disseminated intravascular coagulation is associated with the neurologic outcome of cardiac arrest survivors. *Am J Emerg Med* 2017;35:1617-1623
- Lemiale V, Dumas F, Mongardon N, et al. Intensive care unit mortality after cardiac arrest: the relative contribution of shock and brain injury in a large cohort. *Intensive Care Med*. 2013;39(11):1972-80

- Levine RL, Wayne MA, Miller CC. End-tidal carbon dioxide and outcome of out-of-hospital cardiac arrest. *N Engl J Med* 1997;337:301-6
- Levraut J, Iwase H, Shao ZH, et al. Cell death during ischemia: relationship to mitochondrial depolarization and OS generation. *Am J Physiol Heart Circ Physiol* 2003;284:H549-58
- Lewis CM, Weil MH. Hemodynamic spectrum of vasopressor and vasodilator drug. *JAMA* 1969; 208:1391-1398
- Li Y, Ristagno G, Bisera J, et al. Electrocardiogram waveforms for monitoring effectiveness of chest compression during cardiopulmonary resuscitation. *Crit Care Med* 2008; 36:211-215
- Li Y, Bisera J, Geheb F, et al. Identifying potentially shockable rhythms without interrupting cardiopulmonary resuscitation. *Crit Care Med* 2008b; 36:198-203
- Li Y, Tang W. Techniques for artefact filtering from chest compression corrupted ECG signals: good, but not enough. *Resuscitation* 2009; 80:1219–1220
- Li Y, Bisera J, Weil MH, et al. An algorithm used for ventricular fibrillation detection without interrupting chest compression. *IEEE Trans Biomed Eng* 2012; 59:78-86
- Li Z, et al. Selective beta-blocker esmolol improves cerebral cortex microcirculation in a swine ventricular fibrillation model. *J. Cell. Biochem.* 2019; 120:3679–3688. doi: 10.1002/jcb.27647
- Liachenko S, Tang P, Hamilton RL, et al. Regional dependence of cerebral reperfusion after circulatory arrest in rats. *J Cereb Blood Flow Metab* 2001; 21:1320
- Lin L, Lo M, Ko PC, et al. Detrended fluctuation analysis predicts successful defibrillation for out-of-hospital ventricular fibrillation cardiac arrest. *Resuscitation* 2010; 81:297-301
- Lindner KH, Ahnefeld FW, Schuermann W. Epinephrine and norepinephrine in cardiopulmonary resuscitation: effects on myocardial oxygen delivery and consumption. *Chest* 1990; 97:1458–1462
- Lindner KH, Strohmenger HU, Ensinger H, et al. Stress hormone response during and after cardiopulmonary resuscitation. *Anesthesiology* 1992;77:662–8
- Link MS, Atkins DL, Passman RS, et al. Part 6: Electrical Therapies Automated External Defibrillators, Defibrillation, Cardioversion, and Pacing 2010 American Heart Association Guidelines for Cardiopulmonary Resuscitation and Emergency Cardiovascular Care. *Circulation* 2010; 122:S706–S719
- Lipton P. Ischemic cell death in brain neurons. *Physiol Rev* 1999; 79:1431-1568
- Livesay JJ, Follette DM, Fey KH et al. Optimizing myocardial supply/demand balance with alpha-adrenergic drugs during cardiopulmonary resuscitation. *J Thorac Cardiovasc Surg* 1978;76:244-51
- Lo MT, Lin LY, Hsieh WH, et al. A new method to estimate the amplitude spectrum analysis of ventricular fibrillation during cardiopulmonary resuscitation. *Resuscitation* 2013; 84:1505-11
- Longstreth Jr WT, Copass MK, Dennis LK, et al. Intravenous glucose after out-of-hospital cardiopulmonary arrest: a community-based randomized trial. *Neurology* 1993; 43:2534-2541

- Longstreth Jr WT, Diehr P, Inui TS. Prediction of awakening after out-of-hospital cardiac arrest. *N Engl J Med* 1983; 308:1378-1382
- Longstreth Jr WT, Inui TS. High blood glucose level on hospital admission and poor neurological recovery after cardiac arrest. *Ann Neurol* 1984; 15:59-63
- Lu G, Brittain JS, Holland P, et al. Removing ECG noise from surface EMG signals using adaptive filtering. *Neurosci Lett*. 2009;462(1):14-9
- Lui CT, Poon KM, Tsui KL. Abrupt rise of end tidal carbon dioxide level was a specific but non-sensitive marker of return of spontaneous circulation in patient with out-of-hospital cardiac arrest. *Resuscitation* 2016;104:53-8

M

- Ma JH, Luo AT, Zhang PH. Effect of hydrogen peroxide on persistent sodium current in guinea pig ventricular myocytes. *Acta Pharmacol Sin* 2005; 26:828–834
- Madathil RJ, Hira RS, Stoeckl M, et al. Ischemia reperfusion injury as a modifiable therapeutic target for cardioprotection or neuroprotection in patients undergoing cardiopulmonary resuscitation. *Resuscitation* 2016;105: 85–91
- Magliocca A, Olivari D, De Giorgio D, et al. LUCAS Versus Manual Chest Compression During Ambulance Transport: A Hemodynamic Study in a Porcine Model of Cardiac Arrest. *J Am Heart Assoc*. 2019;8;8(1):e011189
- Martin DR, Brown CG, Dzwonczyk R. Frequency analysis of the human and swine electrocardiogram during ventricular fibrillation. *Resuscitation* 1991; 22:85–91
- Maxwell MP, Hearse DJ, Yellon DM. Species variation in the coronary collateral circulation during regional myocardial ischaemia: a critical determinant of the rate of evolution and extent of myocardial infarction. *Cardiovasc Res*. 1987;21:737-46
- Mentzelopoulos SD, Malachias S, Chamos C, et al. Vasopressin, steroids, and epinephrine and neurologically favorable survival after in-hospital cardiac arrest: a randomized clinical trial. *JAMA* 2013; 310:270-279
- Meybohm P, Gruenewald M, Albrecht M, et al. Hypothermia and postconditioning after cardiopulmonary resuscitation reduce cardiac dysfunction by modulating inflammation, apoptosis and remodeling. *PLoS One* 2009; 4:e7588
- Monsieurs KG, De Cauwer H, Wuyts FL, et al. A rule for early outcome classification of out-of-hospital cardiac arrest patients presenting with ventricular fibrillation. *Resuscitation* 1998; 36:37–44

- Müllner M, Sterz F, Binder M, Schreiber W, Deimel A, Laggner AN. Blood glucose concentration after cardiopulmonary resuscitation influences functional neurological recovery in human cardiac arrest survivors. *J Cereb Blood Flow Metab* 1997;17:430-436
- Munoz C, Carlet J, Fitting C, et al. Dysregulation of in vitro cytokine production by monocytes during sepsis. *J Clin Invest* 1991;88:1747–1754

N

- Nakagawa Y, Amino M, Inokuchi S, et al. Novel CPR system that predicts return of spontaneous circulation from amplitude spectral area before electric shock in ventricular fibrillation. *Resuscitation*. 2017; 113:8–12
- Nas J, van Dongen LH, Thannhauser J, et al. The effect of the localisation of an underlying ST-elevation myocardial infarction on the VF-waveform: A multi-centre cardiac arrest study. *Resuscitation* 2021; 168:11-18
- Negovsky VA, Gurvitch AM. Post-resuscitation disease: a new nosological entity: its reality and significance. *Resuscitation* 1995; 30:23–27
- Negovsky VA. Postresuscitation disease. *Crit Care Med* 1988; 16:942–946
- Negovsky VA. The second step in resuscitation: the treatment of the “post-resuscitation disease.” *Resuscitation* 1972; 1:1–7
- Neumar RW, Nolan JP, Adrie C, et al. Post-cardiac arrest syndrome: epidemiology, pathophysiology, treatment, and prognostication. A consensus statement from the International Liaison Committee on Resuscitation (American Heart Association, Australian and New Zealand Council on Resuscitation, European Resuscitation Council, Heart and Stroke Foundation of Canada, InterAmerican Heart Foundation, Resuscitation Council of Asia, and the Resuscitation Council of Southern Africa); the American Heart Association Emergency Cardiovascular Care Committee; the Council on Cardiovascular Surgery and Anesthesia; the Council on Cardiopulmonary, Perioperative, and Critical Care; the Council on Clinical Cardiology; and the Stroke Council. *Circulation* 2008; 118:2452-2483
- Neumar RW, Otto CW, Link MS, et al. Part 8: Adult Advanced Cardiovascular Life Support 2010 American Heart Association Guidelines for Cardiopulmonary Resuscitation and Emergency Cardiovascular Care. *Circulation* 2010; 122:S729-S767
- Neumar RW. Molecular mechanisms of ischemic neuronal injury. *Ann Emerg Med* 2000;36:483-506
- Neurauter A, Eftestøl T, Kramer-Johansen J, et al. Improving countershock success prediction during cardiopulmonary resuscitation using ventricular fibrillation features from higher ECG frequency bands. *Resuscitation* 2008; 79:453-459

- Neurauter A, Eftestøl T, Kramer-Johansen J, et al. Prediction of countershock success using single features from multiple ventricular fibrillation frequency bands and feature combinations using neural networks. *Resuscitation* 2007; 73:253-263
- Nichol G, Leroux B, Wang H, et al. Trial of Continuous or Interrupted Chest Compressions during CPR. *N Engl J Med* 2015;373(23):2203-14
- Niemann JT, Cairns CB, Sharma J, et al. Treatment of prolonged ventricular fibrillation: immediate countershock versus high-dose epinephrine and CPR preceding countershock. *Circulation* 1992; 85:281-287
- Niemann JT, Criley JM, Rosborough JP, et al. Predictive indices of successful cardiac resuscitation after prolonged arrest and experimental cardiopulmonary resuscitation. *Ann Emerg Med* 1985; 14:521–528
- Niemann JT, Rosborough JP, Youngquist S, et al. Is all ventricular fibrillation the same? A comparison of ischemically induced with electrically induced ventricular fibrillation in a porcine cardiac arrest and resuscitation model. *Crit Care Med* 2007;35:1356-61
- Noc M, Weil MH, Gazmuri RJ, et al. Ventricular fibrillation voltage as a monitor of the effectiveness of cardiopulmonary resuscitation. *J Lab Clin Med* 1994; 124:421–426
- Noc M, Weil MH, Tang W, et al. Electrocardiographic prediction of the success of cardiac resuscitation. *Crit Care Med* 1999; 27:708–714
- Nolan JP, Neumar RW, Adrie C, et al. Post-cardiac arrest syndrome: epidemiology, pathophysiology, treatment, and prognostication. A Scientific Statement from the International Liaison Committee on Resuscitation; the American Heart Association Emergency Cardiovascular Care Committee; the Council on Cardiovascular Surgery and Anesthesia; the Council on Cardiopulmonary, Perioperative, and Critical Care; the Council on Clinical Cardiology; the Council on Stroke. *Resuscitation* 2008;79(3):350-79
- Nolan JP, Soar J, Zideman DA, et al. European Resuscitation Council Guidelines for Resuscitation 2010 Section 1. Executive summary. *Resuscitation* 2010; 81:1219-1276
- Nolan JP, Sandroni C, Böttiger BW et al. European Resuscitation Council and European Society of Intensive Care Medicine Guidelines 2021: Post-resuscitation care. *Resuscitation* 2021; 161:220-269
- Novack TA, Dillon MC, Jackson WT. Neurochemical mechanisms in brain injury and treatment: A review. *J Clin Exp Neuropsychol* 1996; 18:685–706
- Nurmi J, Rosenberg P, Castren M. Adherence to guidelines when positioning the defibrillation electrodes. *Resuscitation* 2004;61:143

O

- *Olasveengen TM, Eftestøl T, Gundersen K, et al. Acute ischemic heart disease alters ventricular fibrillation waveform characteristics in out-of hospital cardiac arrest. Resuscitation 2009; 80:412–7*
- *Olasveengen TM, Wik L, Sunde K, et al. Outcome when adrenaline (epinephrine) was actually given vs. not given - post hoc analysis of a randomized clinical trial. Resuscitation 2012; 83:327-332*
- *Olasveengen TM, Mancini ME, Perkins GD, et al. Adult Basic Life Support: 2020 International Consensus on Cardiopulmonary Resuscitation and Emergency Cardiovascular Care Science With Treatment Recommendations. Circulation 2020; 142:S41-S91*
- *Ono Y, Hayakawa M, Maekawa K, et al. Fibrin/fibrinogen degradation products (FDP) at hospital admission predict neurological outcomes in out-of-hospital cardiac arrest patients. Resuscitation 2017;111:62-67*
- *Osswald S, Trouton TG, O’Nunain SS, et al. Relation between shock-related myocardial injury and defibrillation efficacy of monophasic and biphasic shocks in a canine model. Circulation 1994; 90:2501-2509*
- *Ouyang P, Brinker JA, Bulkley BH, et al. Ischemic ventricular fibrillation: the importance of being spontaneous. Am J Cardiol 1981; 48:455-459*
- *Ouyang YB, Tan Y, Comb M, et al. Survival- and death-promoting events after transient cerebral ischemia: phosphorylation of Akt, release of cytochrome C and Activation of caspase-like proteases. J Cereb Blood Flow Metab 1999;19:1126-35*

P

- *Paiva EF, Paxton JH, O’Neil BJ. The use of end-tidal carbon dioxide (ETCO₂) measurement to guide management of cardiac arrest: A systematic review. Resuscitation 2018;123:1-7*
- *Panchal AR, Bartos JA, Cabañas JG, et al. Part 3: Adult Basic and Advanced Life Support: 2020 American Heart Association Guidelines for Cardiopulmonary Resuscitation and Emergency Cardiovascular Care. Circulation 2020;142:S366-S468*
- *Panfilov A. Spiral breakup as a model of ventricular fibrillation. Chaos 1998; 8:57-64*
- *Paradis NA, Martin GB, Rosenberg J, et al. Coronary perfusion pressure and the return of spontaneous circulation in human cardiopulmonary resuscitation. JAMA 1990; 263:1106–1113*
- *Peberdy MA, Callaway CW, Neumar RW, et al. Part 9: post-cardiac arrest care: 2010 American Heart Association Guidelines for Cardiopulmonary Resuscitation and Emergency Cardiovascular Care. Circulation 2010;122:S768-86*

- Pellis T, Weil MH, Tang W, et al. Evidence favoring the use of an alpha2-selective vasopressor agent for cardiopulmonary resuscitation. *Circulation* 2003;108:2716–2721
- Perkins GD, Ji C, Deakin CD, et al. A Randomized Trial of Epinephrine in Out-of-Hospital Cardiac Arrest. *N Engl J Med* 2018;379:711-721
- Parnat AM, Weil MH, Tang W, et al. Optimizing timing of ventricular defibrillation. *Crit Care Med* 2001; 29:2360-2365
- Podbregar M, Kovacic M, Podbregar-Mars A, et al. Predicting defibrillation success by 'genetic' programming in patients with out-of-hospital cardiac arrest. *Resuscitation* 2003; 57:153-159
- Pokorna M, Necas E, Kratochvil J et al. A sudden increase in partial pressure end-tidal carbon dioxide (P(ET)CO₂) at the moment of return of spontaneous circulation. *J Emerg Med* 2010;38:614-21
- Polderman KH. Mechanisms of action, physiological effects, and complications of hypothermia. *Crit Care Med* 2009;37:S186-202
- Poppe M, Stratil P, Clodi C, et al. Initial end-tidal carbon dioxide as a predictive factor for return of spontaneous circulation in nonshockable out-of-hospital cardiac arrest patients: A retrospective observational study. *European Journal of Anaesthesiology* 2019;36:524-30
- Povoas HP, Bisera J. Electrocardiographic waveform analysis for predicting the success of defibrillation. *Crit Care Med* 2000; 28:N210-N211
- Prengel AW, Lindner KH, Ensinger H, et al. Plasma catecholamine concentrations after successful resuscitation in patients. *Crit Care Med* 1992;20:609–614
- Prengel AW, Linstedt U, Zenz M, et al. Effects of combined administration of vasopressin, epinephrine, and norepinephrine during cardiopulmonary resuscitation in pigs. *Crit Care Med* 2005;33:2587–2591
- Pulsinelli WA. Selective neuronal vulnerability: morphological and molecular characteristics. *Prog Brain Res* 1985;63:29-37

Q

- Qin H, Walcott GP, Killingsworth CR, Rollins DL, Smith WM, Ideker RE. Impact of myocardial ischemia and reperfusion on ventricular defibrillation patterns, energy requirements, and detection of recovery. *Circulation* 2002; 105:2537-2542

R

- Radhakrishnan J, Ayoub IM, Gazmuri RJ. Activation of caspase-3 may not contribute to postresuscitation myocardial dysfunction. *Am J Physiol Heart Circ Physiol* 2009; 296:H1164-H1174
- Radhakrishnan J, Wang S, Ayoub IM, et al. Circulating levels of cytochrome c after resuscitation from cardiac arrest: a marker of mitochondrial injury and predictor of survival. *Am J Physiol Heart Circ Physiol* 2007; 292:H767-H775
- Rea TD, Fahrenbruch C, Culley L, et al. CPR with chest compression alone or with rescue breathing. *N Engl J Med* 2010;363(5):423-433
- Rea TD, Pearce RM, Raghunathan TE, et al. Incidence of out-of-hospital cardiac arrest. *Am J Cardiol* 2004; 93:1455–1460
- Reimer KA, Jennings RB. The "wavefront phenomenon" of myocardial ischemic cell death. II. Transmural progression of necrosis within the framework of ischemic bed size (myocardium at risk) and collateral flow. *Lab Invest* 1979; 40:633-644
- Raymond TT, Pandit SV, Griffis H, et al. Effect of Amplitude Spectral Area on Termination of Fibrillation and Outcomes in Pediatric Cardiac Arrest. *J Am Heart Assoc* 2021;10:e020353
- Reis C, Akyol O, Araujo C, et al. Pathophysiology and the monitoring methods for cardiac arrest associated brain injury. *Int J Mol Sci* 2017:18
- Ringgaard VK, Wemmelund KB, Sloth E, et al. Esmolol does not affect circulation negatively during resuscitation. *Am J Emerg Med* 2019;37:690-695
- Ringh M, Herlitz J, Hollenberg J, Rosenqvist M, Svensson L. Out of hospital cardiac arrest outside home in Sweden, change in characteristics, outcome and availability for public access defibrillation. *Scand J Trauma Resusc Emerg Med* 2009;17:18
- Ristagno G, Tang W, Chang YT, et al. The quality of chest compressions during cardiopulmonary resuscitation overrides importance of timing of defibrillation. *Chest* 2007; 132:70-75
- Ristagno G, Tang W, Xu TY, et al. Outcomes of CPR in the presence of partial occlusion of left anterior descending coronary artery. *Resuscitation* 2007b; 75:357-365
- Ristagno G, Tang W, Sun S, et al. Cerebral cortical microvascular flow during and following cardiopulmonary resuscitation after short duration of cardiac arrest. *Resuscitation* 2008; 77:229-234
- Ristagno G, Gullo A, Berlot G, et al. Prediction of successful defibrillation in human victims of out-of-hospital cardiac arrest: a retrospective electrocardiographic analysis. *Anaesth Intensive Care* 2008b; 36:46-50

- Ristagno G, Tang W, Russell JK, et al. Minimal interruption of cardiopulmonary resuscitation for a single shock as mandated by automated external defibrillations does not compromise outcomes in a porcine model of cardiac arrest and resuscitation. *Crit Care Med* 2008c; 36:3048-3053
- Ristagno G, Tang W, Huang L, et al. Epinephrine reduces cerebral perfusion during cardiopulmonary resuscitation. *Crit Care Med* 2009;37(4):1408-15
- Ristagno G, Li Y, Gullo A, et al. Amplitude spectrum area as a predictor of successful defibrillation. In Gullo A. (ed.): *Anaesthesia Pharmacology Intensive Care and Emergency Medicine* 23. Springer Verlag Italia 2011, pp. 141-160
- Ristagno G, Li Y, Fumagalli F et al. Amplitude spectrum area to guide resuscitation-a retrospective analysis during out-of-hospital cardiopulmonary resuscitation in 609 patients with ventricular fibrillation cardiac arrest. *Resuscitation* 2013; 84:1697-703
- Ristagno G, Latini R, Vaahersalo J, et al. Early activation of the kynurenine pathway predicts early death and long-term outcome in patients resuscitated from out of-hospital cardiac arrest. *J Am Heart Assoc* 2014;3 4::e001094
- Ristagno G, Mauri T, Cesana G, et al. Amplitude spectrum area to guide defibrillation: a validation on 1617 patients with ventricular fibrillation. *Circulation* 2015; 131:478-87
- Rivers EP, Wortsman J, Rady MY, et al. The effect of the total cumulative epinephrine dose administered during human CPR on hemodynamic, oxygen transport, and utilization variables in the postresuscitation period. *Chest* 1994;106:1499 –1507
- Rodriguez E, Echeverria JC, Alvarez-Ramirez J. Fractality in electrocardiographic waveforms for healthy subjects and patients with ventricular fibrillation. *Chaos, Solitons and Fractals* 2009; 39:1046-1054
- Ruggeri L, Franco A, Alba AC, et al. Coagulation Derangements in Patients With Refractory Cardiac Arrest Treated With Extracorporeal Cardiopulmonary Resuscitation. *J Cardiothorac Vasc Anesth.* 2019;33:1877-1882
- Ruggeri L, Nespoli F, Ristagno G, et al. Esmolol during cardiopulmonary resuscitation reduces neurological injury in a porcine model of cardiac arrest. *Sci Rep.* 2021 20;11(1):10635
- Ruiz J, Irusta U, Ruiz De Gauna S, et al. Cardiopulmonary resuscitation artefact suppression using a Kalman filter and the frequency of chest compressions as the reference signal. *Resuscitation* 2010; 81:1087-1094
- Ruiz-Bailén M, Aguayo de Hoyos E, Ruiz-Navarro S, et al Reversible myocardial dysfunction after cardiopulmonary resuscitation. *Resuscitation* 2005; 66:175–181
- Ruiz de Gauna S, Ruiz J, Irusta U, et al. A method to remove CPR artefacts from human ECG using only the recorded ECG. *Resuscitation* 2008;76:271-8

S

- Sahni D, Kaur GD, Jit H et al. Anatomy & distribution of coronary arteries in pig in comparison with man. *Indian J Med Res* 2008;127:564-70
- Salcido DD, Schmicker RH, Kime N et al. Effects of intra-resuscitation antiarrhythmic administration on rearrest occurrence and intra-resuscitation ECG characteristics in the ROC ALPS trial. *Resuscitation* 2018 ;129:6-12
- Sanders AB, Kern KB, Atlas M, et al. Importance of the duration of inadequate coronary perfusion pressure on resuscitation from cardiac arrest. *J Am Coll Cardiol* 1985b; 6:113–118
- Sanders AB, Ogle M, Ewy GA. Coronary perfusion pressure during cardiopulmonary resuscitation. *Am J Emerg Med* 1985; 2:11–14
- Sandroni C, Cavallaro F, Callaway CW, et al. Predictors of poor neurological outcome in adult comatose survivors of cardiac arrest: a systematic review and meta-analysis. Part 1: patients not treated with therapeutic hypothermia. *Resuscitation* 2013;84(10):1310-23
- Sandroni C, Cavallaro F, Callaway CW, et al. Predictors of poor neurological outcome in adult comatose survivors of cardiac arrest: a systematic review and meta-analysis. Part 2: Patients treated with therapeutic hypothermia. *Resuscitation* 2013b;84(10):1324-38
- Sandroni C, Ristagno G. End-tidal CO₂ to detect recovery of spontaneous circulation during cardiopulmonary resuscitation: We are not ready yet. *Resuscitation* 2016;104:A5-6
- Sasson C, Rogers MA, Dahl J, et al. Predictors of survival from out-of-hospital cardiac arrest: a systematic review and meta-analysis. *Circ Cardiovasc Qual Outcomes* 2010;3:63-81
- Sato Y, Weil MH, Sun Tang W, et al. Adverse effects of interrupting precordial compression during cardiopulmonary resuscitation. *Crit Care Med* 1997; 25:733–736
- Savastano S, Baldi E, Raimondi M, et al. End-tidal carbon dioxide and defibrillation success in out-of-hospital cardiac arrest. *Resuscitation* 2017; 121:71-75
- Schöchl H, Cadamuro J, Seidl S, et al. Hyperfibrinolysis is common in out-of-hospital cardiac arrest: results from a prospective observational thromboelastometry study. *Resuscitation* 2013;84:454-9
- Schoene P, Coult J, Murphy L et al. Course of quantitative ventricular fibrillation waveform measure and outcome following out-of-hospital cardiac arrest. *Heart Rhythm*. 2014; 11:230-6
- Schoenenberger RA, von Planta M, von Planta I. Survival after failed out-of-hospital resuscitation. Are further therapeutic efforts in the emergency department futile? *Arch Intern Med* 1994;154(21):2433-7
- Schultz CH, Rivers EP, Feldkamp CS, et al. A characterization of hypothalamic-pituitary-adrenal axis function during and after human cardiac arrest. *Crit Care Med* 1993; 21:1339-1347

- Scquizzato T, Landoni G, Paoli A et al. Effects of COVID-19 pandemic on out-of-hospital cardiac arrests: A systematic review. *Resuscitation*. 2020; 157:241-247
- Shandilya S, Ward K, Kurz M, et al. Non-linear dynamical signal characterization for prediction of defibrillation success through machine learning. *BMC Med Inform Decis Mak* 2012; 12:116
- Shanmugasundaram M, Valles A, Kellum MJ, et al. Analysis of amplitude spectral area and slope to predict defibrillation in out of hospital cardiac arrest due to ventricular fibrillation (VF) according to VF type: Recurrent versus shock-resistant. *Resuscitation* 2012; 83:1242-1247
- Sharma HS, Miclescu A, Wiklund L. Cardiac arrest -induced regional blood-brain barrier breakdown, edema formation and brain pathology: a light and electron microscopic study on a new model for neurodegeneration and neuroprotection in porcine brain. *J Neural Transm* 2011;118: 87-114
- Sheak KR, Wiebe DJ, Leary M, et al. Quantitative relationship between end-tidal carbon dioxide and CPR quality during both in-hospital and out-of-hospital cardiac arrest. *Resuscitation* 2015;89:149-54
- Sherman LD, Rea TD, Waters JD, et al. Logarithm of the absolute correlations of the ECG waveform estimates duration of ventricular fibrillation and predicts successful defibrillation. *Resuscitation* 2008; 78:346-354
- Sherman L, Niemann J, Youngquist ST, et al. Beta-blockade causes a reduction in the frequency spectrum of VF but improves resuscitation outcome: A potential limitation of quantitative waveform measures. *Resuscitation* 2012; 83:511-516
- Siesjo BK, Bengtsson F, Grampp W, et al. Calcium, excitotoxins, and neuronal death in brain. *Ann NY Acad Sci* 1989; 568:234-251
- Skrifvars MB, Pettila V, Rosenberg PH, et al. A multiple logistic regression analysis of in-hospital factors related to survival at six months in patients resuscitated from out-of-hospital ventricular fibrillation. *Resuscitation* 2003; 59:319-328
- Slezak J, Tribulova N, Pristacova J, et al. Hydrogen peroxide changes in ischemic and reperfused heart. *Am J Pathol* 1995; 147:772-781
- Small DL, Morley P, Buchan AM. Biology of ischemic cerebral cell death. *Prog Cardiovasc Dis* 1999;42:185-207
- Snyder D, Morgan C. Wide variation in cardiopulmonary resuscitation interruption intervals among commercially available automated external defibrillators may affect survival despite high defibrillation efficacy. *Crit Care Med* 2004; 32:S421-S424
- Soar J, Nolan JP, Böttiger BW et al. European Resuscitation Council Guidelines for Resuscitation 2015: Section 3. Adult advanced life support. *Resuscitation* 2015;95:100-47

- Soar J, Maconochie I, Wyckoff MH et al. 2019 International Consensus on Cardiopulmonary Resuscitation and Emergency Cardiovascular Care Science With Treatment Recommendations: Summary From the Basic Life Support; Advanced Life Support; Pediatric Life Support; Neonatal Life Support; Education, Implementation, and Teams; and First Aid Task Forces. *Circulation* 2019;140(24):e826-e880
- Soar J, Böttiger BW, Carli P, et al. European Resuscitation Council Guidelines 2021: Adult advanced life support. *Resuscitation* 2021;161:115-151
- Song Y, Shryock JC, Wagner S, et al. Blocking late sodium current reduces hydrogen peroxide-induced arrhythmogenic activity and contractile dysfunction. *J Pharmacol Exp Ther* 2006; 318:214–222
- Steen S, Liao Q, Pierre L, et al. The critical importance of minimal delay between chest compressions and subsequent defibrillation: a haemodynamic explanation. *Resuscitation* 2003; 58:249-258
- Stewart AJ, Allen JD, Adgey AA. Frequency analysis of ventricular fibrillation and resuscitation success. *Q J Med* 1992; 85:761–769
- Strohmenger HU, Lindner KH, Lurie KG, et al: Frequency of ventricular fibrillation as predictor of defibrillation success during cardiac surgery. *Anesth Analg* 1994; 79:434-438
- Strohmenger HU, Lindner KH, Keller A, et al. Spectral analysis of ventricular fibrillation and closed-chest cardiopulmonary resuscitation. *Resuscitation* 1996; 33:155–161
- Strohmenger HU, Lindner KH, Brown CG. Analysis of the ventricular fibrillation ECG signal amplitude and frequency parameters as predictors of countershock success in humans. *Chest* 1997; 111:584–589
- Sutton RM, French B, Meaney PA, et al. Physiologic monitoring of CPR quality during adult cardiac arrest: A propensity-matched cohort study. *Resuscitation* 2016;106:76-82
- Swindle MM, Horneffer PJ, Gardner TJ, et al. Anatomic and anesthetic considerations in experimental cardiopulmonary surgery in swine. *Lab Anim Sci.* 1986;36:357-61

T

- Tang W, Snyder D, Wang J, et al. One-shock versus three-shock defibrillation protocol significantly improves outcome in a porcine model of prolonged ventricular fibrillation cardiac arrest. *Circulation* 2006; 113:2683–2689
- Tang W, Weil MH, Gazmuri RJ, et al. Pulmonary ventilation/perfusion defects induced by epinephrine during cardiopulmonary resuscitation. *Circulation* 1991; 84:2101-2107
- Tang W, Weil MH, Sun RJ, et al. The effects of biphasic and conventional monophasic defibrillation on post resuscitation myocardial function. *J Am Coll Cardiol* 1999; 4:815-822

- Tang W, Weil MH, Sun S, et al. Epinephrine increases the severity of postresuscitation myocardial dysfunction. *Circulation* 1995;92:3089-93
- Tang W, Weil MH, Sun S, et al. Progressive myocardial dysfunction after cardiac resuscitation. *Crit Care Med* 1993;21(7):1046-50
- Tang W, Weil MH, Sun S, et al. The effects of biphasic waveform design on post-resuscitation myocardial function. *J Am Coll Cardiol* 2004; 43:1228-1235
- Taraszewska A, Zelman IB, Ogonowska W, et al. The pattern of irreversible brain changes after cardiac arrest in humans. *Folia Neuropathol* 2002;40:133-141
- Thannhauser J, Nas J, van Grunsven PM. The ventricular fibrillation waveform in relation to shock success in early vs. late phases of out-of-hospital resuscitation. *Resuscitation* 2019;139:99-105
- Thannhauser J, Nas J, Rebergen DJ, et al. Computerized Analysis of the Ventricular Fibrillation Waveform Allows Identification of Myocardial Infarction: A Proof-of-Concept Study for Smart Defibrillator Applications in Cardiac Arrest. *J Am Heart Assoc* 2020;9:e016727
- Thannhauser J, Nas J, Vart P, et al. Electrocardiographic recording direction impacts ventricular fibrillation waveform measurements: A potential pitfall for VF-waveform guided defibrillation protocols. *Resusc Plus*. 2021; 6:100114
- Theochari E, Xanthos T, Papadimitriou D et al. Selective beta blockade improves the outcome of cardiopulmonary resuscitation in a swine model of cardiac arrest. *Ann Ital Chir* 2008;79:409-14
- Travers AH, Rea TD, Bobrow BJ, et al. Part 4: CPR Overview 2010 American Heart Association Guidelines for Cardiopulmonary Resuscitation and Emergency Cardiovascular Care. *Circulation* 2010; 122:S676-S684
- Trentini F, Marziano V, Guzzetta G, et al. The pressure on healthcare system and intensive care utilization during the COVID-19 outbreak in the Lombardy region: a retrospective observational study on 43,538 hospitalized patients. *Am J Epidemiol* 2022; 191:137-146

V

- Vaillancourt C, Verma A, Trickett J, et al. Evaluating the effectiveness of dispatch-assisted cardiopulmonary resuscitation instructions. *Acad Emerg Med* 2007; 14:877–883
- Vaillancourt C, Everson-Stewart S, Christenson J, et al. The impact of increased chest compression fraction on return of spontaneous circulation for out-of-hospital cardiac arrest patients not in ventricular fibrillation. *Resuscitation* 2011; 82:1501-1507
- Vakeva AP, Agah A, Rollins SA, et al. Myocardial infarction and apoptosis after myocardial ischemia and reperfusion: role of the terminal complement components and inhibition by anti-C5 therapy. *Circulation* 1998; 97:2259-2267

- Valenzuela TD, Roe DJ, Cretin S, et al. Estimating effectiveness of cardiac arrest interventions: a logistic regression survival model. *Circulation* 1997; 96:3308–3313
- Valenzuela TD, Roe DJ, Nichol G, et al. Outcomes of rapid defibrillation by security officers after cardiac arrest in casinos. *N Engl J Med* 2000; 343:1206–1209
- van Alem AP, Post J, Koster RW. VF recurrence: characteristics and patient outcome in out-of-hospital cardiac arrest. *Resuscitation* 2003;59(2):181-8
- van Genderen ME, Lima A, Akkerhuis M, et al. Persistent peripheral and microcirculatory perfusion alterations after out-of-hospital cardiac arrest are associated with poor survival. *Crit Care Med* 2012;40:2287–2294
- Van Hoeyweghen RJ, Bossaert LL, Mullie A, et al. Quality and efficiency of bystander CPR: Belgian Cerebral Resuscitation Study Group. *Resuscitation* 1993; 26:47–52
- Vendrell M, Hessheimer AJ, Ruiz A, et al. Coagulation profiles of unexpected DCDD donors do not indicate a role for exogenous fibrinolysis. *Am J Transplant* 2015;15:764-71
- Viersen VA, Greuters S, Korfage AR, et al. Hyperfibrinolysis in out of hospital cardiac arrest is associated with markers of hypoperfusion. *Resuscitation* 2012;83:1451-5
- von Planta M, von Planta I, Weil MH, et al. End tidal carbon dioxide as an haemodynamic determinant of cardiopulmonary resuscitation in the rat. *Cardiovasc Res* 1989; 23:364–368

W

- Waalewijn RA, Tijssen JG, Koster RW. Bystander initiated actions in out-of-hospital cardiopulmonary resuscitation: results from the Amsterdam Resuscitation Study (ARREST). *Resuscitation* 2001; 50:273–279
- Wada T, Gando S, Ono Y, et al. A Disseminated intravascular coagulation with the fibrinolytic phenotype predicts the outcome of patients with out-of-hospital cardiac arrest. *Thromb J* 2016;14:43
- Wada T. Coagulofibrinolytic Changes in Patients with Post-cardiac Arrest Syndrome. *Front Med (Lausanne)*. 2017 29;4:156
- Wang J, Weil MH, Tang W, et al. A comparison of electrically induced cardiac arrest with cardiac arrest produced by coronary occlusion. *Resuscitation* 2007b; 72:477–483
- Wang S, Radhakrishnan J, Ayoub IM, et al. Limiting sarcolemmal Na⁺ entry during resuscitation from ventricular fibrillation prevents excess mitochondrial Ca²⁺ accumulation and attenuates myocardial injury. *J Appl Physiol* 2007; 103:55-65
- Watson JN, Uchaipichat N, Addison P, et al. Improved prediction of defibrillation success for out-of-hospital VF cardiac arrest using wavelet transform methods. *Resuscitation* 2004; 63:269–275

- Watson JN, Addison PS, Clegg GR, et al. Wavelet transform-based prediction of the likelihood of successful defibrillation for patients exhibiting ventricular fibrillation. *Mea. Sci Technol* 2005; 16:L1-L6
- Weaver MD, Cobb LA, Dennis D, et al. Amplitude of ventricular fibrillation waveform and outcome after cardiac arrest. *Ann Intern Med* 1985; 102:53–55
- Weil MH, Bisera J, Trevino RP, et al. Cardiac output and end-tidal carbon dioxide. *Crit Care Med* 1985; 13:907-909
- Weisfeldt ML, Becker LB. Resuscitation after cardiac arrest: a 3-phase timesensitive model. *JAMA* 2002; 288:3035–3038
- Werther T, Klotz A, Granegger M, et al. Suppression of the cardiopulmonary resuscitation artefacts using the instantaneous chest compression rate extracted from the thoracic impedance. *Resuscitation* 2012; 83:692-698
- Wiggers CJ. Studies of ventricular fibrillation caused by electrical shock: cin-ematographic and electrocardiographic observations of the natural process in the dog's heart: its inhibition by potassium and the revival of coordinated beats by calcium. *Am Heart J* 1930; 5:351—365
- Wik L, Steen PA, Bircher NG. Quality of bystander cardiopulmonary resuscitation influences outcome after prehospital cardiac arrest. *Resuscitation* 1994; 28:195–203
- Wik L, Naess PA, Ilebekk A, et al. Effects of various degrees of compression and active decompression on haemodynamics, end-tidal CO₂, and ventilation during cardiopulmonary resuscitation of pigs. *Resuscitation* 1996; 31:45–57
- Wik L, Hansen TB, Fylling F, et al. Delaying defibrillation to give basic cardiopulmonary resuscitation to patients with out-of-hospital ventricular fibrillation: a randomized trial. *JAMA* 2003;289:1389-95
- Wik L, Kramer-Johansen J, Myklebust H, et al. Quality of cardiopulmonary resuscitation during out-of-hospital cardiac arrest. *JAMA* 2005; 293:299–304

X

- Xie J, Weil MH, Sun S, et al. High-energy defibrillation increases the severity of postresuscitation myocardial dysfunction. *Circulation* 1997;96:683-8
- Xu K, Puchowicz MA, Sun X, et al. Decreased brainstem function following cardiac arrest and resuscitation in aged rat. *Brain Res* 2010; 1328:181-189

Y

- Yang Q, Li M, Huang Z, Xie Z, et al. Validation of spectral energy for the quantitative analysis of ventricular fibrillation waveform to guide defibrillation in a porcine model of cardiac arrest and resuscitation. *J Thorac Dis* 2019; 11:3853-3863
- Yeh ST, Lee HL, Aune SE, et al. Preservation of mitochondrial function with cardiopulmonary resuscitation in prolonged cardiac arrest in rats. *J Mol Cell Cardiol* 2009; 47:789-797
- Young C, Bisera J, Gehman S, et al. Amplitude spectrum area: measuring the probability of successful defibrillation as applied to human data. *Crit Care Med* 2004; 32:S356-S358
- Yu T, Weil MH, Tang W, et al. Adverse outcome of interrupted precordial compression during automated defibrillation. *Circulation* 2002; 106:368-372

Z

- Zaza A, Belardinelli L, Shryock JC. Pathophysiology and pharmacology of the cardiac “late sodium current”. *Pharmacol Ther* 2008; 119:326–339
- Zhang Q, Li C. Combination of epinephrine with esmolol attenuates post-resuscitation myocardial dysfunction in a porcine model of cardiac arrest. *PLoS One* 2013;8:e82677
- Zuo F, Ding Y, Dai C et al. Estimating the amplitude spectrum area of ventricular fibrillation during cardiopulmonary resuscitation using only ECG waveform. *Ann Transl Med* 2021;9:619

11 DISCLOSURE AND ACKNOWLEDGEMENTS

11.1 FUNDING FOR THE THESIS WORK

AMSA trial was funded by the Horizon 2020 Programme under grant agreement no. 733381 (EU Framework “European Sudden Cardiac Arrest network: towards Prevention, Education and New Treatment - ESCAPE-NET” and received an additional unrestricted grant from ZOLL Medical Corp., Chelmsford, USA.

11.2 CONFLICT OF INTEREST

The student declares no conflicts of interest.

11.3 PUBLICATIONS DERIVED FROM THE THESIS WORK

11.3.1 Full articles

- Ruggeri L, Semeraro F, Ristagno G. Amplitude spectrum area: The "clairvoyance" during resuscitation in the era of predictive medicine. *Resuscitation*. 2017 Nov;120:A5-A6. doi: 10.1016/j.resuscitation.2017.09.011. Epub 2017 Sep 18. PMID: 28928017
- Ruggeri L, Nespoli F, Ristagno G, Fumagalli F, Boccardo A, Olivari D, Affatato R, Novelli D, De Giorgio D, Romanelli P, Minoli L, Cucino A, Babini G, Staszewsky L, Zani D, Pravettoni D, Belloli A, Scanziani E, Latini R, Magliocca A. Esmolol during cardiopulmonary resuscitation reduces neurological injury in a porcine model of cardiac arrest. *Sci Rep*. 2021 May 20;11(1):10635. doi: 10.1038/s41598-021-90202-w. PMID: 34017043; PMCID: PMC8138021
- Babini G, Ruggeri L, Ristagno G. Optimizing defibrillation during cardiac arrest. *Curr Opin Crit Care*. 2021 Jun 1;27(3):246-254. doi: 10.1097/MCC.0000000000000821. PMID: 33797430

11.3.2 Abstracts

- Olivari Davide, Daria De Giorgio, Francesca Fumagalli, Aurora Magliocca, Laura Ruggeri, Giuseppe Ristagno. Preclinical feasibility of real time AMSA measurement during CPR using a modified clinical defibrillator. European Resuscitation Council Congress 2022

11.4 COLLABORATING PERSONNEL FOR THE THESIS WORK

The student Laura Ruggeri truly thanks the following colleagues for their determinant help and support. Indeed, the experimental and clinical studies described in the thesis were possible thanks to their collaboration and enthusiasm:

- Prof. Giuseppe Ristagno from the Mario Negri Institute, for having mentored, with his valuable experience of experimental and clinical studies in the field of cardiac arrest, the student during the 4-year course. His support and guidance were determinant to achieve the results described in the thesis
- Dr. Roberto Latini from the Mario Negri Institute for the support in every phase of the studies
- Prof. Derek J. Hausenloy from the Duke-NUS Medical School, Singapore, for the 4-year supervision
- Dr. Francesca Fumagalli and all the experimental team of the Cardiovascular Department of Mario Negri Institute, for the help in running all the studies
- Prof. Antonio Pesenti, Prof. Roberto Fumagalli, Prof. Giacomo Bellani, Dr. Maurizio Migliari, Dr. Filippo Bernasconi and all the personnel of Azienda Regionale Emergenza-Urgenza of Milano and Monza, Italy, in particular to all the Heads of local EMS (CLEU) and the nurses involved, for the support and collaboration in conducting AMSA Trial
- Dr. Giovanni Gordini, Dr. Federico Semeraro and all the personnel of EMS of Bologna, Italy, for the collaboration in conducting AMSA Trial
- Prof. Markus Skrifvars, Dr. Tomi Mäkiäho and all the personnel of EMS of Espoo, Finland, for the collaboration in conducting AMSA Trial
- Prof. Lars Wik, from Oslo University Hospital, for his support and advice in conducting AMSA Trial
- The Italian Resuscitation Council and all its personnel for the support
- Drs. Jennifer Meessen and Adriana Blanda for revision of statistics
- ZOLL Medical Corporation (USA) for the technical support necessary in all phases of the experimental studies.